A genetic screening identifies a component of the SWI/SNF complex, Arid1b as a senescence regulator

Sadaf Khan

A thesis submitted to Imperial College London
for the degree of Doctor in Philosophy

MRC Clinical Sciences Centre
Imperial College London, School of Medicine

July 2013

Statement of originality

All experiments included in this thesis were performed by myself unless otherwise stated.

Copyright Declaration

The copyright of this thesis rests with the author and is made available under a Creative Commons Attribution Non-Commercial No Derivatives license. Researchers are free to copy, distribute or transmit the thesis on the condition that they attribute it, that they do not use it for commercial purposes and that they do not alter, transform or build upon it. For any reuse or redistribution, researchers must make clear to others the license terms of this work.

Abstract

Senescence is an important tumour suppressor mechanism, which prevents the proliferation of stressed or damaged cells. The use of RNA interference to identify genes with a role in senescence is an important tool in the discovery of novel cancer genes. In this work, a protocol was established for conducting bypass of senescence screenings, using shRNA libraries together with next-generation sequencing. Using this approach, the SWI/SNF subunit Arid1b was identified as a regulator of cellular lifespan in MEFs. SWI/SNF is a large multi-subunit complex that remodels chromatin. Mutations in SWI/SNF proteins are frequently associated with cancer, suggesting that SWI/SNF components are tumour suppressors.

Here the role of ARID1B during senescence was investigated. Depletion of ARID1B extends the proliferative capacity of primary mouse and human fibroblasts. Furthermore, in cells expressing mutant RAS^{G12V} and $PIK3CA^{H1047R}$, ARID1B is necessary for the maintenance of oncogene-induced senescence (OIS). Knockdown of ARID1B during OIS results in reduced expression of the CKIs $p21^{Cip1}$ and $p16^{INK4a}$. Many SWI/SNF proteins are post-transcriptionally induced during both replicative senescence and OIS, suggesting a broader role for the SWI/SNF complex in senescence.

Ectopic expression of components of the SWI/SNF complex induced premature senescence associated with an increase in $p21^{Cip1}$ and $p16^{INK4a}$ protein levels. SILAC analysis of global changes in protein levels identified enrichment of mitochondrial proteins and depletion of mitotic proteins upon ARID1B expression. Mitochondrial dysfunction and ROS production are important in ARID1B expressing cells as growth arrest was rescued using antioxidant N-acetyl-cysteine. Finally, analysis of cancer genome sequencing data has identified ARID1B as a mutational-driver gene in some cancers. In these tumours, ARID1B mutations are often associated with mutations in *TP53* and *PTEN.* Altogether the present evidence suggests that regulation of senescence by different mechanisms contributes to explain the tumour suppressive properties of the SWI/SNF complex.

Acknowledgements

All thanks is for God and Jesus. I am truly grateful for the opportunity to do what I love every day.

Throughout my life I have been blessed with amazing teachers who are very important to me. Thank you to Ana, for always going the extra mile to help me. Thank you for always being there for me ♥. You are “the buzz lightyear to my woody”.

Thank you to Juan Carlos and to Selina for the continual encouragement and help over the last few years, and for advising me with your experience every step of the way!! Much of the work wouldn’t have been possible without ‘the horrids’. Marta, thank you for being my inspiration, thank you for all that you did for me, I will never forget it. The day the two big slaves left the little slave was very Meireles, but Nik, YNWA! Thanks Migi for bringing me into your group of “kids” and for being a great friend.

I would like to thank ALL the cool people in the CSC for making my time here so fun. Thank you my partner in distraction, Ines for teaching me ChIP sukhi para me :D. Where were you when Aguero scored 94th minute vs QPR? I was in Bram’s office destroying his ear drums :’), thanks for SO many things, not least the MS, and Vesela thanks for your 5% input ;). Thanks Tom for introducing me to Ronald ‘The Don’ Fisher and the Genomics lab for the NGS optimisation. Thanks also to Angeles, Nuria, Joao and Rita for fun times ☺ and everyone in CP.

Thank you to Mike, for always checking up on me in the night, and Curtis for bringing my 20 boxes with a huge smile. You guys were “The Constant” when I was “unstuck in time”. To all the footie boys thanks for making Mondays worth it: thanks to my “favourite” Fico for filling a huge gap (fatass!) when Ana left. Jorge + Vlad your feedback on my work was absolutely priceless thank you! Fede, Ben, Olivier, Peter thank you for holding back the shots, you’re all true gentlemen ☺. Francesco, I hope I finally convinced you fate exists, after you gave me ‘The Fall’ 4 days before I was that girl…thank you for giving me a break :oP!

For Ken. Thank you for encouraging me to apply for studentships. If it wasn’t for your kind words and confidence in me, I never would have thought to take this path. Thank you for instilling in me your passion for science.

Thank you to my friends who stood by me through all the late dinners, birthdays and engagement parties!

Thank you to my big nurturing family for your unconditional love and prayers, especially to my Mummy. Thanks Chibbies for the room cleaning and Sally for ‘praying that I get a life one day’. Thank you for letting me follow my dreams.

All praise for any good in this work belongs to God. Our helper when all doors are closed and our shelter when all solutions fail. Thank you for your guidance.

Table of Contents

Statement of originality 2

Copyright declaration 2

Abstract 3

Acknowledgments 4

Table of contents 5

List of Figures and Tables 10

Abbreviations 13

Chapter 1. Introduction 20

1.1. Senescence 20

1.1.1. The senescence signature 21

1.1.2. Replicative senescence 24

1.1.3. Stress-induced senescence 25

1.1.4. Molecular mechanisms regulating senescence 28

1.1.5. Epigenetic regulation of senescence 31

1.1.5.1. Epigenetic regulation of the *INK4b-ARF-INK4a* locus 31

1.1.5.2. Chromosomal architecture during senescence 32

1.1.6. Senescence and ageing *in vivo* 34

1.2. Loss-of-function screenings using RNA interference (RNAi) 36

1.2.1. Systems for pooled shRNA screenings 38

1.2.2. Genetic screenings to identify novel senescence regulators 39

1.3. The SWI/SNF complex in senescence and cancer 44

1.3.1. The SWI/SNF complex of chromatin remodellers 44

1.3.1.1. A multi-subunit complex 45

1.3.1.2. ATP-dependent nucleosome remodelling 47

1.3.1.3. Regulation of transcription 50

1.3.1.4. Specialised domains and exchangeable isoforms 50

1.3.2. Role of the SWI/SNF complex in senescence and cancer 51

1.3.2.1. SWI/SNF subunits are frequently mutated in cancer 52

1.3.2.2. Relationship between the SWI/SNF complex and senescence 57

1.3.2.2.1. SNF5 57

1.3.2.2.2. BRG1/BRM 58

1.3.2.2.3. ARID1A/ARID1B 60

1.3.2.2.4. PBRM1/BRD7 61

1.3.2.2.5. Role of SWI/SNF in SAHF formation 62

Chapter 2. Materials and Methods 64

2.1. Libraries 64

2.1.1. HCC deletion library 64

2.1.2. pGIPZ genome-wide library 64

2.2. Cell lines and tissue culture methods 65

2.3. Retrovirus production and transduction of target cells 65

2.4. Lentivirus production and transduction of target cells 66

2.5. Generation of custom Solexa libraries 67

2.5.1. Genomic DNA isolation 67

2.5.2. Solexa PCR 67

2.5.3. DNA purification and quantification 68

2.6. Next-generation sequencing 68

2.6.1. Solexa library quality control 68

2.6.2. High-throughput sequencing 69

2.6.3. Bioinformatics 69

2.7. Growth assays 72

2.7. 1. Growth curves and colony formation assays 72

2.7.2. BrdU (5-Bromo-2'-deoxyuridine) incorporation assay 73

2.7.3. Senescence-associated β-galactosidase (SA-β-gal) assay 73

2.7.3.1. Cytochemical staining 73

2.7.3.2. Fluorescence visualisation 74

2.8. Generation of shRNA expressing retroviral vectors 74

2.8.1. shRNA constructs 74

2.8.2. Plasmid DNA purification 75

2.8.3. Agarose gel electrophoresis and DNA purification 75

2.8.4. DNA sequencing 75

2.9. RNA expression analysis 76

2.9.1. Total RNA purification 76

2.9.2. Gene expression profiling 76

2.9.2.1. RNA quality control 76

2.9.2.2. Microarray analysis 77

2.9.3. Quantitative RT-PCR (RT-qPCR) analysis 77

2.10. Protein expression analysis 78

2.10.1. Immunofluorescence 78

2.10.1.2. High throughput microscopy (HTM) 78

2.10.1.3. High content analysis (HCA) 78

2.10.1.4. Confocal microscopy 81

2.10.2. SILAC to identify changes in protein expression 81

2.10.2.1. Whole cell protein extraction 81

2.10.2.2. Protein quantification 82

2.10.2.3. Sodium-dodecyl-sulphate polyacrylamide gel electrophoresis (SDS-PAGE) 82

2.10.2.4. Co-immunoprecipitation of nuclear protein complexes 83

2.10.2.5. Identification of proteins by LC–MS/MS 83

Chapter 3. Screening for regulators of lifespan extension in MEFs using NGS 85

3.1. Optimisation of the bypass of senescence screening 85

3.2. Proof of concept experiment verifies feasibility of the screening 86

3.3. NGS used to identify shRNAs from bypass of replicative senescence screen in MEFs 87

3.4. ARID1B is a candidate regulator of replicative senescence in MEFs 91

3.5. Depletion of Arid1b extends cellular lifespan in MEFs 93

3.6. ARID1B regulates cell proliferation and replicative senescence in IMR-90 93

3.7. Conclusions and perspectives 96

3.7.1. Screening for regulators of replicative senescence in MEFs 96

3.7.2 Advances in pooled shRNA screenings using NGS 97

Chapter 4. ARID1B a component of the SWI/SNF complex regulates senescence 100

4.1. Knockdown of ARID1B attenuates OIS 100

4.2. ARID1B regulates $p21^{CIP1}$, $p16^{INK4a}$ and p53 expression during OIS 100

4.3. Gene expression profiling identifies multiple senescence effectors regulated by ARID1B 103

4.4. Expression of oncogenic $PIK3CA^{H1047R}$ induces senescence 105

4.5. Knockdown of ARID1B attenuates $PIK3CA^{H1047R}$ mediated senescence 106

4.6. ARID1B regulates $p16^{INK4a}$ and $p21^{CIP1}$ expression during PIK3CA-induced senescence 110

4.7. High expression of SWI/SNF complex components during replicative senescence 110

4.8. Expression of SWI/SNF complex components increases during OIS 113

4.9. Post-translational stabilisation of the SWI/SNF complex during senescence 113

4.10. SILAC based quantitative proteomics identifies changes in the levels of ARID1B binding proteins during OIS 116

4.11. ARID1B is excluded from regions of repressed chromatin 119

4.12. Retroviral constructs overexpressing ARID1A and ARID1B 121

4.13. Ectopic expression of SWI/SNF subunits induces premature senescence 121

4.14. Premature senescence induced by ARID1B is mainly p53 dependent 126

4.15. Global changes in protein expression associated with ARID1B 129

4.16. ARID1B is deleted in cancer 132

4.17. Conclusions and perspectives 132

4.17.1. ARID1B depletion can bypass senescence through multiple mechanisms 132

4.17.2. SWI/SNF proteins are induced during senescence 134

4.17.3. Growth arrest induced by SWI/SNF is exerted through different mechanisms 139

4.17.4. ARID1B exhibits tumour-suppressive functions in cancer 141

Chapter 5. Discussion & Future work 144

5.1. Genetic screens are useful tools for identifying novel genes and pathways involved in senescence 144

5.1.1. Genome-wide screening for regulators of OIS in IMR-90 144

5.1.2. Library bias not detected from sequencing pGIPZ library pools 145

5.1.3. Set up of infection conditions for pGIPZ lentiviral screening 146

5.1.4. pGIPZ shp53-1 can be used as a control hairpin that bypasses OIS 146

5.2. ARID1B is an important senescence regulator 150

5.3. The SWI/SNF complex is implicated in cancer and ageing 152

5.4. The clinical utility of targeting the SWI/SNF complex in cancer detection and therapy 15X

5.5. Concluding remark 154

References 159

Appendix 213

List of Figures and Tables

Figure 1.1. Senescence is an intrinsic cellular response to multiple stresses. 21

Figure 1.2. The senescence signature. 24

Table 1.1. Senescent cells are found in pre-malignant lesions *in vivo.* 26

Figure 1.3. Senescence is a barrier to tumourigenesis *in vivo.* 27

Figure 1.4. Key senescence pathways and effectors. 30

Figure 1.5. Epigenetic regulation of senescence. 34

Figure 1.6. Screenings using pooled shRNA libraries. 38

Figure 1.7. Genetic screens for the bypass of replicative senescence. 40

Figure 1.8. Workflow of shRNA identification using different methods. 42

Figure 1.9. The SWI/SNF complex of nucleosome remodellers. 49

Figure 1.10. The SWI/SNF complex interacts with proteins involved in many cancer-related pathways. 52

Figure 1.11. Mutations in SWI/SNF genes are predominantly deleterious. 55

Table 1.2. SWI/SNF mutations occur frequently in human cancers. 56

Figure 2.1. Bioanalyser profile of acceptable custom Solexa library for NGS. 69

Figure 2.2. Solexa sequencing schematic. 71

Figure 2.3. Bioanalyser profile of acceptable RNA profile for gene expression profiling. 77

Figure 2.4. Workflow of establishing filters for High Content Analysis. 80

Figure 3.1. An shRNA library targeting genes frequently deleted in human HCC. 86

Figure 3.2. Proof of concept to establish the feasibility of an shRNA lifespan extension screen in MEFs. 87

Figure 3.3. Strategy for the genetic screening for bypass of replicative senescence

in MEFs. 90

Figure 3.4. Lifespan extension screen in MEFs identifies Arid1b as a candidate senescence regulator. 92

Figure 3.5. Depletion of Arid1b extends cellular lifespan in MEFs. 94

Figure 3.6. Depletion of ARID1B extends cellular lifespan in IMR-90. 95

Figure 4.1. Knockdown of ARID1B attenuates OIS. 101

Figure 4.2. ARID1B regulates different senescence effectors. 102

Figure 4.3. Validation of gene expression changes associated with ARID1B knockdown during OIS. 104

Figure 4.4.1. Expression of oncogenic PIK3CA^{H1047R} induces senescence. 107

Figure 4.4.2. Characterisation of the senescence response induced upon PIK3CA^{H1047R} expression. 108

Figure 4.5. Knockdown of ARID1B attenuates PIK3CA^{H1047R} mediated senescence. 109

Figure 4.6. ARID1B regulates p16^{INK4a} and p21^{CIP1} during PIK3CA-induced senescence. 111

Figure 4.7. Expression of SWI/SNF complex increases during replicative senescence. 112

Figure 4.8. Expression of SWI/SNF complex increases during OIS. 114

Figure 4.9. Increase in expression of SWI/SNF subunits is not transcriptionally regulated. 115

Figure 4.10. SILAC based quantitative proteomics identifies SWI/SNF interactor exchange during OIS. 118

Figure 4.11. ARID1B is excluded from regions of repressed chromatin. 120

Figure 4.12. Retroviral constructs overexpressing ARID1A and ARID1B. 122

Figure 4.13.1. Overexpression of SWI/SNF subunits induces premature senescence. 123

Figure 4.13.2. Molecular analysis of senescence induced by SWI/SNF subunits. 125

Figure 4.14.1. Knockdown of important senescence regulators alleviates ARID1B mediated senescence. 127

Figure 4.14.2. Co-expression of Human papillomavirus (HPV) oncoproteins alleviates

ARID1B-mediated senescence. 128

Figure 4.15.1. Global changes in protein levels upon ARID1B overexpression analysed by SILAC. 130

Figure 4.15.2. Production of oxidative stress may contribute to ARID1B mediated senescence. 131

Figure 5.1. pGIPZ library set up and pool coverage determined by HTS. 145

Figure 5.2. Optimising infection conditions with pGIPZ lentiviral vectors. 148

Figure 5.3. Validation of pGIPZ controls for proof of principle experiment for bypass of OIS screening. 149

Table A1. Inferences from test NGS run at CSC. 213

Table A2. Differential gene expression of ARID1B knockdown cells during OIS. 214

Table A3. pGIPZ pool coverage determined by HTS. 215

Table A4. Copy number deletions in ARID1B is significant across cancers. 215

Table A5. cDNA constructs. 216

Table A6. shRNA target sequences. 216

Table A7. Solexa PCR primers. 217

Table A8. Sequencing primers. 217

Table A9. RT-qPCR primers. 217

Table A10. Primers for cloning. 219

Table A11. Antibodies. 219

Figure A1. Validation of ARID1B antibody for immunoprecipitation 220

Abbreviations

4-OHT	4-hydroxy tamoxifen
A	Adenine
Ac	Acetylated
AKT	v-akt murine thymoma viral oncogene homologue
ARF	Alternative reading frame
ARID	AT-rich interactive domain
ASF	Anti-silencing function
ATCC	American Type Culture Collection
ATM	Ataxia telangiectasia mutated
ATP	Adenosine tri-phosphate
ATR	Ataxia telangiectasia and Rad3 related
BAF	BRG1/BRM associated factors
BAMBI	BMP and activin membrane-bound inhibitor homologue
BCL	B-cell CLL/lymphoma
BH	Benjamini-Hochberg
BMP	Bone morphogenetic protein
bp	Base pair
BRAF	v-raf murine sarcoma viral oncogene homologue B1
BRCA	Breast cancer susceptibility gene
BRD	Bromodomain containing
BrdU	5-bromo-2-deoxyuridine
BRG1	Brahma related gene 1
BRM	Brahma
BSA	Bovine serum albumin
C	Cytosine
c-FOS	Cellular-FBJ osteosarcoma oncogene
C. elegans	*Caenorhabditis elegans*
C(T)	Threshold cycle
C/EBP	CCAAT/enhancer binding protein
C_{12}FDG	Fluorescein-di-β-d-galactopyranoside
CASAVA	Consensus assessment of sequence and variation
cBAF	Cardiac BAF

CBX7	Chromobox protein homologue 7
CDC	Cell division cycle
CDK	Cyclin dependent kinase
CKI	Cyclin dependent kinase inhibitor
CDKN1	cyclin-dependent kinase inhibitor 1A
CDKN2	cyclin-dependent kinase inhibitor 2A
cDNA	Complementary DNA
CGH	Comparative genomic hybridisation
ChIP	Chromatin immunoprecipitation
CML	Chronic myeloid leukaemia
CSC	Clinical Sciences Centre
CSC	Cancer stem cell
CSF	Colony-stimulating factor
CTGF	Connective tissue growth factor
CXCL	CXC chemokine ligand
CXCR	CXC chemokine receptor
DAPI	4,6-diamidino-2-phenylindole
DDR	DNA damage response
DMEM	Dulbecco's modified Eagle's medium
DMSO	Dimethyl sulfoxide
DNA	Deoxyribonucleic acid
DNMT	DNA methyltransferase
dNTP	Deoxyribonucleotide triphosphate
ds	Double strand
DTT	Dithiothreitol
E.coli	*Escherichia coli*
EDTA	Ethylenediaminetetraacetic acid
EIF	Translation initiation factor
ELAND	Efficient large-scale alignment of nucleotide databases
EMBL	European Molecular Biology Laboratory
ER	Oestrogen receptor
esBAF	Embryonic stem cell BAF
ETS	E26 oncogene homologue
EZH2	Enhancer of zeste homologue 2
FBS	Foetal bovine serum
FGF	Fibroblast growth factors

FOXO	Forkhead box, sub-group O
γH2AX	Phosphorylated histone 2, variant X
g	Gram
G	Guanine
GDF	Growth differentiation factor
GFP	Green fluorescent protein
GLB1	Galactosidase, beta 1
GM	granulocyte-macrophage
GO	Gene ontology
GR	Glucocorticoid receptor
GSEA	Gene Set Enrichment Analysis
GSK3	glycogen synthase kinase 3
GUS-B	β-glucuronidase
H	Histone
HAT	Histone acetyl-transferase
HCA	High content analysis
HCC	Hepatocellular carcinoma
HDAC	Histone deacetylase
HEK	Human embryonic kidney
HEPES	4-(2-hydroxyethyl)-1-piperazineethanesulfonic acid
HGPS	Hutchinson–Gilford progeria syndrome
HIF	Hypoxia inducible factor 1
HIRA	Histone repressor A
HMG	High mobility group
HMT	Histone methyltransferase
HP	Heterochromatic protein
HPDE	Human pancreatic duct epithelial
HPV16	Human papilloma virus 16
h	Hour
HRAS	Harvey rat sarcoma gene
HSCs	Hematopoietic stem cells
hTERT	Human telomerase reverse transcriptase
HTM	High throughput microscopy
HUGO	Human genome organisation
HZI	Helmholtz Centre for Infection
ICAM	Intercellular adhesion molecule

ID	Inhibitor of DNA binding
IF	Immunofluorescence
IFI	Interferon, gamma-inducible protein
IFITM	Interferon induced transmembrane protein
IGF	Insulin growth factor
IGFBP	Insulin growth factor binding protein
IL	Interleukin
INK4	Inhibitor of CDK4
INO	Inositol requiring
IP	Immunoprecipitation
iPS	Induced pluripotent stem cell
ISWI	Imitation SWI/SNF
JMJD	Jumonji domain containing
K	Lysine
kb	Kilo base
kDa	Kilo dalton
KLF4	Krüppel-like factor 4
KRTAP	Keratin associated protein
L	Litre
LAMP	Lysosomal-associated membrane protein
LB	Luria Bertani
LC	Liquid chromatography
LCE	Late cornified envelope
LMN	Lamin
LOH	Loss of heterozygosity
LTR	Long terminal repeat
LYAR	Ly1 antibody reactive
Lys	Lysine
m	Milli
M	Molar
MAPK	Mitogen-activated protein kinases
Mb	Mega base pair
MCM	Minichromosome maintenance complex
me	Methylation
MEF	Mouse embryonic fibroblast

min	Minute
miR	MicroRNA
MMP	Matrix metalloproteinase
MNase	Micrococcal nuclease
mRNA	Messenger RNA
MRT	Malignant rhabdoid tumour
MS	Mass spectrometry
MSC	Mesenchymal stem cells
mTOR	Mammalian target of rapamycin
MW	Molecular weight
MYC	Myelocytomatosis gene
NAC	N-acetyl-cysteine
NFκB	Nuclear factor kappa B
nBAF	Neural BAF
NGS	Next generation sequencing
NKI	Netherlands Cancer Institute
NKRF	NFκB repressing factor
NOP	Nucleolar protein
npBAF	Neural progenitor BAF
NPC	Naso-pharyngeal carcinoma
NSCLC	Non-small-cell lung cancer
NuRD/CHD	Nucleosome remodelling and deacetylation/chromatin helicase DNA binding
OCT4	Octamer-binding transcription factor 4
OIS	Oncogene induce-senescence
OPN	Osteopontin
OSKM	Polycistronic cassette containing Oct4, Sox2, Klf4 and c-Myc
PAI	Plasminogen activator inhibitor
PBAF	Polybromo BAF
PBRM	Polybromo
PBS	Phosphate buffered saline
PcG	Polycomb group
PCNA	Proliferating cell nuclear antigen
PCR	Polymerase chain reaction
PEI	Polyethylenimine
PFA	Paraformaldehyde
PGC	Peroxisome proliferative activated receptor gamma coactivator

PLA2R	Phospholipase A2 receptor
Pol II	RNA polymerase II
PRC	Polycomb repressive complex
PSMD	Proteasome (prosome, macropain) 26S subunit, non-ATPase
PTEN	Phosphatase and tensin homologue
RB	Retinoblastoma protein
REST	RE1-silencing transcription factor
RIN	RNA integrity number
RMA	Robust multichip average
RNA	Ribonucleic acid
RNAi	RNA interference
RNase	Ribonuclease
ROS	Reactive oxygen species
rpm	Rotations per minute
rRNA	Ribosomal RNA
RRP	Ribosomal RNA processing protein
s	Second
SA-β-gal	Senescence-associated β-galactosidase
SAHF	Senescence-associated heterochromatic foci
SASP	Senescence associated secretory phenotype
SDS	Sodium dodecyl sulphate
SDS-PAGE	SDS polyacrylamide gel electrophoresis
Ser	Serine
shRNA	Short hairpin RNA
SILAC	Stable isotope labelling with amino acids in cell culture
siRNA	Small interfering RNA
SMAD	Mothers against decapentaplegic homologue
SMARC	SWI/SNF-related, matrix-associated, actin-dependent regulator of chromatin
SMURF	SMAD specific E3 ubiquitin protein ligase
SNF	Sucrose non-fermenting
SNP	Single nucleotide polymorphism
SOX2	SRY (sex determining region Y)-box 2
SPP	Secreted phosphoprotein
SS18	Synovial sarcoma translocation, chromosome 18
STAT	Signal transducer and activator of transcription
SV40 LT	Simian vacuolating virus 40 large antigen
SWI	Switch

T	Thymine
TASCC	TOR autophagy spatial coupling compartment
TGF	Tumour growth factor
tGFP	Turbo green fluorescent protein
TNF	Tumour necrosis factor
TNFAI	TNFα inhibitor
TNFSF	TNFα super family
Trx	Trithorax
U	Unit (of enzyme activity)
UBR	Ubiquitin protein ligase E3 component n-resigning
UV	Ultraviolet
µ	Micro
VDR	Vitamin D (1,25- dihydroxyvitamin D3) receptor
VHL	Von Hippel-Lindau tumour suppressor
VSV-g	Vesicular stomatitis virus glycoprotein
w/v	Weight/volume
WGS	Whole genome sequencing
WNT	Wingless (Wg) and integration site (INT) gene
X-Gal	5-Bromo-4-chloro-3-indolyl-β-D-galactopyranoside

Chapter 1. Introduction

1.1. Senescence

Cellular senescence was first described by Hayflick and Moorhead when they observed normal human diploid cells divide a limited number of times before undergoing a permanent growth arrest they termed senescence (Hayflick and Moorhead, 1961). Despite a loss of proliferative capacity, senescent cells remain viable and metabolically active; they do not express genes required for proliferation even under strong mitogenic conditions, thereby distinguishing the process from quiescence (Hayflick, 1965). Senescence is an intrinsic cellular mechanism, which like apoptosis, is activated by a variety of cell stresses, including oxidative damage, oncogene activation, and telomere shortening. Senescence prevents harmful lesions acquired in cells from being passed on to daughter cells (Figure 1.1).

Although differences exist depending on the stimuli and the cell type in which senescence is studied, the ARF/p53 and $p16^{INK4a}$/retinoblastoma (RB1) pathways are crucial to senescence activation (Shay et al., 1991). The tumour suppressors RB1 and p53 are frequently lost in cancer. This along with the understanding that normal cells senesce in response to oncogenic stress led to the hypothesis that senescence is an important tumour suppression mechanism, preventing the proliferation of stressed or damaged cells (Chen et al., 2005; Collado et al., 2005). Cellular senescence can oppose neoplastic progression *in vivo* and escape from senescence, or immortality, is important for malignant transformation (Dimri, 2005).

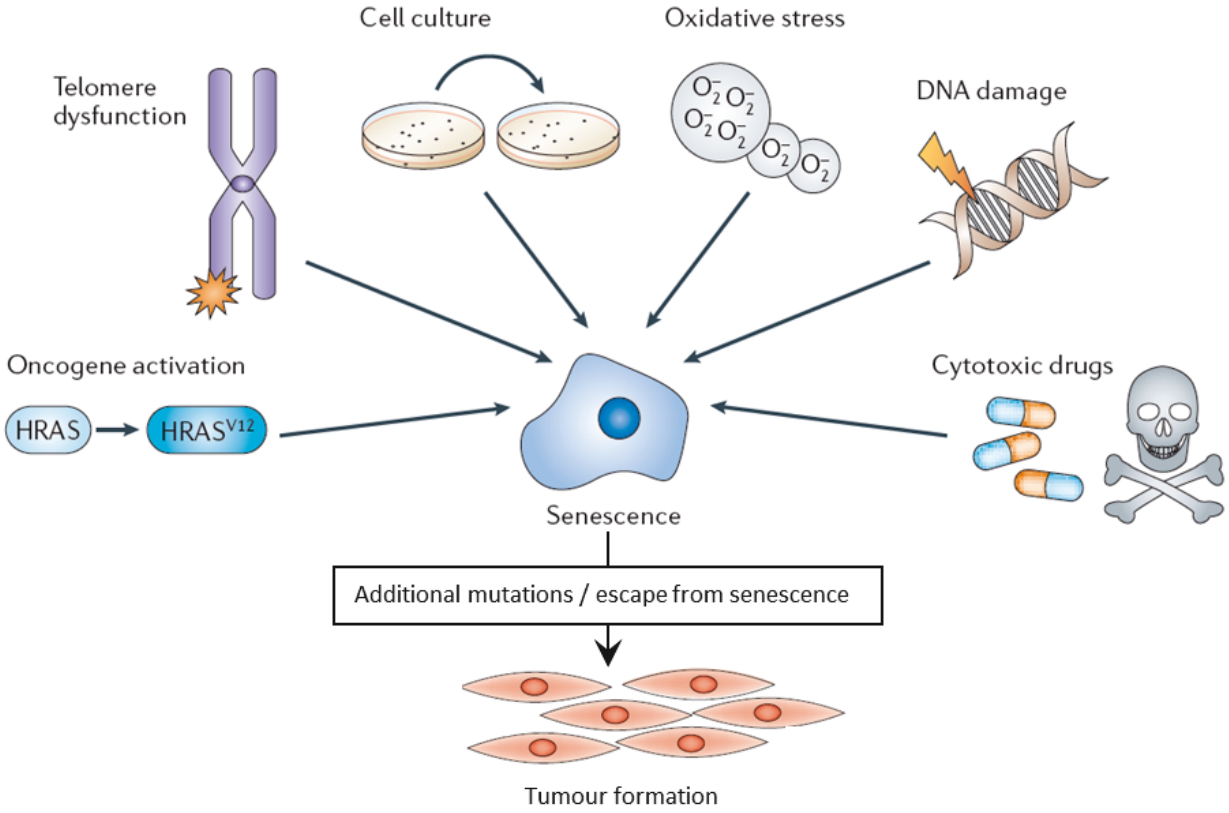


Figure 1.1. Senescence is an intrinsic cellular response to multiple stresses. Many different stress factors can lead to cellular senescence, which is a self-defence mechanism to prevent harmful mutations or lesions being transferred to daughter cells, thereby restraining tumourigenisis. (Adapted from Collado and Serrano 2006)

1.1.1. The senescence signature

Senescent cells possess a distinct phenotype, which allows them to be identified from within a heterogeneous population of senescent and proliferating cells (Figure 1.2). Changes in cell morphology include a flat enlarged size, which in part is due to the high levels of vimentin expression in senescent cells (Nishio et al., 2001; Serrano et al., 1997). Other observable differences found in senescent cells includes the presence of senescence-associated-ß-galactosidase activity (SA-ß-Gal) (Courtois-Cox et al., 2008; Dimri et al., 1995), the formation of senescence-associated heterochromatic foci (SAHF) (Narita et al., 2003), the activation of the DNA damage response (DDR) (d'Adda di Fagagna, 2008), and the induction of the senescence-associated secretory phenotype (SASP) (Kuilman and Peeper, 2009).

As well as having a distinct morphological phenotype, the expression of many cell cycle genes is altered during senescence (Mason et al., 2004; Shelton et al., 1999). This includes the up-regulation of important cyclin-dependent kinase inhibitors (CDIs) *CDKN1a* and *CDKN2a* (encoding $p21^{Cip1}$ and $p16^{INK4a}$ respectively) and the repression of proteins involved in S-phase entry such as cyclin A, cyclin B and proliferating cell nuclear antigen (*PCNA*) (Pang and Chen, 1994; Seshadri and Campisi, 1990; Stein et al., 1991). The repression of these genes is predominantly due to the unphosphorylated status of RB1 in senescent cells, thereby allowing RB1 to repress the expression of E2F target genes by binding to E2F and inhibiting its activity. (Futreal and Barrett, 1991; Stein et al., 1990).

Amongst the most notable changes in gene expression during senescence is the up-regulation of multiple secreted factors, which collectively account for the SASP (Coppe et al., 2010; Shelton et al., 1999). Through the SASP, senescent cells influence their surrounding microenvironment (Acosta et al., 2013; Coppe et al., 2008). Depending on the context, these secreted factors can have tumour promoting or tumour suppressive effects (Krtolica et al., 2001).

The most widely used assay for identifying senescent cells is the detection of perinuclear β-galactosidase activity (Figure1.2) (Courtois-Cox et al., 2008; Dimri et al., 1995). SA-β-Gal is a consequence of increased lysosomal mass in senescent cells, which allows SA-β-Gal activity to be detected at a sub-optimal pH of pH 6.0, as opposed to the optimal pH of 4.0-4.5 (Kurz et al., 2000; Robbins et al., 1970). This increase in β-galactosidase activity can be detected in cultured cells or *in vivo* either by the breakdown of a chromogenic substrate 5-bromo-4-chloro-3-indolyl β-d-galactopyranoside (X-Gal) or by the breakdown of fluorescein-di-β-d-galactopyranoside (C_{12}FDG) (Debacq-Chainiaux et al., 2009; Dimri et al., 1995). A positive SA-β-Gal reaction can also be seen in non-senescent cells and is induced by high confluency and serum starvation in tissue culture (Severino et al., 2000); thus SA-β-Gal must be used in combination with other senescence markers to affirm the senescence phenotype.

Senescent cells also display an increase in the size of autophagic vacuoles (Gerland et al., 2003). Autophagy, a lysosome dependent cellular process, is involved in the digestion of the cell's organelles and like senescence it is activated in response to stress (Hoare et al., 2011). In 2009 Young et al., demonstrated that autophagy associated genes are upregulated during senescence, and the inhibition of autophagy can delay the onset of senescence (Young et al., 2009). Recent work from the same group revealed that the cell's endomembrane system is reorganised to spatially couple lysosomes and mTOR forming a complex called the TOR-autophagy spatial coupling compartment (TASCC). The TASCC resides a short distance from the Golgi apparatus and supports the up-regulation of protein synthesis during senescence (Narita et al., 2011).

Nuclear architecture also changes during senescence (O'Sullivan and Karlseder, 2012). Chromatin in the nucleus is reorganised to include specific regions of heterochromatin termed SAHF (Narita et al., 2003b). These structures can be visualised as DAPI stained foci (Figure 1.2). SAHFs have recently been shown to possess a higher order structure consisting of distinct layers of repressive histone marks, H3K9me^3 forming the core of the SAHF with a H3K27me^3 outer ring (Chandra et al., 2012). The formation of SAHFs requires co-operation between many proteins including heterochromatin protein 1 (HP1), histone H2A variant macroH2A, high mobility group A (HMGA) proteins, histone repressor A (HIRA) and anti-silencing function 1a (ASF1a) (Zhang et al., 2007). These heterochromatic structures are important in silencing E2F target genes to halt cell cycle progression (Narita et al., 2003a). Knockdown of proteins required for SAHF formation, such as ASF1a or HMGA1 can delay senescence (Narita et al., 2006; Zhang et al., 2005).

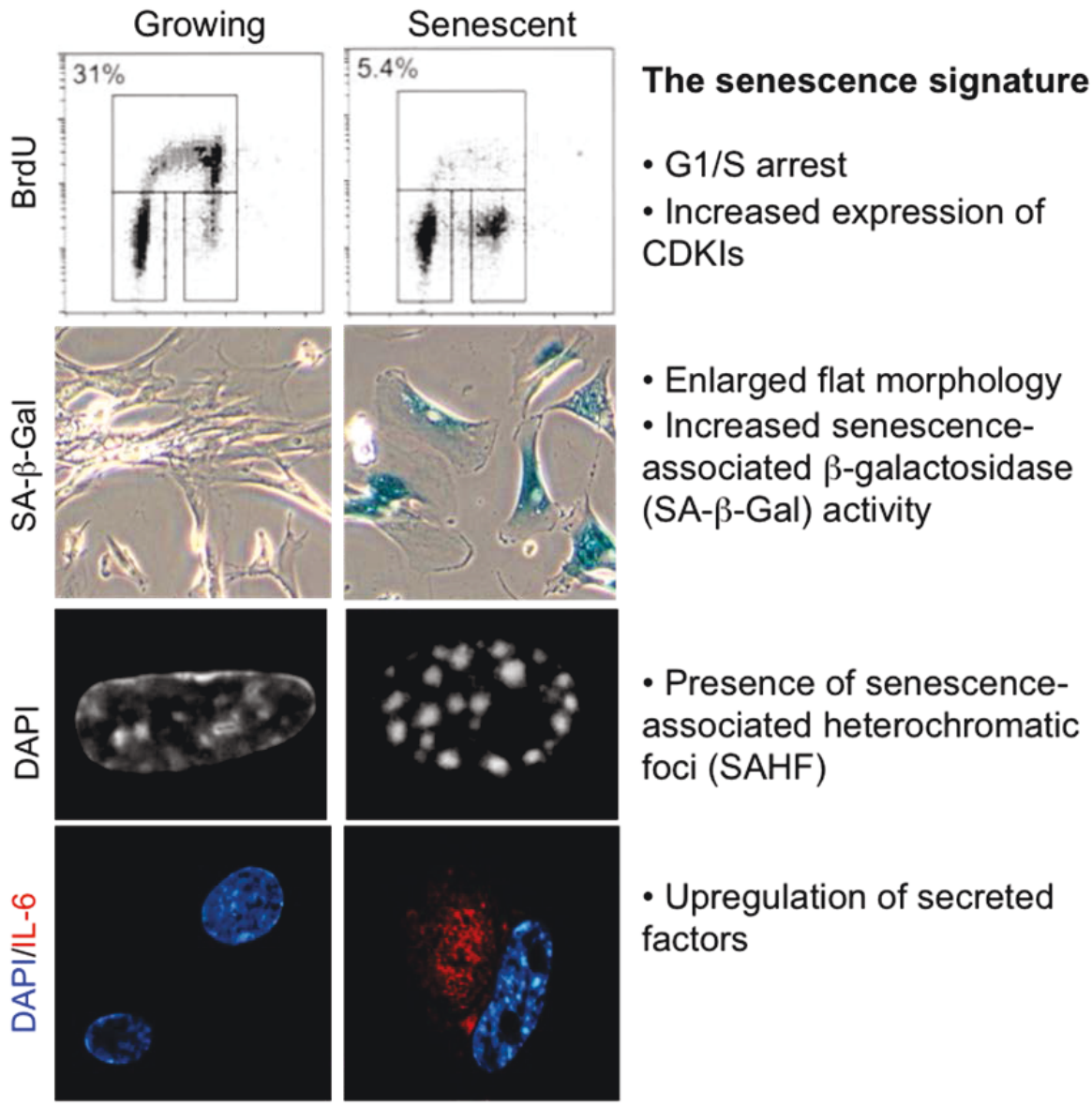


Figure 1.2. The senescence signature. Senescent cells undergo number of different structural and functional changes, which allow them to be identified from non-senescent cells (Adapted with images from Serrano et al. 1997 and Young et al. 2011)

1.1.2. Replicative senescence

Hayflick and Moorhead's observation that normal diploid cells could only divide a finite number of times, gave rise to the idea that cells possess a 'mitotic clock' that counts the number of replications the cell has completed (Hayflick, 1997). It was later understood that human cells reach replicative exhaustion due to telomere attrition with each round of cell division (Harley et al., 1990). Telomere shortening occurs because of the 'end-replication problem' as DNA polymerase is unable to completely synthesise the 5' end of the lagging strand (Olovnikov, 1973; Watson, 1972). This phenomenon is also observed *in vivo* as telomeres decrease in length with increasing age in various

human tissues (Takubo et al., 2010). Replicative senescence, triggered by telomere shortening is sensed as a double-strand break (DSB) initiating a DDR via p53 activation. (Garcia-Cao et al., 2006). The DDR can also be activated by telomere "uncapping" which occurs when the protective structure capping telomeric overhangs is disrupted (Blackburn, 2001; Takai et al., 2003).

In humans, cells which are required to divide indefinitely, such as certain stem cells and in somatic cells of other species, such as mice, telomeric overhangs are maintained by elevated expression of the ribonucleoprotein enzyme telomerase (Greider and Blackburn, 1985; Mathon et al., 2001; Shi et al., 2002). Telomerase is able to extend the 3' end of telomeres preventing the DDR that results from telomere shortening. Immortalised human cell lines and multiple human tumours overexpress telomerase, suggesting that telomerase expression is important in avoiding senescence and in the development of tumours (Counter et al., 1992; Morin, 1989). A clear link between telomerase and senescence was established when the introduction of telomerase in human epithelial cells and fibroblasts resulted in an extension of lifespan (Bodnar et al., 1998).

1.1.3. Stress-induced senescence

Senescence can also be induced as a stress response independent of the replicative state. These responses are termed 'stress-induced senescence' or 'premature senescence' as it occurs before full telomeric attrition has taken place and is characterised by a more rapid onset of senescence (Ben-Porath and Weinberg, 2005). Stimuli which induce premature senescence include aberrant oncogene activation or the use of chemotherapeutic drugs (Kuilman et al., 2010). Oxidative stress can also induce premature senescence. For example, mouse embryonic fibroblasts (MEFs) that express telomerase maintain a long telomere length (~50 kb compared to ~10kb in humans), however still undergo senescence relatively rapidly when propagated in culture (Itahana et al., 2004; Rangarajan and Weinberg, 2003). This 'culture shock' is attributed to non-physiological levels of oxidative stress that results in a DDR (Parrinello et al., 2003; Sherr and DePinho, 2000).

The most commonly studied form of premature senescence, is that elicited by aberrant oncogene activation, termed oncogene-induced senescence (OIS) (Courtois-Cox et al., 2008). In 1997 Serrano et al., demonstrated that overexpression of a constitutively active form of H-RAS (RAS^{G12V}) triggered premature senescence (Serrano et al., 1997). Similarly overexpression of the downstream effectors of RAS, such as BRAF and MEK also induced senescence (Lin et al., 1998; Zhu et al., 1998). During OIS a rise in $p16^{INK4a}$ and p53 provide negative feedback regulation to prevent uncontrolled proliferation (Ohtani et al., 2001; Serrano et al., 1997; Wei et al., 2001). Furthermore, unregulated RAS signalling creates a surplus of mitogenic signals that leads to hyper-replication, triggering a DDR (Bartkova et al., 2006; Di Micco et al., 2006). The discovery that many different types of benign lesions contain senescent cells and that these cells decrease in number during malignant transformation has revealed the importance of OIS as a barrier to tumourigenesis *in vivo* (Table 1.1 and Figure 1.3).

Table 1.1. Senescent cells are found in pre-malignant lesions *in vivo*.

Lesion	Reference
Human melanocytic nevi	(Gray-Schopfer et al., 2006; Michaloglou et al., 2005)
Murine lung adenomas	(Collado et al., 2005; Dankort et al., 2007)
Human dermal neurofibromas	(Courtois-Cox et al., 2006)
Human and murine prostate PIN lesions	(Chen et al., 2005)
Murine pancreatic intraductal neoplasias	(Collado et al., 2005)
Murine papillomas	(Collado et al., 2005)
Murine lymphomas	(Braig et al., 2005)
Early murine melanomas	(Ha et al., 2007)

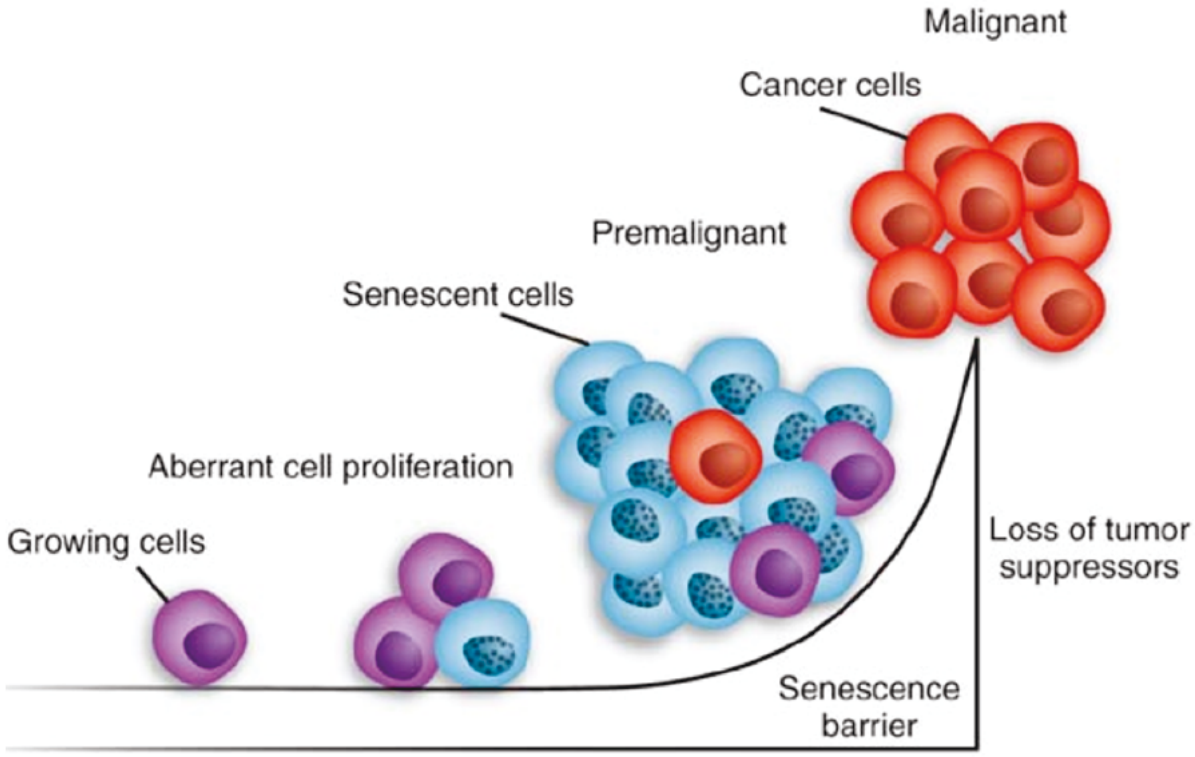


Figure 1.3. Senescence is a barrier to tumourigenesis *in vivo.* Tumours contain a heterogeneous population of growing, senescent and cancer cells. Senescent cells are thought to limit the proliferation of the tumour mass. Alterations in senescent cells or the increase in cancer cells will favour tumourigenesis and malignancy (Adapted from Narita and Lowe, 2005).

The PI3K/PTEN/Akt/mTOR pathway plays an important role in controlling many organismal processes including autophagy, cell proliferation, DDR, and ageing (Harrison et al., 2009; Narita et al., 2011; Selman et al., 2009; Steelman et al., 2011). The *PIK3CA* gene, encoding the PI3K p110α catalytic subunit, is one of the most frequently mutated genes in human cancers (Lee et al., 2005; Ligresti et al., 2009; Samuels et al., 2004). Mutations mostly reside in the helical (E542, E545) and kinase (H1047) domains and generally result in constitutive kinase activity (Huang et al., 2008a; Ligresti et al., 2009; Steelman et al., 2011). Constitutively active PI3K/PTEN/Akt/mTOR pathway signalling is able to induce a stable senescence response (Astle et al., 2012; Collado et al., 2000; Kim et al., 2007; Lee et al., 2007a); however this response is weaker than RAS induced senescence (Kennedy et al., 2011). Inhibitors of the PI3K/PTEN/Akt/mTOR pathway can bypass cellular senescence and extend lifespan in mice (Demidenko et al., 2009a; Demidenko et al., 2009b; Harrison et al., 2009) and

numerous reports have used rapamycin to inhibit mTOR and bypass OIS in human fibroblasts (Demidenko et al., 2009b; Kolesnichenko et al., 2012).

Reprogramming of somatic cells into induced Pluripotent Stem cells (iPS) can be achieved by the expression of four transcription factors, OCT4, SOX2, KLF4 and c-MYC (Takahashi and Yamanaka, 2006). Interestingly the early response to expression of the reprogramming factors induces a senescence arrest coupled to the induction of the DDR and the upregulation of senescence markers such as $p16^{INK4a}$, p53 and $p21^{CIP1}$, suggesting senescence is a barrier to efficient iPS reprogramming (Banito et al., 2009; Hong et al., 2009; Li et al., 2009). The theory that the majority of a tumour mass arises from just a few cells termed cancer stem cells (CSCs), with the ability to self-renew and that cancer cells may trans-differentiate to migrate or form tumour-associated vasculature, has highlighted the importance of this senescence barrier in preventing cells attaining unlimited self-renewal properties in a tumour setting (Reya et al., 2001).

Analogous to excessive oncogene activation, loss of tumour suppressor signalling can also activate a senescence response; generally via the unconstrained activation of downstream oncogenes. The PTEN tumour suppressor protein is an inhibitor of PI3K and is mutated in many cancers (Li et al., 1997; Liaw et al., 1997). PTEN null MEFs have a rapid onset of senescence dependent on p53 activation (Chen et al., 2005). Similarly, loss of NF1, a RAS GTPase activating protein (GAP), results in excessive RAS signalling, triggering a negative feedback loop in human fibroblasts activating OIS (Bollag et al., 1996; Cichowski et al., 2003; Courtois-Cox et al., 2006).

1.1.4. Molecular mechanisms regulating senescence

As mentioned previously, the ARF/p53 and the $p16^{INK4a}$/RB1 pathways are central to the induction and maintenance of senescence (Figure 1.4) (Sherr and McCormick, 2002). Disruption of both of these pathways in humans results in extension of replicative lifespan in normal cells (Shay et al., 1991). In mouse embryonic fibroblasts (MEFs) the critical pathways controlling senescence operate via p53,

with Rb1 having a less important regulatory role (Harvey et al., 1993). Inactivation of either p53 or $p19^{ARF}$ results in a bypass of senescence in MEFs, with these cells maintaining a high proliferative potential (Kamijo et al., 1997). A similar proliferative advantage is seen in triple-knockout MEFs where Rb1, p107 and p130 pocket proteins are all inactivated; suggesting that in mice Rb1 function may be compensated by related proteins (Sage et al., 2000). The p53 and RB1 pathways converge under particular cell stresses, the functional outcome of these pathways is the activation of various CDKIs that prevent cell cycle progression, and at high levels result in a permanent growth arrest (Alcorta et al., 1996; Stein et al., 1999).

P53 is activated under a number of different cell stresses, including replicative senescence, OIS, oxidative damage and the addition of cytotoxic drugs (Vousden and Lu, 2002). In response to DNA damage, p53 is phosphorylated by DDR kinases ATM/Chk2 and ATR/Chk1 (Hirao et al., 2000; Liu et al., 2000). When p53 is phosphorylated it cannot be degraded by p53 inhibitor HDM2 (MDM2 in mice), and therefore the half-life of the protein is increased. During replicative senescence, shortened telomeric overhangs, or telomere uncapping is recognised as a DNA single-strand break activating the ATM/Chk2 pathway; in OIS, an initial burst of hyper-replication results in a number of stalled replication forks recognised as double strand breaks by ATR/Chk1 (d'Adda di Fagagna et al., 2003; Di Micco et al., 2006). P53 is also activated when $p14^{ARF}$ ($p19^{Arf}$ in mice) binds and inhibits HDM2. ARF is expressed in response to aberrant oncogenic activation and as well as playing a critical role in the establishment of senescence in murine cells, its overexpression in human fibroblasts also induces senescence in a p53 dependent manner (Wei et al., 2001; Zindy et al., 1998).

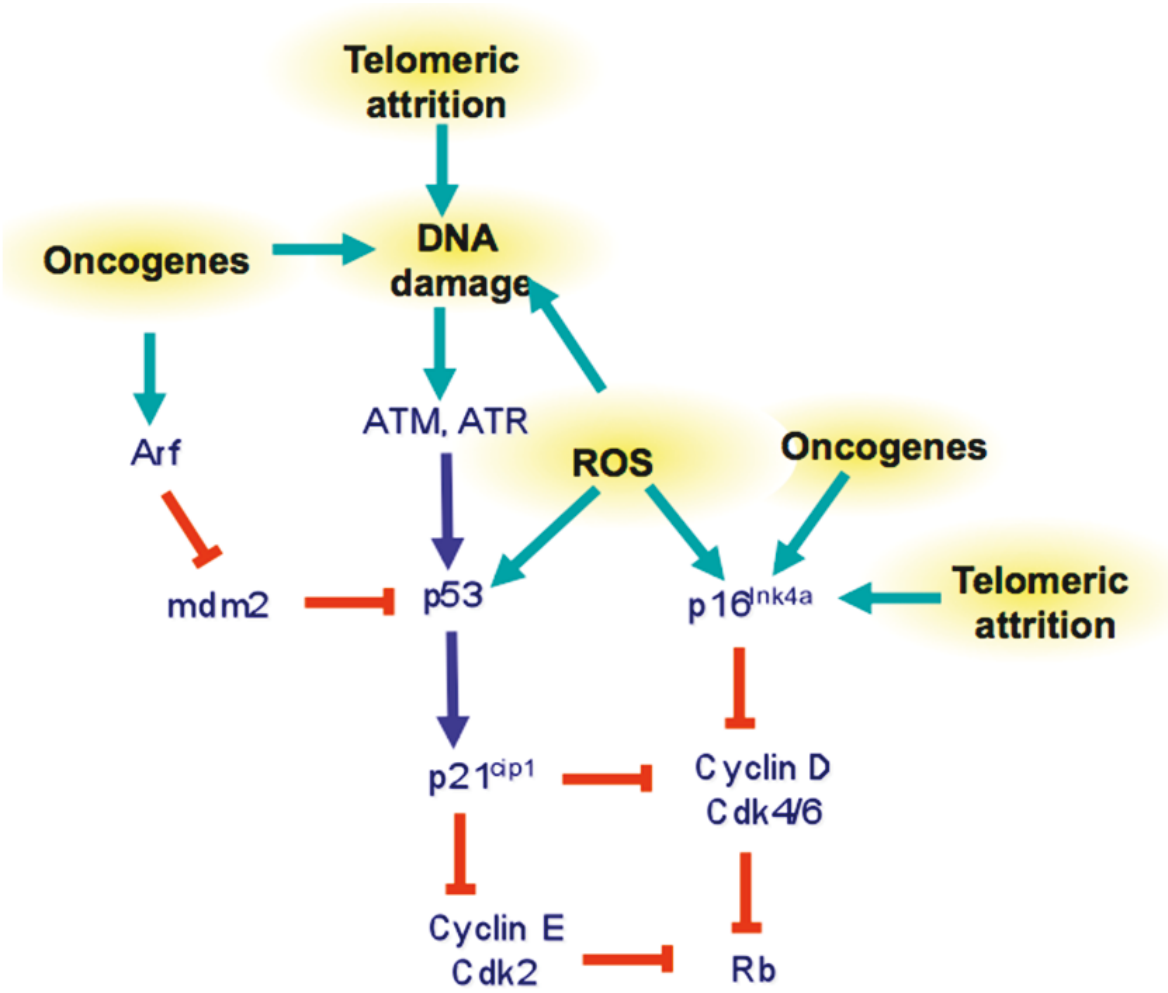


Figure 1.4. Key senescence pathways and effectors. Various stress responses activate senescence all of which converge upon either the ARF/p53 or $p16^{INK4a}$/RB1 pathways. The functional consequence of activation of these pathways is the upregulation of CDKIs, which inhibit cell cycle progression through the activation of RB1, and repression of E2F target genes.

Once activated, p53 is responsible for the transcription of a number of target genes that inhibit cell cycle progression including $p21^{CIP1}$, 14-3-3σ and PAI-1 (el-Deiry et al., 1993; Hermeking et al., 1997; Kortlever et al., 2006). The CDKI $p21^{CIP1}$ prevents the phosphorylation and inactivation of RB1 by binding to and inhibiting the activity of cyclin/CDK complexes.

RB1 is also regulated by a different CDKI, $p16^{INK4a}$. Interestingly $p16^{INK4a}$ is transcribed from the *INK4b-ARF-INK4a* locus, which codes for three important tumour suppressor proteins, $p15^{INK4b}$, ARF and $p16^{INK4a}$ (Gil and Peters, 2006). $P16^{INK4a}$ has a high affinity for CDK4 and CDK6 and prevents their

interaction with cyclins causing a cell cycle arrest (Figure 1.4) (Alcorta et al., 1996; Serrano et al., 1993).

1.1.5. Epigenetic regulation of senescence

Establishment of the irreversible senescent state requires alterations in gene expression and stable changes to chromatin structure, suggesting a role for epigenetic regulators (Rai and Adams, 2012). Chromatin is the template for epigenetic remodelling and facilitates processes such as transcription, DDR, DNA synthesis and mitosis amongst others. Both nucleosomes and DNA can be modified by methylation, acetylation and ubiquitination, and this allows various cellular processes to occur (Kouzarides, 2007).

1.1.5.1. Epigenetic regulation of the *INK4b-ARF-INK4a* locus

When the cell undergoes particular stresses, epigenetic remodelling occurs around the *INK4b-ARF-INK4a* locus to activate gene transcription, a key event in the establishment of senescence (Gil and Peters, 2006; Serrano et al., 1997). Gene expression at the *INK4b-ARF-INK4a* locus is tightly regulated by a number of different transcription factors. This includes v-ets erythroblastosis virus E26 oncogene homologue 2 (ETS2), which positively regulates $p16^{INK4a}$ expression and inhibitor of DNA-binding 1 (ID1), which represses $p16^{INK4a}$ expression (Cummings et al., 2008; Ohtani et al., 2001; Swarbrick et al., 2008).

The ability of transcription factors to bind to the locus during senescence is regulated by additional levels of epigenetic control namely the presence or absence of polycomb complexes (Bracken et al., 2007). In young, unstressed human and mouse cells the *INK4a-ARF* locus is repressed by Polycomb group (PcG) binding and H3 trimethylation at lysine 27 ($H3K27me^3$) (Bracken et al., 2007). Two core polycomb complexes exist, Polycomb repressive complex 2 (PRC2) establishes repressive $H3K27me^3$ marks whereas PRC1 recognises, binds and maintains these repressive marks via histone H2A

monoubiquitination at lysine 119 (H2AK119Ub) (Cao et al., 2002; Czermin et al., 2002; Muller et al., 2002). A number of PcG proteins are thought to have oncogenic properties explained in part by their role in repressing $p16^{INK4a}$ expression. Overexpression of PcG proteins, such as BMI1, CBX7 and CBX8 delays senescence (Dietrich et al., 2007; Gil et al., 2004; Jacobs et al., 1999; Scott et al., 2007).

During senescence, repressive PcG complexes must be evicted from the *INK4b-ARF-INK4a* locus for gene transcription to occur. This is conducted in part by the removal and replacement of PcG proteins with antagonising trithorax (Trx) complexes (Mills, 2010). Trx protein MLL1 is recruited to the *INK4b-ARF-INK4a* locus during OIS and catalyses the methylation of Lysine 4 on H3 ($H3K4me^3$), a mark of transcriptional activation (Kotake et al., 2009). The SWI/SNF complex of nucleosome remodellers also belongs to the Trx family. One of the core components of SWI/SNF, SNF5 mediates polycomb eviction from the *INK4b-ARF-INK4a* locus, thereby restoring $p16^{INK4a}$ expression (Kia et al., 2008). The H3K27 demethylase JMJD3 can also regulate *INK4a/ARF* expression during OIS (Agger et al., 2009; Barradas et al., 2009). JMJD3 is upregulated during OIS and is recruited to the *INK4b-ARF-INK4a* locus. This leads to demethylation of *INK4a/ARF* which counteracts PcG mediated $H3K27me^3$ repression, thereby inducing $p16^{INK4a}$ expression and ARF expression in MEFs (Agger et al., 2009; Barradas et al., 2009).

1.1.5.2. Chromosomal architecture during senescence

Aside from previously mentioned epigenetic characteristics of senescence, such as SAHF formation and telomere uncapping, other forms of nuclear and chromosomal remodelling occur that are important in senescence establishment (O'Sullivan and Karlseder, 2012). A global reorganisation of nucleosome assembly, results in the loss and gains of specific histone variants in the chromatin of senescent cells (Dimauro and David, 2009). For example, the linker histone H1 is replaced by non-histone proteins HMGA1 and HMGA2 on senescent chromatin (Funayama et al., 2006; Narita et al., 2006). Global changes in nucleosome positioning also occurs during senescence. As human

fibroblasts reach replicative senescence the pattern of regularly positioned nucleosomes in young cells is gradually shifted into a more irregular pattern (Ishimi et al., 1987). Human fibroblasts undergoing senescence induced by DNA damaging agents have a large decrease in total H3 and H4 levels, as well as a reduction in H3 biogenesis (O'Sullivan et al., 2010). In ageing budding yeast, H3 loss is also observed and is due to a decrease in H3 Lysine 56 acetylation (H3K56Ac). Yeast which are unable to acetylate H3K56 have a short lifespan and overexpression of H3 or H4 can extend cellular lifespan (Feser et al., 2010).

Nuclear architectural proteins are important in organising chromatin domains and transcriptional regulation (Cremer and Cremer, 2001). Lamins are structural proteins that bind to core histones and are responsible for chromatin positioning within the nucleus. Mutations in the Lamin A gene (*LMNA*) is associated with many disease states, collectively known as laminopathies (Vlcek and Foisner, 2007). The Hutchinson–Gilford progeria syndrome (HGPS) is a disease caused by a single mutation in *LMNA*, resulting in a truncated protein product. HGPS patients suffer from premature ageing resulting in limited growth, accelerated skin wrinkling and tissue degeneration. Fibroblasts from patients with HGPS have deformed nuclear envelope structure, undergo premature senescence and demonstrate a global decreases in repressive histone marks H3K9me^3 and H3K27me^3 (Huang et al., 2008b; Shumaker et al., 2006). In cells lacking Lamin A/C, the half-life of the RB1 protein is dramatically decreased via proteosomal degradation (Johnson et al., 2004). Recently, Lamin B1 has also been linked to senescence, as expression of Lamin B1 decreases during both replicative and OIS (Shimi et al., 2011). Silencing of Lamin B1 triggers premature senescence, and the overexpression of this protein delays senescence in human fibroblasts (Shimi et al., 2011).

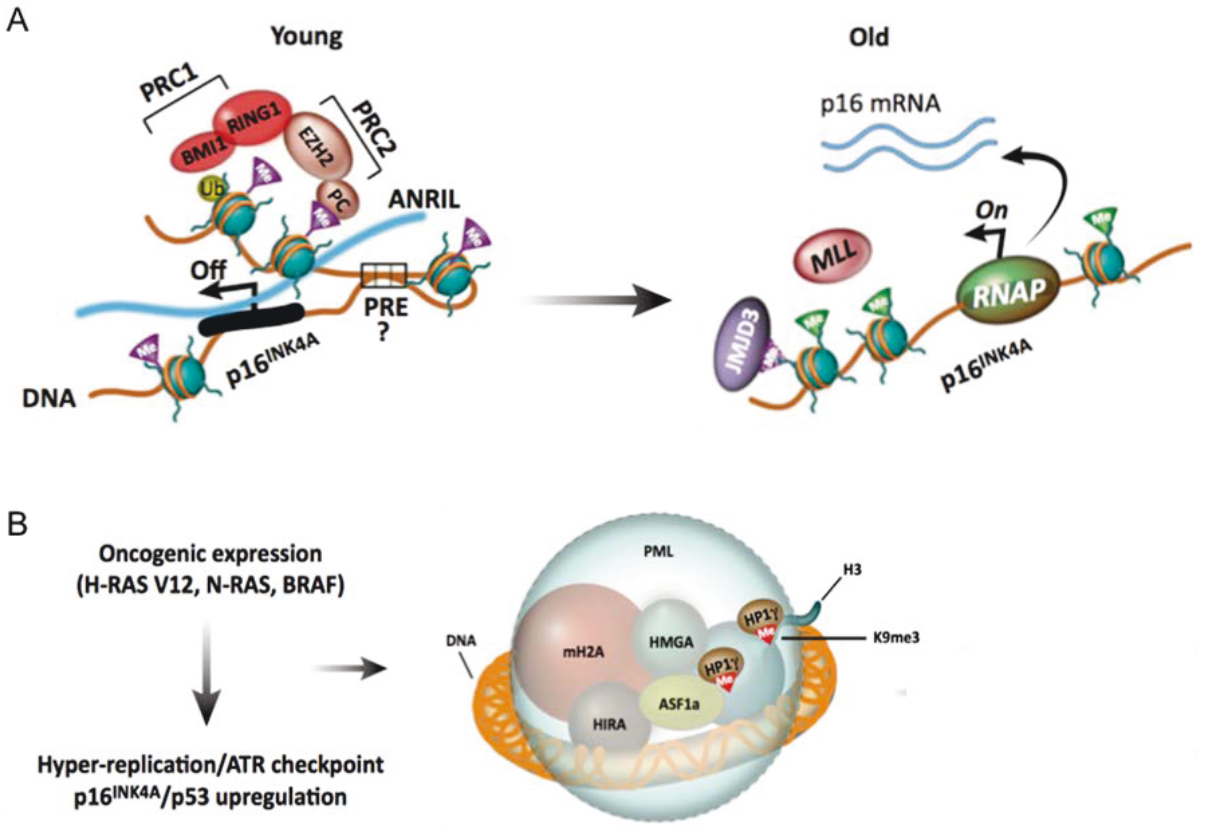


Figure 1.5. Epigenetic regulation of senescence. Various epigenetic mechanisms regulate senescence and ageing including (A) regulation of the *INK4b-ARF-INK4a* locus mediated by Polycomb group proteins, long intergeneic non-coding RNAs and histone demethylases (B) Changes in chromosomal architecture including SAHF formation which involves the establishment of repressive heterochromatic marks orchestrated by histone variants and chromatin remodellers (Adapted from O' Sullivan et al. 2012)

1.1.6. Senescence and ageing *in vivo*

The accumulation of senescent cells with age has led to the belief that senescence is important for the ageing process *in vivo* (Dimri et al., 1995; Paradis et al., 2001; Tacutu et al., 2011). P16^{INK4a} expression is one of the most useful markers of senescence induction *in vitro*. *In vivo* p16^{INK4a} expression increases in skin samples as donor age increases (Krishnamurthy et al., 2004). Recently an elegant study has highlighted the importance of p16^{INK4a} during the ageing process (Baker et al., 2011). In the BubR1 haploinsufficiency mouse model of premature ageing, p16^{INK4a}-positive cells were targeted for apoptosis by being expressed under the same promoter as Caspase-8. Clearance of these p16^{INK4a} positive cells in the mice instigated a number of health benefits which include a delayed onset of cataracts and hunchback and improving fitness levels (Baker et al., 2011). Fewer senescent cells were also found in these mice as identified by reduced SA-β-Gal activity and reduced IL-6

production. Although the healthspan of these mice was greatly improved, no extension of lifespan was seen with the clearance of senescent cells, suggesting $p16^{INK4a}$ independent pathways also contribute to ageing (Baker et al., 2011).

The transcription factor NF-κB, an important mediator of the SASP and oxidative stress and is involved in many age-related pathophysiologies such as atherosclerosis, diabetes and cancer (Adler et al., 2007; Arkan et al., 2005; Cuaz-Perolin et al., 2008; Tilstra et al., 2012) . Adler et al., have used a mouse model to show that when NF-κB is conditionally inhibited in the skin of aged mice the expression profile is more similar to that of younger mice and the skin shows a youthful phenotype including an increase in proliferation and thickness, and a decrease in SA-β-Gal activity and $p16^{INK4A}$ expression (Adler et al., 2007). A different study examined the effect of NF-κB inhibition in mice with XFE progeroid syndrome, a disease of premature ageing resulting from defects in the DDR. In progeroid mice, inhibition of the NF-κB pathway decreased signs of DNA damage and senescence, and alleviated age-related pathologies associated with XFE progeroid syndrome (Tilstra et al., 2012).

Senescent cells secrete a plethora of factors collectively termed the SASP (Kuilman and Peeper, 2009). In the last few years a number of studies have highlighted the importance of the SASP in interacting with the surrounding microenvironment and immune system *in vivo*. In a mouse model, reactivation of silenced p53 expression in tumourigenic liver cells triggers a senescence response, that upregulates the SASP (Xue et al., 2007). SASP upregulation causes clearance of senescent cells via activation and recruitment of the innate immune system (Xue et al., 2007). A different study showed that $NRAS^{G12V}$ expression in liver cells activated senescence and these cells were detected by the adaptive immune system, and cleared by the innate immune system (Kang et al., 2011). The response was mediated by T-lymphocytes that were specific for senescent cells (Kang et al., 2011). Clearance of these senescent cells halted tumourigenesis and mice lacking CD4+ T-lymphocytes

were unable to clear the senescent cells and developed hepatocellular carcinoma (HCC) (Kang et al., 2011).

1.2. Loss-of-function screenings using RNA interference (RNAi)

To identify novel cancer genes, many studies have turned to high throughput technologies to provide a wealth of information with relative ease, and with increasingly reduced costs. Such techniques include whole genome sequencing (WGS), comparative genomic hybridisation (CGH) and SNP analysis to allow mapping of DNA mutations within tumours. Whole-transcriptome RNA-seq and gene expression microarrays have also been used to identify differential expression of genes in cancer samples (Cowin et al., 2010; Lizardi et al., 2011). These studies provide valuable insights into identifying potential tumour-suppressor genes; however they are unable to distinguish commonly found passenger mutations, which do not confer a growth advantage to tumours, from those mutations that are driving tumour formation. The use of RNAi to perform loss-of function screens results in the discovery of candidates with a causal role in the phenotype being studied (Silva et al., 2008; Zender et al., 2008). For these screenings it is pivotal that assay design is optimised to reduce the number of false positive and false negative hits obtained (Hu and Luo, 2012).

RNAi was first used in mammalian cells in 2001 to suppress gene expression (Elbashir et al., 2001). Short double-stranded RNA (dsRNA) fragments are unwound and the sense strand is incorporated into the RISC complex where it binds to complementary mRNAs and causes mRNA transcript degradation (Valencia-Sanchez et al., 2006). Two types of RNAi are successfully used for gene silencing, small interfering RNA (siRNA) are synthetic anti-sense oligonucleotides that are transfected directly into cells, or short hairpin RNA (shRNA) that form a secondary hairpin structure when transcribed from DNA (Echeverri and Perrimon, 2006).

Both strategies have been used successfully to perform loss-of-function screens (Berns et al., 2004; MacKeigan et al., 2005; Meacham et al., 2009). Synthetic siRNAs are easy to produce and in general are very efficient at silencing gene expression. However siRNA libraries are relatively expensive and transfection of these oligonucleotides only produces a transient knockdown, which is unsuitable for long-term assays. SiRNAs are largely used for single-well assays coupled to high-content analysis (HCA) using for example an automated microscope. These assays generally screen for complex phenotypes such as cell morphology, or protein phosphorylation (Neumann et al., 2006; Pepperkok and Ellenberg, 2006). In screenings where long-term gene silencing is required or cells are difficult to transfect, viral vectors are used to stably integrate and express shRNAs within cells (Brummelkamp et al., 2002b). Vector-based shRNA libraries are less expensive then siRNA libraries and may be used indefinitely, however vectors must first be cloned and prepared for transfection, which may be labour intensive depending on the size and complexity of library pools. Vector-based shRNAs are the silencing method of choice for many *in vivo* screens that require stable shRNA expression (Bric et al., 2009; Luo et al., 2009; Wuestefeld et al., 2013).

At present a number of shRNA libraries are available both commercially and through specific laboratories. These include libraries from the Netherlands Cancer Institute (NKI), the Hannon-Elledge lab and from System Biosciences. These libraries vary in the number of shRNAs contained, the genome coverage, the shRNA design and the expression system used (Hu and Luo, 2012). The NKI library uses an RNA Pol III expression system to express hairpins with a 19-base double-strand (ds) stem and a 9-base loop (Bernards et al., 2006). The Hannon-Elledge libraries are designed based on second-generation shRNA libraries that have been developed using an increased knowledge of RNAi. Improvements include silencing triggers that are similar to natural microRNA (miR) and an RNA Pol II promoter, as Pol II promoters transcribe endogenous primary miR transcripts (Bernards et al., 2006; Silva et al., 2005). The hairpins have a 22-base ds stem and a 19-base miR30 loop. Hannon-Elledge

libraries have been cloned into multiple vectors each with particular advantages; these miR30 based shRNA libraries are therefore well suited for pooled shRNA screenings.

1.2.1. Systems for pooled shRNA screenings

Pooled shRNA library screenings have become particularly popular as a relatively inexpensive method to screen large gene sets without the need for high throughput automation. The most common assays conducted using pooled shRNA libraries are those involving the positive selection of shRNAs conferring a cell's enrichment within a population when a particular selection pressure is applied. As shRNA screenings can be extended for long periods of time it allows even shRNAs with a modest phenotypic effect on cells to be selectively enriched during the process.

Different assays have been adapted for these types of screens. Viability assays select for shRNAs which give cells a proliferative advantage to grow under selective pressure (Figure 1.6). In reporter screens, a fluorescent marker can be used to identify shRNAs which affect the expression of constructs. These cells can then be selected from a pool by FACS analysis. Strategies have been adapted to screen for changes in cell morphology, ability to form colonies in soft agar or cells with invasive properties characteristic of epithelial-to-mesenchymal transition (Figure 1.6) (Smolen et al., 2010; Westbrook et al., 2005).

Viral vectors used to infect cells most commonly exist in two types retroviral and lentiviral. Both types of virus efficiently integrate DNA into the cell, however only lentiviral vectors can infect non-dividing cells, and therefore are better suited for screenings using post-mitotic cells or cells that divide very slowly. Hannon-Elledge miR30-shRNA libraries are available as both types; the pSM2 and pSMP based libraries produce retrovirus, whereas the pGIPZ and pTRIPZ libraries produce lentivirus (Hu and Luo, 2012).

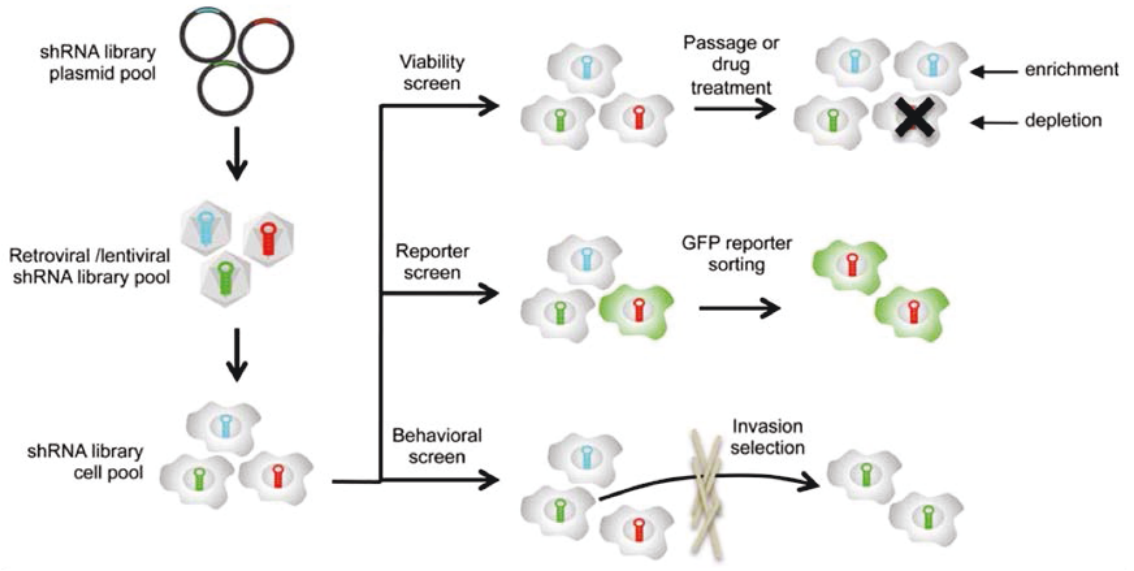


Figure 1.6. Screenings using pooled shRNA libraries. Pooled shRNA library screenings are designed to detect enrichment or depletion of particular shRNAs from amongst a pool of cells, under different selective pressures. (Hu and Luo, 2012)

Vectors where shRNA expression can be tracked are also available. This is particularly useful when studying the progress of a population of infected cells amongst a population of uninfected cells, for example when performing screens *in vivo* (Zender et al., 2008). ShRNA collections also exist such that the shRNA expression is inducible under certain conditions. In these systems the timing of shRNA expression after infection can be controlled by addition or removal of the inducing agent to allow induction and rescue of gene silencing. The diversity of shRNA vectors available broadens the range of possible screenings. As a result shRNA screenings have become a valuable tool in identifying novel candidates in a multitude of cellular pathways and processes.

1.2.2. Genetic screenings to identify novel regulators of senescence

One of the earliest loss-of-function genome-wide screens in mammalian cells was conducted to discover candidate genes able to bypass p53-dependent growth arrest in human fibroblasts (Berns et al., 2004). Through the use of genetic screens, many genes involved in senescence regulation have been identified (Acosta et al., 2008; Brummelkamp et al., 2002c; Gil et al., 2004; Sage et al., 2000). Typically a library of different shRNAs is used to infect cells which are near-senescent. ShRNAs which

can confer a senescence bypass will cause cells to proliferate and become enriched within a pool of cells infected with non-selective shRNAs (Figure 1.7).

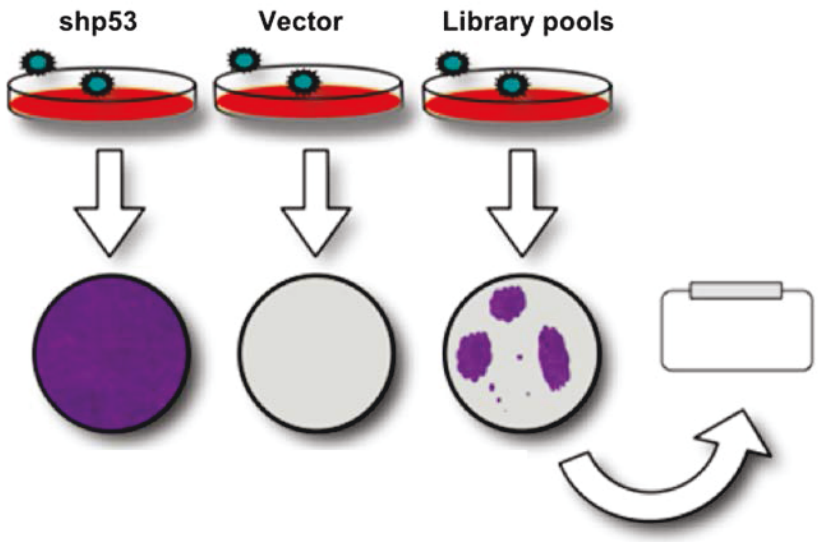


Figure 1.7. Genetic screens for the bypass of replicative senescence. A pooled shRNA library is used to infect near-senescent cells. Cells are passaged until an empty vector control reaches senescence. Cells proliferating in library infected pools are used to identify shRNAs that potentially delay the onset of senescence (Adapted from Acosta et al. 2007).

ShRNAs which cause a bypass of senescence can be recovered from genomic DNA by PCR using primers specific for the vector backbone (Silva et al., 2008). Before the advent of high throughput technology these shRNAs were cloned into an intermediate vector. A limited number of bacterial colonies were picked and sequenced by Sanger capillary sequencing (Figure 1.8). The use of this system has disclosed interesting regulators of senescence. However the process is labour intensive, results in false positives and will only detect shRNAs yielding the strongest phenotypes. High throughput technology provides a faster and more sensitive alternative to methods involving gene cloning. Using these techniques a considerably greater number of candidates can be detected per screen at lower costs and less time than traditional methods.

One alternative method to gene cloning involves using barcode microarrays. In screenings for bypass of replicative senescence, cells must be collected from at-least two time points. The first time-point serves as a reference sample and genomic DNA is taken soon after infection and should contain an

even distribution of hairpins from the library. The second time point is the experimental time-point and is taken at the end of the assay; hairpins causing a bypass in senescence should be enriched in this sample. ShRNAs are amplified similar to previous techniques and samples from different time points are labelled with different fluorescent dyes (Figure 1.8). Labelled shRNA sequences are then mixed together to competitively hybridise to custom made microarrays containing probes that are specific to shRNAs within the library (Schlabach et al., 2008). One advantage of customised microarrays is that they allow detection of positive and negative shRNA selection; however barcoded microarrays are amenable to non-specific cross-probe hybridisation and also variable hybridisation due to the different GC-content of hairpins in the library.

As the cost of next-generation sequencing (NGS) technology has decreased, it has become the method of choice for shRNA screening readout, particularly using illumina Solexa technology (Sims et al., 2011). The shRNA inserts are PCR amplified using primers that incorporate adaptors at the extreme 5' and 3' ends to allow hybridisation to a flow cell (Figure 1.8). At this stage it is also possible to "tag" each sample with an index or a barcode, which usually consists of a unique 3-5 nt sequence within the primer (Meyer and Kircher, 2010). The barcode sequence allows multiple samples to be run on a single flow cell and greatly reduces the cost of sequencing. Once sequenced the indexes can be deconvoluted to assign the reads to each specific sample. After the shRNAs have been amplified and have incorporated adaptors and barcodes, solid support bridge amplification is used to create thousands of amplicons of each hybridised shRNA molecule, generating millions of clusters per flow cell. The clustered template DNA is sequenced using a sequencing-by-synthesis technique utilising reversible terminators and removable fluorophores (Figure 1.8) (Shendure and Ji, 2008).

To assess the feasibility of any screening, it is important to set up assay conditions such that a positive control shRNA is able to produce a good signal-to-noise ratio when diluted in a pool of shRNAs (Birmingham et al., 2009). This will determine the optimal size of the shRNA pools and

optimise other conditions. Background clonal variation is particularly important when a population of cells do not act homogenously during a time period, for example due to selective mutations incurred before or during the screen. These selective mutations or traits may increase the number of false positives detected in the screen, and therefore the timing of the assay must be set to prevent selection of these clones.

Another factor to consider in shRNA screenings are off-target effects caused by shRNAs cross-reacting and silencing genes of near sequence similarity to the intended target (Jackson et al., 2006). Off-target effects will increase the number of false-positive hits, however identifying multiple, independent hairpins targeting the same gene in a screen will increase the confidence that the candidate shRNA is a true positive (Jackson and Linsley, 2010). Libraries comprised of many shRNAs targeting each gene will decrease the number of false negative hits due to ineffective gene silencing of some shRNAs. Both factors may be overcome by analysing common gene set or pathway enrichment within the candidate hits, however this approach is only feasible when conducting large genome-wide shRNA screens. Recent work has begun on the production of validated shRNA libraries, containing shRNAs able to deliver potent and specific gene silencing (Fellmann et al., 2011). These optimised libraries may contain less shRNAs yet result in fewer false positive and false negative hits arising from non-specific or weak gene silencing.

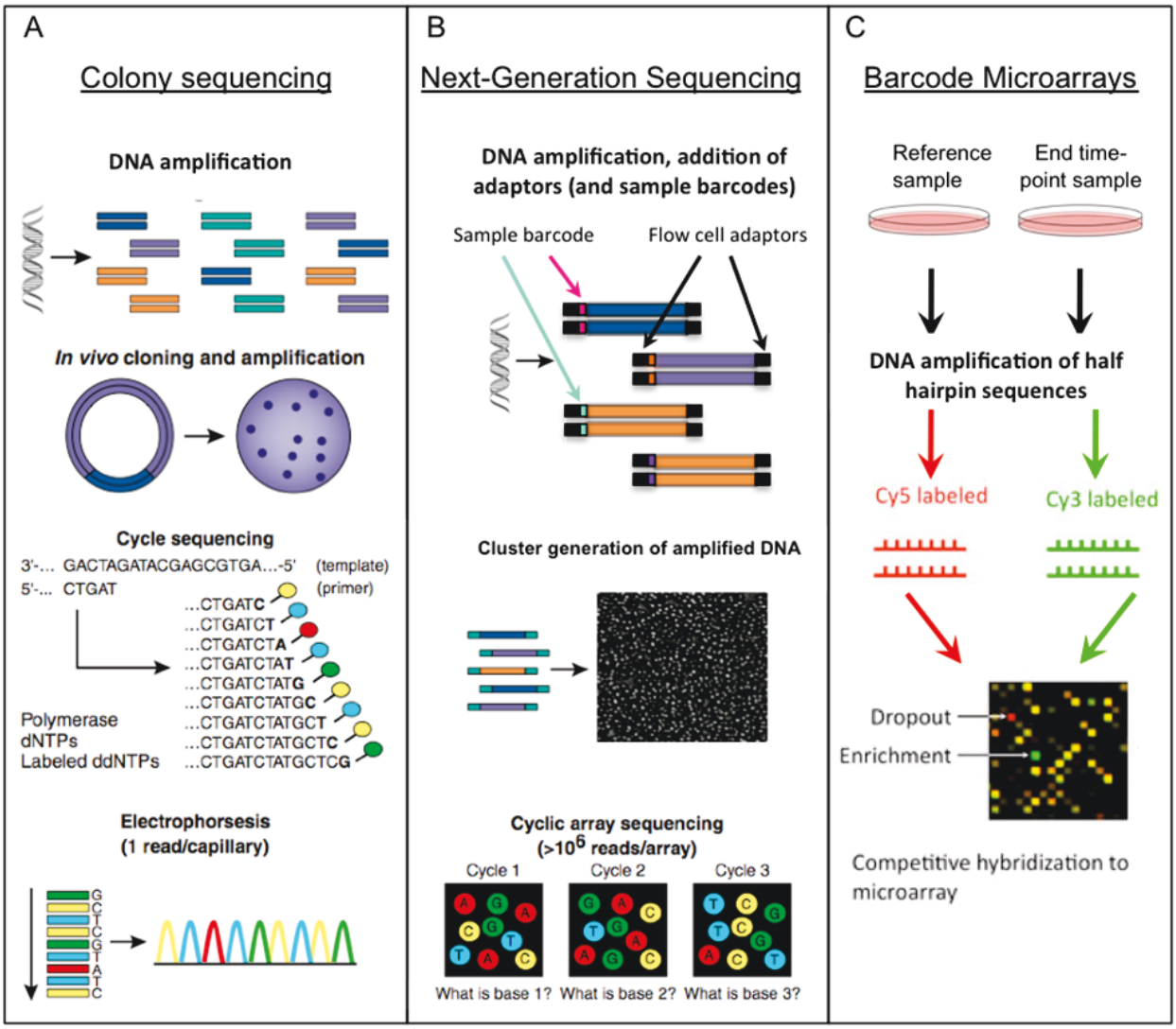


Figure 1.8. Workflow of shRNA recovery using different methods. (A) Sanger sequencing and gene cloning was traditionally used to analyse recovered shRNA fragments. Each shRNA is detected from a single bacterial colony and sequenced as a separate sample. (B) Using Next-generation sequencing, solexa adaptors are incorporated into shRNA sequences during PCR amplification. This allows sequences to hybridise to flow cells and form clusters. Unique barcodes are also incorporated in the PCR primers to allow identification of each sample. Clusters are read by sequencing by synthesis. (C) Barcode microarrays compare the relative levels of shRNA between reference and experimental conditions. The shRNA sequence is amplified and the two time-points are labelled with different colour flourophores. The two samples are then pooled together and hybridise to a custom-made microarray chip containing probes detecting shRNA sequences from the library. ShRNA enrichment and depletion may be detected by measuring the intensity ratio of the two fluorophores at specific probe locations. (Adapted from Shendure and Ji, 2008; Schlabach et al.,2008*)*

Careful statistical analysis is required to select the candidates arising from large-scale screenings and in many cases the top candidates from a screen should be retested in a secondary screen (Birmingham et al., 2009). Retesting candidates often involves including additional RNAi sequences targeting the same gene to discount off-target effects. Candidate shRNAs may also be tested in different cell-types to reduce the possibility of a phenotype being cell-line specific. Finally the genes

may be tested using a different but related phenotypic readout to exclude the possibility that artefacts developed during the primary screen; for example if the primary screen identified regulators of replicative senescence, the candidates can be tested in an OIS system. The possibility of these concerns occurring is greatly reduced by sequencing biological replicates of screenings, which will decrease the number of false positives detected.

1.3. The SWI/SNF complex in senescence and cancer

1.3.1. The SWI/SNF complex of chromatin remodellers

In eukaryotic cells, DNA associates with highly conserved proteins known as histones, to form the basic unit of chromatin, a nucleosome. Each nucleosome consists of 146 base pairs (bp) of DNA wrapped around an octamer of histones H2A, H2B, H3 and H4, with adjacent nucleosomes being connected by DNA and linker histone H1 (Luger et al., 1997; Richmond and Davey, 2003). The abundance of linker histone H1 determines the compaction of DNA such that DNA containing high levels of H1, known as heterochromatin, appears condensed and is relatively inaccessible to transcription machinery and other regulatory factors. In contrast, euchromatin has low levels of H1 and the DNA in these regions is loosely arranged and highly transcribed (Dillon and Festenstein, 2002).

Dynamic chromatin states are regulated by macromolecular complexes such as nucleosome remodellers. These complexes function in two main ways; by using energy from ATP hydrolysis to destabilise DNA-histone interactions, or by covalently modifying histone tails. Both processes result in the mobilisation or eviction of nucleosomes regulating access to DNA. Chromatin-remodelling enzymes are essential for controlling nuclear organisation in multiple cellular processes, including gene expression, DNA replication, DNA repair, development and differentiation. Specifically, the SWItching defective/Sucrose Non-Fermenting (SWI/SNF) family have evolved multiple subunits with various domains to meet the challenges of gene regulation in higher eukaryotes.

1.3.1.1. A multi-subunit complex

Components of the SWI/SNF complex were first discovered in two screenings identifying genes with functions in transcriptional regulation in *Saccharomyces cerevisiae* (Winston and Carlson, 1992). One of the screens identified mutations in genes involved in mating-type switching in yeast. These mutants were unable to express haem oxygenase (HO) an endonuclease required for the switching process and were termed SWI (SWItching defective) (Neigeborn and Carlson, 1984; Stern et al., 1984). The second screen discovered SNF (Sucrose Non-Fermenting) mutants, which could not grow on sucrose because they were unable to express the sucrose hydrolysing enzyme β-fructofuranosidase (*SUC2)* (Carlson et al., 1981). Mutations in *SWI* or *SNF* genes gave rise to pleiotropic defects (Carlson et al., 1981; Stern et al., 1984) suggesting these genes are involved in global transcription regulation in yeast (Guarente, 1987; Nasmyth et al., 1987; Neigeborn and Carlson, 1984).

By the early 1990s numerous reports had found that *Saccharomyces cerevisiae* genes identified from SWI and SNF screenings belonged to the same multi-subunit complex. In addition some of the genes identified in both screenings were in fact identical and were subsequently termed *SWI/SNF* genes (Cairns et al., 1994; Peterson, 1996; Wolffe, 1994). This complex was required for transcriptional enhancement by assisting gene specific regulatory proteins (Laurent et al., 1991; Peterson et al., 1994; Peterson and Herskowitz, 1992). Because *SWI/SNF* genes could alter transcription profiles, these genes were thought to be involved in chromatin regulation. Mutations in *SWI/SNF* genes were suppressed by deletion of either H2A or H2B genes (*hta1, htb1*). Furthermore, nuclease sensitivity assays detected changes in chromatin structure around the *SUC2* promoter, suggesting that the SWI/SNF complex functions by antagonising nucleosome-mediated repression (Hirschhorn et al., 1992). Additional studies found that this nucleosome remodelling was ATP-dependent (Cote et al., 1994; Kwon et al., 1994) and soon after, homologous ATPase complexes were identified in other organisms (Khavari et al., 1993; Tamkun et al., 1992; Wang et al., 1996a).

All ATP-dependent chromatin remodellers exist in large multi-subunit complexes (Vignali et al., 2000). The SWI/SNF complex is highly conserved in eukaryotes and has been purified from a number of organisms including *Arabidopsis*, *Saccharomyces cerevisiae*, *Drosophila*, *Xenopus*, mice and humans (Muchardt and Yaniv, 1999). Mammalian SWI/SNF is thought to be the most complex and diverse owing to its higher molecular mass (>2 MDa) and the fact that it exists in multiple forms (Smith et al., 2003; Wang et al., 1996a).

Essential to SWI/SNF function is the DNA-dependent ATPase activity. In mammalian complexes this activity is executed by one of two mutually exclusive catalytic subunits BRM (Brahma) or BRG1 (Brahma-Related Gene 1), which share 74% amino acid identity in humans (Khavari et al., 1993). A number of subunits bind to either ATPase, and these non-ATPase subunits are known as BRG1/BRM-associated factors (BAFs) which are identified by their molecular size, for example BAF155 has a molecular mass of 155 kDa. Alternatively, SWI/SNF components are sometimes referred to using their official HUGO gene nomenclature as SWI/SNF-related, matrix-associated, actin-dependent regulator of chromatin (SMARCs) these two classification systems are used interchangeably in the literature (Hargreaves and Crabtree, 2011; Ring et al., 1998).

Kingston and co-workers were the first to describe the highly conserved ‘core’ SWI/SNF subunits SNF5 (BAF47), BAF155 and BAF170 (Phelan et al., 1999). These proteins together with either BRG1 or BRM were able to remodel nucleosomes at a level comparable to the entire complex *in vitro* (Phelan et al., 1999). BAF155 and BAF170 are highly homologous (67% identical amino acid sequence) scaffolding proteins and can be present in the complex as homodimers or heterodimers (Chen and Archer, 2005; Ho et al., 2009b). Yeast SNF5 does not possess any DNA binding activity and has not been observed to bind to any specific DNA sequence or motif (Laurent et al., 1990), however SNF5 is thought to enhance the DNA binding activity of the whole complex (Hirschhorn et al., 1992; Peterson et al., 1994).

In vivo chromatin remodelling by SWI/SNF requires further 'accessory' subunits (Sudarsanam et al., 2000; Winston and Carlson, 1992). These subunits stabilise the complex and confer target specificity by interacting with other proteins in response to certain stimuli or developmental cues (Szerlong et al., 2008; Zhao et al., 1998). Purification of SWI/SNF complexes from various cells lines demonstrated that these complexes were highly heterogeneous in composition (Wang et al., 1996a). Two main types of complexes were purified termed the BAF complex and the Polybromo BAF (PBAF) complex (Figure 1.9) (Nie et al., 2000; Wang et al., 1996a). BAF complexes contained either BRG1 or BRM and were associated with one of two AT-Rich Interactive Domain (ARID) containing proteins BAF250A (ARID1A) or BAF250B (ARID1B) (Wang et al., 2004). PBAF complexes only contained BRG1. These complexes also excluded ARID1A/ARID1B however contained a different ARID-subunit, BAF200 (ARID2), as well as a protein with multiple bromodomains, BAF180 (Polybromo-1; PBRM1) giving the name of the complex (Reisman et al., 2009; Xue et al., 2000; Yan et al., 2005).

1.3.1.2. ATP-dependent nucleosome remodelling

SWI/SNF are important regulators of gene expression and various gene profiling studies have shown that mutations in core SWI/SNF components result in changes in gene expression in 1% of human genes, 1-2% of *Drosophila* genes and 5-7% of all yeast genes (Monahan et al., 2008; Ondrusova et al., 2013; Zraly et al., 2006). Nucleosome remodelling is the first and most well studied function of SWI/SNF, however numerous other functions exist largely through interactions with DNA binding proteins and signalling molecules.

Nucleosome positioning varies across the genome, depending on underlying DNA sequences, DNA methylation, nuclear architecture, and promoter/enhancer regions. ATP-dependent chromatin remodelling enzymes are required to mobilise nucleosomes and allow DNA-binding proteins access to chromatin (Clapier and Cairns, 2009). Four families of ATP-dependent chromatin-remodellers exist; SWI/SNF, Imitation SWI (ISWI), NUcleosome Remodelling and Deacetylation/Chromatin Helicase

DNA binding (NuRD/CHD), and INOsitol requiring 80 (INO80) (Wu et al., 2009). These families are categorised depending on which catalytic subunit is utilised as well as unique associated non-catalytic subunits (Clapier and Cairns, 2009). Bromodomains present in BRG1/BRM are unique to SWI/SNF catalytic subunits. Furthermore, SWI/SNF does not require extranucleosomal DNA to remodel nucleosomes, which distinguishes these complexes from the other nucleosome remodellers, ISWI, NuRD/CHD and INO80 which all depend on linker DNA for ATPase activity (Gangaraju and Bartholomew, 2007; Kassabov et al., 2003; Udugama et al., 2011; Whitehouse et al., 1999)

The SWI/SNF family remodel nucleosomes via two main mechanisms. The first mechanism involves disrupting DNA-histone contacts resulting in nucleosome sliding (cis-displacement) and DNA translocation. Alternatively histones can be disassociated with DNA altogether (trans-displacement), resulting in nucleosome transfer to a different DNA molecule (Figure 1.9) (Lorch et al., 1999; Owen-Hughes et al., 1996; Whitehouse et al., 1999).

Nucleosome sliding is achieved in a step-wise process known as the ‘loop-recapture’ model. SWI/SNF binds to either nucleosomes or DNA and histone-DNA contacts are disrupted using energy from ATP hydrolysis (Aoyagi et al., 2002). Loosening of nucleosome-DNA interactions allows DNA to form a loop structure that translocates around the nucleosome in a wave, exposing DNA that was previously bound to histones (Saha et al., 2002).

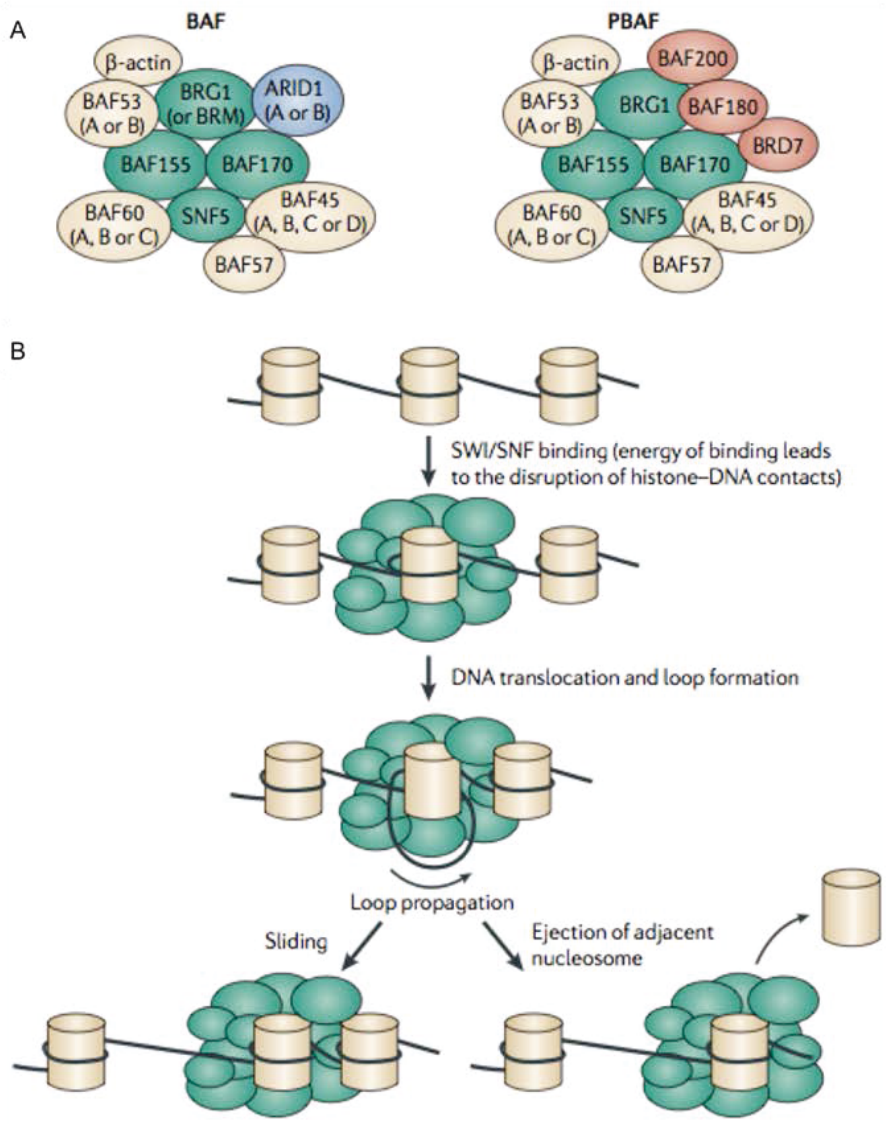


Figure 1.9. The SWI/SNF complex of nucleosome remodellers. (A) Mammalian SWI/SNF is a multi-subunit complex that exists in two main forms the BAF and the PBAF complexes which are defined by targeting subunits that are exclusive to each complex (blue and red components) (B) SWI/SNF disrupt histone-DNA contacts utilising energy coupled to ATP-hydrolysis. Remodelling activity results in the displacement or eviction of nucleosomes (Adapted from Wilson and Roberts, 2011.)

In vitro studies show that SWI/SNF is able to disassemble nucleosomes by rapidly displacing the H2A/H2B dimer, followed by other histones, resulting in nucleosome ejection (Boeger et al., 2003, 2004; Reinke and Horz, 2003). *In vivo* other factors, including histone chaperones, may be required for nucleosome destabilisation. One such histone chaperone Asf1, binds to histones H3 and H4 and assists nucleosome ejection at promoters (Adkins et al., 2004; Adkins et al., 2007; Korber et al., 2006).

1.3.1.3. Regulation of transcription

ATP-independent SWI/SNF function is attributed to the presence of specialised domains within the complex which bind to transcription factors, histone marks and DNA modifying enzymes to regulate gene expression. Although SWI/SNF was initially associated with gene activation, numerous findings have reported that SWI/SNF complexes also repress transcription (Dunaief et al., 1994; Stankunas et al., 2008; Zhan et al., 2011). Various SWI/SNF subunits have been shown to bind to either histone deacetylases (HDACs) or histone acetyl-transferases (HATs) to regulate histone acetylation at target sites (Drost et al., 2010; Zhang et al., 2000; Zhang et al., 2002). Furthermore core SWI/SNF proteins were found to interact with the transcriptional repressor REST and were identified as part of the coREST complex (Battaglioli et al., 2002).

1.3.1.4. Specialised domains and exchangeable isoforms

In 1996 Crabtree and colleagues isolated SWI/SNF complexes from multiple cell lines using an antibody specific to the homologous region of BRG1 and BRM. They discovered many distinct complexes existed and suggested that SWI/SNF is assembled in a combinatorial fashion, beginning with the choice of either BRG1 or BRM as a catalytic subunit (Wang et al., 1996a). Over 10 proteins exist in a single SWI/SNF complex and many subunits are encoded by different isoforms within the same gene family. These isoforms are mutually exclusive such that only one family member will be present in each complex, generating a diverse collection of possible SWI/SNF combinations, each having a particular specificity or function.

Further work from the same group and others identified SWI/SNF complexes that are specific for particular cell lineages. EsBAF is a SWI/SNF complex exclusively found in ES cells that contains BRG1, BAF155 and BAF60a and excludes BRM, BAF170 and BAF60c (Ho et al., 2009b; Kidder et al., 2009). EsBAF is required to maintain pluripotency via interactions with OCT4. Genome-wide mapping of BRG1 in ES cells revealed sites that overlap with OCT4, SOX2 and NANOG occupancy (Ho et al.,

2009a). Intriguingly BRG1 binding correlated with the repressive histone mark H3K27me^3, and expression profiling following BRG1 depletion in ES cells suggests that BRG1 has a mainly repressive function (Rada-Iglesias et al., 2011)

Differentiation of ES cells into different cell lineages requires intermediary cellular states and gene expression changes. These transitions are also regulated by different SWI/SNF complexes. For example, neural progenitors and post-mitotic neurons each contain combinations of SWI/SNF complexes that are specific to either cell type (npBAF and nBAF respectively) (Lessard et al., 2007; Wu et al., 2007; Yoo et al., 2009). In neural progenitors, npBAF is characterised by the inclusion of BAF53a and BAF45a and depletion of these subunits limits self-renewal (Lessard et al., 2007). Upon terminal differentiation BAF45a and BAF53a are substituted by BAF53b and BAF45b and progenitor cells form post-mitotic neurons (Lessard et al., 2007; Wu et al., 2007). In recent years further examples of lineage-specific BAF complexes have been identified including cardiocytes and myocytes that preferentially assemble SWI/SNF complexes containing BAF60c and BAF45c both of which are highly expressed in these tissues (Lei et al., 2012; Lickert et al., 2004; Puri and Mercola, 2012; Willis et al., 2012). Thus combinatorial assembly of SWI/SNF has an important role in cell fate determination, and lineage commitment.

1.3.2. Role of the SWI/SNF complex in senescence and cancer

Aberrant epigenetic regulation is a common feature of cancer cells (Jones and Baylin, 2002). DNA methylation profiling of human tumours has shown that a high frequency of tumour samples contain hypermethylation at CpG island promoters of important senescence regulators such as *CDKN2A* (Gonzalez-Zulueta et al., 1995; Herman et al., 1995; Merlo et al., 1995), *BRCA1* (Esteller et al., 2000), *VHL* (Herman et al., 1994) and *RB1* (Sakai et al., 1991). The high frequency of deletions to the Trx group of proteins (Decristofaro et al., 2001) and overexpression of PcG proteins (Kleer et al., 2003) in cancer supports the notion that different changes in the epigenetic machinery could be important for

tumour progression. Furthermore, SWI/SNF proteins interact with a number of oncogenes and tumour suppressors, to directly affect the function of these proteins (Figure 1.10).

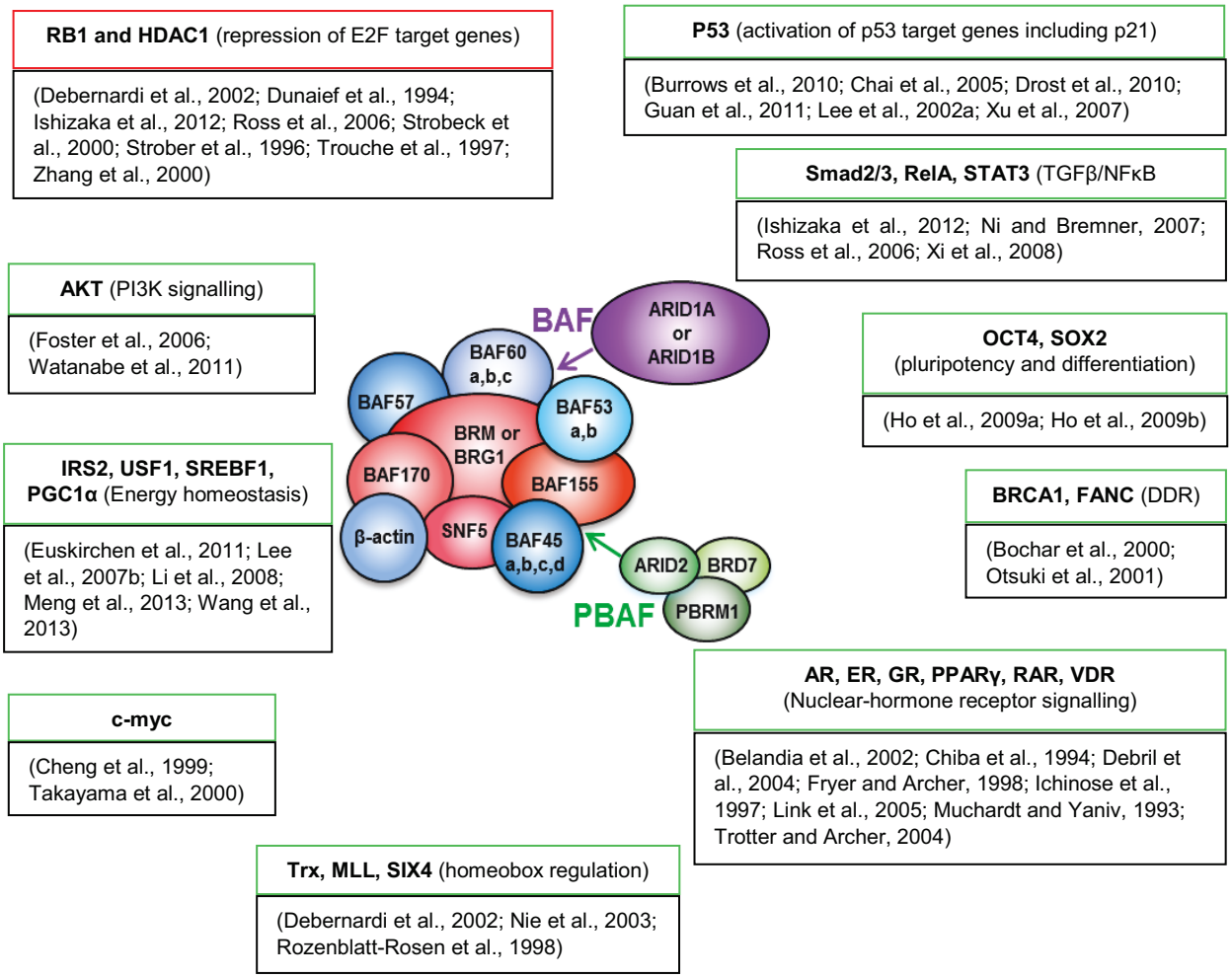


Figure 1.10. The SWI/SNF complex interacts with proteins involved in many cancer-related pathways. SWI/SNF subunits interact with a number of proteins to regulate gene transcription. Many of these proteins are involved in pathways that are frequently de-regulated in cancer.

1.3.2.1. SWI/SNF subunits are frequently mutated in cancer

Over a decade ago, mutations in core SWI/SNF subunit SNF5 were identified in a high frequency of Malignant Rhabdoid Tumours (MRTs) (Versteege et al., 1998). Later, it was shown that another core member of the complex, BRG1 was mutated in multiple cell lines (Wong et al., 2000). The advent of large scale sequencing of cancer genomes has identified mutations in several SWI/SNF complex members (Table 1.1). A study analysing available exome sequencing data sets, has calculated that

19.6% of all cancer samples from exon sequencing studies have mutations in at least one SWI/SNF subunit (Kadoch et al., 2013). Shain and Pollack have also conducted an elaborate study of all the whole-exome sequencing data available to explore the extent of SWI/SNF mutations (Shain and Pollack, 2013). They conclude that deleterious mutations of all SWI/SNF components (19%) approach an overall frequency similar to the highest mutated gene *TP53* (26%) supporting the theory that SWI/SNF proteins are bone fide "Mut-driver genes" (Vogelstein et al., 2013).

Loss of heterozygosity of SNF5 is found in almost all cases of paediatric rhabdoid sarcomas suggesting that SNF5 is a key driver to tumour progression (Biegel et al., 1999; Versteege et al., 1998). These cancers are highly aggressive however tumour cells appear genomically stable, diploid and predominantly devoid of other mutations (McKenna et al., 2008), suggesting that epigenetic alterations may substitute for genomic instability in the progression of MRT (Wilson et al., 2010). SNF5 mutations have also been detected in other tumours at a lower frequency including CML, Hodgkin's lymphoma, paediatric brain tumours (choroid plexus carcinomas) and familial schwannomatosis amongst others (Hulsebos et al., 2007; Kohashi et al., 2009; Kreiger et al., 2009; Modena et al., 2005; Sevenet et al., 1999; Trobaugh-Lotrario et al., 2009; Yuge et al., 2000)

The catalytic subunit BRG1 is the only SWI/SNF subunit that can act alone to remodel nucleosomes *in vitro*, and it is therefore unsurprising that BRG1 is one of the most commonly mutated subunits across all cancers (Table 1.1) (Modena et al., 2005; Shain and Pollack, 2013). Interestingly mutually exclusive catalytic subunit BRM has a much lower mutation rate (0.5% compared to 3% for BRG1) (Shain and Pollack, 2013). Studies have shown that loss of BRG1 or BRM expression occurs in approximately 30% of non-small-cell lung cancer (NSCLC) cell lines, and although a high frequency of these cell lines have BRG1 mutations, none show mutations in BRM (Decristofaro et al., 2001; Glaros et al., 2007; Reisman et al., 2003; Wong et al., 2000). Instead it was revealed that BRM was

epigenetically silenced in cell lines and BRM expression could be restored using histone deacetylase (HDAC) inhibitors (Glaros et al., 2007; Yamamichi et al., 2005).

Mutations in accessory SWI/SNF components are also frequent in cancer, particularly in the 'targeting subunits' ARID1A, ARID1B and PBRM1 (Shain and Pollack, 2013). ARID1A mutations have been observed in approximately 50% of ovarian clear cell carcinoma and 30% of endometrioid carcinomas (Guan et al., 2011; Jones et al., 2010; Wiegand et al., 2010). A similarly high PBRM1 mutation rate (41%) was observed in clear cell renal carcinoma (Varela et al., 2011). ARID1A and ARID1B mutations account for 11% of childhood cancer neuroblastomas and these mutation were associated with early treatment failure and decreased patient survival (Sausen et al., 2013). Various other studies have identified these subunits as driver mutations in breast, colon, pancreatic and hepatocellular cancers amongst others (Table 1.1).

Although alterations in SWI/SNF genes are frequently loss-of-function mutations, a subset of cancers overexpress certain subunits suggesting that SWI/SNF may have an oncogenic role in these cancers. In particular, primary and metastatic melanoma samples have significantly higher BRG1 expression levels than dysplastic naevi (Lin et al., 2010). Furthermore knockdown of BRG1 in melanoma cell lines reduces cell proliferation (Lin et al., 2010). A similar expression pattern is seen in prostate cancer, as the expression of BRG1 increases in malignant and invasive prostate cancer compared to benign lesions, however the opposite was seen for BRM suggesting that elevated levels of BRG1 may be a consequence of BRM loss in these tumours (Sun et al., 2007).

In conclusion, mutations in SWI/SNF subunits are predominantly "tumour-driving" events as opposed to background passenger mutations. This concept is strengthened by the evidence that inactivating mutations in SWI/SNF proteins make up 71% of all SWI/SNF mutations whereas only 41% of mutations in all exome sequenced genes are deleterious (Figure 1.11.) (Shain and Pollack, 2013).

Furthermore, these numbers are probably an underestimation as exome sequencing studies do not consider other subunit inactivation mechanisms including chromosomal rearrangements, DNA methylation, and aberrant post-translational modifications.

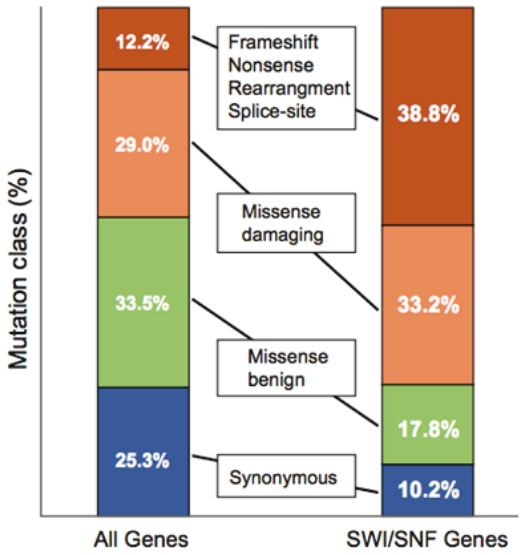


Figure 1.11. Mutations in SWI/SNF genes are predominantly deleterious. Bar-graph representing the distribution of mutation types in SWI/SNF genes (right) compared to all exome-sequenced genes (left) illustrates that mutations in SWI/SNF genes are more commonly inactivating. (Shain and Pollack, 2013)

Sub-complex	Gene symbol	Alias	Domains	Frequent mutations in cancer	Mutation frequency (%)*	References
Core	SMARCA4	BRG1, BAF190a	ATPase (DExx and HELICc), BROMO, HAS, LXCXE, QLQ, Proline, BRK	Hepatocellular, Burkitt lymphoma, pancreatic, lung	3	(Endo et al., 2013; Love et al., 2012; Medina et al., 2008; Reisman et al., 2003; Shain et al., 2012; Wong et al., 2000)
	SMARCA2	BRM, BAF190b	ATPase (DExx and HELICc), BROMO, HAS, LXCXE, QLQ, Proline, BRK, PolyQ	Hepatocellular, pancreatic	0.5	(Endo et al., 2013; Shain et al., 2012)
	SMARCB1	SNF5, BAF47, INI1	SNF5	Rhaboid, schwannomatosis.	0.3	(Biegel et al., 1999; Versteege et al., 1998)
	SMARCC1	BAF170	CHROMO, SWIRM, SANT, Leu-zipper, RSC8		0.4	
	SMARCC2	BAF155	CHROMO, SWIRM, SANT, Leu-zipper		0.6	
BAF	ARID1A	BAF250a, p270, SMARCF1, OSA1	ARID, LXXLL	Hepatocellular, Burkitt lymphoma, endometrial, ovarian, pancreatic, neuroblastoma, DLBCL, esophageal adenocarcinoma, gastric, breast	9	(Biankin et al., 2012; Giulino-Roth et al., 2012; Le Gallo et al., 2012; Love et al., 2012; Sausen et al., 2013; Zhang et al., 2013) (Dulak et al., 2013; Streppel et al., 2013) (Dulak et al., 2013; Fujimoto et al., 2012; Jones et al., 2010; Kandoth et al., 2013; Shain et al., 2012; Stephens et al., 2012; Wang et al., 2011; Wiegand et al., 2010)
	ARID1B	BAF250b, BRIGHT, OSA2	ARID, LXXLL	Hepatocellular, pancreatic, neuroblastoma, DLBCL, breast	2	(Fujimoto et al., 2012; Sausen et al., 2013; Shain et al., 2012; Stephens et al., 2012; Trifonov et al., 2013)
PBAF	ARID2	BAF200, p200	ARID, LXXLL, RFX, Zn finger	Hepatocellular, pancreatic, breast	2	(Biankin et al., 2012; Fujimoto et al., 2012; Li et al., 2011; Stephens et al., 2012)
	BRD7	BP75,	BROMO		0.1	
	PBRM1	BAF180, PB1	BROMO, BAH, HMG, Zn finger	Pancreatic, renal	4	(Numata et al., 2013; Shain et al., 2012; Varela et al., 2011)
Accessory	SMARCE1	BAF57	HMG-box	Spinal meningiomas		(Smith et al., 2013)
	SMARCD1	BAF60B		Breast		(Stephens et al., 2012)

Table 1.2. SWI/SNF mutations occur frequently in human cancers. SWI/SNF sub-complexes contain exclusive components with specialised domains. Many of the SWI/SNF core and targeting subunits found to be significantly mutated in specific cancers are shown from analysing large sequencing studies up to May 2013. *Frequency calculated from Shain and Pollack, 2013 through the analysis of 24 exome sequencing studies until December 2012.

Abbreviations: **DExx**; Asp-Glu-X-X helicase superfamily. **HELICc**; Helicase superfamily c-terminal domain. **BROMO**; Bromodomain. **HSA**; domain in helicases and associated with SANT domains. **BRK**; domain in transcription and CHROMO domain helicases. **CHROMO**; Chromatin organization modifier domain. **SWIRM**; Swi3p, Rsc8p, and Moira domain. **SANT**; ySWI3, yADA2, hNCoR, hTFIIIB binding domains. **RSC8**; RSC chromatin remodeling complex subunit RSC8. **ARID**; AT-Rich Interaction Domain. **RFX**; RFX-DNA-binding domain. **BAH**; Bromo Adjacent Homology domain. **HMG**; High Mobility Group.

1.3.2.2. Relationship between the SWI/SNF complex and senescence

Although the profile of SWI/SNF mutations in cancer has been studied in great depth, mechanisms of tumour suppression are not well defined. The SWI/SNF complex has been associated with the regulation of numerous signalling pathways in cancer (Figure 1.10.) (Wilson and Roberts, 2011). The exact role of SWI/SNF in specific cell types or conditions is difficult to predict because of the diverse number of complexes available. However some patterns of SWI/SNF activity are emerging across cell types, in particular the overlap between SWI/SNF function and activation of senescence pathways.

1.3.2.2.1. SNF5

One of the core subunits of the SWI/SNF complex, SNF5 has been shown modulate senescence via the activation of $p16^{INK4a}$, $p21^{CIP1}$ and $p19^{ARF}$ expression. SNF5 can displace PcG complexes at the *INK4a/ARF* locus (Kia et al., 2008). This displacement of PcG, results in de-repression of the INK4a*/ARF* promoter via loss of the repressive $H3K27me^3$ mark and re-activation of gene expression through recruitment of BRG1 and Pol II (McKenna et al., 2008; Wilson et al., 2010). Similarly in mice expressing $K\text{-}RAS^{G12D}$, SNF5 opposes the action of Polycomb and activates $p19^{ARF}$ expression (Young and Jacks, 2010). As a result Snf5 null mice form tumours from an early onset, with a median age of 11 weeks (Wilson et al., 2010). These tumours have high levels of PcG protein Enhancer of Zeste Homologue 2 (Ezh2), and Ezh2 is essential for tumour formation in these mice; supporting the idea that Snf5 represses PcG activity to prevent tumour formation (Wilson et al., 2010; Young and Jacks, 2010).

In mouse models for conditional bi-allelic inactivation of *Snf5*, heterozygous *Snf5* mice form tumours that are phenotypically similar to human rhabdoid tumors (Isakoff et al., 2005; Tsikitis et al., 2005; Zhang et al., 2002). P53 loss in these mice further accelerates tumour formation suggesting that Snf5 and p53 may co-operate in tumour-suppression (Isakoff et al., 2005). Levels of cyclin D1 are also elevated in tumours formed in this mouse model. When heterozygous Snf5 mice were crossed with cyclin D1 null mice the number of tumours arising during Snf5 inactivation was significantly decreased

compared to parental Snf5 heterozygous mice, suggesting increased cyclin D1 expression is important for the tumour promoting mechanisms in Snf5 null mice (Tsikitis et al., 2005).

Various groups have reported that expression of SNF5 in SNF5-null rhabdoid tumour cell-lines results in a growth arrest defined by a flattened cellular morphology and increase in SA-β-Gal activity (McKenna et al., 2008; Wilson et al., 2010). One proposed mechanism is that SNF5 binds to p53 and BRG1 to activate $p21^{CIP1}$ transcription (Chai et al., 2005; Lee et al., 2002a). In a similar cell line, reintroduction of SNF5 brings HDAC1 to the cyclin D1 promoter and results in transcriptional repression of cyclin D1 (Zhang et al., 2002). Thus, SNF5 is able to bind to the promoters of important cell cycle proteins and regulate transcription through recruitment of transcriptional activators and repressors (Chai et al., 2005; Kuwahara et al., 2010; Lee et al., 2002a; Xu et al., 2010).

1.3.2.2.2. BRG1/BRM

BRG1 was first associated with senescence when it was found to bind to hypo-phosphorylated RB1 and induce cell cycle arrest (Dunaief et al., 1994). Soon after, BRM was also shown to interact with RB1 and both BRG1 and BRM can also interact with other members of the pocket-protein family p107 and p130 (Strober et al., 1996; Trouche et al., 1997). BRG1/BRM contain an LXCXE motif which was initially thought to bind to the pocket domain, an interaction which is disrupted in the presence of viral oncoproteins SV40 T antigen, adenovirus E1 A and HPV16 E7 which bind to the same region of RB1 (Dunaief et al., 1994). Further investigations showed that mutations in the LXCXE domain of BRG1/BRM did not hinder RB1 binding and that neighboring regions were responsible for the observed interaction (Strober et al., 1996; Trouche et al., 1997). In the SW13 cell-line, which does not express BRG1/BRM, overexpression of either BRG1/BRM induces a senescence like arrest, with cells acquiring a flat enlarged morphology and increased SA-β-gal activity (Dunaief et al., 1994; Strober et al., 1996). RB1 is necessary for this arrest as it forms a repressive transcriptional complex through the recruitment of HDAC1 (Trouche et al., 1997; Zhang et al., 2000). This BRG1/BRM-RB1-HDAC

complex represses transcription of E2F target genes such as cyclin E, cyclin A and cdc2 (Trouche et al., 1997; Zhang et al., 2000). HDACs also contain the LXCXE motif, which interacts with the RB1 pocket domain (Siddiqui et al., 2003). A similar transcriptional repressor complex was identified in the livers of old mice but not young ones. BRM is induced in old mice initiating the formation of a C/EBPα-Rb-E2F4-Brm complex (Iakova et al., 2003). This complex represses transcription of E2F regulated genes, including c-myc, in quiescent and regenerating livers of old mice (Iakova et al., 2003). Thus the BRM-Rb complex present in livers of ageing mice, causes a lack of proliferative response and growth arrest in old mice (Iakova et al., 2003).

A study in 2009 identified BRG1 as a binding partner of the important senescence regulator $p16^{INK4a}$ (Becker et al., 2009). A yeast two-hybrid screen using human $p16^{INK4a}$ as bait, captured the C-terminal region of BRG1. Verification of this interaction was performed by co-immunoprecipitating over-expressed MYC-tagged $p16^{INK4a}$ and over-expressed FLAG-tagged BRG1 in U2OS osteosarcoma cells. Visualisation of these tagged proteins expressed in the SW13 adrenocortical carcinoma cell line showed nuclear co-localisation further supporting an interaction (Becker et al., 2009). However no similar reports supporting this interaction with endogenous proteins have emerged. Contrary to other reports the study also claimed that BRG1 was not required for RB1 mediated senescence, and that BRG1 has no role in $p16^{INK4a}$-mediated cell cycle arrest (Becker et al., 2009; Strobeck et al., 2000).

BRG1/BRM can also regulate the p53/$p21^{CIP1}$ pathway. BRG1 has been shown to bind to the $p21^{CIP1}$ promoter and facilitate its transcriptional activation (Giraud et al., 2004; Guan et al., 2011; Kang et al., 2004; Tu et al., 2013). BRG1 can activate $p21^{CIP1}$ expression by binding to Signal Transducer and Activator of Transcription 3 transcription factor (STAT3) (Giraud et al., 2004). The STAT3-BRG1 interaction occurs under specific stimuli, in particular through IL-6 induction (Ni and Bremner, 2007). Interestingly, rapid induction of certain IL-6-responsive genes including *IFITM3 and IFI16* is dependent on BRG1 recruitment to these gene promoters (Ni and Bremner, 2007).

BRG1 has been shown to interact with p53 in a number of different cell lines, although the outcome of this interaction appears to be cell-type specific. In U2OS and Saos-2 cells BRG1 mediates p53 transactivation function and suppresses cell proliferation (Lee et al., 2002a). In MCF7 cells BRG1 is required to activate transcription of a subset of p53 genes (Xu et al., 2007). Similarly in rat mesenchymal stem cells (MSC), ectopic Brg1 expression induces senescence or apoptosis that is dependent on the presence of p53 (Napolitano et al., 2007). Intriguingly the same group observed that in rat MSC, knockdown of BRG1 also induced cell senescence but not apoptosis. This senescence response was coupled to p53 activation measured by an increase in phosphorylated Ser15-p53 and acetylated Lys379-p53 (Alessio et al., 2010). Depletion of BRG1 in HeLa, G401 and RK0 cell lines also showed that BRG1 silencing stabilises p53, and results in an upregulation of p53 target genes (Naidu et al., 2009). In these cell lines BRG1 regulates p53 levels by forming a complex with CREB-binding protein (CBP) that mediates p53 poly-ubiquitination and degradation (Naidu et al., 2009).

1.3.2.2.3. ARID1A/ARID1B

ARID1A and ARID1B are mutually exclusive components of the BAF complex. These proteins are the largest subunits of the SWI/SNF complex and target the complex to DNA through the ARID domain (Kortschak et al., 2000). Initial studies on the role of ARID1A/ARID1B suggested that they have antagonistic roles during differentiation (Nagl et al., 2005; Nagl et al., 2007). Recent evidence from overexpression studies show that both ARID1A and ARID1B control cell proliferation (Guan et al., 2011; Inoue et al., 2011).

Mutations in *ARID1A* occur in a high frequency of ovarian cancers and are mutually exclusive to *TP53* and *RAS* mutations suggesting functional redundancy (Jones et al., 2010; Wiegand et al., 2010). Knockdown of ARID1A in a non-transformed ovarian epithelial cell line enhances the proliferation and tumourigenicity of these cells (Guan et al., 2011). Furthermore, re-introduction of ARID1A in cell lines or tumours with ARID1A knockdown results in a significant reduction in cell and tumour growth (Guan

et al., 2011). Analysis of the mechanism of ARID1A tumour suppression identified ARID1A as a p53 binding partner (Guan et al., 2011). The p53-ARID1A interaction recruited BRG1 and Pol II to the promoters of known p53 target genes such as *CDKN1a* and *SMAD3* and enhanced their transcriptional activation (Guan et al., 2011). Activation of $p21^{CIP1}$ is an important event in ARID1A mediated tumour suppression as $p21^{CIP1}$ knockdown is able to bypass the growth arrest caused by ARID1A overexpression in ovarian epithelial cell lines (Guan et al., 2011).

ARID1A and ARID1B are highly mutated in pancreatic cancer suggesting a tumour suppressive function (Shain et al., 2012). Depletion of either ARID1A/ARID1B with siRNA, results in an increase in proliferation in some pancreatic cancer cell lines (Shain et al., 2012). Gene expression profiling in human pancreatic duct epithelial (HPDE) cells shows Polycomb-related gene sets are significantly enriched following ARID1A/ARID1B knockdown, supporting the idea that SWI/SNF opposes PcG function in tumourigenesis (Shain et al., 2012; Wilson et al., 2010). In contrast, a different study showed that ectopic expression of ARID1B into the MiaPaCa2 pancreatic cancer cell line did not affect cell growth but affected their ability to grow in soft agar (Khursheed et al., 2013).

In HeLa cells, overexpression of ARID1B reduced cell proliferation and a higher percentage of cells were found in the G0/G1 cell cycle phase (Inoue et al., 2011). ARID1B caused an increase in $p21^{CIP1}$, and p53 levels in these cells and depleted c-myc levels (Inoue et al., 2011). ChIP analysis showed ARID1B bound to $p21^{CIP1}$ and c-myc promoters, however association with p53 was not investigated (Inoue et al., 2011). Furthermore, ARID1B depletion promotes cell proliferation in human HCC cell lines, however the mechanism of increased cell growth is unknown (Fujimoto et al., 2012).

1.3.2.2.4. PBRM1/BRD7

BAF180 and BRD7 are components of the PBAF complex with an important role in p53 regulation. A genome-wide shRNA screening in primary BJ fibroblasts identified BRD7 and BAF180 as regulators of

replicative senescence (Burrows et al., 2010). Further investigation showed that depletion of these proteins prevented OIS, and reduced levels of $p21^{CIP1}$ (Burrows et al., 2010; Drost et al., 2010). Over-expression of BRD7 induced premature senescence, coupled to an upregulation of $p21^{CIP1}$ levels (Burrows et al., 2010; Drost et al., 2010). Two reports have identified the interaction between BRD7 and p53 as necessary for transcriptional activation of a subset of p53 target genes, including $p21^{CIP1}$ (Burrows et al., 2010; Drost et al., 2010). BRD7 forms a complex with PBAF-p300-p53 to acetylate target gene promoters and activate gene expression (Drost et al., 2010). ChIP analysis demonstrated that BRD7 also binds to non-p53 target gene promoters during OIS, suggesting BRD7 may also function independently of p53 (Drost et al., 2010). BRD7 overexpression in naso-pharyngeal carcinoma (NPC) causes a G1 cell arrest that is characterised by upregulation of genes involved in the RAS/MEK/ERK and RB1/E2F pathways (Peng et al., 2007; Zhou et al., 2004).

1.3.2.2.5. Role of SWI/SNF in SAHF formation

Senescent cells undergo dramatic changes in chromatin structure and contain SAHFs (Chandra et al., 2012; Narita et al., 2003a; Zhang et al., 2005). The SWI/SNF complex interacts with multiple SAHF components and plays a role in SAHF formation. SAHFs contain HP1 and histone variant macroH2A which assist in the formation of heterochromatic structures (Zhang et al., 2005). It has been shown that BRG1/BRM catalytic activity is required to recruit HP1 proteins to chromatin *in vitro* (Lavigne et al., 2009). BRG1/BRM facilitate access to the HP1 contact site inside of the nucleosome so that HP1 can enter and compete with SWI/SNF for binding, preventing further remodelling (Lavigne et al., 2009). Furthermore the histone chaperone ASF1a, an essential factor in SAHF formation, is a known interactor of BRM (Moshkin et al., 2002; Zhang et al., 2005). It has been proposed, but not proven, that BRM may be required for the incorporation of macroH2A into SAHFs as BRM activity is necessary for the formation of RB1/HP1β foci in senescent melanocytic nevi (Bandyopadhyay et al., 2007).

More recently Zhang and colleagues have described a clear link between BRG1 and SAHF formation (Tu et al., 2013). In this study it was shown that chromatin-associated BRG1 levels increase during OIS, as does the association between BRG1 and RB1 (Tu et al., 2013). Furthermore, knockdown of BRG1 during OIS inhibits SAHF formation and overexpression of BRG1 induced senescence and increased SAHF formation (Tu et al., 2013). BRG1-induced SAHF formation was dependent on its interaction with RB1 (Tu et al., 2013).

Chapter 2. Materials and Methods

2.1. Libraries

2.1.1. HCC deletion library

An shRNA library targeting the mouse orthologues of genes frequently deleted in human HCC (hereafter referred to as HCC library) was obtained from Lars Zender (Zender et al., 2008). The HCC library consists of 624 shRNA constructs divided into 13 pools (Figure 3.1). 1.54 µg from each pool was mixed to create a HCC library super pool for transfections.

2.1.2. pGIPZ genome-wide library

Aliquots of the pGIPZ human genome-wide shRNA library were obtained from Lars Zender. 60,000 shRNA constructs were divided into 60 pools. 1 µL of aliquot from a pool was used to transform one vial of One Shot® Stbl3™ Chemically Competent *E. coli* following manufacturer's recommendations. *E. coli* were mixed with SOC media to a final volume of 500 µL. After incubating for 1 h at 37°C with gentle shaking, 480 µL of the transformation mixture was plated on a 15 cm dish (containing low salt LB Agar with 100 µg/mL Ampicillin and 25 µg/mL Zeocin). The remaining transformation mixture was diluted 1,000 and 10,000 times and plated on 10 cm dishes to determine the number of individual transformants. All dishes were incubated at 37°C overnight. The following day bacterial growth from the 15 cm dish was scraped into 300 mL of low salt LB broth containing 100 µg/mL Ampicillin and 25 µg/mL Zeocin and was grown for 10 h at 30°C (to reduce recombination of viral vectors) with vigorous shaking. Plasmid DNA was purified as described below. The number of colonies arising from the 10 cm dishes were counted and used to calculate the average efficiency of the transformation. Colonies arising from the 10 cm dishes were also analysed by PCR to assess if constructs had recombined. 5 colonies were picked at random and plasmid recombination was assessed by PCR, using primers designed to amplify a region spanning the full length of the hairpin between the two LTRs (primer

sequences are given in Table A8). PCR products were run on an agarose gel to check the size of the amplicon as described below.

2.2. Cell lines and tissue culture methods

All tissue culture reagents were purchased from Invitrogen (Invitrogen Ltd, Paisley, UK), unless otherwise stated. All chemicals were purchased from Sigma (Sigma-Aldrich, Dorset, UK), unless otherwise stated.

IMR-90 human foetal lung fibroblasts and HEK293T packaging cells were obtained from the American Type Culture Collection (ATCC). HEK293T packaging cells expressing retrovirus structural genes (gag-pol and env) were obtained from Takara BIO INC. MEFs were prepared from 13.5-day-old embryos of CD1 mice. The head and viscera were removed and the remaining tissue was minced using scalpels. A single cell suspension was obtained by trypsinisation (0.25% (v/v)) at 37°C for 15 min with periodic mincing. Cells were cultured for 1-2 days until they became confluent and were then frozen in foetal bovine serum (FBS; PAA) containing 10% dimethyl sulfoxide (DMSO) (v/v). IMR-90, HEK293T and MEFs and were cultured in complete medium (Dulbecco's Modified Eagle Medium (DMEM) supplemented with 10% (v/v) FBS and 1% (v/v) antibiotic-antimycotic), and grown in humidity at 37°C with 5% CO2. Inducible ER:RAS cells were prepared from IMR-90 infected with pLNC-ER:RAS, a vector expressing the constitutively active form of RAS (RAS^{G12V}) fused to the ligand-binding domain of the oestrogen receptor (ER). Cells are treated 1 day post seeding with 4OHT (100 nM reconstituted in DMSO) to induce senescence as previously described (Acosta et al., 2008; Barradas et al., 2009).

2.3. Retrovirus production and transduction of target cells

HEK293T cells were seeded the previous day to obtain a confluence of 70-80% for the day of transfection. For each transfection, 1 mL of DMEM was mixed with 20 µg of expression plasmid, 2.5

µg of VSV-g and 75 µL of linear 25 kDa linear polyethylenimine (PEI; 1 mg/mL (w/v), Polysciences). The transfection mixture was incubated at room temperature for approximately 30 min and added drop-wise to each plate of HEK293T. Transfection efficiency was monitored the next day by the presence of GFP (green fluorescent protein) or mCherry fluorescent protein expressed from a reporter plasmid (for a list of plasmids see Table A5). The day after transfection, the media of the transduced packaging cells was replaced (6 mL/plate). On the same day, target cells (MEFs or IMR-90) were plated at a density of 10^6 cells per 10 cm plate.

After 48 h viral supernatants produced by packaging cells were collected and filtered through 0.45 µm pore-sized acetate filters (Anachem) and supplemented with 4 µg/mL of polybrene. The culture media of the target cells was then replaced by the filtered virus-containing supernatant. Infection took place 2-3 times to maximize the transduction efficiency and a period of 3-5 h was left between each round for virus production. The media of the infected cells was replaced with fresh complete medium post infection.

The percentage of infected cells was determined by flow cytometry using reporter plasmids expressing GFP or mCherry and using uninfected cells as a negative control. Two days after infection, cells were split and grown for 5-7 days in the presence of puromycin (0.5 µg/mL) or for 1-2 weeks in 200 µg/mL G418 in order to select for infected cells.

2.4. Lentivirus production and transduction of target cells

HEK293T cells were seeded the previous day to obtain a confluency of 70-80% for the day of transfection. For each transfection, 1 mL of DMEM containing 10 µg of expression plasmid, 10 µg of psPAX2 helper plasmid, 2 µg of VSV-g plasmid and 75 µL of PEI (1 mg/mL) was used (unless otherwise stated) and added to cells as before. The following day media of the transduced packaging cells was replaced (6 mL/plate). In parallel target IMR-90 cells were plated at a density of 10^6 cells

per 10 cm plate for each infection. After 48 h, viral supernatants were collected from packaging cells and filtered through 0.45 µm pore-sized acetate filters. 1.5 mL of supernatant was mixed with 4.5 mL of complete media (to obtain a viral supernatant dilution of 4). Polybrene was added to a final concentration of 4 µg/mL. The culture media of the target cells was replaced with diluted viral supernatant for 5 h. The media of infected cells was replaced with fresh complete medium post infection.

2.5. Generation of custom Solexa libraries

2.5.1. Genomic DNA isolation

Cells infected with the library were collected by trypsinisation and centrifugation. Genomic DNA was extracted from pellets using DNeasy Blood and Tissue Kit (QIAGEN) following manufacturer's instructions. The final elution volume was 50 µL in sterile distilled water. The DNA concentration was determined by measuring the absorbance at 260 nm (A_{260}) using a NanoDrop® ND-1000 UV-Vis spectrophotometer.

2.5.2. Solexa PCR

Duplicate PCR reactions were performed for each sample. 1 µg of extracted DNA was added to 45 µL of PCR SuperMix High Fidelity and 1 µL of each forward and reverse primers (10 µM). Primers are ligated to Solexa adaptors and also contain a 3 nt barcode for assigning sample specificity (Figure 2.2). Blank samples containing no genomic DNA were prepared in parallel for each primer set to assess the presence of contaminants. PCR conditions are as follows: 95°C 10 min, 95°C 30 s, 52°C 45 s, 72°C 60 s. Repeat steps 2-4 34 times. Final incubation 72°C for 10 min. For a list of Solexa PCR primers see Table A7.

2.5.3. DNA purification and quantification

Solexa PCR products were analysed on an agarose gel. DNA loading buffer (Orange G 0.2% (w/v) in 3% glycerol (v/v)) was added to the samples, which were then resolved on a 2.5% agarose (w/v) gel with 0.5 µg/mL ethidium bromide. A one lane gap was left between samples to prevent cross contamination. Samples were separated at 100 V in TAE buffer (40 mM Tris and 1 mM EDTA (pH 8.0) in 0.1% HAc (v/v)). For DNA visualisation, the gel was exposed to UV using the Bio-Rad Gel Doc™ 2000 system. Image analysis was carried out using the Quantity One® (version 4.4.1) software (Bio-Rad). The size of the DNA fragments was estimated by using a 100 bp DNA ladder (New England Biolabs) as a reference. PCR products should be in the range of 115 bp (barcoded) to 117 bp (non-barcoded). The band corresponding to each PCR product was extracted from agarose gels using a clean scalpel. QIAquick Gel Extraction kit (QIAGEN) was used to recover PCR products following manufacturer's instructions. DNA was eluted in 20 µL of sterile distilled water.

Gel extracted DNA was quantified using Qubit® dsDNA HS Assay kit and measured on the Qubit® 2.0 Fluorometer following manufacturer's guidelines. The individual barcoded PCR-products were then pooled in equal quantities to form a Solexa sequencing library.

2.6. Next-generation sequencing

2.6.1. Solexa library quality control

Quality control of the Solexa library involved precise assessment of the Solexa PCR product size and purity using Agilent High Sensitivity DNA Kit and Agilent 2100 Bioanalyser. An aliquot of library was diluted to 100-300 pg/µL and profiles shown in Figure 2.1 were deemed of sufficient purity to run. The amount of amplifiable DNA amenable for clustering on Solexa flowcells was determined after qPCR using Solexa flow cell primers. QPCRs were performed by CSC genomic lab staff.

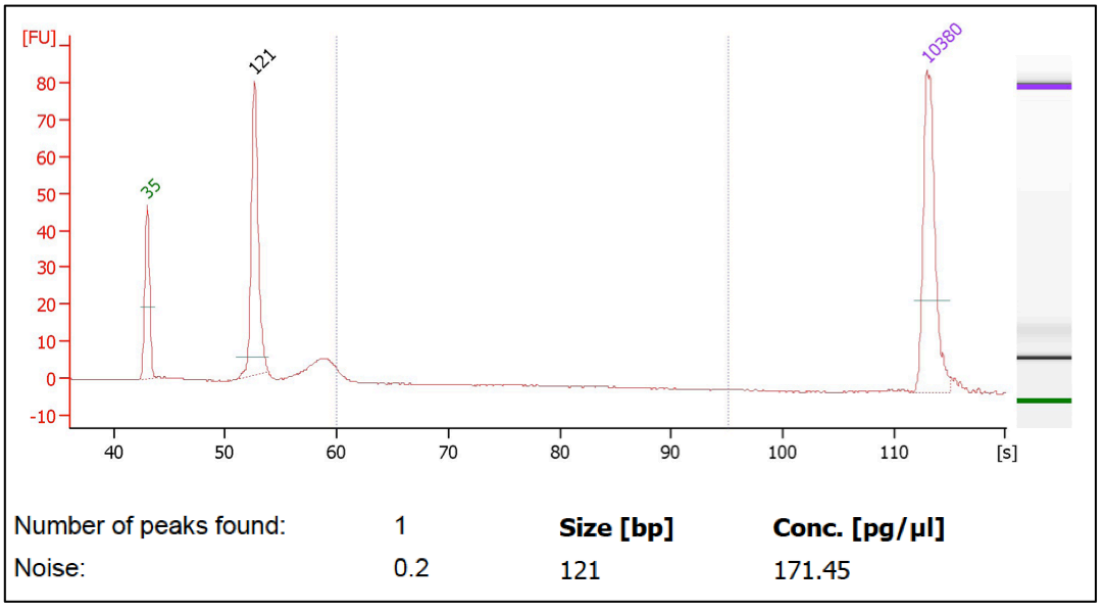


Figure 2.1. Bioanalyser profile of acceptable custom Solexa library for NGS. Diluted Solexa libraries were run on the Agilent 2100 Bioanalyser using the Agilent High Sensitivity DNA Kit. A profile deemed of suitable purity to use for HTS should contain a single dominant peak in the range of 117-125 bp.

2.6.2. High-throughput sequencing

6 pM of the Solexa library was used to create clusters by bridge amplification on a single lane of a Solexa flowcell and sequenced on the Genome Analyser IIx (GAIIx) at either the Helmholtz Centre for Infection Research (HZI) or the CSC Genomics Laboratory, Clinical Sciences Centre (CSC). The miR30 sequencing primer used was HPLC purified and reconstituted in sterile distilled water (for a list of sequencing primers see Table A8).

2.6.3. Bioinformatics

FASTA files produced from the sequencing runs were processed by Adam Geiss using RTA version 1.8.70.0, with default filter and quality settings against a PhiX control lane. Sequences were first de-multiplexed with CASAVA 1.7 to allow 'binning' of samples by barcode bases 35-37. The reverse complement of each read was aligned to the custom HCC or pGIPZ libraries using the ELAND extended implementation of CASAVA 1.7. Bases 3-19 of each read were used, reporting exact matches only (Figure 2.2). Hairpin sequence proportions were calculated for samples and ranked

using a Fisher's combined p-value by Tom Carroll using R (v2.13.0). The Fisher's combined test allows p-values across independent data sets to be combined (Fisher, 1925).

ers

::

AAACTGTTTGGTAAATAGTGAAGCCACAGATGTATTTACCAAACAGTTTCGAGCTGTGCCTACTGCCTCGGAattcaagggctactttag
TTTGACAAACCAATTTATCACTTCGGTGTCTACATAAATGGTTTGTCAAAGCTCGACACGGATGACGGAGCCTtaagttccccgatgaaatc

'-GAAGCTCGAAACTGTTTGGTAAATAGTGAAGCCACAGATGTATTTACCAAACAGTTTCGAGCTGTGCCTACTGCCTCGGAattcaagggg
←gttcccc

'CAGAAGACGGCATACGAxxxAAGCCACAGATGTA→
TTTGACAAACCAATTTATCACTTCGGTGTCTACATAAATGGTTTGTCAAAGCTCGACACGGATGACGGAGCCTtaagttccccgatgaaatc

'-GAAGCTCGAAACTGTTTGGTAAATAGTGAAGCCACAGATGTATTTACCAAACAGTTTCGAGCTGTGCCTACTGCCTCGGAattcaagggg
AAATGGTTTGTCAAAGCTCGACACGGATGACGGAGCCTtaagttccccc

CAGAAGACGGCATACGAxxxAAGCCACAGATGTATTTACCAAACAGTTTCGAGCTGTGCCTACTGCCTCGGAatt
TTTGACAAACCAATTTATCACTTCGGTGTCTACATAAATGGTTTGTCAAAGCTCGACACGGATGACGGAGCCTtaagttccccgatgaaatc

CACAGATGTATTTACCAAACAGTTTCGAGCTGTGCCTACTGCCTCGGAattcaagggctactttagTCGGTGGTCGCCGTATCATT
GTGTCTACATAAATGGTTTGTCAAAGCTCGACACGGATGACGGAGCCTtaagttccccgatgaaatcAGCCACCAGCGGCATAGTAA

CACAGATGTATTTACCAAACAGTTTCGAGCTGTGCCTACTGCCTCGGAattcaagggctactttagTCGGTGGTCGCCGTATCATT

Figure 2.2. Solexa sequencing schematic. Design of Solexa library samples for sequencing on a 39 bp run.

2.7. Growth assays

2.7.1. Growth curves and colony formation assays

For growth curves 5×10^5 (IMR-90) or 10^6 (MEFs) cells were seeded per 10 cm plates in duplicate. Cell number was estimated every 5-7 days (IMR-90) or 3-4 days (MEFs) until the empty vector (control) reached senescence. Cells were trypsinised and resuspended in 3-12 mL of complete media. 50 µL of

resuspended cells was diluted in 150 µL of Guava® ViaCount® reagent (Millipore) and applied to the Guava microcapillary flow cytometry system (Millipore). Debris and non-viable cells were gated to be excluded from the final cell count and cell numbers were quantified using Guava® ViaCount® assay software (Millipore).

Short-term growth curves were conducted by plating 500-1000 cells per 96-well dish in triplicate. Cells were washed with PBS once and fixed for 20 min with 4% paraformaldehyde (PFA, (w/v)) every 2 days. Cells were stained with 1 µM 4',6-diamidino-2-phenylindole (DAPI) for 10 min and fluorescent images of stained cells were acquired using the IN Cell Analyzer 1000 automated high-throughput microscope (GE Healthcare). Image processing and quantification of nuclei was performed using the IN Cell Investigator (v1.7) software (GE Healthcare) (see High Content Analysis). Growth curves were normalised relative to the average number of cells in the 'day 0' sample fixed one day post plating.

For colony formation assays cells were plated at a low density of either 5×10^4 or 10^5 in 10 cm plates and between 10^4 - $2x10^5$ per 6-well dish. Cells were washed with PBS and fixed with 0.5% glutaraldehyde (w/v) in PBS for 10 min. Cells were washed twice with distilled water and all plates were stained simultaneously with 0.2% crystal violet (w/v). Crystal violet was extracted with 10% acetic acid (v/v) and the absorbance at 595 nm (A_{595}) was measured using the Bio-Rad 680XR microplate reader. Absorbance values were used to quantify relative cell growth and were plotted normalised to cells transduced with an empty vector.

2.7.2. BrdU (5-Bromo-2'-deoxyuridine) incorporation assay

Cells ($1\text{-}4x10^3$) were plated in 96-well plates in duplicate and allowed to adhere overnight. The following day, cells were incubated with 5-Bromo-2′-deoxyuridine (BrdU, 50 µM) for 16-20 h. After incubation, cells were washed with PBS and fixed for 20 min with 4% PFA (w/v). For immunofluorescence staining, cells were first permeabilised for 10 min with 0.25% (v/v) Triton X-100 in

PBS and incubated for 1 h with blocking solution (0.5% (w/v) BSA, 0.2% (w/v) fish skin gelatine). Treatment with DNase I (0.5 U/μL) in presence of 1 mM $MgCl_2$ was performed simultaneously with Alexa Fluor® 488 mouse anti-BrdU antibody (1:100, Invitrogen) and incubated for 30 min at room temperature. Cells were washed three times with PBS and incubated with 1 μM DAPI for 10 min. Plates were examined using the IN Cell Analyzer 1000 automated high-throughput microscope (GE Healthcare) with a 10x objective. High Content Analysis (HCA) was used to quantify the proportion of BrdU positive nuclei. Image processing was performed using the IN Cell Investigator (v1.7) software (GE Healthcare) (see High Content Analysis).

2.7.3. Senescence-associated β-galactosidase (SA-β-gal) assay

2.7.3.1. Cytochemical staining

10^3 - $6x10^4$ cells were plated per 6-well dish and 2-7 days later cells were washed once with PBS and fixed with 0.5% glutaraldehyde (w/v) for 5 min. Fixed cells were washed twice with 1 mM $MgCl_2$ in PBS (pH 6.0) and then incubated with X-Gal staining solution (1 mg/mL X-Gal (Promega), 5 mM $K_3[Fe(CN)_6]$ and 5 mM $K_4[Fe(CN)_6]$ in 1 mM $MgCl_2$/PBS (pH 6.0)) for 8–24 h, after which the cells were washed with water and stored at 4 °C, in the dark. Bright field (BF) colour images were taken using the Olympus CKX41 inverted fluorescence microscope, supplied with a DP20 digital camera. The percentage of SA-β-Gal-positive cells was determined by counting at least 150 cells.

2.7.3.2. Fluorescence visualisation

SA-β-gal activity was detected as described in Debacq-Chainiaux et al., 2009. $4x10^3$ cells were plated per 96-well dish in duplicate wells. 2 days later cells were incubated with fresh complete medium containing C_{12}FDG (33 μM) and incubated for 2 h. Following incubation cells were washed twice with PBS and were fixed for 20 min with 4% PFA (w/v). Fixative was removed by washing twice with PBS

and cells were stained with 1 µM DAPI for 10 min. Fluorescence was visualised using the IN Cell Analyzer 1000 automated high-throughput microscope (GE Healthcare). Image processing and quantification of nuclei was performed using the IN Cell Investigator (v1.7) software (GE Healthcare) (see High Content Analysis). At least 500 cells were counted per replicate.

2.8. Generation of shRNA expressing retroviral vectors

2.8.1. shRNA constructs

Retroviral plasmids for knockdown of human and mouse genes were constructed by sub-cloning oligonucleotides into pRetroSuper (pRS), as previously described (Brummelkamp et al., 2002a). Oligonucleotides were designed using the BIOPREDsi (www.biopredsi.org) or DSIR (http://biodev.extra.cea.fr/DSIR/DSIR.html) algorithms to computationally predict shRNA target sequences with an optimal knockdown effect. A minimum of three independent shRNA constructs were designed and tested for each gene. The forward and reverse strands of the oligonucleotides were annealed in shRNA annealing buffer (100 mM NaCl and 50 mM HEPES, pH 7.4). The oligonucleotides were then incubated for 4 min at 90 °C, then for 10 min at 70 °C and slowly cooled to 10 °C or room temperature. The annealed oligos were cloned between the unique BglII and HindIII enzyme sites of the pRS vector using T4 DNA ligase (New England Biolabs). One Shot® TOP10 competent cells were transformed and plated on LB agar plates following manufacturer's guidelines. The presence of positive clones was verified by colony PCR, using primers spanning the full hairpin region (for a full list of shRNA target sequences see Table A6). The PCR products were resolved on a 2.5% agarose (w/v) gel (see Agarose gel electrophoresis). Positive colonies were grown in 300 mL of LB medium containing 100 µg/mL Ampicillin for 12–16 h at 37 °C, with vigorous shaking.

2.8.2. Plasmid DNA purification

Bacterial cell cultures were pelleted by centrifugation at 6000 × g for 15 min at 4 °C. Large-scale plasmid DNA preparation was carried out using the HiSpeed® Plasmid Purification kit (QIAGEN)

following manufacturer's guidelines. DNA was eluted with 1 mL sterile distilled water. The concentration was determined by measuring the absorbance at 260 nm (A_{260}) in a NanoDrop® ND-1000 UV-Vis spectrophotometer. The DNA was stored at –20 °C for future applications.

2.8.3. Agarose gel electrophoresis and DNA purification

Restriction enzyme-digested DNA and PCR products were analysed by their electrophoretic mobility on an agarose gel. DNA loading buffer (Orange G 0.2% (w/v) in 3% glycerol (v/v)) was added to the samples, which were then resolved on a 1–2.5% agarose (w/v) gel with 0.5 µg/mL ethidium bromide. Samples were separated at 100 V for 30–60 min in TAE buffer (40 mM Tris and 1 mM EDTA (pH 8.0) in 0.1% HAc (v/v)). DNA bands were visualised as before.

The QIAquick Gel Extraction kit (QIAGEN) was used to extract and purify DNA (70 bp–10 kb) from agarose. The DNA fragment was excised from the agarose gel using a clean scalpel and DNA was purified following manufacturer's instructions. DNA was eluted in 30–50 µL sterile distilled water.

2.8.4. DNA sequencing

For each sequencing reaction 600 ng of plasmid DNA was added to distilled water to make a final volume of 9.6 µL. 0.4 µL of either forward or reverse primer (10 µM) was added to give a final volume of 10 µL. DNA sequencing was carried out at the CSC Genomics Laboratory using an automated ABI3730xl DNA analyser (Applied Biosystems). Sequences were viewed using 4Peaks (version 1.7) and Serial cloner (version 2.6) software (a list of sequencing primers is shown in Table A8).

2.9. RNA expression analysis

2.9.1. Total RNA purification

Total RNA was extracted using the RNeasy mini kit (QIAGEN). Cells were plated at a density of $3x10^5$-$5x10^5$ cells per 6 or 10 cm dish and washed with ice cold PBS two days later. All samples were

collected in parallel. 350-600 µL of buffer RLT (cell lysis buffer) was added directly to the plate and cell lysate was collected using a cell scraper and applied onto a QIAshredder spin column placed on ice. All other steps were performed at RT following manufacturer's guidelines. RNA was eluted in 30–50 µL RNase-free water into RNase-free tubes. The concentration was determined by measuring the absorbance at 260 nm (A_{260}) using a NanoDrop® ND-1000 UV-Vis spectrophotometer. The RNA was stored at –80 °C for future applications.

2.9.2. Gene expression profiling

2.9.2.1. RNA Quality Control

Purity and integrity of RNA samples were assessed before microarray analysis. RNA integrity and size representation was validated by RT-PCR primed by oligo(dT)18. 1 µg of RNA was used to generate cDNA using iScript™ cDNA Synthesis Kit (BioRad) following manufacturer's instructions. A 1.1Kb product was amplified from cDNA by PCR using primers spanning the full-length *LUMICAN* transcript (for a list of cDNA primers see Table A10). PCR products were run on a gel to check amplicon size and quantity as described previously. RNA quality was also assessed using the Agilent 2100 Bioanalyser and Agilent RNA 6000 Nano kit, following manufacture's guidelines. 28s/18s rRNA ratio should be approximately 2.0 An RIN (RNA integrity number) score of above 7 indicates high quality RNA extraction (Figure 2.3).

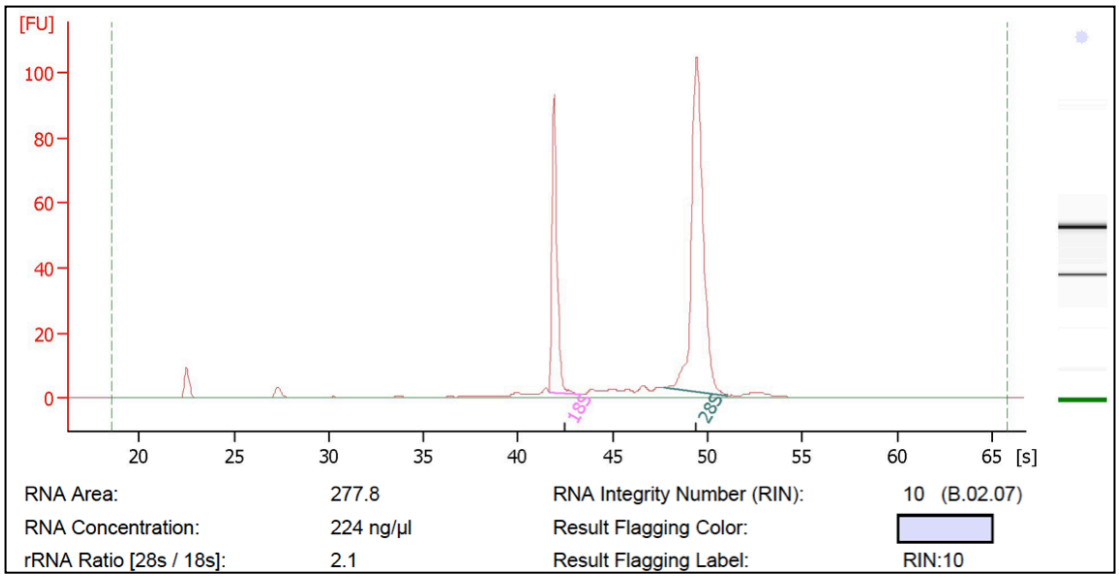


Figure 2.3. Bioanalyser profile of acceptable RNA extraction for gene expression profiling. Profile of RNA obtained showing intact and pure RNA with a maximum RIN score of 10. 18S and 28S rRNA peaks are prominent with a relatively flat baseline before, in-between and after the two peaks.

2.9.2.2. Microarray analysis

For microarray experiments, cRNA was hybridized to Human Gene 1.0 ST arrays (Affymetrix) following manufacturer's instructions. Three biological replicates were performed for each condition. Microarray data processing and analysis was carried out at EMBL-GeneCore (Heidelberg, Germany). Microarray data was normalised using Robust Multichip Average (RMA) and differentially expressed genes were identified using Linear Models for Microarray data (LIMMA). A cutoff of a Benjamini-Hochberg (BH) false discovery rate <0.05 was used to identify significant genes. All analyses were carried out in R (v2.13.0).

2.9.3. Quantitative RT-PCR (RT-qPCR) Analysis

1 µg of RNA was used to generate cDNA using iScript™ cDNA Synthesis Kit (BioRad) following manufacturer's instructions. RT-qPCR reactions were performed on the CFX96™ Real-Time PCR Detection System (BioRad) Using SYBR Green PCR Master Mix (Applied Biosystems). Gene expression data was normalised to β-glucuronidase (GUS-B) (a list of RT-qPCR primers used is given in Table A9).

2.10. Protein expression analysis

2.10.1. Immunofluorescence

For immunofluorescence, cells were fixed with 4% PFA (*w*/*v*) for 30 min, washed with PBS and permeabilised with 0.25% Triton X-100 (v/v) for 10 min. To block unspecific binding of primary antibody, cells were incubated for 1 h in blocking solution (0.5% BSA (w/v) and 0.2% fish skin gelatin (v/v) in PBS). The cells were then incubated with the primary antibody, diluted in blocking buffer, for 1

h at room temperature. Fixed cells were washed three times with PBS (5 min per wash, with agitation) to remove unbound primary antibody and were subsequently incubated with the secondary antibody, diluted in blocking buffer, for 1 h at room temperature. Cells were washed with PBS three times before adding 1 μM DAPI for 10 min for nuclear staining. Stained samples were stored at 4°C in the dark until further use (a list of antibodies used is given in Table A11).

2.10.1.1. High throughput microscopy (HTM)

Immunofluorescence was performed using the IN Cell Analyzer 1000 or 2000 automated high-throughput microscope (GE Healthcare) with 10x, 20x or 40x objectives. Two or three (where double staining is used) fluorescence images were acquired for each field, and fields were distributed randomly within each well. A minimum of 500 cells were acquired for each sample per replicate.

2.10.1.2. High content analysis (HCA).

High content analysis (HCA) was conducted using IN Cell Investigator (v1.7) software (GE Healthcare) as described in Banito et al. 2009, DAPI staining of the nuclei was used to identify cells. The nuclei were segmented using top-hat segmentation, specifying a minimum nucleus area of 100 μm^2. To define the cell area, a collar segmentation approach was used with a border of 1 μm around DAPI staining. The cellular expression of the analysed protein was determined by measuring the average intensity of pixels detected in the reference channel wavelength within the specified nuclear region (Object Nuclear Intensity).

Each cell was assigned a nuclear intensity value (and cell intensity value when applicable) for the specific protein being studied. A histogram of the nuclear intensity values of the cells in a sample was produced and this was used to set a threshold filter to determine positive and negative expressing cells (Figure 2.4A). The cut-off for the filter was selected by establishing the negative population on the histogram, for example for ARID1B expression - using shARID1B-infected cells (mostly red

population on the histogram), and the positive population on the histogram, high ARID1B expression in empty vector infected cells (mostly green population on the histogram) (Figure 2.4A). Once the cut-off filter was established all sample images were analysed using the same filter. Each cell was classified as either positive (pos) or negative (neg) for the expression of the analysed protein (Figure 2.4B) and percentage of both cell populations (positive and negative) was generated per well. The mean of the nuclear intensity was also routinely analysed and equivalent results were obtained.

The antibodies used for the analysis were validated with robust controls (shRNAs and/or overexpression) to test their specificity. Where possible, alternative antibodies were tested in control experiments to confirm the results obtained. Statistical analysis of IF data was conducted using GraphPad software Prism® (version 6.0b). Unpaired t-test using Welch's correction was used to calculate p-values.

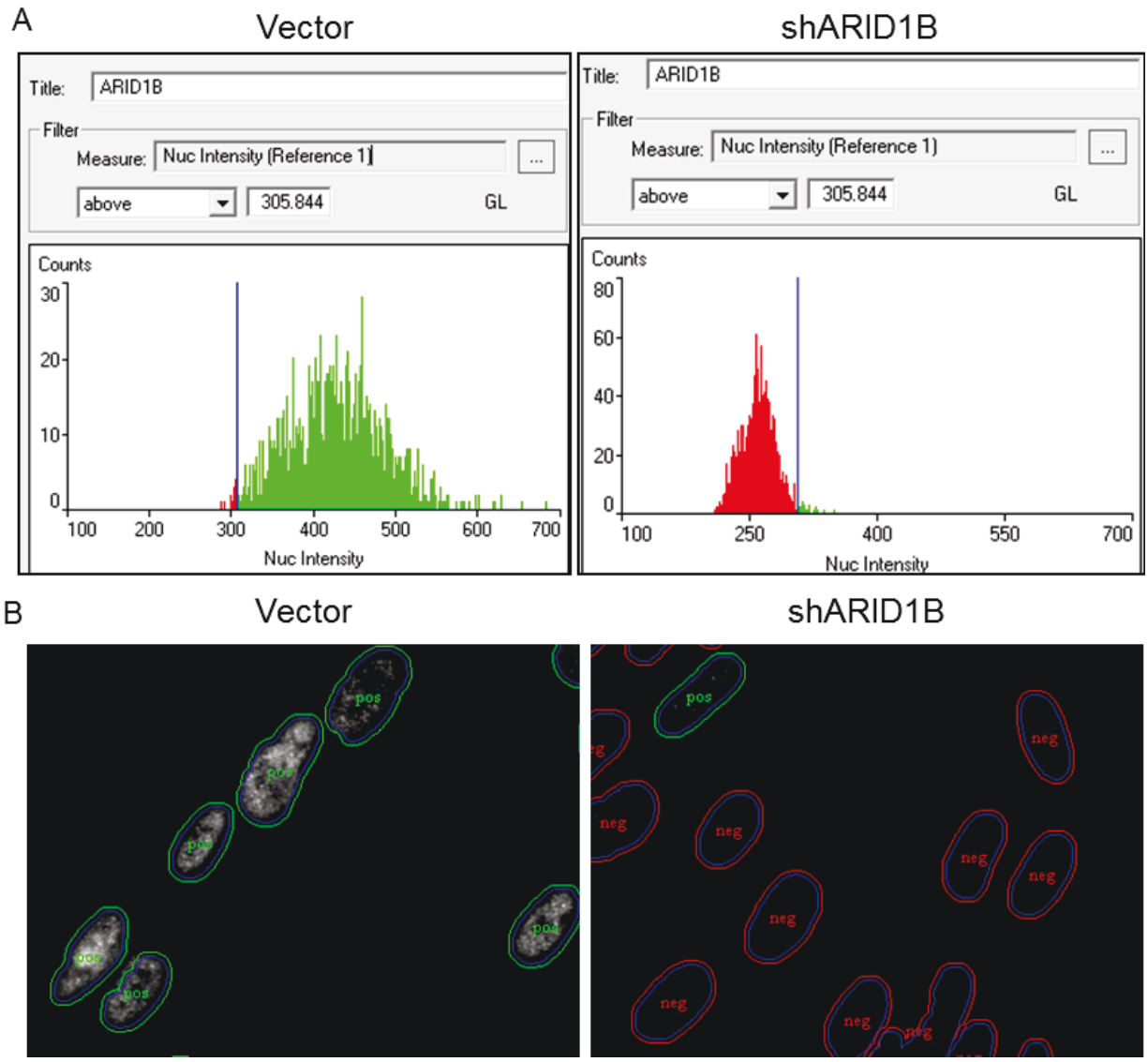


Figure 2.4. Workflow of establishing filters for High Content Analysis. IMR-90 cells were infected with either empty vector or shARID1B. $4x10^3$ cells were seeded per well in 96-well plates and the following day, cells were stained by immunofluorescence for ARID1B and DAPI and subjected to High throughput microscopy (HTM). Acquired images were analysed by high content analysis (HCA). (A) The nuclear intensity of ARID1B is determined for each cell (Nuc Intensity (Reference 1)) and the nuclear intensity of cells in a sample produces a histogram (A, B). A threshold filter was set to discriminate cells expressing high (pos) or low (neg) levels of ARID1B$^-$.

2.10.1.3. Confocal microscopy

Coverslips (Fisher Scientific) were treated with 70% ethanol (v/v) for sterilisation and plated in a 10cm dish. 10^6 cells were plated per dish on top of the coverslips and the media was changed the following day to remove unattached cells. 2 days after plating, coverslips were fixed with 4% PFA (w/v) for 20 min and immunofluorescence was conducted as before. Following DAPI staining, coverslips were washed twice with PBS and once with water and inverted onto glass slides (Fisher Scientific) with a drop of VECTASHIELD® Mounting Media (Vector Labs). Clear nail varnish was used to fix coverslips to slides, and slides were left to dry for 20 min. Fluorescence Images were taken with the Leica SP5 confocal microscope using the 40x objective.

2.10.2. SILAC to identify changes in protein expression

Stable isotope labelling with amino acids in cell culture (SILAC) is a method used to identify differential changes in proteins by mass spectrometry-based quantitative proteomics. Early passage IMR90 cells were grown for two passages in SILAC media containing either 'light' or 'heavy' amino acids, to allow production of newly synthesised labelled proteins. 500 mL of SILAC DMEM (Thermo Fisher Scientific (89985)) and was supplemented with either 50 mg of Light-Arginine and Light-Lysine or 50 mg of Heavy-Arginine (L-Arginine-HCl, 13C6, 15N4, 89990, Thermo Fisher Scientific) and Heavy-Lysine (L-Lysine-2HCl, 13C6, 15N2, 88209, Thermo Fisher Scientific). Media was supplemented with 10% Dialyzed FBS for SILAC (89986, Thermo Fisher Scientific) and Antibiotic-Antimycotic as before. Cells were transduced with virus suspended in SILAC complete medium and two days later were split for selection in SILAC complete medium supplemented with 0.5 µg/mL puromycin for 7 days. In total cells were grown in SILAC media for a minimum of three passages.

2.10.2.1. Whole cell protein extraction

SILAC labelled cells were counted and equal numbers of 'heavy' and 'light' cells (approximately $5x10^6$ cells each) were mixed together and pelleted by centrifugation. Cell pellets were washed once with ice

cold PBS and were resuspended in RIPA buffer (1% NP-40, 0.1% SDS, 50 mM Tris-HCl pH 7.4, 150 mM NaCl, 0.5% Sodium Deoxycholate, 1 mM EDTA) supplemented with protease inhibitors. Cells were incubated on ice for 30 min and cell lysates were subjected to centrifugation for 15 min at maximum speed. The supernatant containing proteins was transferred to a fresh tube.

2.10.2.2. Protein quantification

Proteins were quantified using the DC Protein Assay (BioRad) in a microtitre 96-well plate following manufacturer's guidelines for microplate assay. Absorbance at 660 nm (A_{660}) was measured using the Bio-Rad 680XR. Protein concentration was determined relative to known standards prepared in the same buffer as analysed samples. 70 µg of protein was used for analysis of proteins differentially expressed using SILAC whole cell extracts.

2.10.2.3. Sodium-dodecyl-sulphate polyacrylamide gel electrophoresis (SDS-PAGE)

Protein samples were diluted with 5x Laemmli sample buffer (1x concentration; 60 mM Tris-Cl pH 6.8, 2% Sodium-dodecyl-sulphate (SDS, w/v), 10% glycerol (v/v), 5% β-mercaptoethanol (v/v), 0.01% bromophenol blue(w/v)) and were heated at 90°C for 7 min. Following a brief centrifugation step samples were loaded onto a 10% Mini-PROTEAN® TGX™ Precast Gel (BioRad) in running buffer (25 mM Tris, 190 mM Glycine, 0.1% SDS (w/v)). Electrophoresis was conducted at 100V for 15-20 min to allow sample to just enter the resolving gel. Proteins were fractionated alongside Precision Plus Protein™ Dual Color Standards (BioRad) as a reference. After resolving, the protein gel was washed 3 times in distilled water for 5 min each with gentle agitation. Proteins were stained for visualisation with Coomassie Brilliant Blue R-250 (BioRad) for 6 h and washed with copious amounts of water over night.

2.10.2.4. Co-immunoprecipitation of nuclear protein complexes

To identify changes in nuclear complexes in senescent cells, proteins were labelled using SILAC as before. Equal numbers of cells were counted and mixed (approximately $1.5x10^7$ cells per condition) and nuclear material was extracted using the Nuclear Complex Co-IP Kit (Active Motif) following manufacturer's recommendations. 5% of the nuclear fraction was kept as "input" to assess the mixing error and the remainder was halved to immunoprecipitate ARID1B complexes and isotype matched IgG (as a negative control) at 4°C overnight. The next day 50 µL of magnetic beads coupled with recombinant protein G (Dynabeads® Protein G, Invitrogen) was added to each sample for 4 h at 4°C. Bound complexes were washed using magnetic recovery of beads following manufacturer's guidelines, and eluted in 30 µL of 5x Laemmli sample buffer by heating at 90°C for 10 min. Immunoprecipitated protein samples were subjected to SDS-PAGE as described previously.

2.10.2.5. Identification of proteins by LC–MS/MS

Mass spectrometry and peptide quantification analysis was performed in the Biomolecular Mass Spectrometry and Proteomics Laboratory (CSC). Gel bands were reduced with dithiothreitol, alkylated with iodoacetamide and then subjected to overnight trypsin digestion. The peptide extracts underwent a second round of trypsin digestion to minimise the number of missed cleavages. Peptide mixtures were analyzed using an UltiMate 3000 Rapid Separation LC, coupled to a LTQ-Orbitrap-Velos mass spectrometer (ThermoFisher Scientific). Separation was performed in a 3 h gradient using a 50 cm Acclaim pepmap C18 column (ThermoFisher Scientific). Protein identification and quantification was performed using Maxquant v1.2.0.13, with the embedded Andromeda 1.2.0.0 search engine and the IPI_Human_v3.37 database. The initial minimum ratio H/L count was set to 1 to obtain raw data, however the stringency was later increased to a minimum count of 3.

For identification of ARID1B associated proteins, further stringency parameters were included. Confident interactors were defined as proteins that had a total count higher than that obtained in the 5% input and cytoplasmic proteins were excluded from the final list.

Chapter 3. Screening for regulators of lifespan extension in MEFs using NGS

Functional shRNA screens combined with NGS has led to the discovery of important regulators of various cellular processes including senescence and cell proliferation (Burrows et al., 2010; Silva et al., 2008). In order to identify novel genes involved in the regulation of senescence, an shRNA screening coupled to NGS was planned. Many conditions must be optimised prior to conducting shRNA screenings including the size of the shRNA pools to be tested and the duration of the screen.

3.1. Optimisation of the bypass of senescence screening

To screen for regulators of replicative senescence in MEFs, assay conditions must first be optimised. I used a relatively small shRNA library to screen for senescence regulators in MEFs, to establish the screening protocol using NGS. The HCC shRNA library consists of 624 shRNAs and was provided by Lars Zender. The library contains mouse orthologues of genes frequently deleted in approximately 100 human HCC tumours. 58 regions in the genome were recurrently deleted, and these regions held 362 genes. Of these 362 genes, 301 mouse orthologues were identifiable and corresponding shRNAs were obtained from the Cold Spring Harbor Laboratory RNAi CODEX library (Figure 3.1A). Hairpins were shuttled from the pSM2 vector to pLMS which contains GFP expression to allow identification of infected cells (Figure 3.1B). 624 shRNAs were divided into 13 pools each containing 48 shRNAs; each deleted gene was therefore represented by 2 mouse shRNAs on average.

The HCC library has previously been used to identify tumor-promoting shRNAs in a mouse model of HCC (Zender et al., 2008). The advantage of using this library, as opposed to a library of randomly pooled shRNAs, is that the library contains genes deleted in cancer and therefore may be enriched for important tumour suppressors.

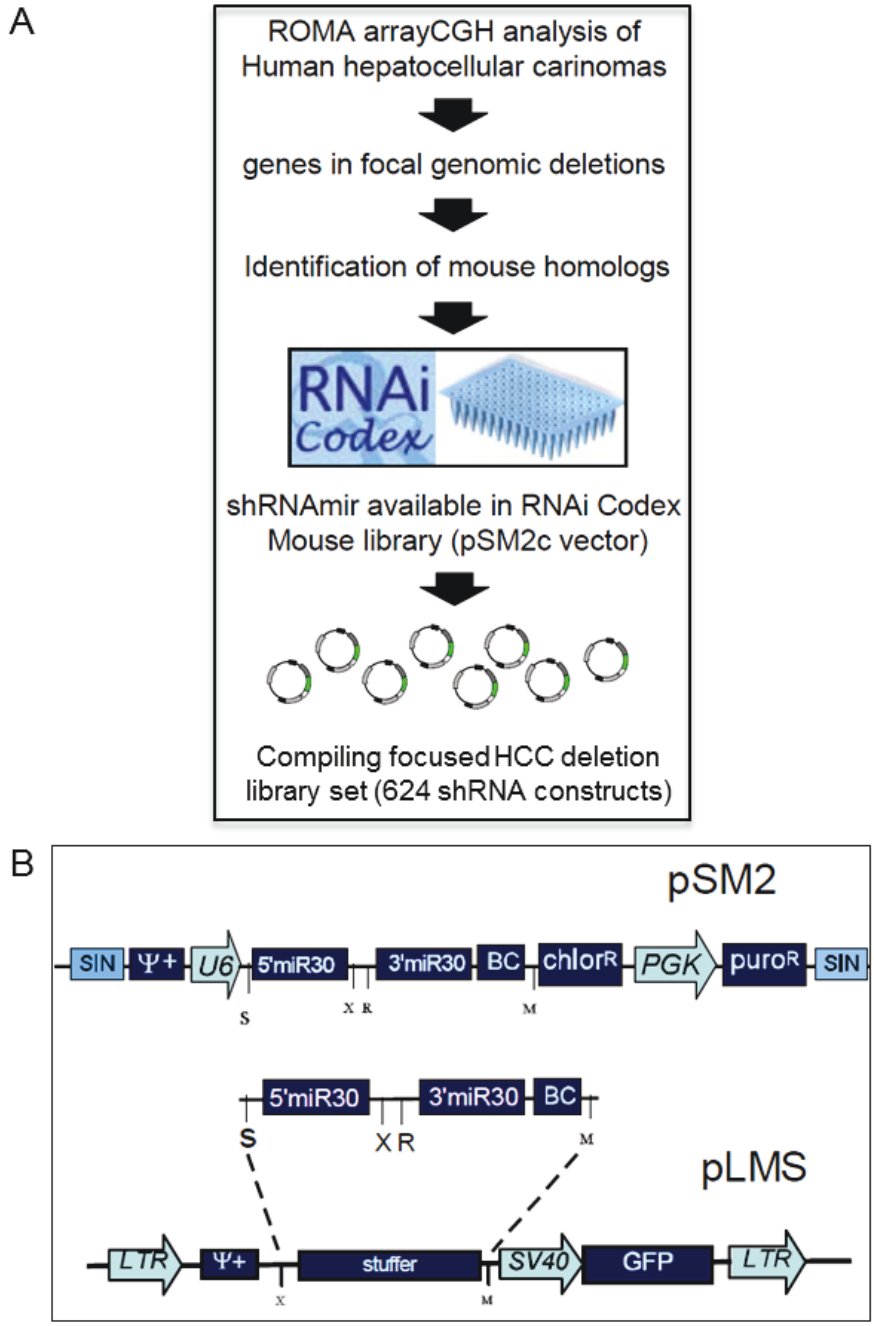


Figure 3.1. An shRNA library targeting genes frequently deleted in human HCC. (A) Strategy of the workflow for creating a mouse HCC shRNA library (B) shRNAs available in the RNAi codex library were subcloned from the pSM2 vector into pLMS which contains GFP to allow identification of infected cells. Figures (A) and (B) were adapted from Zender et al., 2008.

3.2. Proof of concept experiment verifies feasibility of the screening

To establish the time duration for the screen and assess the feasibility of conducting a pooled shRNA screen with the HCC library, a proof of principle experiment was conducted. MEFs infected with an empty vector were passaged to establish when the cells would reach senescence. When cell growth

was assessed 26 days after infection, vector control cells had a very limited growth potential and were not substantially affected by dense colony formations arising from spontaneous mutations (Figure 3.2). To determine if a single shRNA diluted in the HCC library (comprised of 624 shRNAs) can increase the colony formation ability of cells, I infected MEFs with different dilutions of shp53 constructs; as shp53 is known to bypass senescence it can be used as a positive control to assess which dilutions of shRNAs can give a proliferative advantage to cells. An shp53 dilution of 1:1000 can increase the colony formation ability of the cells when compared to the vector control sample (Figure 3.2). Therefore it can be concluded that screening for replicative senescence in MEFs using the pooled HCC library is feasible and day 26 is a suitable end time point for the screening.

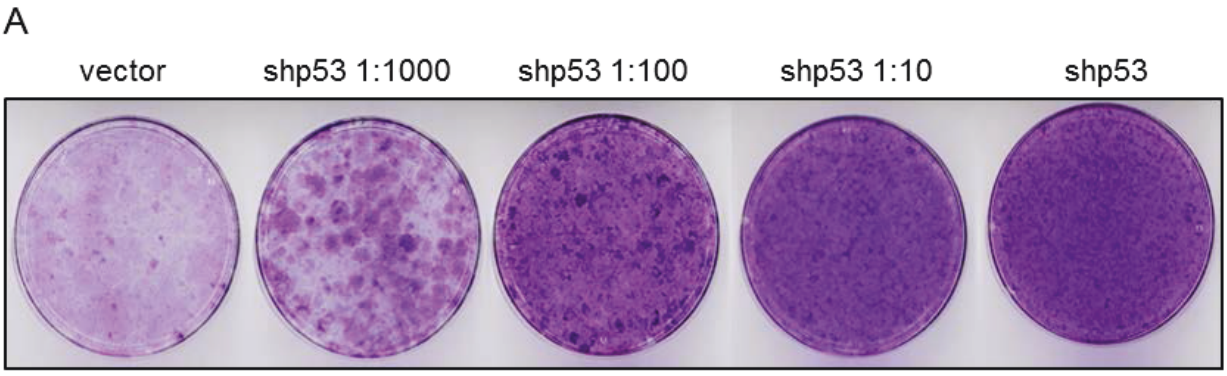


Figure 3.2. Proof of concept to establish the feasibility of an shRNA lifespan extension screen in MEFs. (A) MEFs were infected with different dilutions of the positive control vector shp53 and an empty vector control to assess the feasibility of the screening. Following infection, 10^6 cells were seeded per 10 cm dish, and 10^6 cells were re-seeded upon each serial passage. Enrichment of cells infected with shp53 was analysed by colony formation assay by seeding 10^5 cells in a 10 cm dish at passage 5, cells were fixed at day 26 post infection, corresponding to the latest time point of the screen. Crystal violet staining of fixed plates indicates that MEFs infected with a vector control have very limited growth potential and are not substantially affected by spontaneous mutations.

3.3. NGS used to identify shRNAs from bypass of replicative senescence screen in MEFs

In order to identify shRNAs regulating senescence in MEFs, MEFs were infected with the pooled HCC library or empty vector and were passaged until vector cells reached senescence. This was done to allow shRNAs conferring a growth advantage to become enriched within the cell population. To

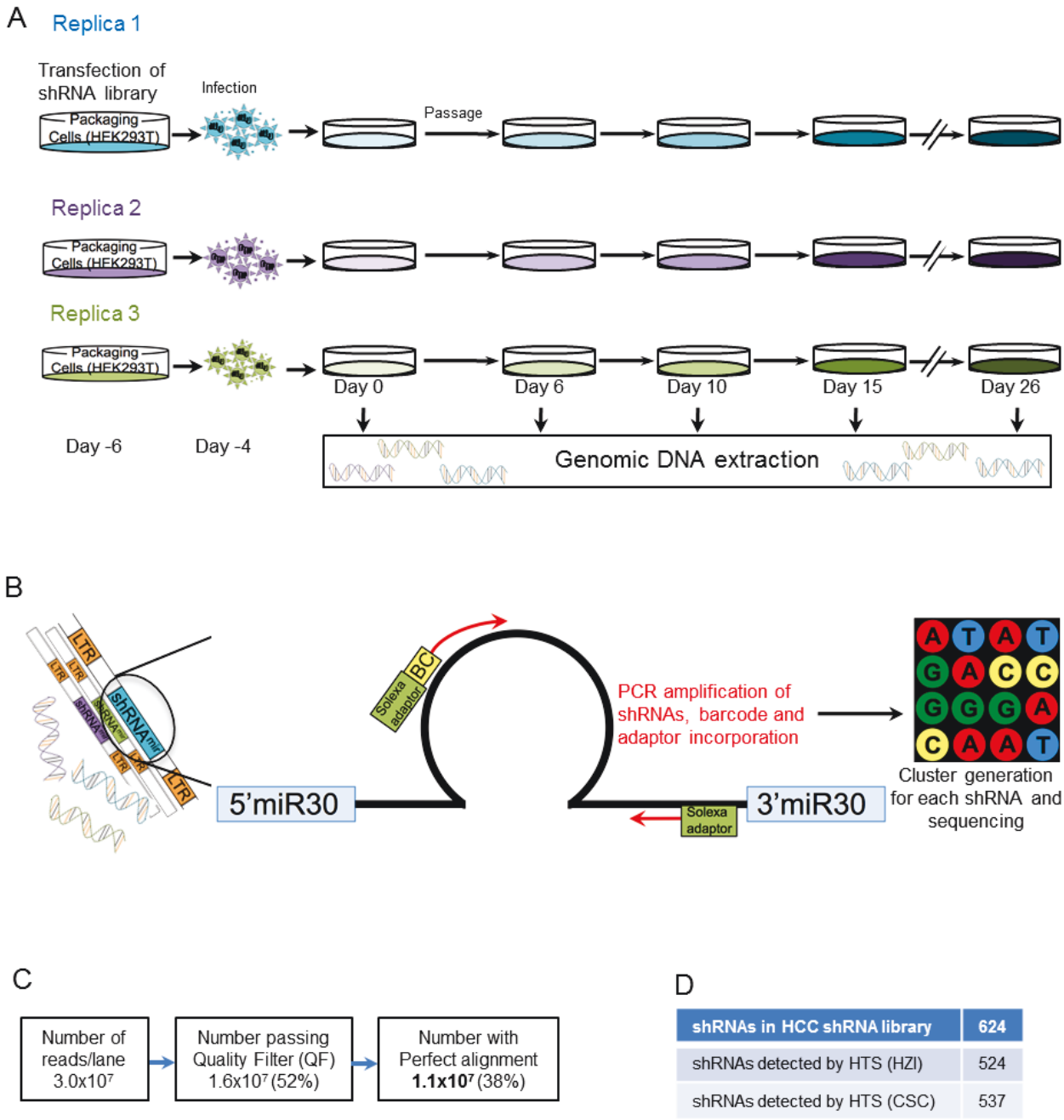
improve the reliability of the screening and decrease the number of false positives obtained, the screening was conducted in biological triplicate. For each independent replicate MEFs were infected at passage 1. 4 days later, cells were trypsinised and counted. $4x10^5$ cells were plated in duplicate and the remaining cells were collected for genomic DNA extraction, DNA from this aliquot was assigned as the reference sample. Cells were passaged and a fraction of the cells were collected at days 6 (passage 2), 10 (passage 3), 15 (passage 4) and 26 (passage 5) (Figure 3.3A).

Genomic DNA was extracted from cells and the hairpin sequences integrated into the genomic DNA were recovered by PCR amplification (Figure 3.3B). PCR primers were designed such that the extreme 5' and 3' ends of the final PCR product are complementary to the sequence of the Solexa flow cell adaptors, allowing the amplified PCR product to hybridise to the Solexa flow cell (Figure 3.3B). Each sample (biological replicates and time points) was assigned a specific 3 nt barcode, incorporated into the 5' PCR primer which allows shRNA reads amplified from the same sample to be identified. All barcoded samples were combined in equal amounts and sequenced on the same lane of the Solexa flow cell.

Sequencing of samples from the HCC screen was conducted at the Helmholtz Centre for Infection Research (HZI, Germany) in the first instance and later at the Clinical Sciences Centre (CSC, UK) to verify the sequencing protocol. Solexa libraries at the CSC were sequenced on the Illumina GAIIx using a 39 bp cycle run. Primers were slightly modified from the conventional primers used for miR30 shRNA recovery (Sims et al., 2011; Zender et al., 2008) to allow the full hairpin plus barcode to be sequenced within 39 bp (Figure 2.2). In a test-sequencing run at the CSC, 6 pM of Solexa library was run on 2 lanes of a single flowcell. On average, over 10^7 reads were recovered per lane, with perfect hairpin alignment to miR30 shRNA libraries, and with perfect barcode sequencing match (Figure 3.3C).

Comparison of enriched hairpins detected from the same Solexa library run on two different lanes of a flowcell, shows there is very little variability in the sequencing output between the lanes (variation may arise during the clustering step involving bridge amplification) (Table A1). Variation between lanes is higher in 'Day 0' samples where all shRNAs in a sample are relatively equally distributed, and variability is almost minimal in 'Day 26' samples, which contain enriched hairpins (Table A1). Sequencing of 'Day 0' samples verified that the number of shRNAs detected in the test sequencing run is comparable to the number detected in the HZI sequencing run (Figure 3.3D).

The test-sequencing run allowed verification of the establishment of an NGS protocol for massive parallel sequencing of miR30 shRNAs using a 39 cycle base run. On average, $7.3x10^5$ sequencing reads per sample can be obtained from a screen with 5 time-points, conducted in triplicate (a total of 15 samples). For screenings using the pooled HCC deletion library, this allows each shRNA to be represented on average over 1,000 times in each of the 15 samples.



shRNAs in HCC shRNA library	624
shRNAs detected by HTS (HZI)	524
shRNAs detected by HTS (CSC)	537

Figure 3.3. Strategy for the bypass of replicative senescence screen in MEFs. (A) MEFs are infected with a library of shRNAs. Three independent replicates are conducted. Upon serial passage there is an enrichment of shRNAs that give cells a proliferative advantage. Genomic DNA was collected from infected cells at specified time points. (B) Solexa libraries were prepared from extracted DNA by PCR amplification using primers specific for the shRNA loop and backbone. Primers incorporate Solexa adaptor sequences to allow flow cell hybridisation. The forward primer used for PCR also contains a unique 3-nucleotide barcode, which will be used to identify each sample. 6 pM of the gel extracted Solexa library was used to create clusters and was sequenced by massive parallel sequencing. (C) Workflow for sequencing reads acquired on the GAIIx. The number of reads shown is the average calculated from running 6 pM of Solexa library on 2 lanes of a single flowcell. (D) The number of HCC library shRNAs detected in the test sequencing run are comparable to the number detected in the HZI sequencing run.

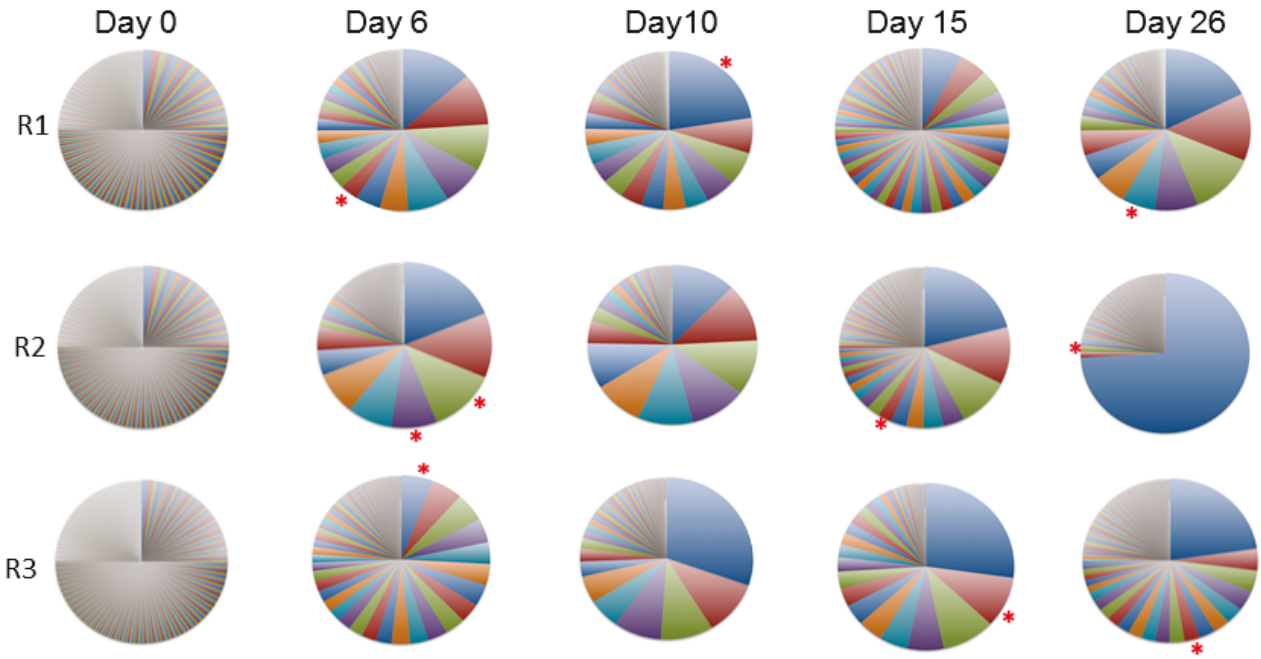
3.4. ARID1B is a candidate regulator of replicative senescence in MEFs

Sequencing data from the screen was analysed by measuring the enrichment of a gene across the entire dataset. Sequencing data has been represented as pie charts to show the relative abundance of particular shRNAs within a sample (Figure 3.4A). This representation shows there is no initial library bias as reference samples (Day 0) have a similar distribution of all shRNAs whereas in later time-points there is a change in the distribution (Figure 3.4A).

Z-scores were first calculated to assess the distribution of shRNA sequences in each sample. From this a p-value was given. To analyse the enrichment of shRNAs, each gene was assigned a Fisher's combined p-value, which allows the independent p-values across all samples to be combined (Figure 3.4B). Arid1b was identified as the gene with the most significant Fisher's combined p-value as it was frequently enriched in different time-points and in different replicates (Figure 3.4A red asterisks, Figure 3.4B). Furthermore, independent shRNAs targeting Arid1b were also found in the screen (Figure 3.4A Replicate 2, day 6, red asterisks) suggesting that Arid1b is a strong candidate implicated in replicative senescence in MEFs.

ARID1B is a component of the SWI/SNF complex of nucleosome remodellers. This complex is involved in numerous cellular processes and its subunits are frequently mutated in cancer (Hargreaves and Crabtree, 2011). Previous studies on ARID1B have shown that it plays an important role in differentiation (Nagl et al., 2007; Yan et al., 2008) and that it is involved in transcriptional regulation of cell cycle effectors $p21^{CIP1}$ and c-myc (Inoue et al., 2011). However a role for Arid1b in senescence regulation has not been previously identified.

A



B

Gene	Fisher's Combined p-value
Arid1b	1.35×10^{-37}
MGC103372	2.21×10^{-17}
Slc9a3	6.25×10^{-17}
Ankrd22	7.17×10^{-14}
Elac1	2.85×10^{-08}
Fgf5	1.79×10^{-4}
Tnmd	2.30×10^{-4}
Arl8b	7.09×10^{-4}
Bhlhb9	2.42×10^{-2}
BC050789	3.00×10^{-2}

Figure 3.4. Lifespan extension screen in MEFs identifies Arid1b as a candidate senescence regulator. (A) Proportions of sequencing reads of unique shRNAs relative to total shRNAs detected per sample. Samples are arranged by replicates (rows) and time-points (columns). Pie graphs show the representation of an shRNA relative to each standalone sample and pie colours are indicative of shRNAs within a sample only and not across the dataset. Red asterisks indicate the high occurrence of shRNAs targeting Arid1b appearing within the top 10 enriched shRNAs per sample. (B) after caluclating the Z-score and p-value of shRNAs in each sample, candidate shRNAs extending cellular lifespan were ranked by Fisher's combined p-value. This combines independent p-values across the data set for each gene. Arid1b is identified as the shRNA with the most significant Fisher's combined p-value.

3.5. Depletion of Arid1b extends cellular lifespan in MEFs

To confirm the role of Arid1b in lifespan extension, three hairpins targeting *Arid1b* were designed and cloned, of which, one hairpin produced an efficient knockdown of Arid1b at the protein level and mRNA level (Figure 3.5A, B). Knockdown of Arid1b resulted in an observable increase in colony formation (Figure 3.5D) and extended the replicative lifespan of MEFs (Figure 3.5C). The data confirms the result from the screening and suggests that Arid1b knockdown delays senescence in MEFs.

3.6. ARID1B regulates cell proliferation and replicative senescence in IMR-90

In order to establish whether the effect of Arid1b was more general and conserved in humans, three independent shRNAs targeting human *ARID1B* mRNA were designed. The efficiency of ARID1B knockdown was judged by RT-qPCR and by immunofluorescence. Both shARID1B-2 and shARID1B-3 resulted in significantly depleted ARID1B expression; however shARID1B-3 had a greater knockdown efficiency than shARID1B-2 (Figure 3.6A, B). Knockdown of ARID1B increased the lifespan of IMR-90 cells (Figure 3.6C) and also increased the ability of these cells to form colonies at low density (Figure 3.6E). The efficiency of ARID1B knockdown, correlated with the ability to delay senescence. These experiments confirm that ARID1B ablation extends cellular lifespan of both human and mouse fibroblasts.

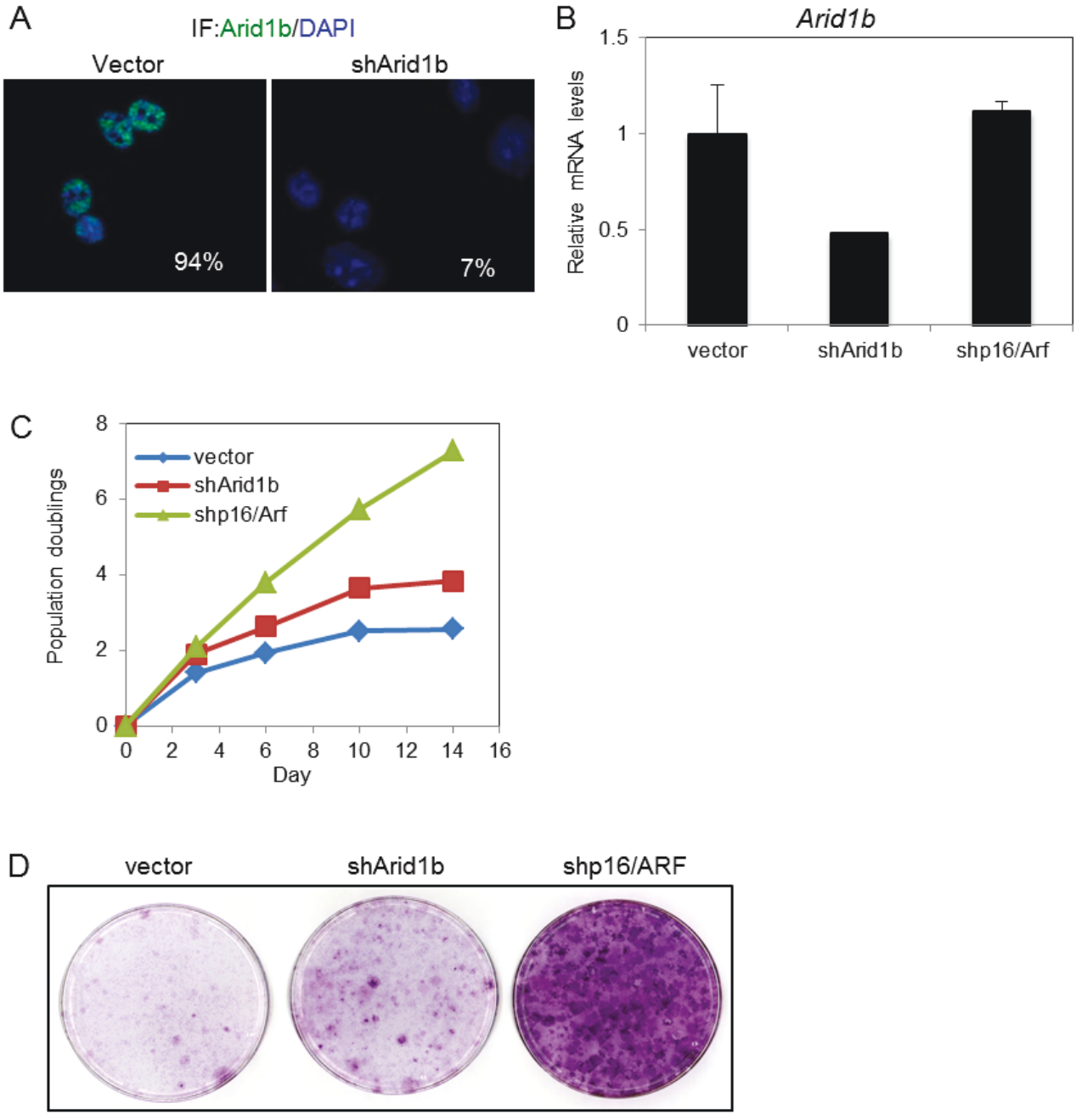


Figure 3.5. Depletion of Arid1b extends cellular lifespan in MEFs. (A) Confirmation of Arid1b knockdown in MEFs by immunofluorescence, numbers indicate percentage of Arid1b positive cells assessed by quantitative IF. (B) Confirmation of the levels of Arid1b knockdown in MEFs by qRT-PCR. (C) MEFs were infected at passage 1 with vector, shArid1b and shp16/Arf. After selection growth curves were performed by plating 10^6 cells in a 10 cm dish and counting cells every 3 or 4 days. (D) MEFs were infected with the indicated vectors and following selection $4x10^4$ cells were seeded per 10 cm dishes. After 14 days plates were fixed and stained with crystal violet.

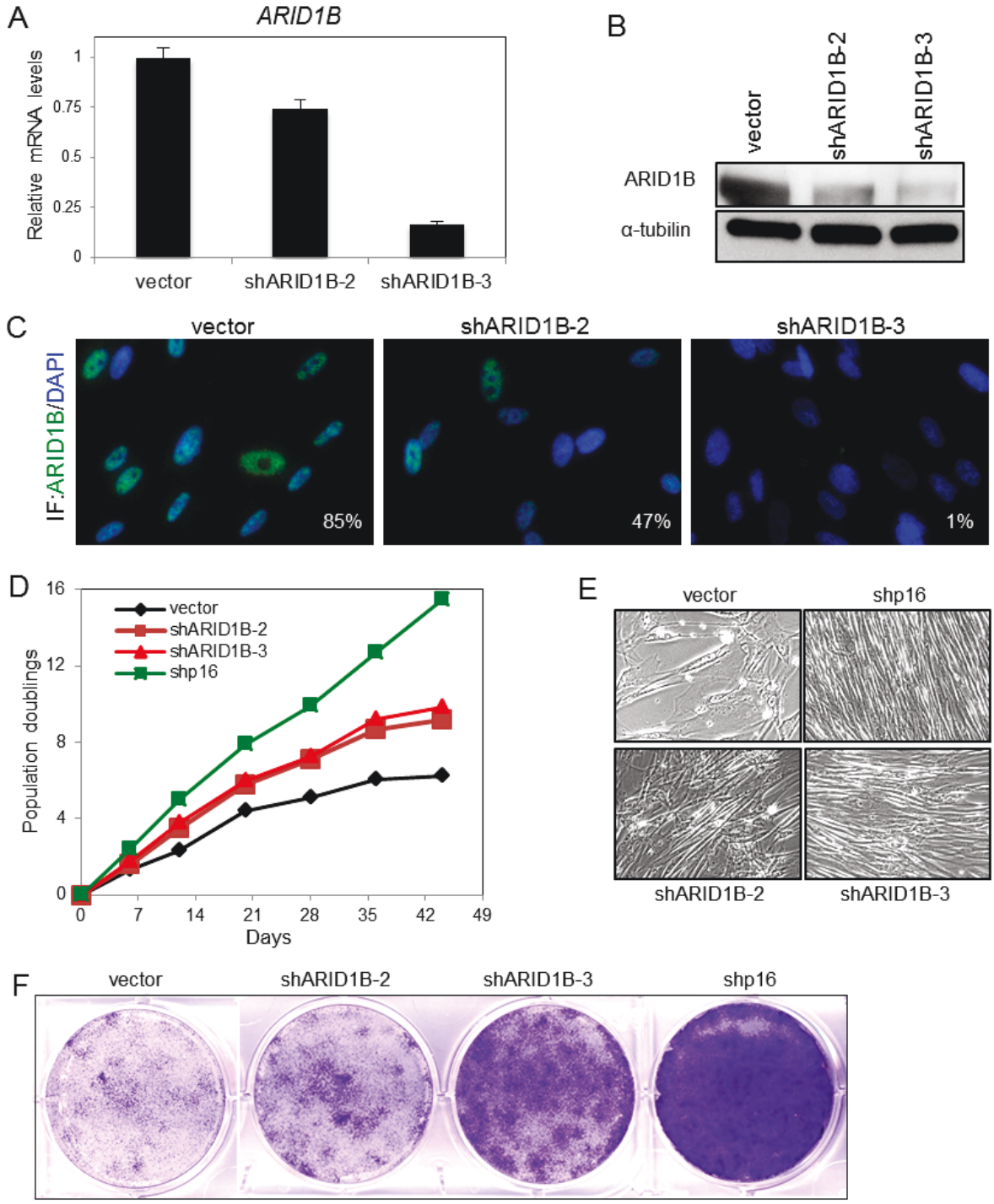


Figure 3.6. Depletion of ARID1B extends cellular lifespan in IMR-90. (A-c) Confirmation of the levels of ARID1B knockdown in IMR-90 by RT-QPCR, western blot and quantitative immunofluorescence, numbers indicate percentage of ARID1B positive cells assessed by quantitative IF. (D-F) IMR-90 cells were infected at passage 17 with the indicated constructs. (D) After selection, passage 19 cells were seeded at $5x10^5$ cells per 10 cm dish and growth curves were performed by counting cells approximately every 7 days. (E) Representative microphotographs of cells at passage 21 taken 5 days after plating for growth curves showing the effect of two independent constructs targeting ARID1B over growth and morphology of IMR-90 cells. (F) Colony formation assays were performed by seeding 10^4 cells infected with the indicated constructs at passage 15 in a 6-well plate. 11 days later cells were fixed and stained with crystal violet to show that knockdown of ARID1B increases proliferation.

3.7. Conclusions and perspectives

3.7.1. Screening for regulators of replicative senescence in MEFs

Genetic screenings for the bypass of senescence have served to identify genes associated with cancer (Acosta et al., 2008; Burrows et al., 2010; Gil et al., 2004). In this work I used a small HCC shRNA library to establish a protocol for senescence screenings coupled to NGS. The screening was conducted in primary MEFs which have a limited replicative lifespan and quickly undergo senescence attributed to high levels of oxidative stress, a phenomenon known as 'culture shock' (Parrinello et al., 2003; Sherr and DePinho, 2000). The HCC shRNA library used was well suited for this purpose, the library is relatively small (624 shRNAs) and therefore pooled shRNA screens can be conducted with relative ease, and the sequencing data obtained had a high depth of coverage, with each shRNA represented on average 1000 times in 15 different time-points and replicates. Furthermore, the library targets genes that are frequently deleted in human HCC, and therefore the HCC library is enriched for tumour suppressor genes that may have a role in senescence. Indeed, the library has previously been used to identify novel HCC tumour suppressor genes as well as genes involved in liver regeneration (Wuestefeld et al., 2013; Zender et al., 2008).

The limited replicative lifespan of MEFs has served as a valuable system for identifying senescence regulators (Jacobs et al., 2000; Leal et al., 2008; Shvarts et al., 2002). A potential problem of using MEFs in a lifespan extension screen is that mutations accumulate in MEFs upon prolonged culture, which allows escape from senescence (Busuttil et al., 2003). These mutations give rise to dense highly proliferating colonies. Such colonies may be infected with 'passenger' shRNAs which will become enriched and therefore will contribute to 'false positive' candidates. At day 26 the control cells were not substantially affected by dense colony formations arising from clonal variation and therefore day 26 was chosen as a suitable end time point for the screening.

To confirm that ARID1B is a true regulator of senescence, it was important to reproduce the result of the senescence bypass observed in MEFs. For this purpose a mouse shArid1b hairpin was created that had an independent target sequence to the hairpins in the HCC library. This independent hairpin also extended the cellular lifespan of MEFs. A similar growth advantage was seen when ARID1B was depleted in late passage IMR-90 cells. Taken together the data suggests that ARID1B has a role in senescence.

3.7.2 Advances in pooled shRNA screenings using NGS

Over the last decade the speed, lowered costs and data output of NGS has progressed rapidly and massive parallel sequencing has been adapted for use with a number of different techniques. NGS has previously been used to identify shRNAs from pooled library screenings (Schlabach et al., 2008; Silva et al., 2008). Here I established a protocol for use of NGS to identify miR30 based shRNAs on a 39 bp GAIIx Solexa run. For this purpose, PCR primers were adjusted from conventional primers (Sims et al., 2011; Zender et al., 2008) to permit sequencing of the full hairpin and barcode in 39 bp.

Conditions were optimised to maximise data output. Initially, the amount of DNA loaded onto flow cells for bridge amplification (clustering) was tested. Accurate measurement of the concentration of the template library is critical to maximise the cluster density while simultaneously avoiding cluster detection issues due to overcrowding and cluster focusing. An initial sequencing run tested 8 pM and 6 pM based on the sample concentrations used previously for ChIP-sequence. 6 pM produced the highest number of clusters passing filter (254204 compared to 197931) and was used for sequencing runs thereafter. I also assessed the variability due to clustering by comparing the highest-ranked hairpins from the same Solexa library run on two different lanes of a flowcell. I detected very little variability in the highest ranked hairpins confirming that variation in cluster generation does not substantially affect the ranking of hairpins detected.

The Solexa sequencing primer begins sequencing within the variable region of the hairpin. It is important that the first four bases of the amplicon have no sequence bias as these sequencing cycles are used to detect the position of all the clusters and to calculate expected signal intensities for each channel, which should be equal for the four bases (A, T, C and G). Samples which have an even distribution of the four bases across the run are 'high-diversity' whereas samples which have a sequence imbalance (i.e. high levels of certain bases in certain positions) are 'low-diversity'. Sequencing libraries from senescence screenings may contain bias as some shRNAs are expected to be enriched in the sample, especially at later time points and therefore the distribution of the four bases will not be even. When low-diversity samples are being sequenced a control lane is run parallel to the samples to set up sequencing and alignment. This control lane sequences DNA from 'PhiX' a high-diversity viral genome. The Genomics facility found the PhiX control lane is essential for obtaining reads with a high percentage pass filter rate. They also tested using a PhiX "spike" in the sample, which is less expensive then sequencing a separate control lane; however this decreased the number and quality of the amplicons obtained.

The swift advances in NGS technology means that protocols must be continuously optimised to suit upgrades in machines and improvements in reagents. In most institutes, including the CSC, the GAIIx has been replaced by the HiSeq 2000, which no longer has the option of 39 bp reads. The minimum read length of 50 bp will increase the percentage of perfectly matched reads, as hairpins sequenced using 50 cycle sequencing kits will not be affected by the drop in peak intensity due to limited reagents when the run is nearing completion. Obtaining a high read accuracy at the end positions of the sequence is critical as sample barcodes are situated there. Using a longer cycle run also allows longer barcodes to be used. In this way, barcodes can be designed to be redundant, such that single base mismatches within the barcode region would still allow for correct identification of the amplicon to the corresponding sample, therefore lowering the percentage of discarded reads. The HiSeq 2000 is able to produce 4.5 GB of data per 50 bp sequencing lane compared to 1 GB of data per 39 bp lane on the

GAIIx. The increased data output makes the HiSeq 2000 better suited for genome-wide shRNA screens. However this comes at a greater overall cost of £500 compared to £371 for the GAIIx. For screenings using small shRNA libraries the GAIIx may still be the most cost-effective method of sequencing however with the advent of the HiSeq 2500 (August 2012), it is likely that the GAIIx will soon be replaced.

As the popularity of pooled shRNA screenings using NGS has increased, a number of statistical packages have become available for analysing data from high-throughput screens (Sims et al., 2011; Yu et al., 2013). This will aid processing the increasing amounts of data retrieved from NGS screenings. Packages can be modified to suit the preferences of the user, for example in our screenings only reads with perfect alignment to the reference library were selected, however others have allowed reads with up to two mismatches to pass filter (Sims et al., 2011). As with statistical packages, the number of commercial shRNA libraries available is also increasing. Efforts are now focused on developing validated genome-wide libraries which will ease the use of shRNA screens, especially *in vivo* when smaller pools containing potent shRNAs are required (Fellmann et al., 2011). The rapid advances in RNAi and NGS means that large pooled shRNA screenings have become a powerful and widely available tool to identify regulators of important pathways *in vitro* and *in vivo*.

Chapter 4. ARID1B a component of the SWI/SNF complex regulates senescence

4.1. Knockdown of ARID1B attenuates OIS

The ability of ARID1B knockdown to delay replicative senescence in primary mouse and human fibroblasts led to the investigation of the role of ARID1B during OIS. For this purpose, IMR-90 ER:RAS cells were infected with ARID1B shRNAs and control constructs. When compared to vector infected cells, cells with ARID1B knockdown proliferated faster (Figure 4.1A, D). ARID1B knockdown also resulted in an increase in the percentage of replicating cells as measured by BrdU incorporation. To understand whether this increase in proliferation was due to a bypass in senescence, cells were stained for SA-β-Gal activity to identify senescent cells (Dimri et al., 1995). As expected the percentage of SA-β-Gal positive cells increased when IMR-90 ER:RAS cells were treated with 4OHT (Figure 4.1C, D). ARID1B depleted cells had lower SA-β-Gal activity compared to vector cells (Figure 4.1C, D). Together these results suggest that ARID1B is an important regulator of OIS.

4.2. ARID1B regulates $p21^{CIP1}$, $p16^{INK4a}$ and p53 expression during OIS

OIS is mediated by different senescence effectors, including $p21^{CIP1}$, $p16^{INK4a}$, and p53. As ARID1B knockdown abrogates OIS, it is important to understand its effects on these pathways. I compared the expression of these senescence effectors using quantitative IF. $P21^{CIP1}$, $p16^{INK4a}$ and p53 expression was lower when ARID1B was depleted during OIS (Figure 4.2A-D). Knockdown of ARID1B also decreased the mRNA levels of *CDKN1a* and *INK4a* during OIS demonstrating that ARID1B regulates the expression of important cell cycle regulators (Figure 4.2E, F).

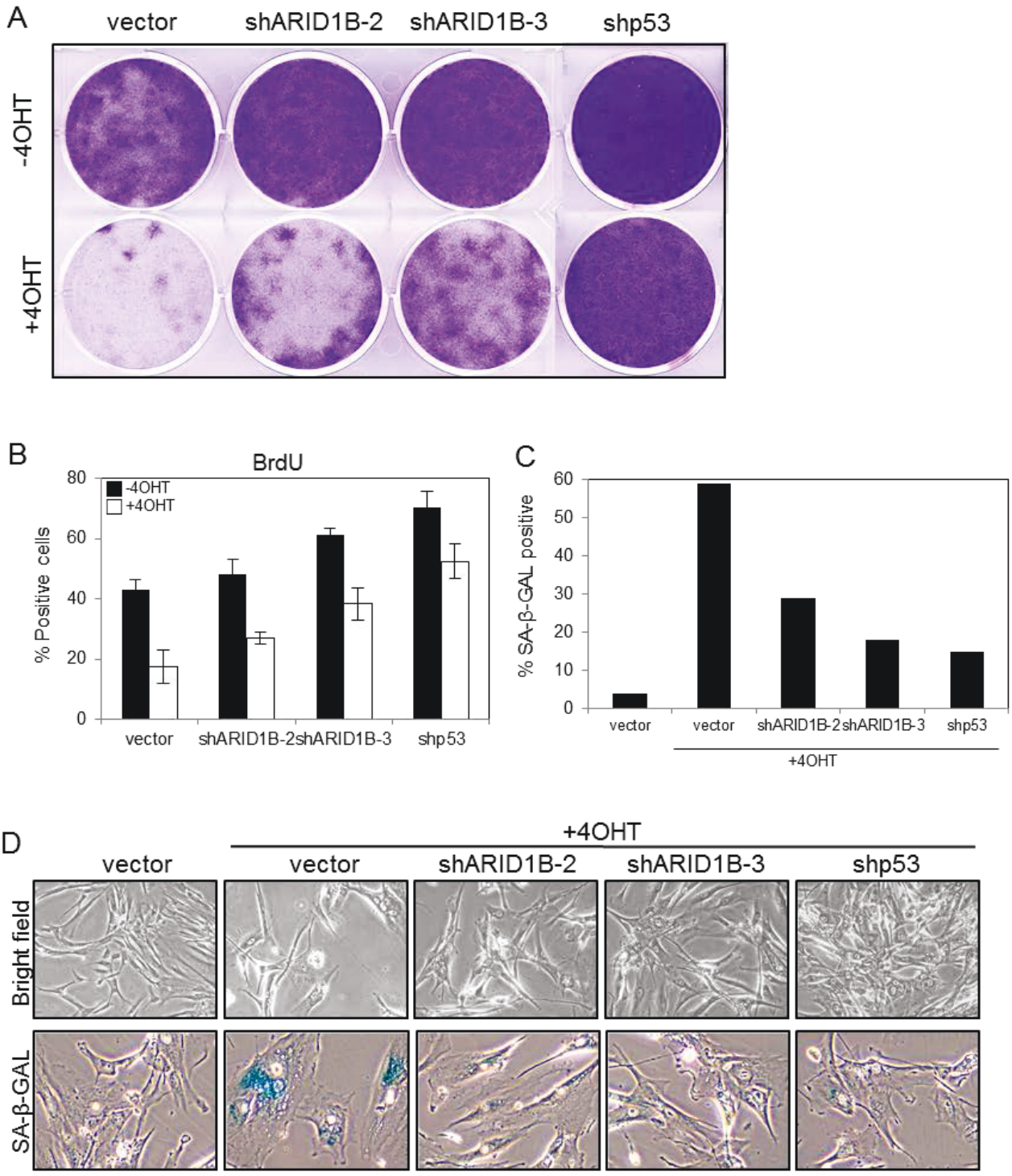


Figure 4.1. Knockdown of ARID1B attenuates OIS. (A-D) IMR-90 ER:RAS at passage 13 were infected with the indicated constructs and selected. Cells were grown with either 100 nM 4OHT to activate the ER:RAS protein or DMSO to act as a control (A) $1.5x10^4$ cells were seeded per 6-well plate and treated with or without 4OHT. 16 days later cells were fixed and stained with crystal violet. (B) Cells were grown with or without the addition of 100 nM 4OHT for 5 days. Proliferation was evaluated by BrdU incorporation. (C) $6x10^4$ cells were plated per 6-well plate and fixed 2 days later. SA-β-GAL activity was assessed and calculated from counting at least 150 cells. Bright field images of indicated cells 5 days after plating $5x10^5$ cells per 10 cm plate. Representative bright field images of SA-β-GAL activity shown in (C).

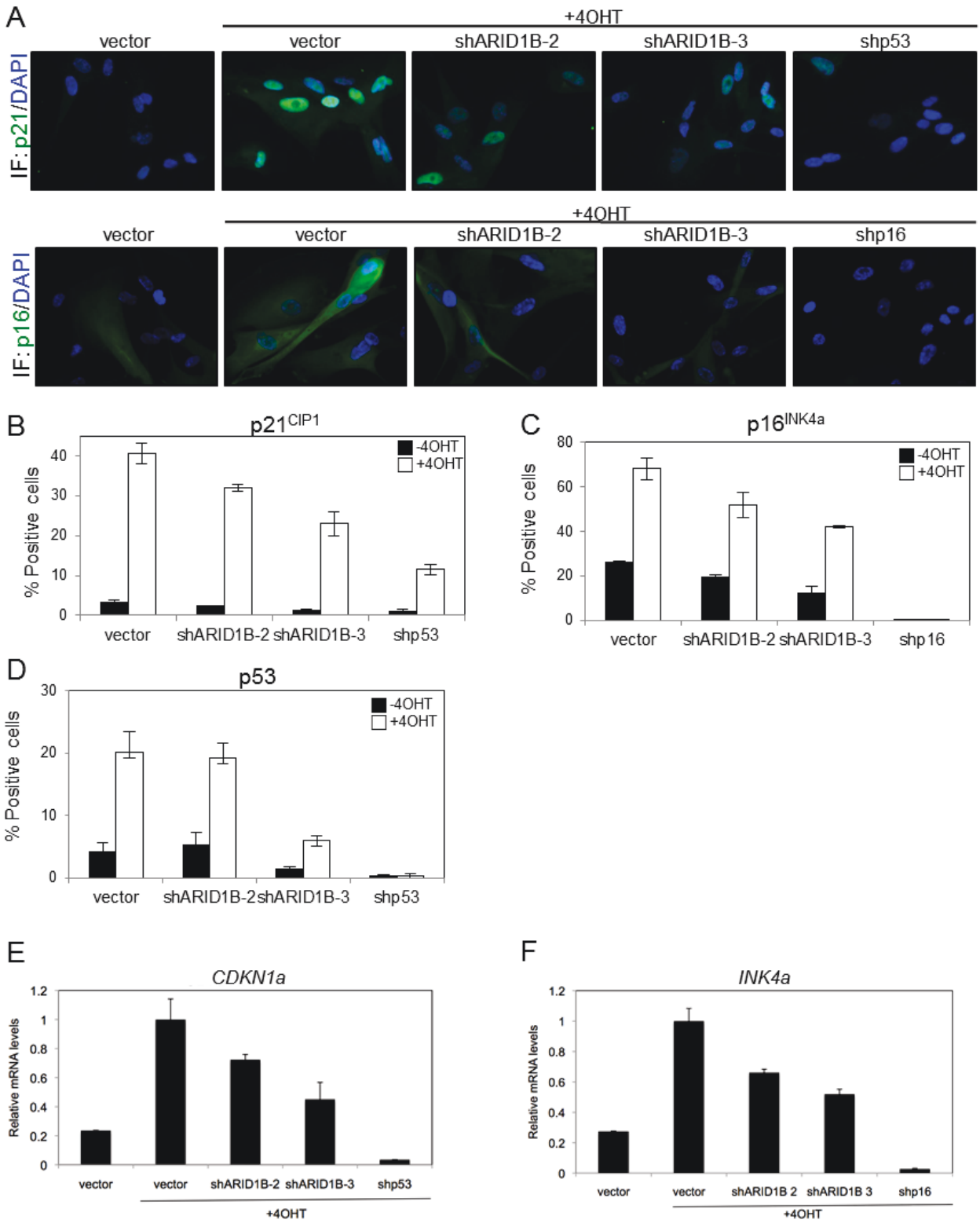


Figure 4.2. ARID1B regulates different senescence effectors. (A-F) IMR-90 ER:RAS at passage 13 were infected with the indicated constructs and selected. Cells were grown with either 100 nM 4OHT to activate the ER:RAS protein or DMSO (A) IF images of $p21^{CIP1}$ and $p16^{INK4a}$ (B-D) Quantification of $p21^{CIP1}$, $p16^{INK4a}$ and p53 levels assessed by quantitative IF. (E,F) *CDKN1A* and *CDKN2A* expression is decreased in ARID1B depleted cells during OIS.

4.3. Gene expression profiling identifies multiple senescence effectors regulated by ARID1B

To further elucidate the mechanisms by which ARID1B controls senescence, I analysed the gene expression profile of cells undergoing OIS. For this purpose I used IMR-90 ER:RAS cells infected with empty vector or shARID1B-3 and induced senescence (by addition of 4OHT). 6 days later RNA was collected for gene expression profiling using the Human Gene 1.0 ST arrays (Affymetrix).

A total of 108 genes were identified, in which transcript levels were either up- or down-regulated by at least 2-fold in ARID1B knockdown cells compared to vector cells. Genes downregulated by at least 2 fold during ARID1B knockdown include components of the SASP including *SPP1 (OPN)* and *MMP3.* Genes upregulated by at least two-fold when ARID1B is depleted include the $p16^{INK4a}$ inhibitor *ID1* as well as *ID2* and *ID3* (Table A2). The expression levels of other genes relevant for senescence were also ablated upon ARID1B knockdown including *ETS1, GDF15, E2F7* and *CDKN1a* (Table A.2). Interestingly, many proteins associated with keratinocyte differentiation including four members of the Late cornified envelope (*LCE*) gene cluster on chromosome 1q and two members of the Keratin–associated protein 2 (*KRTAP2*) gene cluster on chromosome 17q were also significantly downregulated (Table 4.1). Some of these gene expression changes were investigated by RT-qPCR in IMR-90 ER:RAS cells infected with either vector, shARID1B, shp53 and shp16 (Figure 4.3). This data served to confirm that ARID1B ablation during OIS results in gene expression changes in important senescence pathways.

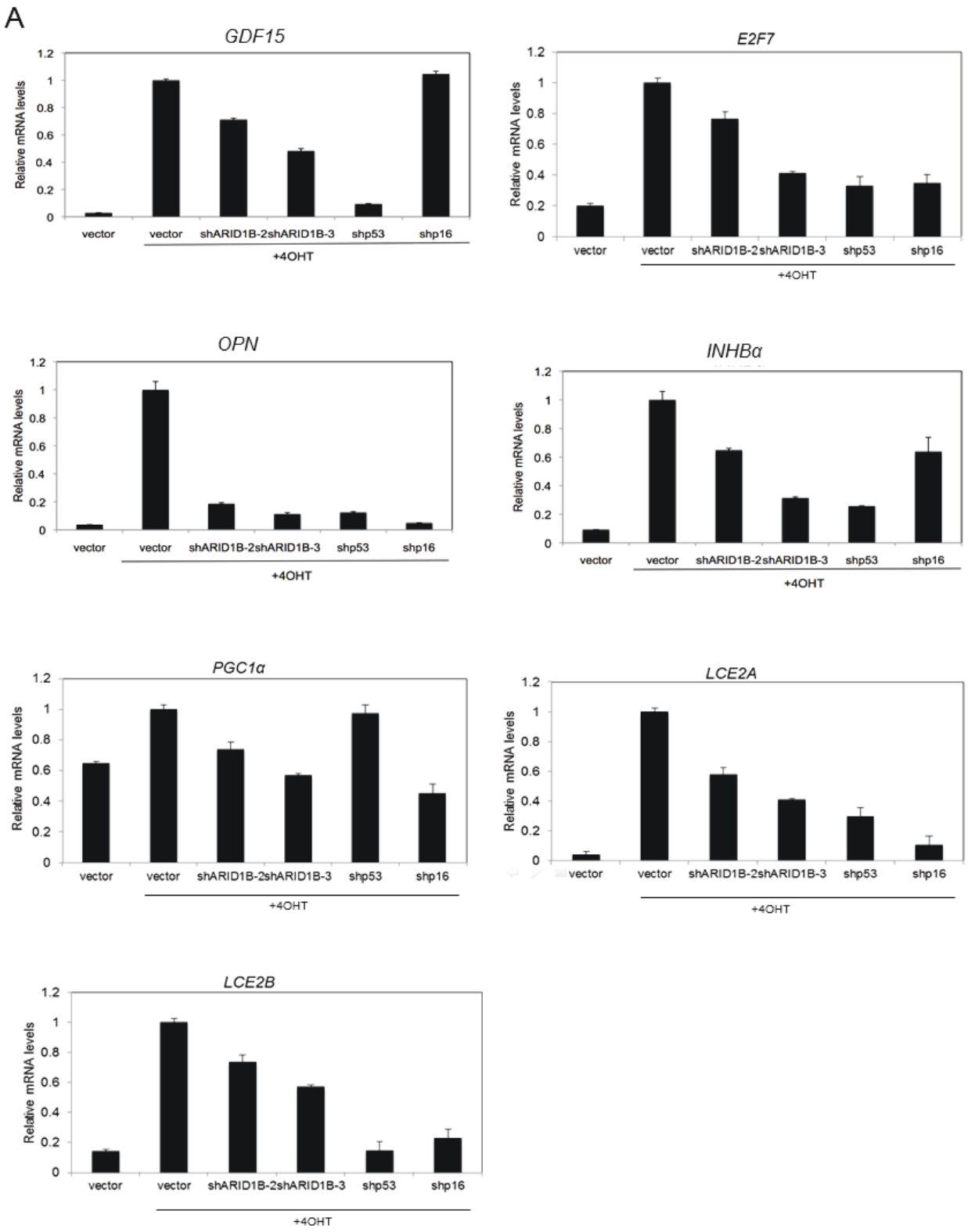


Figure 4.3. Validation of gene expression changes associated with ARID1B knockdown during OIS. (A) IMR-90 ER:RAS at passage 13 were infected with the indicated constructs and selected. Cells were grown with 100 nM 4OHT to activate the ER:RAS protein or with DMSO to act as a control. $3x10^5$ cells were grown in a 10 cm plate and treated and untreated cells were collected 6 days later. Graphs show changes in selected genes upon depletion of ARID1B during OIS.

4.4. Expression of oncogenic PIK3CA^{H1047R} induces senescence

As previously discussed, aberrant activation of the PI3K pathway induces a stable senescence response (Astle et al., 2012; Steelman et al., 2011). To study the effect of ARID1B on PI3K induced senescence, I first overexpressed several PIK3CA mutants (data not shown). One such mutant, PIK3CA^{H1047R}, harbours a mutation in the PIK3CA kinase domain resulting in constitutive activation of the kinase (Ligresti et al., 2009). To test if PIK3CA^{H1047R} induces senescence, I infected IMR-90 cells with PIK3CA^{H1047R}, mutant RAS^{G12V} or a control. Activation of PI3K was investigated by measuring the phosphorylation status of AKT (a downstream target of PI3K) using quantitative IF. PIK3CA^{H1047R} expressing cells had elevated levels of phospho-AKT (Serine 473) when compared to vector expressing cells confirming that the PIK3CA^{H1047R} mutant is active (Figure 4.4.1A). In response to PIK3CA^{H1047R} expression, IMR-90 cells adopted a flattened, enlarged morphology with numerous vesicles contained within the cytoplasm and cell growth was limited substantially compared to vector cells (Figure 4.4.1B, C and Figure 4.5C). PIK3CA^{H1047R} infected cells also displayed a higher level of SA-β-Gal activity when compared to vector infected cells. However the levels of SA-β-Gal activity were lower than that observed in RAS^{G12V} expressing cells (Figure 4.4.1D). Therefore expressing PIK3CA^{H1047R} can induce senescence in IMR-90 cells.

Recently, ARID1B was identified as a cancer gene, frequently mutated in breast cancer (Stephens et al., 2012). Tumours harbouring ARID1B mutations were also associated with mutations in PIK3CA and PTEN, suggesting possible cooperation between ARID1B mutations and abrogated PI3K signalling during tumourigenesis . Similarly in ovarian clear cell carcinoma (OCCC), ARID1A mutations occur in 57% of tumours (Jones 2010). Loss of ARID1A frequently coexists with PIK3CA mutations in OCCC, suggesting that these events are not mutually exclusive (Jones et al., 2010; Yamamoto et al., 2012a, b).

To further characterise the senescence response observed upon PIK3CA^{H1047R} expression. IMR-90 cells infected with control, mutant PIK3CA^{H1047R} or mutant RAS^{G12V} were subjected to quantitative IF. Protein expression of p16^{INK4a}, p21^{CIP1} and p53 increased upon PIK3CA^{H1047R} expression; however levels of the effectors were not as high as that induced by RAS^{G12V} (Figure 4.4.2A). Similar results were observed by RT-qPCR (Figure 4.4.2B). In conclusion, a senescence response is induced by ectopically expressing PIK3CA^{H1047R}.

4.5. Knockdown of ARID1B attenuates PIK3CA^{H1047R} mediated senescence

To test if ARID1B has a role in PIK3CA^{H1047R} mediated senescence, I investigated the effect of ARID1B knockdown in PIK3CA^{H1047R} expressing cells. IMR-90 were double infected with either mutant PIK3CA^{H1047R} or empty vector and with hairpins targeting either ARID1B or control hairpins. PIK3CA^{H1047R} expressing cells, infected with shARID1B-3, had a higher percentage of BrdU positive cells and formed more colonies at low density compared to control PIK3CA^{H1047R} expressing cells, confirming that ARID1B depletion increases proliferation in PIK3CA^{H1047R} expressing cells (Figure 4.5A, B). Furthermore, cells appeared less flat and contained less vesicular structures when ARID1B was knocked down during PIK3CA^{H1047R} induced senescence (Figure 4.5C). PIK3CA^{H1047R} expressing cells with p16^{INK4a} knockdown were able to form highly dense colonies, which did not appear to be contact inhibited (Figure 4.5C). Together these data suggest that ARID1B is important in PIK3CA^{H1047R} mediated senescence.

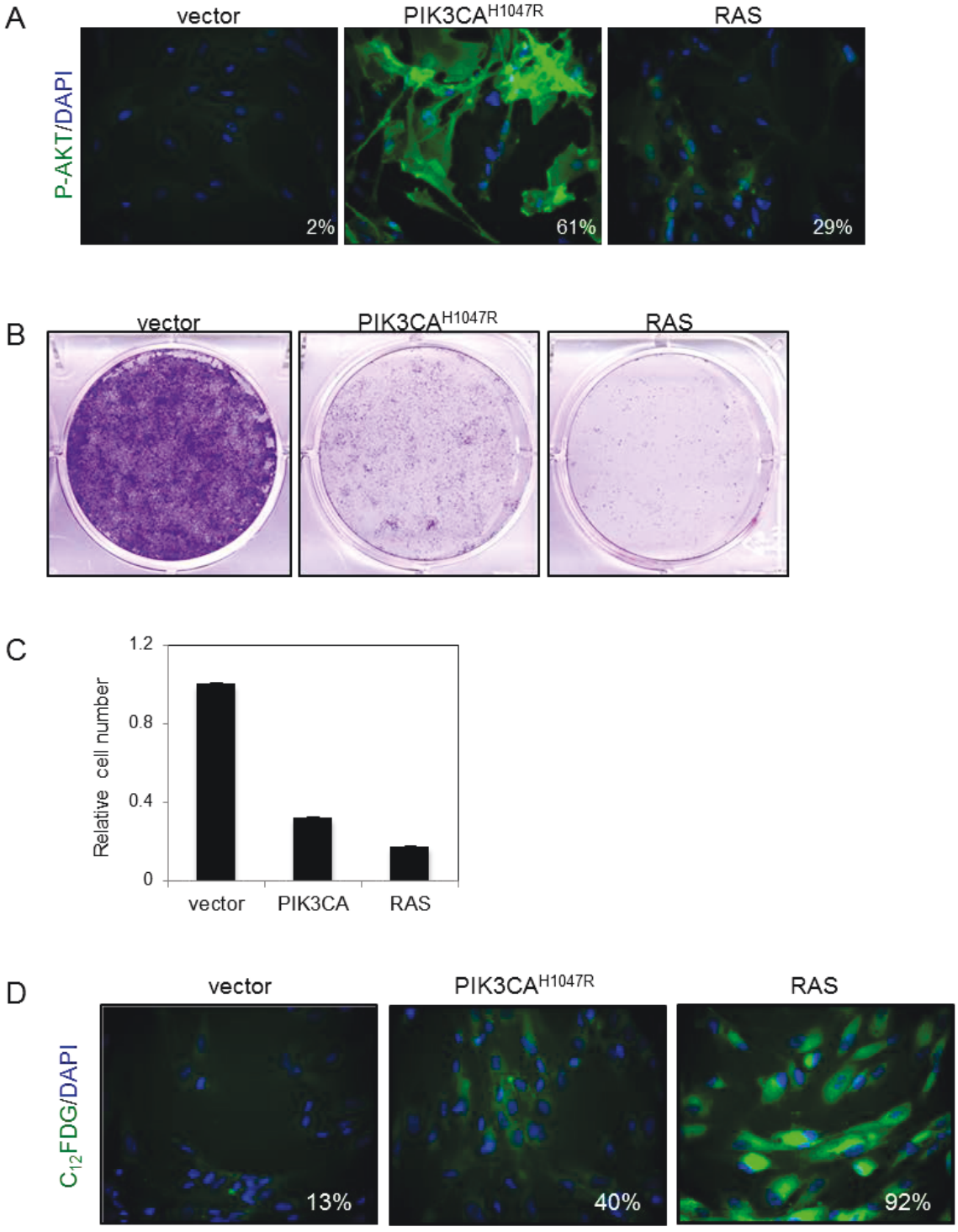


Figure 4.4.1. Expression of oncogenic PIK3CA^{H1047R} induces senescence. (A) IMR-90 cells were infected with the indicated constructs and following selection 4x10^4 cells were plated per well in a 96-well plate. 2 days later cells were fixed and stained with Phospho-AKT (Ser473) to assess PI3K activation, numbers indicate percentage of positive cells assessed by quantitative IF. **(**B,C) IMR-90 cells were infected with a control vector, mutant PIK3CA^{H1047R} or mutant RAS^{G12V}. Following selection 10^4 cells were seeded per 6-well plate. (A) Cells were fixed 12 days later and stained with crystal violet. (B) Crystal violet was extracted with acetic acid and quantified by measuring absorbance levels. Relative cell number was calculated by normalising quantities to vector. (C) Percentage of indicated cells positive for SA-β-Gal activity using fluorescence visualisation of the product of hydrolysed C_{12}FDG, a non-fluorogenic substrate for β-galactosidase.

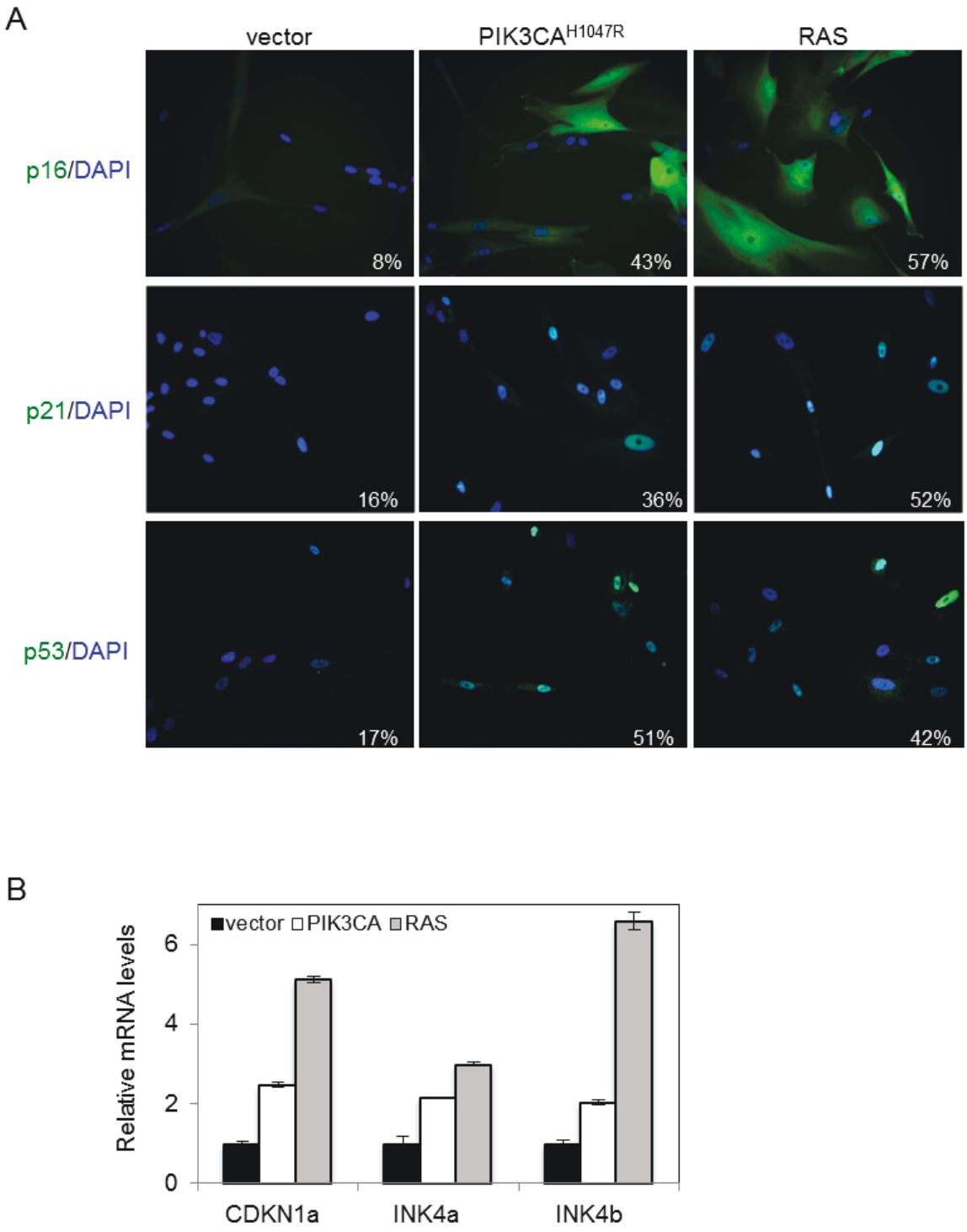


Figure 4.4.2. Characterisation of the senescence response induced upon PIK3CA^{H1047R} expression. (A) IMR-90 cells infected with vector, mutant PIK3CA^{H1047R} or mutant RAS^{G12V} were subjected to IF to assess levels of p21^{CIP1}, p16^{INK4a} and p53. Numbers indicate percentage of positive cells assessed by quantitative IF. (B) Gene expression was assessed in IMR-90 cells infected with the indicated constructs, showing cells overexpressing PIK3CA^{H1047R} express higher levels of important CDKIs.

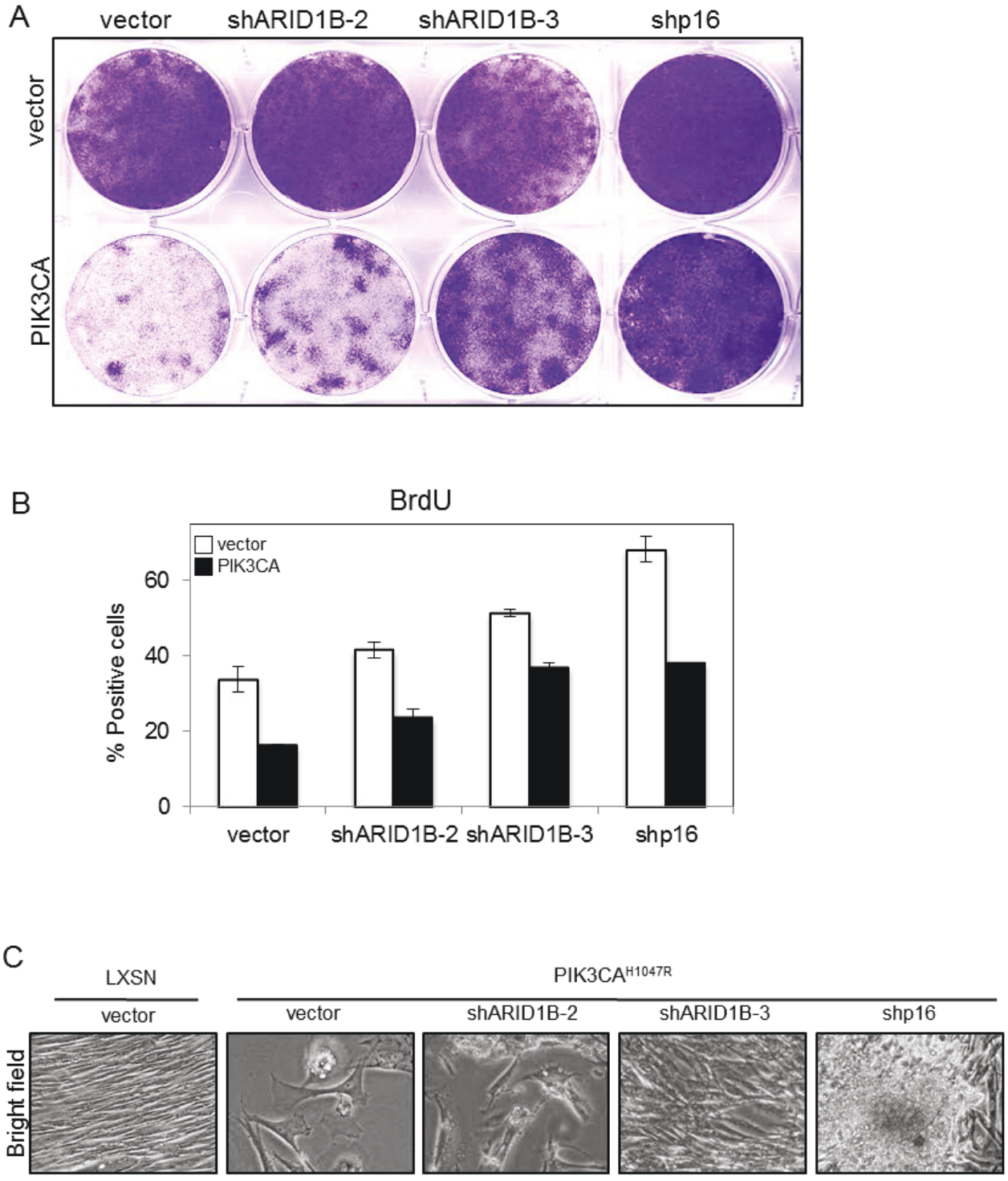


Figure 4.5. Knockdown of ARID1B attenuates PIK3CA^{H1047R} mediated senescence. (A-C) passage 13 IMR-90 were double infected with either mutant PIK3CA or LXSN empty vector and the indicated constructs, and selected. (A) 1.5x10^4 cells were seeded in a 6-well plate. 20 days later cells were fixed and stained with crystal violet. (B) Proliferation was evaluated by BrdU incorporation. (C) 5x10^5 cells were seeded per 10 cm dish and bright field images were taken 13 days later.

4.6. ARID1B regulates $p16^{INK4a}$ and $p21^{CIP1}$ expression during PIK3CA-induced senescence

I next investigated whether the senescence bypass mediated by ARID1B knockdown in $PIK3CA^{H1047R}$ expressing cells is similar to that seen in RAS expressing cells when ARID1B is depleted. Quantitative IF and RT-qPCR was used to assess changes in levels of $p16^{INK4a}$ and $p21^{CIP1}$ in ARID1B ablated cells. As with OIS, the levels of both CDKIs decreased when ARID1B was depleted in cells expressing $PIK3CA^{H1047R}$ suggesting ARID1B controls gene expression of *CDKN1a* and *INK4a* during PIK3CA-induced senescence (Figure 4.6A-C).

4.7. High expression of SWI/SNF complex components during replicative senescence

As ARID1B knockdown delays senescence, I next asked whether the levels of ARID1B change as cells approach senescence. In young IMR-90 (passage 11), ARID1B expression was low and gradually increased during replicative senescence (from passage 19 to passage 26), as detected by immunofluorescence (Figure 4.7A). Similar changes were observed with core SWI/SNF components BRG1, BRM and SNF5 (Figure 4.7A). Furthermore, ARID1B levels also increased upon serial passage of MEFs (Figure 4.7B).

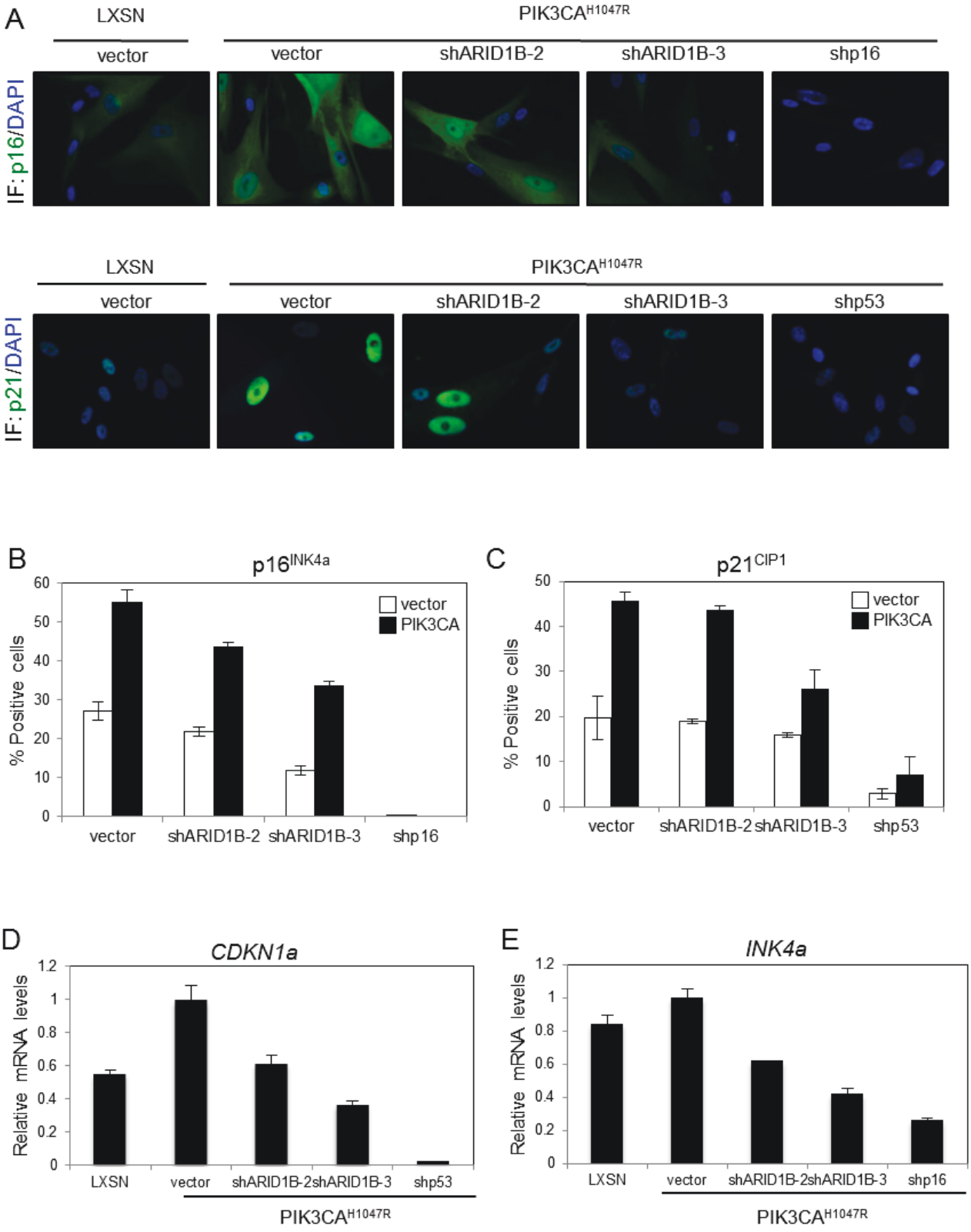


Figure 4.6. ARID1B regulates $p16^{INK4a}$ and $p21^{CIP1}$ during PIK3CA-induced senescence. (A-E) passage 13 IMR-90 were double infected with either mutant PIK3CA or LXSN empty vector and the indicated constructs, and selected. (A-C) $4x10^3$ cells were plated in a 96-well dish and fixed 2 days later. $p21^{CIP1}$ and $p16^{INK4a}$ levels were assessed by quantitative IF. (D,E) Knockdown of ARID1B in $PIK3CA^{H1047R}$ expressing cells reduces the gene expression of *CDKN1a* and *INK4a*.

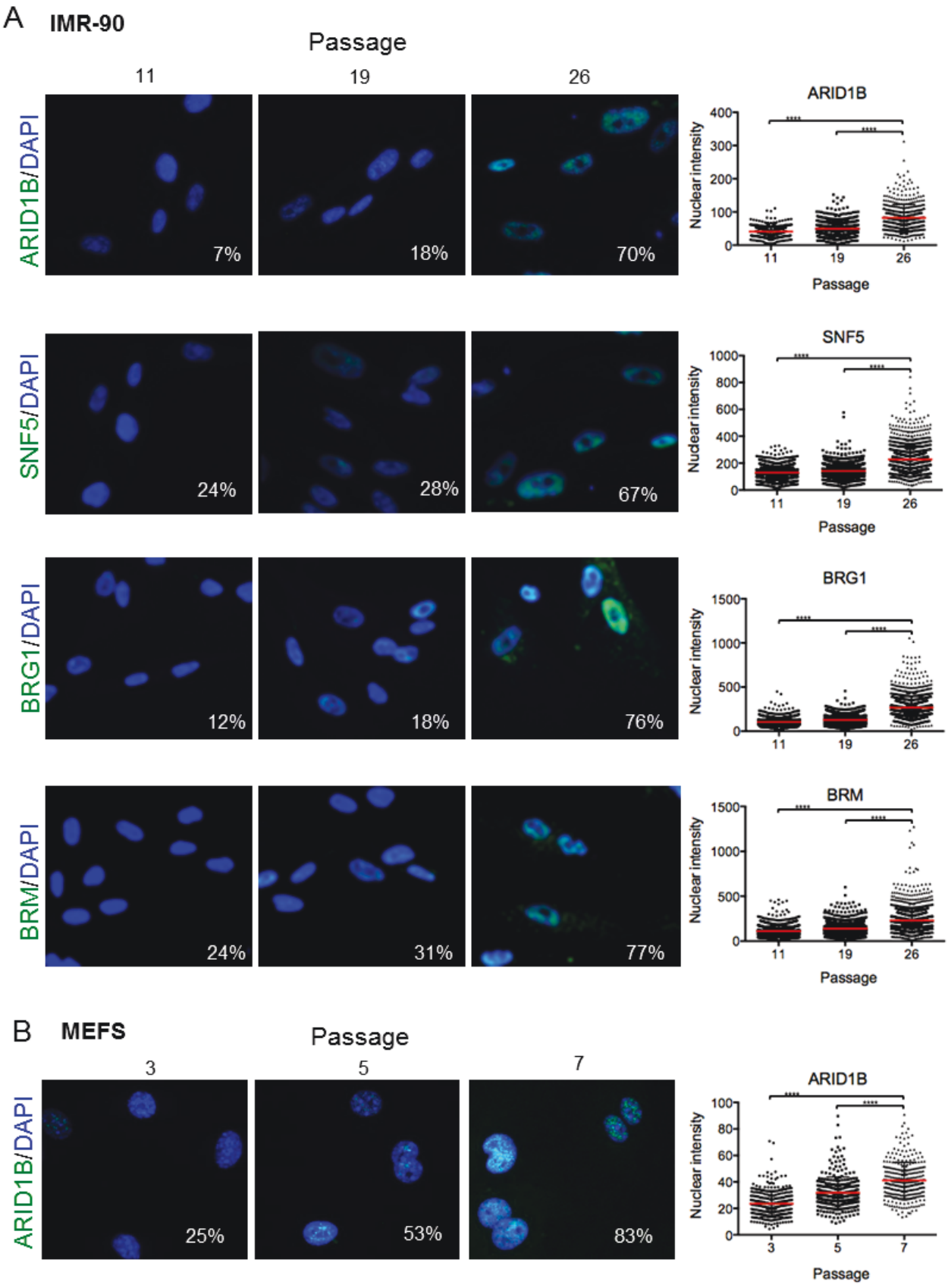


Figure 4.7. Expression of SWI/SNF complex increases during replicative senescence. (A,B) Human (IMR-90) and mouse (MEFs) fibroblasts at the indicated passages subjected to quantitative IF using antibodies targeting indicated SWI/SNF components. Numbers represent percentage of positive cells. ****P<0.0001.

4.8. Expression of SWI/SNF complex components increases during OIS

To see if the expression of SWI/SNF components is increased during OIS, Iassessed the levels of SWI/SNF proteins in IMR-90 and MEFs expressing RAS^{G12V}. I found that cells expressing RAS^{G12V} displayed elevated protein levels of certain SWI/SNF components (Figure 4.8A, B). Elevated SWI/SNF protein levels were also detected during $PIK3CA^{H1047R}$ induced senescence, and ARID1B levels also increase in IMR-90 ER:RAS cells upon 4OHT treatment (data not shown). In contrast quiescent cells, arrested by serum starvation, show similar levels of SWI/SNF proteins to proliferating cells (Figure 4.8A). Taken together the data indicates there are increased levels in SWI/SNF proteins during senescence consistent with a recent study demonstrating the upregulation of chromatin-associated BRG1 in cells expressing RAS^{G12V} (Tu et al., 2013). I also show that this is not associated with reversible forms of cell cycle arrest but is specific to senescence.

4.9. Post-translational stabilisation of the SWI/SNF complex during senescence

I next sought to investigate if the increase in SWI/SNF levels during senescence was mediated by changes in transcription. For this purpose I conducted RT-qPCR analysis in senescent cells and non-senescent cells using primers specific to SWI/SNF subunits and to senescence associated CDKIs as a control (Figure 4.9A, B). Furthermore, I utilised data from gene expression profiling to assess the differential gene expression of IMR-90 ER:RAS cells undergoing OIS (Figure 4.9C). In both cases, mRNA levels of the majority of SWI/SNF subunits remained constant during both replicative senescence and OIS, suggesting that the increase in SWI/SNF expression during senescence is regulated post-transcriptionally.

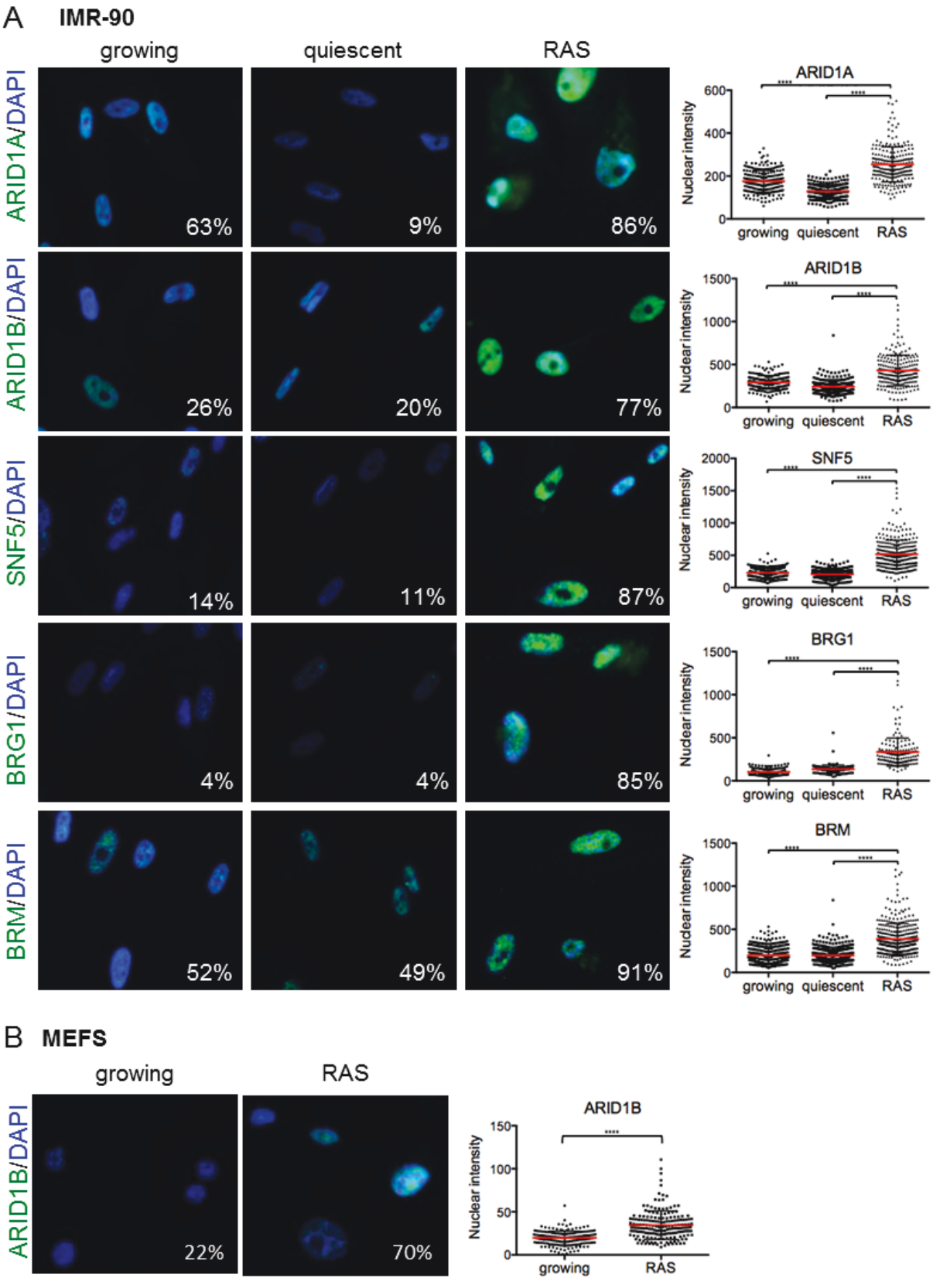
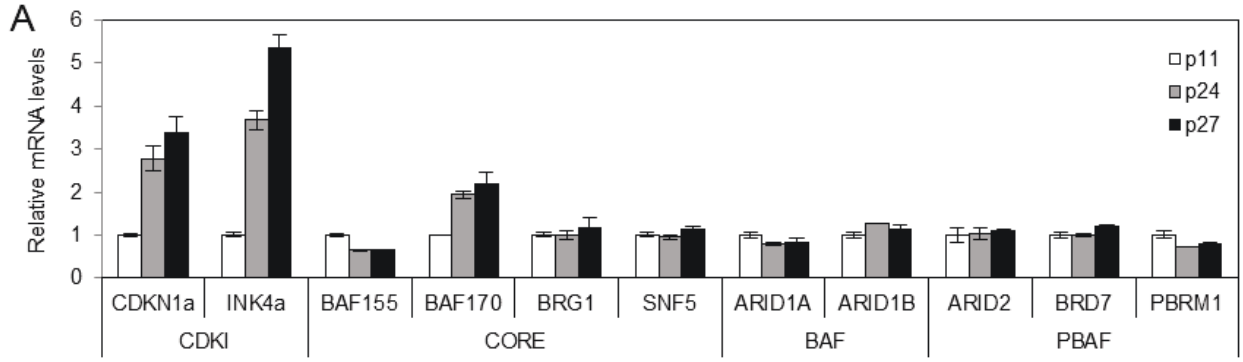
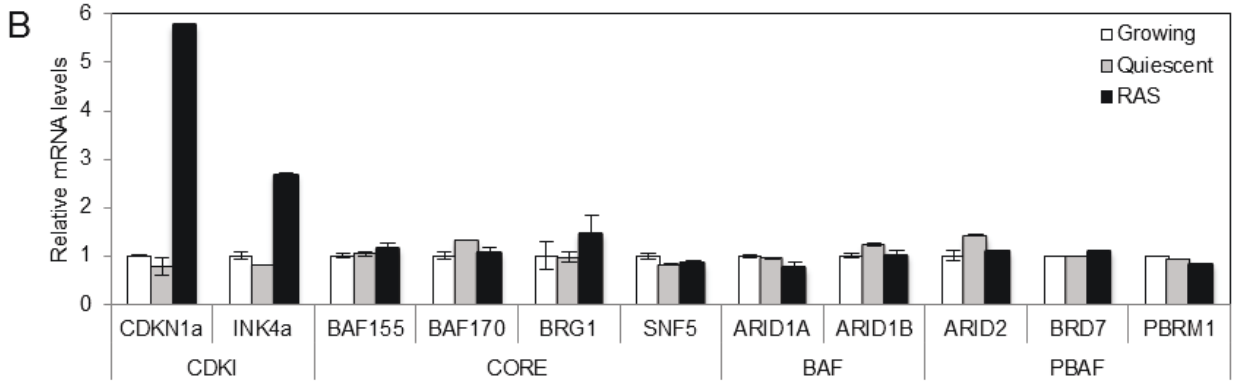


Figure 4.8. Expression of SWI/SNF complex increases during OIS. (A) Growing, quiescent (serum starved) or senescent (RAS^{G12V} expressing) cells were subjected to IF using antibodies targeting various SWI/SNF components. Numbers represent percentage of positive cells. (B) Quantitative IF of Arid1b expressing cells in MEFs infected with empty vector or RAS^{G12V}. Numbers represent percentage of positive cells. ****P<0.0001.





C

		4OHT/control
CDKI	CDKN1a	1.61
	INK4a	1.41
CORE	BAF155	0.99
	BAF170	0.83
	BRG1	1.17
	BRM	0.73
	SNF5	0.81
BAF	ARID1A	0.83
	ARID1B	0.92
PBAF	ARID2	1.09
	BRD7	0.88
	PBRM1	0.85
ACCESSORY	BAF45A	1.11
	BAF45B	1.02
	BAF45C	0.99
	BAF45D	0.48
	BAF53A	0.99
	BAF53B	1.08
	BAF57	0.67
	BAF60A	1.00
	BAF60B	1.02
	BAF60C	0.76
	ACTIN	0.96



Figure 4.9. Increase in expression of SWI/SNF subunits is not transcriptionally regulated. (A) IMR-90 cells were collected for RNA extraction at indicated passages. Gene expression levels of CDKIs and various SWI/SNF components were assessed by RT-qPCR. (B) Growing, quiescent (serum starved) and senescent (RAS^{G12V} expressing) cells were collected for RNA extraction. Gene expression levels of CDKIs and various SWI/SNF components were assessed by RT-qPCR. (C) IMR-90 ER:RAS cells treated with 4OHT or with DMSO were collected for expression profiling. Fold changes of important CDKIs and SWI/SNF components are shown as a ratio of 4OHT treated cells to control cells.

4.10. SILAC based quantitative proteomics identifies changes in the levels of ARID1B binding proteins during OIS

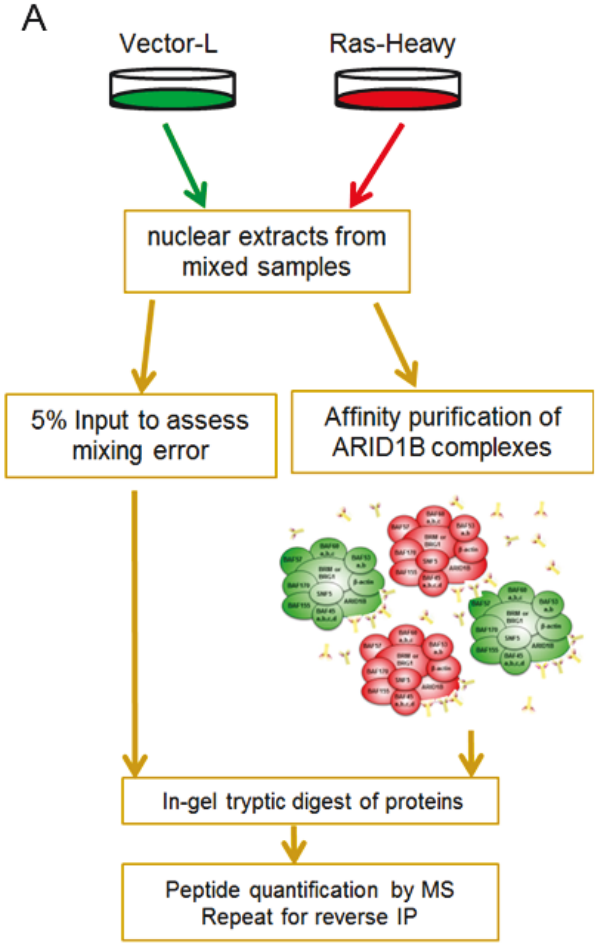
As previously described, mammalian SWI/SNF complexes undergo subunit exchange during differentiation and other processes (Takeuchi and Bruneau, 2009; Wang et al., 1996a; Yoo et al., 2009). To further understand how the complex functions it is important to identify the composition of the complex and its interactors. Quantification of protein-protein interactions is favourable to discriminate specific interactions from background binding (Vermeulen et al., 2008). SILAC can be used to quantify changes in SWI/SNF subunit compositions in different cell types (Ong et al., 2002). Co-immunoprecipitations (co-IPs) coupled to MS have previously facilitated the discovery of the esBAF, npBAF and nBAF complexes (Ho et al., 2009b; Wu et al., 2007; Yoo et al., 2009). It is therefore worth investigating if a 'senescence-associated SWI/SNF complex' exists or whether there is an indiscriminative upregulation of all subunits associated with the complex. Furthermore, it may be possible to determine if the post-transcriptional increase in various SWI/SNF proteins is due to stabilisation of the complex via interactions with other proteins specifically in senescence.

SILAC-IPs were performed to identify changes in proteins interacting with ARID1B in cells infected with either RAS^{G12V} or vector (Figure 4.10A). Importantly a "5% input" sample was taken to assess the mixing error and to determine if a protein was enriched in the immunoprecipitated sample (Figure 4.10A). ARID1B immunoprecipitation antibody was validated by performing IP-Western using two ARID1B antibodies that recognize different epitopes (Figure A1.A). Similarly the ability to co-immunoprecipitate SWI/SNF components was tested by performing an ARID1B IP followed by BRG1 detection using Western blot (Figure A1.B). Initial analysis of the data indicated that the IPs were specific, detecting all core components of the SWI/SNF complex (BRG1, BRM, SNF5, BAF155, BAF170). As expected, mutually exclusive subunits, ARID1A and PBAF specific peptides (PBRM1, ARID2, BRD7, BAF45A) were not detectable in ARID1B IPs however were present in similar IP/MS performed with BRG1 (data not shown).

Although the IPs did not show a change in the levels of most SWI/SNF components during OIS, a number of proteins were associated with ARID1B preferentially during OIS (Figure 4.10B). Strikingly, proteins with the greatest increase in ARID1B binding in RAS^{G12V} expressing cells were associated with the nucleolar compartment (KRI1, KRR1, RRP8, NO66, LYAR), which may reflect an overall change in nucleolar structure during OIS (Narita et al., 2003a) (Figure 4.10B). Some of the detected proteins shown to interact with ARID1B were involved in cell proliferation including Ly1 antibody reactive (LYAR), putative ribosomal RNA methyltransferase (NOP2), Lamin-A (LMNA) eukaryotic initiation factors 3D and 3E (EIF3D, EIF3E) and regulator of chromosome condensation 2 (RCC2), (Figure 4.10B) (Fonagy et al., 1994; Huang et al., 2008b; Mollinari et al., 2003; Su et al., 1993; Watkins and Norbury, 2004).

Further SILAC-IPs were conducted to establish proteins associated with ARID1B in cells overexpressing ARID1B. The majority of the SWI/SNF complex was enriched in the pull downs when ARID1B is expressed; notably the only isoform of BAF45 that was enriched when ARID1B is overexpressed was BAF45D (Figure 4.10C) and this protein together with KRI1 homologue (KRI1) and NFκB repressing factor (NKRF) were found enriched in the complex in both RAS^{G12V} and ARID1B expressing cells (Figure 4.10B, C). The majority of the proteins interacting with ARID1B were associated with transcription and elongation, in support of previous evidence for a role of SWI/SNF in this process (Drost et al., 2010; Staal et al., 2000).

A



B

Gene	Ratio Ras/Vec
KRI1	2.48
KRR1	1.81
RRP8	1.79
NO66	1.78
INTS1	1.78
ZNF687	1.76
INTS2	1.76
INTS10	1.73
INTS3	1.73
LYAR	1.73
NKRF	1.71
WDR18	1.69
NOP2	1.68
ZGPAT	1.67
BAF60B	1.66
LMNA	0.75
EIF3D	0.75
BAF60C	0.74
RCC2	0.73
EIF3E	0.72
FXR1	0.7
LEPREL4	0.57
BAZ1B	0.53

C

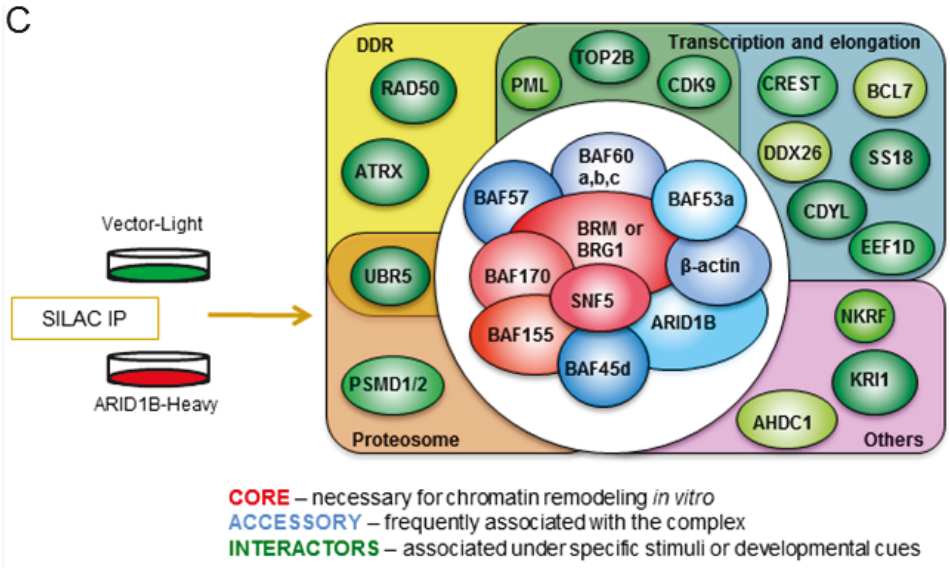


Figure 4.10. SILAC based quantitative proteomics identifies SWI/SNF interactor exchange during OIS. (A) Protocol for detection of proteins associated with ARID1B in growing and senescent cells. (B) Table of ARID1B associated proteins identified as having the greatest change in abundance during senescence. (C) Proteins bound to ARID1B when ARID1B is overexpressed and stabilised, most notably levels of the majority of SWI/SNF subunits increase upon ARID1B overexpression as well as proteins associated with transcription and elongation.

4.11. ARID1B is excluded from regions of repressed chromatin

As ARID1B was shown to bind to a number of transcriptional regulators, it was of interest to dissect the relationship between ARID1B and active or repressed chromatin. In particular it was recently shown that BRG1 is an important factor required for SAHF formation (Tu et al., 2013), and that overexpression of SWI/SNF subunits increases the formation of SAHFs (Figure 4.13.2) (Tu et al., 2013). SAHFs can be identified by the presence of H3K9me^3 and H3K27me^3 layers at the site of condensed heterochromatin (Chandra et al., 2012; Narita et al., 2003a). To identify the correlation between ARID1B and SAHFs, cells expressing RAS^{G12V} were probed with antibodies targeting either H3K9me^3 or H3K27me^3 simultaneously with ARID1B (Figure 4.11A). Expression of RAS^{G12V} in IMR-90 human fibroblasts resulted in the formation of SAHFs and the presence of a single large nucleolus as previously described (Figure 4.11A) (Narita et al., 2003a). Interestingly, ARID1B appeared to be excluded from SAHFs as shown by confocal imaging (Figure 4.11A). Fluorescence intensity profiles demonstrated the non-overlapping nature of ARID1B with both H3K9me^3 and H3K27me^3 (Figure 4.11A). In particular areas stained with ARID1B were void of the H3K27me^3 mark, suggesting that ARID1B is generally associated with active chromatin (Figure 4.11A white arrow heads).

In support of this notion, growing cells were probed with BrdU, to identify sites of DNA replication, that correlate with H3K27me^3, in IMR-90 (Chandra et al., 2012). Similarly to H3K27me^3 staining, ARID1B was shown to exclude BrdU staining and vice versa (Figure 4.11B white arrow heads). This data, together with the binding of ARID1B to proteins involved in transcription and elongation, suggest ARID1B is associated with active chromatin regions.

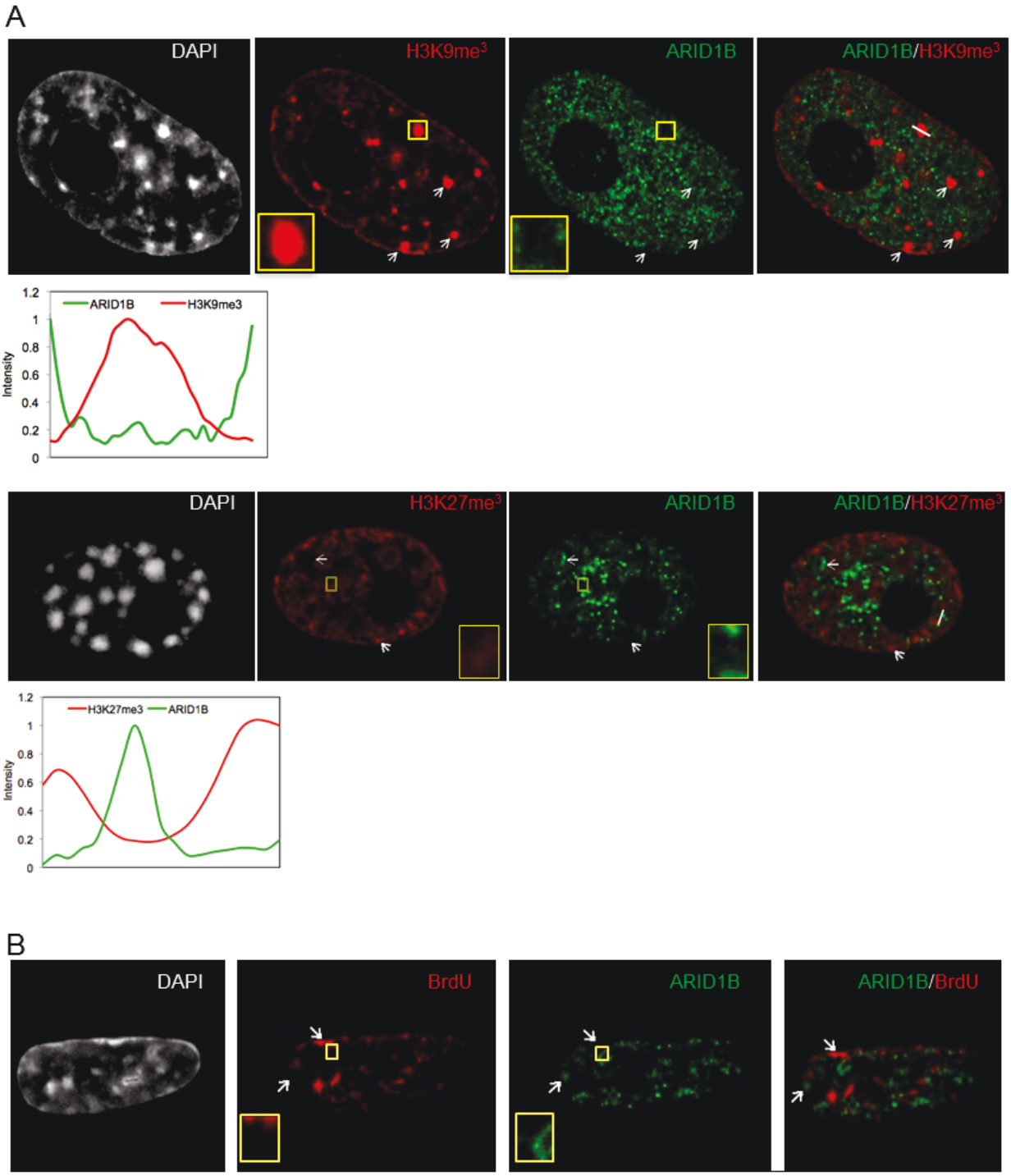


Figure 4.11. ARID1B is excluded from regions of repressed chromatin. (A) IMR-90 cells expressing RAS^{G12V} were fixed and stained with antibodies targeting ARID1B and either of two repressive histone marks $H3K9me^3$ or $H3K27me^3$. Confocal images acquired using a 40x objective demonstrate that ARID1B is excluded from areas stained with $H3K9me^3$ or $H3K27me^3$ and vice versa. The region indicated by the yellow rectangle is magnified. The white line indicates the path over which the fluorescent intensity was profiled as shown in the corresponding graph. White arrowheads depict areas where exclusion of either ARID1B or indicated histone marks is seen. (B) IMR-90 cells were incubated with BrdU for 16hrs and fixed. Cells were stained with antibodies targeting ARID1B and BrdU. Confocal images show ARID1B does not localise to sites of DNA synthesis.

4.12. Retroviral constructs overexpressing ARID1A and ARID1B

As components of the SWI/SNF complex are induced during senescence, it was important to determine the effect of overexpression of SWI/SNF proteins in young IMR-90 cells. For this end, retroviral vectors expressing ARID1A and ARID1B were cloned. The expression of proteins from these vectors was first verified by quantitative IF (Figure 4.12A, B). Expression of ARID1A and ARID1B was simultaneously probed using antibodies raised in different species. Interestingly the results showed that overexpression of ARID1B resulted in a significant decrease in ARID1A protein levels (Figure 4.12A, B). A similar effect was not seen at the transcriptional level, as overexpression of ARID1B did not significantly change *ARID1A* mRNA levels. The data verifies that ectopic expression of ARID1A and ARID1B retroviral constructs increases the levels of the respective proteins at both the protein and RNA level.

4.13. Ectopic expression of SWI/SNF subunits induces premature senescence

To complement the findings observed using ARID1B shRNAs, ARID1B and other SWI/SNF proteins were ectopically expressed to explore their effects on cell proliferation. Expression of SWI/SNF components in IMR-90 cells caused a reduction of cell growth and cells exhibited characteristic features of senescence (Figure 4.13.1-2). The induction of growth arrest was confirmed by colony formation assays, and by the appearance of enlarged flat cells (Figure 4.13.1A). Although in IMR-90 human fibroblasts the SWI/SNF induced growth arrest was not as striking as that produced by RAS^{G12V}, the proportion of cells staining positively for SA-β-Gal activity increased greatly from <1% in vector expressing cells to around 36-47% in cells expressing various components of the SWI/SNF complex (Figure 4.13.1A).

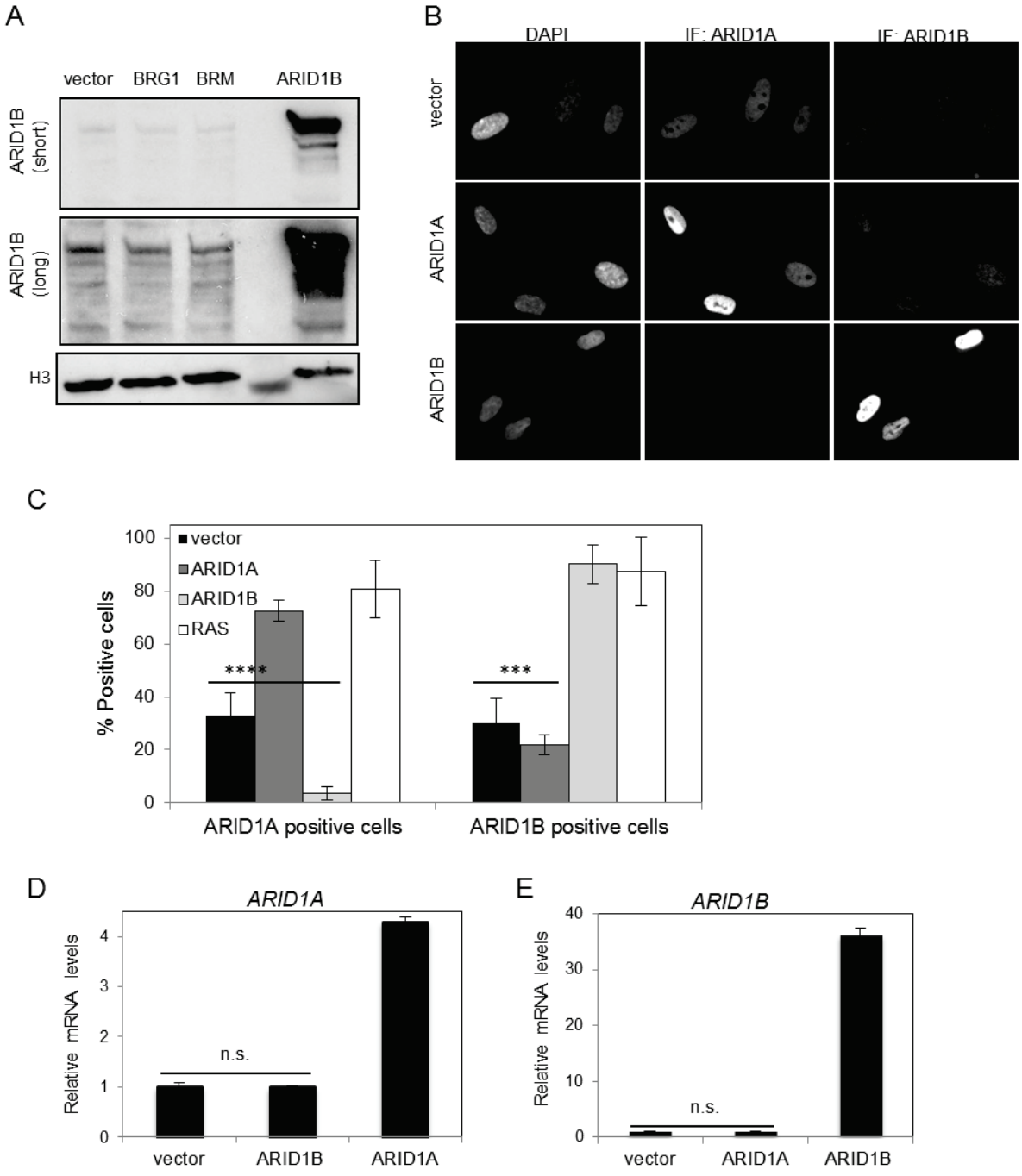


Figure 4.12. Retroviral constructs overexpressing ARID1A and ARID1B. (A) IMR-90 were infected with the indicated constructs and western blot analysis was used to assess the expression of ARID1B protein (B,C) IMR-90 were infected with the indicated constructs and IF was used to simultaneously assess the expression levels of ARID1A and ARID1B in cells. Overexpression of ARID1B results in a dramatic decrease in ARID1A protein levels as assessed by quantitative IF. (C,D) IMR-90 were infected with the indicated constructs. Following selection total RNA was extracted from cells and RT-qPCR was used to assess the level of ARID1A and ARID1B expression in indicated cells showing no change in transcript levels of mutually exclusive subunits upon overexpression of either ARID1A or ARID1B. ****P<0.0001, ***P<0.0002, n.s., not significant

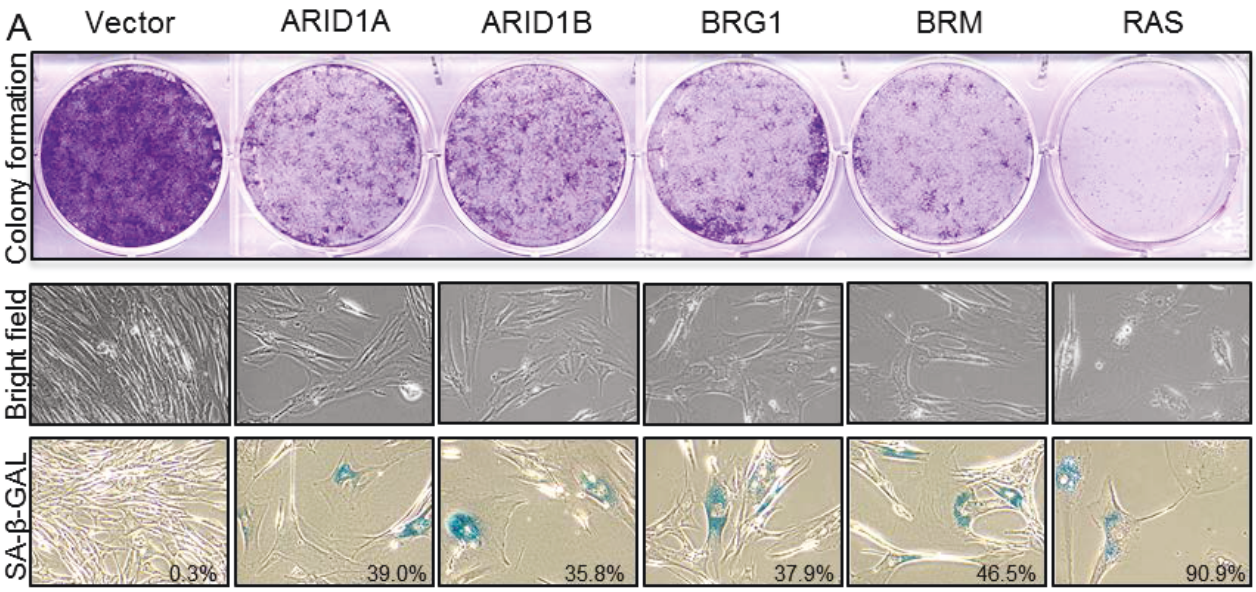


Figure 4.13.1. Overexpression of SWI/SNF subunits induces premature senescence. (A) Passage 10 IMR-90 were infected with the indicated constructs and selected. 10^4 cells were plated in a 6-well plate and stained with crystal violet after 12 days. Overexpression of various components of the SWI/SNF complex decreases the colony formation ability of cells. $5x10^5$ cells were plated per 10 cm plate and bright field images of the indicated cells were taken 5 days later showing overexpression of SWI/SNF components induces a flat enlarged morphology in cells. SA-β-Gal activity was assessed by plating $3x10^3$ cells in a 6-well plate and fixed 13 days later. Cells overexpressing SWI/SNF components have a higher percentage of SA-β-Gal positive cells.

Expression of SWI/SNF components also decreased the population of cells in S-phase as seen by a decrease in BrdU incorporation (Figure 4.13.2). SAHF formation increased upon expression of specific SWI/SNF subunits (Figure 4.13.2). This increase in SAHF formation was particularly prominent in ARID1A and BRG1 expressing cells, in addition to this, ARID1A expressing cells had a higher level of $p16^{INK4a}$ expression (82.1% ± 0.6%) than other SWI/SNF components and vector cells (25.0% ± 0.8%) suggesting that ARID1A mediated senescence is predominantly achieved through activation of the $p16^{INK4a}$/Rb pathway (Figure 4.13.2). Aside from ARID1A, expression of other SWI/SNF components increased the levels of $p21^{CIP1}$ expression. The upregulation of $p21^{CIP1}$ was highest in ARID1B expressing cells where the increase went from 39.9% ± 0.3% in vector cells to 81.1% ± 3.5% in cells expressing ARID1B (Figure 4.13.2). Taken together these results as well as results from others suggest growth arrest mediated by expression of SWI/SNF components is achieved through activation of multiple pathways important in establishing senescence, including the $p16^{INK4a}$/RB1 pathway and

the p53/p21^{CIP1} pathway (Drost et al., 2010; Dunaief et al., 1994; Guan et al., 2011; Inoue et al., 2011; Lee et al., 2002a).

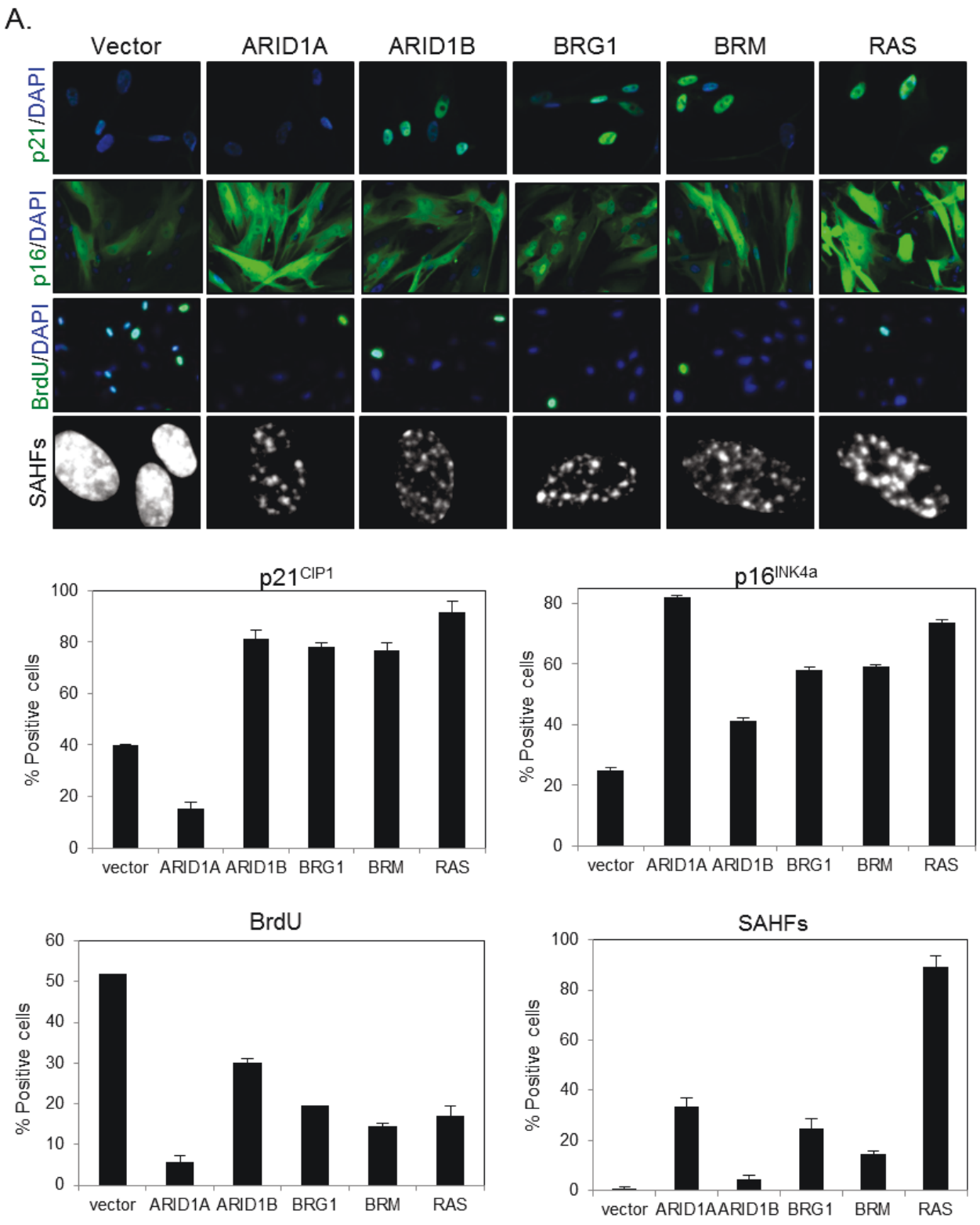


Figure 4.13.2. Molecular analysis of senescence induced by SWI/SNF subunits. (A) Expression of SWI/SNF subunits increases the percentage of $p21^{CIP1}$ and $p16^{INK4a}$ positive cells as determined by quantitative IF. Expression of indicated SWI/SNF components also delayed entry of cells into S-phase as measured by BrdU incorporation. For identification of SAHFs, cells were stained with DAPI and visualised by high-throughput microscopy using a 40x objective. Overexpression of ARID1A and BRG1 induces the formation of distinct SAHFs.

4.14. Premature senescence Induced by ARID1B is mainly p53 dependent

As ARID1B regulates the levels of p53 and $p21^{CIP1}$ in HeLa cells (Inoue et al., 2011), and induces $p21^{CIP1}$ and $p16^{INK4a}$ expression in IMR-90 human fibroblasts (Figure 4.13.2), it was important to explore the role of various senescence effectors in ARID1B-mediated growth arrest. For this purpose ARID1B was expressed together with hairpins targeting either $p21^{CIP1}$, $p16^{INK4a}$, p53 or an empty vector to act as a control. The knockdown efficiency of the hairpins was tested by RT-qPCR (Figure 4.14.1D).

Knockdown of $p21^{CIP1}$ and $p16^{INK4a}$ partially alleviated the growth arrest induced by ARID1B. In particular ARID1B cells with $p21^{CIP1}$ ablation formed colonies with reduced cell size (Figure 4.14.1C). P53 knockdown fully suppressed ARID1B-mediated proliferative arrest (Figure 4.14.1A-C), and a similar result was observed when ARID1B was expressed alongside Human Papilloma virus (HPV) proteins E6/E7 (E6 alone conferred a partial rescue of ARID1B mediated arrest), suggesting that p53 is important in ARID1B-mediated growth arrest (Figure 4.14.2).

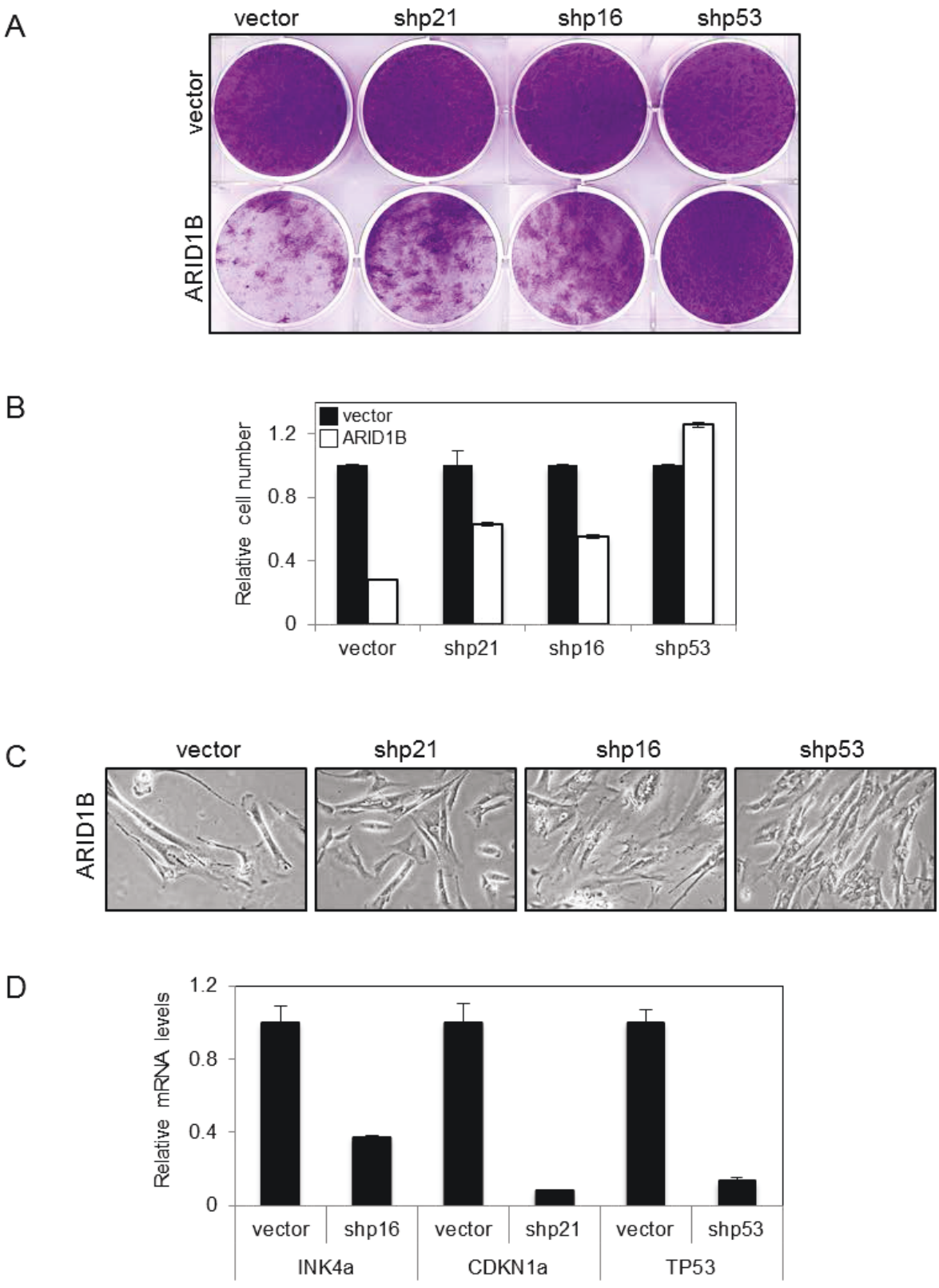


Figure 4.14.1. Knockdown of important senescence regulators alleviates ARID1B mediated senescence. (A,B) The ability of ARID1B to decrease proliferation in IMR-90 fibroblasts was fully rescued by co-expression of shRNAs targeting p53. $2x10^4$ cells were plated per 6-well plates and fixed and stained with crystal violet after 11 days. (B) Crystal violet was extracted with acetic acid and quantified. Graph indicates cell numbers relative to control cells. (C) $5x10^5$ cells were plated per 10 cm dish and bright field images were taken 6 days later (D) RT-qPCR showing the level of knockdown given by indicated hairpins in cells co-infected with pBabe puro (vector).

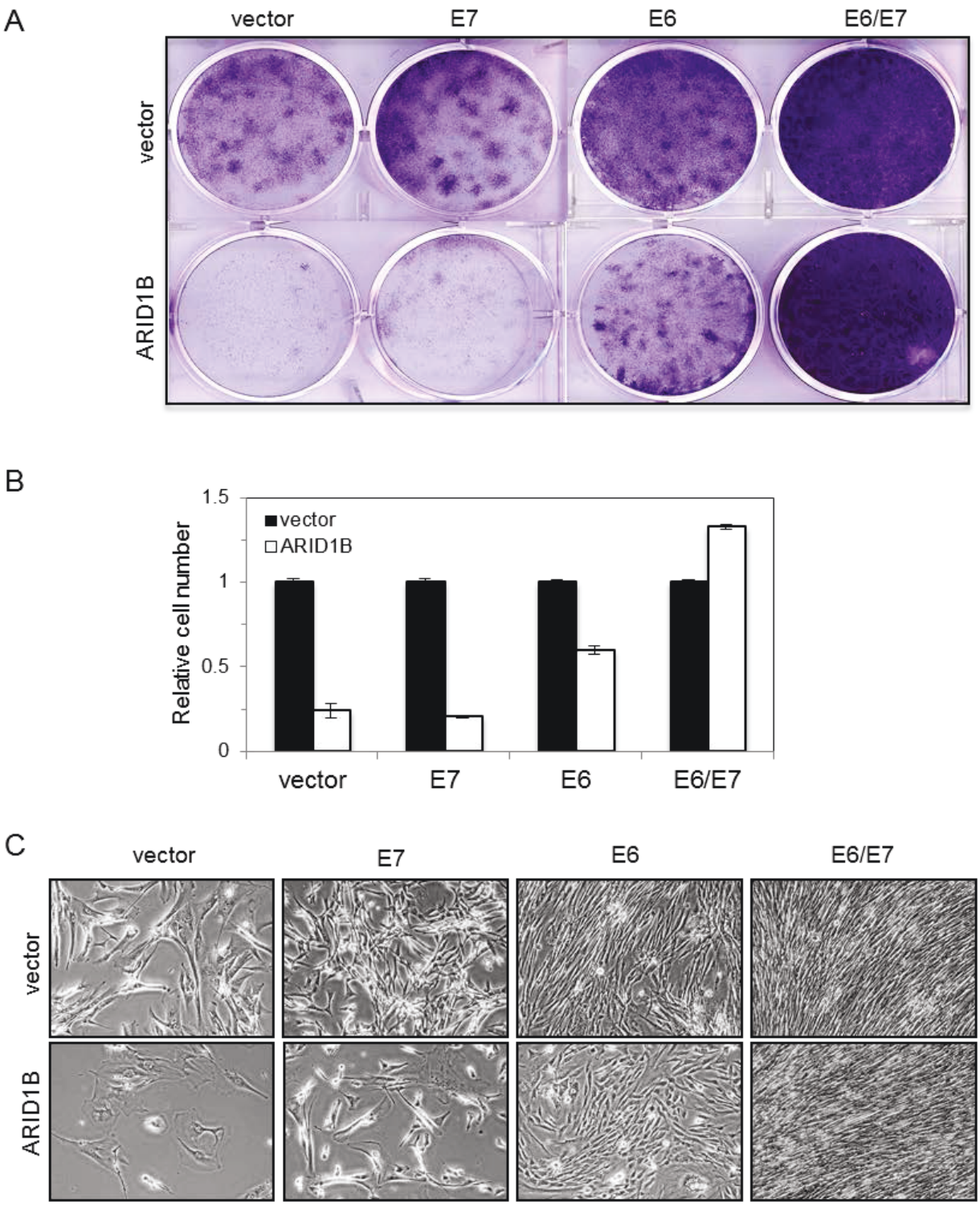


Figure 4.14.2. Co-expression of Human papillomavirus (HPV) oncoproteins alleviates ARID1B-mediated senescence. (A) Cells were co-infected with either a control vector or ARID1B and vectors containing E6, E7, E6/E7 or a control. After selection $2x10^4$ cells were plated per 6-well plate and fixed after 7 days. (B) Quantification of crystal violet staining of cells in (A) relative to control cells. (C) Bright field images of representative colonies formed from cells in (A).

4.15. Global changes in protein expression associated with ARID1B

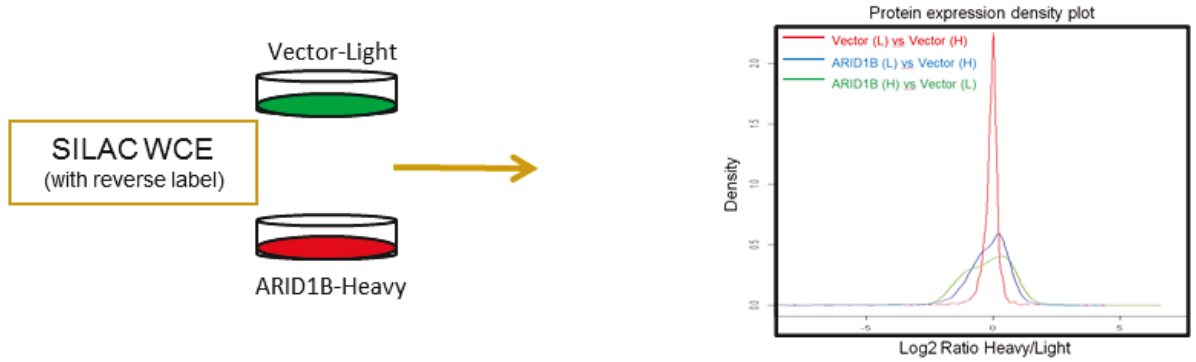
Mass spectrometry (MS)-based proteomics is a powerful tool to characterise changes in protein levels in different cell types. Here, SILAC was utilised to quantify global changes in protein levels upon ARID1B expression (Figure 4.15.1A). Protein identification and quantification was analysed as described in materials and methods and a total of 3312 proteins were detected above the threshold criteria. A protein density plot verified that there are changes in protein expression in IMR-90 cells expressing ARID1B, in both 'forward' and 'reverse' experiments (Figure 4.15.1A).

Proteins with the highest fold increase in ARID1B expressing cells were components of the SASP (including GDF15, IGFBP7 and ICAM1) and a change was observed in several other senescence-associated proteins (Figure 4.15.1B). Amongst the proteins that were downregulated in IMR-90 expressing ARID1B, were a number of cell cycle proteins (including CDC2, PCNA and MCM2) (Figure 4.15.1B). In corroboration with this Gene Ontology (GO) annotation showed that proteins associated with mitosis were negatively regulated by ARID1B expression (p-value 0.001) (Figure 4.15.1C). During senescence, cells increase the number of certain organelles including peroxisomes, lysosomes and mitochondria (Kurz et al., 2000; Lee et al., 2002b; Legakis et al., 2002). GSEA showed lysosomal proteins were highly enriched in ARID1B expressing cells (www.genome.jp/kegg/pathway), and proteins such as GLB1, LAMP1 and LAMP2 were all enriched more than 2.5 times (Figure 4.15.1C).

Interestingly the levels of many mitochondrial proteins were higher in IMR-90 expressing ARID1B, as shown by GSEA (www.geneontology.org) (Figure 4.15.2A). Other gene sets enriched upon ARID1B expression were also mitochondria related; the most highly enriched pathways were oxidative phosphorylation (www.genome.jp/kegg/pathway) and electron transport chain (www.reactome.org) (Figure 4.15.2A, B). As these processes are also altered in senescence, mitochondrial dysfunction may have a role in ARID1B mediated growth arrest (Hutter et al., 2004). In support of this hypothesis, ARID1B cells treated with the ROS scavenger N-acetyl-l-cysteine (NAC) proliferated faster than

untreated cells and did not present a senescent morphology (Figure 4.15.2C, D). Therefore ROS production plays an important role in ARID1B-mediated senescence.

A



B

Protein	Fold change (ARID1B/vector)
GDF15	9.43
IGFBP7	6.07
ICAM1	3.73
LAMP2	2.80
LAMP1	2.74
GLB	2.65
ARID1B	2.50
MMP2	2.07
MMP1	1.97
p21^{CIP1}	1.85
β-actin	0.98
MAPK1	0.49
MCM2	0.42
PCNA	0.36
CDC2	0.26

C

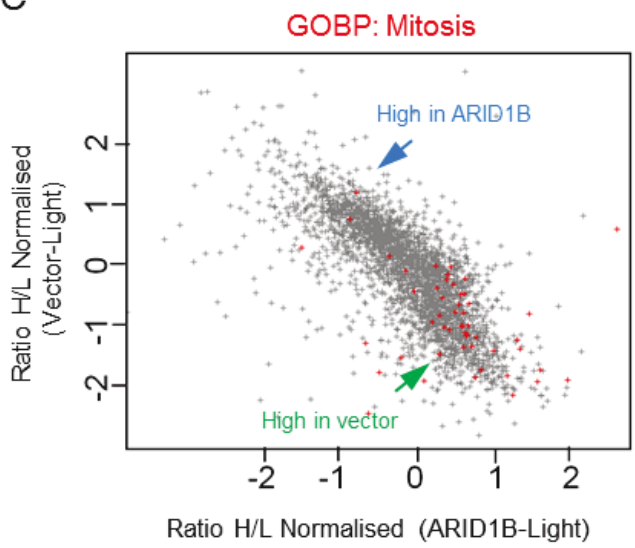


Figure 4.15.1. Global changes in protein levels upon ARID1B overexpression analysed by SILAC. (A) Cartoon summarising the SILAC-based experiments used to catalogue global changes in protein levels upon ARID1B overexpression. (B) SILAC identifies important senescence regulators as ARID1B targets including p21^{CIP1} (C) Gene Ontology Biological Process (GOBP) analysis detects a depletion of mitotic proteins in ARID1B expressing cells.

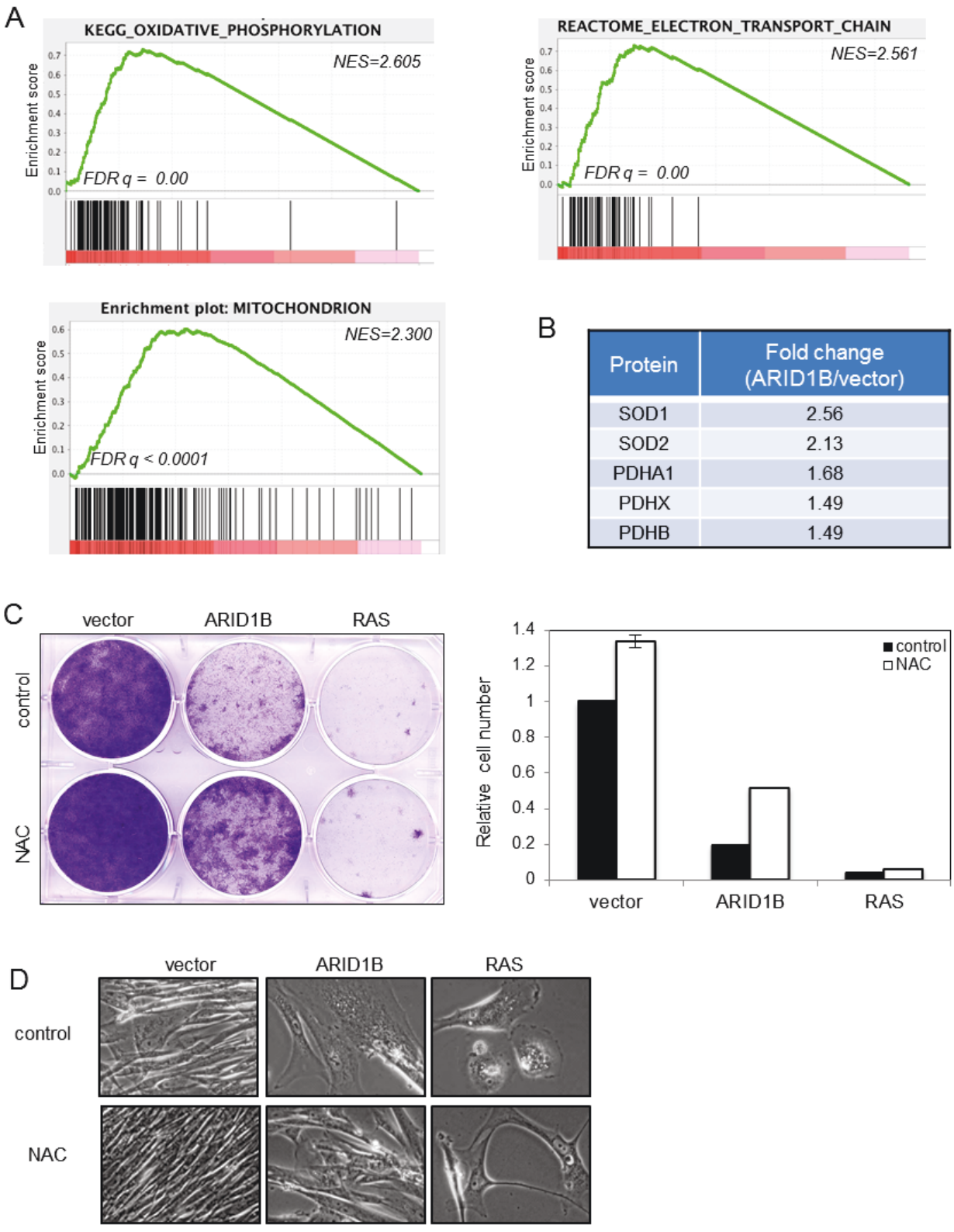


Figure 4.15.2. Production of oxidative stress may contribute to ARID1B mediated senescence. (A) GSEA of genesets associated with mitochondrial function correlate with proteins enriched in ARID1B overexpression as quantified in SILAC analysis. (B) Proteins involved in regulating oxidative phosphorylation and ROS levels are enriched in ARID1B expressing cells. (C) Addition of anti-oxidant *N*-acetylcysteine (NAC) alleviates ARID1B mediated senescence. $1.5x10^4$ cells were plated per 6 cm dish and treated with 100 uM of NAC. Cells were fixed 10 days later and crystal violet was extracted with acetic acid for quantification. (D) Bright-field images of cells in (A) showing differences in cell morphology in ARID1B cells treated with NAC.

4.16. ARID1B is deleted in cancer

Recurrent mutations in ARID1B occur in specific pancreatic, hepatic, brain and breast cancers, such that the alterations are considered to be 'driver mutations' in these cancers (Fujimoto et al., 2012; Sausen et al., 2013; Shain et al., 2012; Stephens et al., 2012). In 2010, an extensive study cataloguing mutations in over 3000 cancer specimens was conducted (Beroukhim et al., 2010). Data from this study showed ARID1B was significantly deleted (but not significantly amplified) across all 54 cancer types, and had a particularly high occurrence of deletion in breast and ovarian cancers (Table A4). Senescence is an important barrier to tumourigenesis *in vivo*, and *ARID1B* alterations frequently occur in particular cancers. Thus, *ARID1B* may be targeted for deletion to bypass senescence in pre-cancerous cells.

4.17. Conclusions and perspectives

4.17.1. ARID1B depletion can bypass senescence through multiple mechanisms

In the previous chapter, Arid1b was identified as a candidate regulator of replicative senescence. I then showed that knockdown of ARID1B extended the cellular lifespan of IMR90 and MEFs. Using the IMR-90 RAS:ER system of OIS I demonstrated that knockdown of ARID1B during OIS decreased the protein and mRNA levels of important senescence regulators $p16^{INK4a}$ and $p21^{CIP1}$.

To further elucidate how ARID1B controls senescence I compared the mRNA expression profile of vector and ARID1B knockdown IMR-90 ER:RAS cells treated with 4OHT as well as vector untreated control cells. The transcript levels of a number of SASP components and secreted factors increased when cells were treated with 4OHT including SPP1, MMP3, MMP10, GDF15, CFS2, CFS3, TNFAIP6, TNFSF18 and TNFSF15. Interestingly, these factors were significantly depleted in shARID1B cells treated with 4OHT compared to vector cells treated with 4OHT. The SWI/SNF complex has previously been linked to the regulation of secreted factors. In activated T-cells the BRG1-containing BAF complex binds to and regulates the IL-3/GM-CSF cytokine cluster in an NF-κB dependent manner

(Wurster et al., 2011). Furthermore, two independent groups have shown that SWI/SNF interacts with SMAD2/3 in response to TGFβ signalling and that this interaction activates SMAD2/3 target genes (Ross et al., 2006; Xi et al., 2008). In TGFβ stimulated cells, BRG1 depletion prevents cells from expressing a number of TGFβ-response genes including CTGF, BAMBI, SMAD7 and JMJD3 (Xi et al., 2008). Importantly, The SWI/SNF sub-complex associated with activated SMAD2/3 contained core subunits BRG1, BAF155 and BAF170 and accessory subunit ARID1B (Xi et al., 2008). In a recent study gene expression profiling of ovarian cancer cells expressing wild-type ARID1A, showed that knockdown of ARID1A reduced the expression of senescence-related secreted factors IL-8, and GDF15 (Guan et al., 2011). Furthermore, ARID1A and BRG1 directly bound to the *SMAD3* promoter, regulating SMAD3 gene expression (Guan et al., 2011). Therefore, it is likely that binding of SWI/SNF to these promoters is necessary for transcriptional regulation of secreted factors.

As with other components of the SWI/SNF complex, ARID1B is known to regulate differentiation (Singhal et al., 2010; Yan et al., 2008). Interestingly our data showed that knockdown of ARID1B affected the expression of multiple differentiation associated genes belonging to the same gene family. Four members of the Late Cornified Envelope (*LCE*) gene cluster on chromosome 1q and two members of the Keratin-Associated Protein 2 (*KRTAP2*) gene cluster on chromosome 17q were significantly downregulated. KRTAP proteins are regulated by GR activation, and therefore depletion of *KTRAP* gene expression may be a result of aberrant SWI/SNF regulation of GR signalling (Donet et al., 2008). Recently, KRTAP proteins have been linked to senescence and ageing. A microarray analysis comparing grey and black hair from individuals, identified greater than two fold expression of *KRTAP* in grey hair (Choi et al., 2011). Furthermore, the *KRTAP13-3* promoter is significantly hypomethylated during replicative senescence; the loci is amongst six CpG methylation sites in the genome that undergo highly significant DNA-methylation changes during senescence (Koch et al., 2012; Koch et al., 2013). Amongst the genes upregulated upon ARID1B depletion were *ID1, ID2, ID3* and *ID4*. ID1 is a negative regulator of *INK4a* expression and is strongly implicated in senescence

control (Alani et al., 2001; Ohtani et al., 2001). Deregulation of ID family proteins has been associated with cancer (Lasorella et al., 1996; Perk et al., 2005; Zebedee and Hara, 2001).

The next step in elucidating the mechanism of ARID1B regulation would be to establish if ARID1B has a direct effect on the transcriptional regulation of particular senescence effectors such as $p16^{INK4a}$ and $p21^{CIP1}$. Alternatively the changes in expression of these genes could be due to ARID1B regulating expression of specific transcription factors such as SMURF2, VDR or p53 which control *INK4a* and *CDKN1a* expression (Kong et al., 2011; Liu et al., 1996; Macleod et al., 1995; Saramaki et al., 2006; Tanaka et al., 2007). For this purpose it would be worthwhile to conduct ChIP analysis to identify ARID1B binding sites in senescent and non-senescent cells and also ARID1B knockdown cells as a control.

PIK3CA is one of the most frequently mutated genes in cancer. Breast tumours with *ARID1B* mutations often contain mutations in *PIK3CA* and *PTEN* (Stephens et al., 2012), suggesting possible cooperation between ARID1B mutations and abrogated PI3K signalling during tumourigenesis. Thus I sought to investigate the relationship between ARID1B and PIK3CA. ARID1B depletion could bypass $PIK3CA^{H1047R}$ induced senescence and these cells had lower levels of $p21^{CIP1}$ and $p16^{INK4a}$. The SWI/SNF complex is linked to the PI3K/PTEN/AKT pathway through regulation of PTEN expression and direct interaction with AKT (Foster et al., 2006; Watanabe et al., 2011). Furthermore, I see an induction in protein expression of many SWI/SNF subunits during $PIK3CA^{H1047R}$ induced growth arrest (data not shown) suggesting SWI/SNF has a key role in $PIK3CA^{H1047R}$ mediated senescence.

4.17.2. SWI/SNF proteins are induced during senescence

As ARID1B was shown to be important in the maintenance of both replicative- and oncogene induced-senescence, I next sought to identify how SWI/SNF is regulated during senescence. The mRNA levels of the majority of SWI/SNF components did not change during senescence. However I did observe an

increase in the protein level of ARID1B, BRG1, BRM and SNF5 during replicative senescence and ARID1A, ARID1B, BRG1, BRM and SNF5 during OIS. This is in agreement with recent findings showing that chromatin-associated BRG1 levels increase during OIS (Tu et al., 2013) and supports the concept that SWI/SNF proteins are important in the induction and maintenance of senescence.

Interestingly I and others have observed that many SWI/SNF proteins are absent from mitotic cells. BRG1 and BRM are excluded from mitotic chromosomes, and BRM is partially degraded during mitosis (Muchardt et al., 1996; Sif et al., 1998). Similarly ARID1A is also degraded during mitosis, and I have observed exclusion of ARID1A, ARID1B and SNF5 from mitotic chromosomes (data not shown) (Flores-Alcantar et al., 2011). BRG1 and BRM are inactivated by phosphorylation during the G2/M transition. The resulting exclusion from chromatin may be important in halting transcription during mitosis (Muchardt et al., 1996).

I next conducted SILAC-based quantitative proteomics to establish whether the composition of the SWI/SNF complex is significantly different in senescent cells. I performed SILAC-IPs to identify changes in proteins interacting with ARID1B in cells infected with either RAS^{G12V} or vector, or expressing ARID1B. The ARID1B IPs were specific, as all core SWI/SNF subunits (BRG1, BRM, SNF5, BAF155, BAF170) were detected in both experiments and enriched in ARID1B expressing cells. Furthermore, subunits that are known to be excluded from SWI/SNF-ARID1B complexes, including ARID1A and PBAF specific peptides (PBRM1, ARID2, BRD7, BAF45A) were not detected in ARID1B IPs however were present in a similar IP/MS experiment performed with BRG1 (data not shown). Interestingly, BAF specific subunit BAF45B was not detected in ARID1B or BRG1 IPs, confirming other reports that suggest it is exclusively expressed in post-mitotic neurons (Figure 4.17B) (Wu et al., 2007).

A recent study of proteins associated with BRG1/BRM in T-cells described BCL7A-C, BCL11A-B, SS18 and BRD9 as permanent, un-exchangeable SWI/SNF subunits, as opposed to proteins that

temporarily interact with the complex (Kadoch and Crabtree, 2013; Kadoch et al., 2013). In the IPs for both ARID1B and BRG1 I detected BCL7A-C and SS18 however BCL11A-B and BRD9 was not detected, suggesting that although these proteins may bind to the SWI/SNF complex with a high affinity, the interaction may be stimulus or cell-type specific (Kadoch et al., 2013).

Isoform exchange in the SWI/SNF complex is important in controlling specificity and function. Many SWI/SNF proteins are present as mutually exclusive exchangeable isoforms, including ARID1A and ARID1B. Ihave observed that overexpression of ARID1B causes ARID1A protein levels to decrease, however mRNA levels of *ARID1A* remain stable, suggesting levels of ARID1A and ARID1B are post-translationally regulated and that free ARID1A or ARID1B proteins not integrated into the SWI/SNF complex are degraded. Such mechanisms controls the pool of SWI/SNF proteins available, including core components SNF5 and BRG1, as well as important accessory proteins such as BAF57 (Chen and Archer, 2005; Keppler and Archer, 2010; Sohn et al., 2007).

Although I did not detect an exchange of particular SWI/SNF subunit isoforms during senescence, I did observe changes in SWI/SNF-associated proteins. Nucleolar proteins (KRI1, KRR1, RRP8, NO66, LYAR) were amongst the interactors highly enriched during OIS. This is particularly intriguing as myself as well as many others have observed by immunofluorescence that SWI/SNF components are not predominantly localised in the nucleoli (Muchardt et al., 1996; Reyes et al., 1997; Vradii et al., 2006). This finding may be significant as there is a prominent change in nucleolar structure during OIS, the mechanism and reason for which are currently unknown (Narita et al., 2003a).

SWI/SNF subunit BAF45D, KRI1 and NKRF preferentially bind to ARID1B in both RAS^{G12V} and ARID1B expressing cells compared to vector cells. The protein with the highest increase in ARID1B-binding during senescence was KRI1. In *C. elegans* Kri-1 is linked to lifespan extension. Kri-1 binds to and promotes nuclear localisation of longevity regulator DAF16/FOXO (Berman and Kenyon, 2006).

DAF-16 controls lifespan in *C. elegans* by inhibiting insulin/IGF-1 signalling (Berman and Kenyon, 2006; Kenyon, 2010). Recently it was shown that SWI/SNF is recruited to targeted DAF-16 promoters (Riedel et al., 2013). Although SWI/SNF subunits were identified as cofactors for DAF-16 function, a direct endogenous interaction between DAF-16 and SWI/SNF was not shown, suggesting they may be present within a larger complex (Riedel et al., 2013; Webb and Brunet, 2013). Considering this scenario, Kri-1 is a possible candidate to bridge the interaction between DAF-16 and SWI/SNF.

Components of the ubiquitin mediated proteasome (UBR5, PSMD1 and PSMD2) were also detected binding to ARID1B. A previous study has shown that ARID1B acts as an E3 ubiquitin ligase targeting H2B Lys 119 for degradation (Li et al., 2010). However I have not observed any global changes in H2B ubiquitination upon ARID1B depletion or expression (data not shown). Other proteins interacting with ARID1B were associated with transcription and elongation, in support of previous evidence for a role of SWI/SNF in this process (Burrows et al., 2010; Drost et al., 2010).

Proteins associated with senescence, previously identified as SWI/SNF interactors were not detected in the IPs; these include, RB1, p53 and SMAD2/3. This may be due to the difficulty in detecting phosphorylated proteins using SILAC LC-MS/MS. Sample preparation and instrumentation must be modified to detect proteins that exist in multiple phosphorylation states. In this study, I identified changes in ARID1B interactors during senescence. To further characterise the repertoire of SWI/SNF interactors in growing and senescent cells I could take advantage of an antibody that binds both BRG1 and BRM. This will allow changes in the PBAF complex as well as ARID1A containing complexes to be studied. The JI antibody available from Crabtree and colleagues would be well suited for this purpose as it recognises the C-terminus of BRG1 and BRM and has been used to detect novel SWI/SNF binding partners in many studies (Dallas et al., 1998; Dunaief et al., 1994; Ho et al., 2009b; Kadoch and Crabtree, 2013; Khavari et al., 1993; Shanahan et al., 1999; Wurster et al., 2011; Zhao et al., 1998).

Proteins identified as SWI/SNF interactors by IP-MS must be verified by conducting reverse IPs or by validating immunoprecipitated proteins by western-blot. Density sedimentation analysis or glycerol gradients may be utilised to assess the stability of the protein interactions with SWI/SNF (Ho et al., 2009b; Kadoch and Crabtree, 2013; Wang et al., 1996a). Previous studies have also used urea based denaturation methods to test the strength of protein interactions with core SWI/SNF subunits and in this way have identified novel SWI/SNF subunits (Kadoch and Crabtree, 2013).

As ARID1B binds to a number of proteins involved in transcription and elongation I investigated the nuclear distribution of ARID1B to identify whether it is associated with active or repressed chromatin. In senescent cells, ARID1B was excluded from areas of repressed chromatin, particularly SAHFs, which are strongly marked with H3K9me^3 and H3K27me^3. Similarly, in proliferating cells ARID1B was excluded from replicating DNA (correlates with H3K27me^3) identified by BrdU incorporation (Chandra et al., 2012). The observations suggest that ARID1B is associated with active chromatin regions. These observations are similar to findings that BRD7, a PBAF accessory component, is required for the establishment of OIS, however is excluded from SAHFs and is associated with actively transcribed chromatin (Drost et al., 2010; Staal et al., 2000). Furthermore, BRG1, BRM and SNF5 are similarly excluded from condensed chromatin and associated with highly transcribed chromatin (Reyes et al., 1997). SWI/SNF may be important in the formation of active and repressed chromatin domains within the nucleus. In IMR-90 cells the formation of SAHFs during OIS is dependent on BRG1; in MEFs deletion of BRG1 causes a disruption in the formation of otherwise highly discrete heterochromatic domains (Bourgo et al., 2009; Tu et al., 2013).

4.17.3. Growth arrest induced by SWI/SNF is exerted through different mechanisms

To further investigate the role of SWI/SNF in senescence, I used vectors expressing human isoforms of BRG1, BRM, ARID1A and ARID1B into the same vectors. Expression of the SWI/SNF proteins induced a premature growth arrest. Cells expressing BRG1, BRM, ARID1A or ARID1B possessed an enlarged flat morphology and had a lower percentage of BrdU incorporation. SWI/SNF protein expression also induced the formation of SAHFs and increased SA-β-Gal activity in cells.

Expression of SWI/SNF proteins induces a growth arrest or a senescence response in multiple cell types (Drost et al., 2010; Dunaief et al., 1994; Guan et al., 2011; Inoue et al., 2011). One of the first studies identifying a role for SWI/SNF in senescence, showed that BRG1 bound to RB1 and HDAC1 and repressed the transcription of E2F target genes (Dunaief et al., 1994). More recently BRG1 and other SWI/SNF proteins have been shown to bind to the *CDKN1a* and *CDKN2a* promoters (Kuwahara et al., 2010; Tu et al., 2013). SWI/SNF subunits also interact with p53 and co-operate in activating transcription of p53 target genes (Drost et al., 2010; Guan et al., 2011). In this work I show that expression of SWI/SNF subunits elevates $p16^{INK4a}$ and $p21^{CIP1}$ levels.

When we compare the effect of expressing individual SWI/SNF subunits, I found ARID1A infected cells have the highest $p16^{INK4a}$ induction and do not show an increase in $p21^{CIP1}$ levels. $P16^{INK4a}$ mediated hyperphosphorylation of RB1 decreases the transactivation of E2F1 target genes including $p21^{CIP1}$ and may explain why ARID1A expressing cells that have very high $p16^{INK4a}$ levels do not induce $p21^{CIP1}$ expression (Gartel et al., 1998; Hiyama et al., 1998). ARID1A expressing cells also contain many distinctly formed SAHF, which act to repress E2F target genes (Narita et al., 2003a), supporting the notion that ARID1A mediated growth arrest is dependent on the $p16^{INK4a}$/RB1 pathway. Conversely, ARID1B infected cells have less prominent SAHF formation, and have higher $p21^{CIP1}$ protein levels compared to ARID1A expressing cells. In HeLa cells, ectopic ARID1B expression increases $p21^{CIP1}$ protein levels and ARID1B-SWI/SNF complexes are enriched at the *CDKN1a*

promoter compared with ARID1A-SWI/SNF complexes (Inoue et al., 2011; Ryme et al., 2009), supporting a role for ARID1B in $p21^{CIP1}$ regulation. In contrast to this view, expression of ARID1A in HEC-1-A and OVISE cell lines containing ARID1A deletions induced $p21^{CIP1}$ expression, suggesting that the function of SWI/SNF proteins is highly cell-type and context dependent (Euskirchen et al., 2011; Wang et al., 1996b).

To assess the contribution of important senescence effectors during ARID1B induced growth arrest, I co-infected young IMR-90 with either vector or ARID1B and with shRNAs targeting either $p21^{CIP1}$, $p16^{INK4a}$, p53 or an empty vector to act as a control. Knockdown of $p21^{CIP1}$ and $p16^{INK4a}$ increased proliferation in ARID1B expressing cells, however p53 ablation conferred a full rescue of ARID1B mediated growth arrest, comparable to vector cells. Similarly, ARID1B cells co-expressing HPV E6/E7 also had a proliferation rate higher than that of vector cells co-expressing HPV E6/E7, suggesting that p53 expression is important in ARID1B induced growth arrest. The observation that ARID1B expressing cells with p53 depletion proliferate faster than vector/shp53 cells could be due to the reduction in ARID1A protein levels in ARID1B expressing cells, and therefore there may be additional disruption of the $p16^{INK4a}$/RB1 pathway. This decrease in ARID1A levels may confer a further proliferative advantage in ARID1B/shp53 cells.

To understand the mechanism of senescence induction, global changes in protein levels were quantified in ARID1B expressing cells using SILAC. Amongst the proteins with the highest fold increase, were senescence-associated secreted factors GDF15, IGFBP7 and ICAM1. Lysosomal proteins associated with senescence were also induced upon ARID1B expression, including GLB1; the protein responsible for SA-β-gal activity (Lee et al., 2006). As expected, mitotic proteins were downregulated in ARID1B cells, suggesting these cells undergo cell cycle arrest.

Intriguingly, GSEA of SILAC data showed that the gene sets correlating with ARID1B expression are associated with mitochondrial dysfunction. There was a significant enrichment of proteins involved in oxidative phosphorylation and the electron transport chain. Mitochondrial production of reactive oxygen species (ROS) is known to contribute to the establishment of OIS (Lee et al., 1999; Moiseeva et al., 2009),and mitochondrial dysfunction plays a key role in replicative senescence and ageing (Hutter et al., 2004; Melov et al., 1999; Passos et al., 2007). Further investigation showed that the ROS scavenger N-acetyl-l-cysteine (NAC) suppressed the ARID1B mediated phenotype. Cells treated with NAC proliferated faster and appeared less flat and enlarged suggesting that ROS production mediates ARID1B induced growth arrest.

It is of interest that both p53 ablation and ROS scavengers are able to rescue ARID1B mediated senescence, as these pathways are connected through numerous cellular processes, including mitochondrial dysfunction and apoptosis (Li et al., 2011b; Liu et al., 2008). Many studies have linked SWI/SNF to oxygen regulation. SWI/SNF is involved in the transactivation of hypoxia-inducible factor-1α (HIF1α) in hypoxic conditions and SWI/SNF interacts with PPARγ coactivator-1α (PGC1α) to regulate mitochondrial fatty acid oxidation (Kenneth et al., 2009; Li et al., 2008). A recent study in yeast demonstrated that SWI/SNF proteins undergo rapid nuclear localisation in response to hypoxia and that many of the SWI/SNF target genes were involved in oxygen regulation (Dastidar et al., 2012).

4.17.4. ARID1B exhibits tumour-suppressive functions in cancer

The results presented in this work as well as work by others, demonstrates a link between various SWI/SNF proteins and senescence. Recently two elaborate studies cataloguing available exome sequencing data showed that, collectively, inactivating mutations in SWI/SNF subunits occur in around 19% of all cancers, a frequency similar to *TP53* (Kadoch et al., 2013; Shain and Pollack, 2013). As senescence acts as a barrier to tumour progression *in vivo*, mutations in SWI/SNF may drive cancer by inactivating senescence reinforcement programs.

ARID1B in particular is significantly deleted in cancers of the breast, pancreas, brain and liver (Fujimoto et al., 2012; Sausen et al., 2013; Shain et al., 2012; Stephens et al., 2012). In breast cancer *ARID1B* mutations are commonly associated with mutations in *TP53* and *PTEN* (Stephens et al., 2012). It would be of interest to analyse if this mutual inclusivity is true in other cancer genomes, in an attempt to shed light on the pathways cooperating during ARID1B mediated senescence. In agreement with our proposed mechanism of ARID1A-mediated senescence, reports have suggested that ARID1A and TP53 mutations are mutually exclusive (Bosse et al., 2013; Shain and Pollack, 2013; Wang et al., 2011). This mutual exclusivity however, is only seen in ovarian and gastric cancers and is not reported in other cancer types.

ARID1B expression may also be deregulated at the epigenetic level in cancers. A recent study demonstrated that the *ARID1B* promoter was hypermethylated in multiple pancreatic cancer cell lines causing ARID1B transcriptional repression (Khursheed et al., 2013). The investigators next sought to identify the effect of ectopic ARID1B expression in these cell lines. Although they were able to detect an increase in ARID1B mRNA expression by RT-qPCR, they could not detect any increase in ARID1B protein expression (Khursheed et al., 2013). Ectopic ARID1B expression did not affect the proliferation of cells, however the ability to form colonies in soft agar was reduced and ARID1B expressing cells had higher levels of SA-β-gal activity (Khursheed et al., 2013).

In the work presented, ARID1B was identified from a screening for regulators of senescence in MEFs, utilising a library containing genes frequently deleted in HCC. The HCC deletion library was thought to be enriched with potential tumour suppressors. It is therefore encouraging that mutations in ARID1B were recently described as ‘cancer driving’ in HCC (Fujimoto et al., 2012). Knockdown of ARID1B in some HCC cell lines increased cell proliferation by more than two-fold, however ARID1B knockdown had no effect in HCC cell lines when ARID1B was mutationally inactivated (Fujimoto et al., 2012). To

characterise the tumour suppressive role of ARID1B in HCC, it could be useful to ectopically express ARID1B in HCC cell lines that do not express ARID1B to see if this has a growth suppressive effect.

Chapter 5. Discussion & Future work

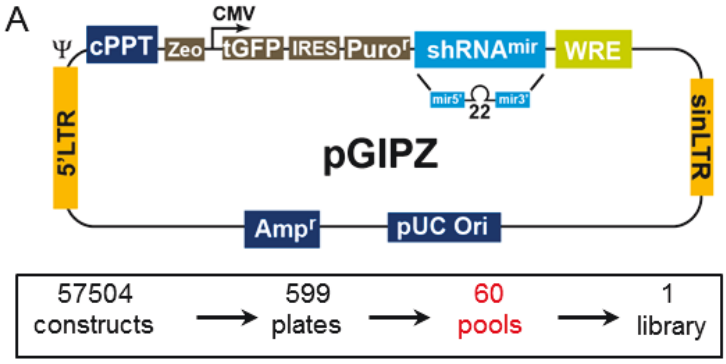
5.1. Genetic screens are useful tools for identifying novel genes and pathways involved in senescence

In the 50 years since senescence was first described by Hayflick and Moorhead, the field has progressed from what was once thought to be an exclusively *in vitro* phenomenon, to now being recognised as an important process involved in cancer and ageing (Collado et al., 2007; Hayflick and Moorhead, 1961). Genetic screenings for the bypass of cellular senescence has led to the identification of novel cancer genes. ShRNA screenings are increasing in popularity as the method of choice for conducting screenings as they are less expensive and require less specialised laboratory equipment when compared to screenings using siRNAs. Recently, the use of NGS as a readout of bypass of senescence screenings has vastly increased the amount of data generated per screen. As the cost of NGS has progressively decreased and with technology rapidly improving, it is now easier to conduct screenings using genome wide shRNA libraries. The protocol established in this work is ideally suited for genome-wide screens based on the miR30 hairpin design. Genome-wide screens provide an un-biased method of identifying important genes, and possibly pathways, involved in establishing senescence.

5.1.1. Genome-wide screening for regulators of OIS in IMR-90

An example of such a genome-wide screening involves the use of the pGIPZ library to identify regulators of OIS. The pGIPZ library consists of 60,000 shRNA constructs (Figure 5.1A). This library can be used to screen for regulators of OIS using the IMR-90 ER:RAS system. Addition of 4OHT to IMR-90 ER:RAS cells triggers OIS in a highly controlled manner and it is therefore a suitable system to use to set up a screen to identify OIS regulators (Acosta et al., 2008; Barradas et al., 2009). The advantage of using human fibroblasts is that they are not as prone to spontaneous mutations as MEFs and they have a longer replicative lifespan (Wu and Li, 1985). The ER:RAS system is preferred over

using cells that are infected with vectors expressing constituitively active RAS^{G12V}, because the induction of the RAS^{G12V} response can be controlled in ER:RAS cells and the population of ER:RAS cells is more homogeneous compared to cells infected with RAS^{G12V} vectors (for the population to be more homogeneous, cells expressing ectopic RAS^{G12V} must first be selected by drug resistance to remove uninfected cells from the population).



Vector Element	Utility
CMV Promoter	RNA Polymerase II promoter
cPPT	Central Polypurine tract helps translocation into the nucleus of non-dividing cells
WRE	Enhances the stability and translation of transcripts
turbo GFP	Marker to track shRNAmir expression
$Puro^r$	Mammalian selectable marker
AMP^r	Ampicillin bacterial selectable marker
5'LTR	5' long terminal repeat
pUC ori	High copy replication and maintenance in *E.coli*
SIN-LTR	3' Self inactivating long terminal repeat
RRE	Rev response element
ZEO^r	Bacterial selectable marker

Figure 5.1. pGIPZ library set up. (A) Notable features of pGIPZ plasmid and library set up (Adapted from http://www.thermoscientificbio.com).

5.1.2. Library bias not detected from sequencing pGIPZ library pools

The pGIPZ library was received in aliquots of 60 pools; each pool contains 1000 shRNAs which were amplified. Quality control of library amplification was conducted through sequencing of cells infected by library pools. IMR-90 cells infected with pGIPZ library pool 9 were collected 2 days after infection. Custom Solexa libraries were prepared as before. Sequencing data was filtered to remove sequences with less than 2 reads. Using this cut-off, sequencing of DNA from cells infected with pool 9 identified 1065 shRNAs. Representation of each shRNA as a proportion of the total reads per sample

demonstrates that the level of library bias was minimal as shRNAs were evenly represented (Table A3). Furthermore, the most abundant shRNAs identified from sequencing were pool specific (shRNAs from pool 9 originate from plates (91-100) indicating that the level of cross-contamination between pools is also minimal.

5.1.3. Set up of infection conditions for pGIPZ lentiviral screening

The pGIPZ library is cloned into lentiviral vectors, which allows higher infection efficiencies to be achieved in target cells when compared to retroviral infection efficiencies. When using lentiviral vectors, infection conditions must be carefully controlled to minimise infection mediated cell stress or cytotoxicity, and alterations to cell physiology, which is a consequence of using high viral titers on primary cells.

Infection conditions were optimised by testing transfection parameters to identify the best conditions for infection efficiency and cell viability. Amount of helper packaging plasmids psPAX2 and VSV-G, as well as viral dilution, were controlled to achieve optimal infection efficiencies (Figure 5.2B red asterisk). Higher infection efficiencies resulted in changes in cell morphology and cytotoxicity, and therefore an infection efficiency of 50% was deemed ideal to limit multiple infections and cell stress (Figure 5.2A).

5.1.4. pGIPZ shp53-1 can be used as a control hairpin that bypasses OIS

As with the lifespan extension screening in MEFs, a proof of principle experiment must first be conducted to assess the feasibility of a screening using a genome-wide shRNA library for bypass of OIS. For this end, a positive control shRNA able to bypass OIS must be selected. The control hairpin must be from the same vector backbone as constructs in the library to control for possible changes in infection efficiency and toxicity caused by using a control from a different vector backbone. I tested 6 different shRNAs targeting either shp16 or shp53 alongside validated lentiviral constructs. I found that

the pGIPZ shRNAs produced a weak knockdown effect using the selected infection conditions (Figure 5.3). The weak knockdown observed may be a result of a low MOI, however the infection conditions have been optimised such that the cells do not become stressed during infection and therefore the MOI should not be increased. A colony formation assay showed that pGIPZ shp53-1 was able to bypass OIS, and this hairpin should be used for further assay design experiments (Figure 5.3A, B).

The pools size used for a genome wide screening will be larger than that of the HCC screen and therefore the proof of principle experiment must be more stringent to see if a bypass can take place. A preliminary colony formation assay showed that pGIPZ shp53 dilutions of 1:1000 did not result in an OIS bypass, however using the same dilutions of p156 RRL shp53 and pRS shp53 did produce an observable effect. An alternative method to assess the bypass of OIS in screening pools, is to measure proliferation rates and GFP enrichment during the screen. Samples which contain shRNAs able to bypass OIS will have higher proliferation rates, or a higher GFP positive population as uninfected cells (GFP negative) will not divide as rapidly; and these pools can be selected for sequencing.

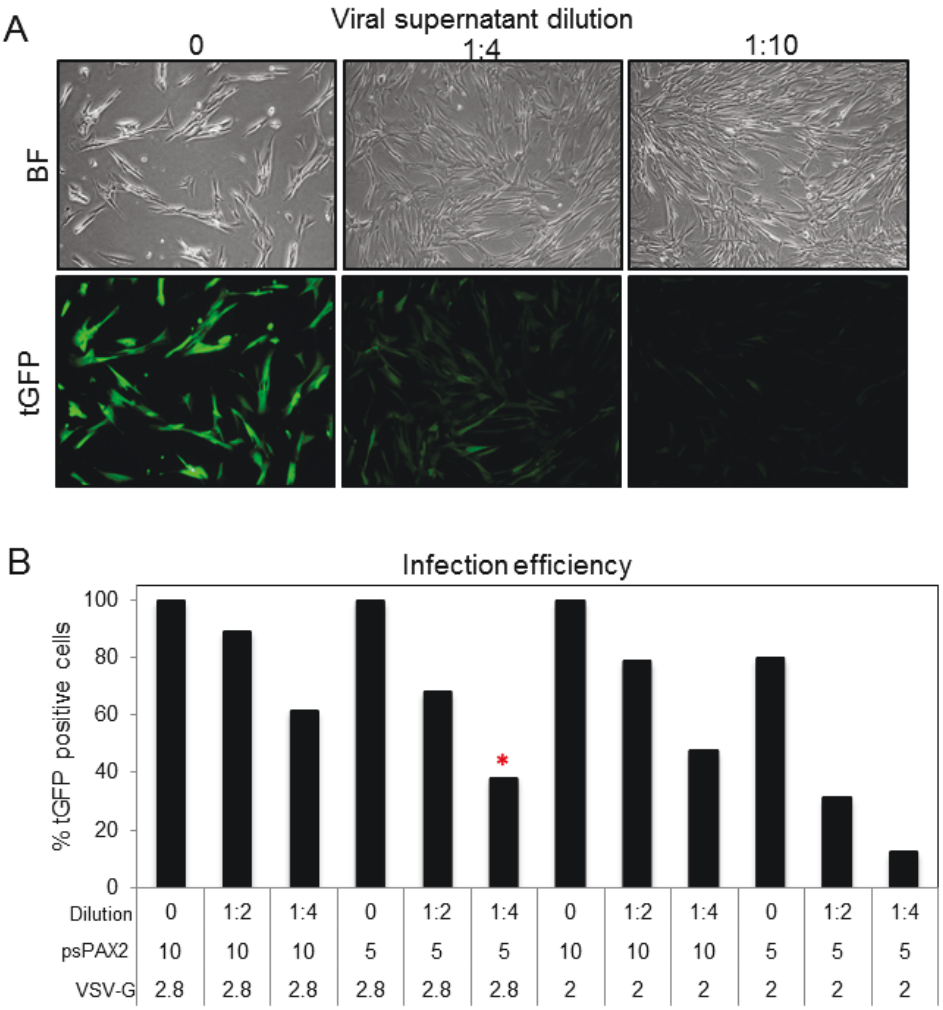


Figure 5.2. Optimising infection conditions with pGIPZ lentiviral vectors. (A) Cells were infected with the pGIPZ vector (transfection conditions: 20 µg of plasmid, 2.8 µg of VSV-G, and 10µg of psPAX2) to assess the infection efficiency and viability of cells using different viral supernatant dilutions with a 5 hr infection duration. 10^6 passage 14 IMR-90 cells were seeded one day pre-infection, and pictures were taken 5 days post infection. (B) 10^6 cells were seeded one day pre-infection, and cells were infected with viral supernatant using indicated conditions. FACs analysis was used to analyse the percentage of tGFP positive cells.

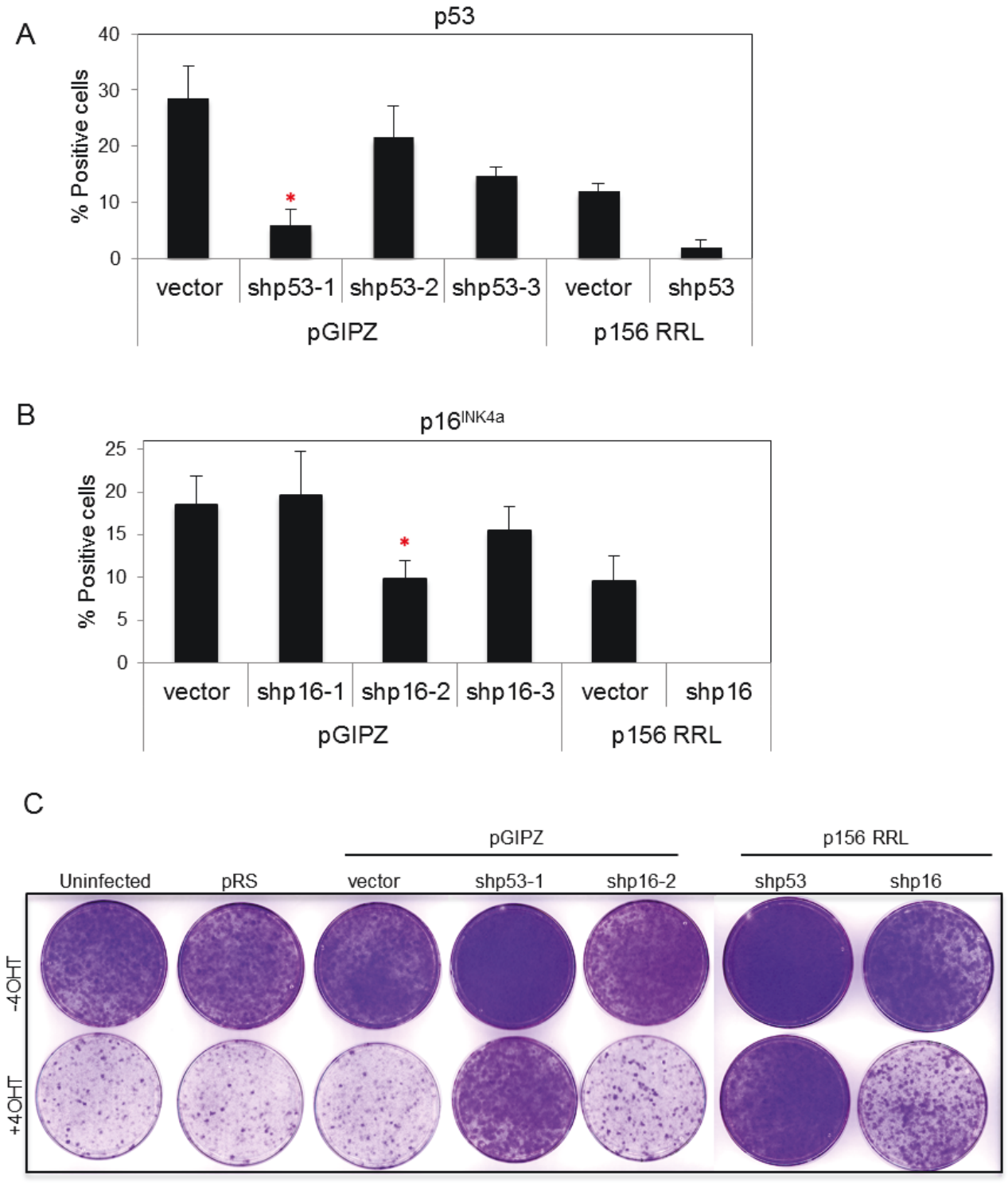


Figure 5.3. Validation of pGIPZ controls for proof of principle experiment for bypass of OIS screening. (A) Levels of p53 protein knockdown in tGFP positive IMR-90 cells infected by indicated constructs as assessed by HCA. (B) Levels of $p16^{INK4a}$ protein knockdown in tGFP positive IMR-90 cells infected by indicated constructs as assessed by HCA. (C) p15 IMR-90 ER:RAS cells were infected with indicated constructs and 10^5 cells were seeded in a 10 cm plate. Cells were treated with 100 nM 4OHT or DMSO. Bypass of OIS was assessed by the ability of infected cells to form colonies upon addition of 4OHT.

5.2. ARID1B is an important senescence regulator

In this work a genetic screen coupled to NGS was used to identify a component of the SWI/SNF complex ARID1B as a senescence regulator. Recently, a number of SWI/SNF components have been identified in screenings for bypass of senescence including PBRM1, BRD7 and SNF5 (Burrows et al., 2010; Drost et al., 2010; Wajapeyee et al., 2008). In mammalian cells, a variety of SWI/SNF complexes exist, all of which use the energy generated by an integral ATPase subunit to remodel chromatin (Clapier and Cairns, 2009). The regulation of chromatin dynamics by the SWI/SNF complex is thought to play an essential role in many cellular processes including differentiation and proliferation

ARID1B is a BAF-specific accessory component of the SWI/SNF complex. Previous work has shown that ARID1B has important cell cycle regulatory effects and controls the expression of cell cycle proteins $p21^{CIP1}$ and c-myc, although its involvement in senescence has not been described (Inoue et al., 2011). SWI/SNF components have previously been implicated in senescence; however the mechanisms exerted by specific components differ depending on the conditions and cell types studied.

In this study, a novel function of ARID1B in regulating senescence is described. I have shown that knockdown of ARID1B extends the cellular lifespan of both human and mouse fibroblasts and abrogates OIS induced by RAS^{G12V} and $PIK3CA^{H1047R}$. During OIS, ARID1B ablation reduces the expression of important senescence effectors including $p16^{INK4a}$ and $p21^{CIP1}$. Gene expression profiling of ARID1B-depleted cells during OIS, revealed that ARID1B regulated the expression of different gene families involved in differentiation, including the ID proteins that have an important role in oncogenesis and senescence regulation (Perk et al., 2005). This suggests, as others have seen, that ARID1B has a function during differentiation, and de-regulation of these pathways may have implications in tumourigenesis.

I observed a post-transcriptional increase in ARID1B and other SWI/SNF proteins during both replicative and oncogene-induced senescence, supporting the theory that these proteins are important senescence regulators. Pull-downs of ARID1B-associated complexes showed that a number of nucleolar proteins were enriched in senescent fractions compared to proliferating cells. I found that ARID1B bound to a number of proteins involved in transcription and elongation; in support of a role for ARID1B in this process, confocal imaging showed that ARID1B is excluded from areas of repressed chromatin, including SAHFs.

Ectopic expression of SWI/SNF proteins ARID1A, ARID1B, BRG1 and BRM induced premature senescence as seen by a decrease in proliferation and an increase in senescence markers such as SAHFs and SA-β-gal activity. SAHFs were most prominent in ARID1A expressing cells and these cells had a high increase in $p16^{INK4a}$ expression, suggesting ARID1A-mediated senescence occurs via the activation of the $p16^{INK4a}$/RB1 pathway. In ARID1B cells the increase in $p16^{INK4a}$ expression was moderate; however these cells had high levels of $p21^{CIP1}$ expression. As knockdown of p53 was able to bypass ARID1B-induced growth arrest it suggests that ARID1B mediates senescence through the p53/$p21^{CIP1}$ pathway. These findings imply, as others have proposed, that SWI/SNF proteins regulate senescence through multiple pathways.

SILAC analysis of global changes in protein levels identified enrichment of mitochondrial proteins and depletion of mitotic proteins upon ARID1B expression. In particular proteins involved in oxidative phosphorylation and the electron transport chain were highly enriched. It was recently shown that cells undergoing $BRAF^{V600E}$-induced senescence increase oxidative metabolism, which is essential for the maintenance of OIS (Kaplon et al., 2013). Higher levels of oxidative phosphorylation during OIS, results in the formation of ROS, which can also induce senescence (Lee et al., 1999; Moiseeva et al., 2009). Mitochondrial dysfunction and ROS production are important features of the ARID1B-induced phenotype as treatment with antioxidant NAC suppressed growth arrest.

Deleterious mutations in *ARID1B* are present in various cancer databases cataloguing mutations in human tumours and human cell lines. *ARID1B* mutations found in breast tumours are associated with mutations in other tumour suppressor genes including *TP53* and *PTEN* (Stephens et al., 2012). Future work may focus on the effect of ectopically expressing these ARID1B mutants compared to wildtype ARID1B expression to determine if these mutants affect cell proliferation. Furthermore, it may be of interest to overexpress wildtype ARID1B in cell-lines harbouring deleterious ARID1B mutations to see if ARID1B expression can limit uncontrolled division in these cells.

In addition, it will be important to carefully analyse genes regulated by ARID1B from the microarray and SILAC data, and establish if ARID1B affects the expression of these genes by altering histone modifications or nucleosome positioning at these loci. For this purpose ChIP and MNase-mapping assays may be conducted to elucidate the mechanism of ARID1B-mediated senescence.

5.3. The SWI/SNF complex is implicated in cancer and ageing

The data presented so far has identified a role for SWI/SNF proteins in replicative senescence and OIS *in vitro*. As previously discussed SWI/SNF proteins are implicated in ageing and cancer *in vivo*. The first report linking the SWI/SNF complex to ageing showed that a BRM-RB1-C/EBPα complex forms in old rat and mouse livers, but not in young livers, and promotes growth arrest (Iakova et al., 2003). Furthermore, the work suggests the increase of BRM is responsible for the weak proliferative response to partial hepatectomy in aged livers and therefore suppresses liver regeneration (Iakova et al., 2003)

More recently, the SWI/SNF-BAF complex has been linked to longevity in *C. elegans* (Riedel et al., 2013). In mutant strains where insulin signalling is blocked, SWI/SNF associates with longevity factor DAF-16/FOXO and this interaction is necessary for promoting stress resistance and lifespan extension (Riedel et al., 2013). Although forkhead box proteins regulate senescence in mammalian cells, no

interaction between FOXO proteins and SWI/SNF has been observed, both in our studies and others (Courtois-Cox et al., 2006; Kyoung Kim et al., 2005; Li et al., 2013; Wang et al., 1996b). Indeed the work in *C. elegans* did not demonstrate a direct interaction between the endogenous proteins (Riedel et al., 2013). Furthermore, the association between SWI/SNF and DAF-16 was only seen in stressful conditions, suggesting that other factors, which may be activated by particular stimuli only, are required to recruit SWI/SNF to DAF-16 promoters (Riedel et al., 2013; Webb and Brunet, 2013).

In human cancers, mutations in SWI/SNF subunits occur more frequently than mutations in any other chromatin remodelling complex (Kadoch et al., 2013). This has led to the belief that particular components of the SWI/SNF complex are *bona fide* tumour suppressors (Vogelstein et al., 2013). Importantly, it appears loss of one SWI/SNF allele is sufficient to promote the formation of aggressive cancers whereas other tumour suppressor genes often undergo loss of heterozygosity (LOH) in both alleles in tumours (Jones et al., 2010; Kadoch et al., 2013; Varela et al., 2011; Versteege et al., 1998). Extensive analysis of available tumour exome sequencing data, has revealed that mutations in SWI/SNF components are generally inactivating and target the core subunits and the DNA-binding accessory proteins (Shain and Pollack, 2013).

Further support that SWI/SNF acts as a tumour-suppressor complex has hailed from results showing that overexpression of SWI/SNF proteins in cell-lines harbouring inactivating SWI/SNF mutations, suppressed cell division. This was first seen when reintroduction of BRG1 into the SW13 cancer cell line induced senescence, and similarly ectopically expressing SNF5 in MRT cell lines results in a G1 cell cycle arrest (Dunaief et al., 1994; Versteege et al., 2002). More recently, overexpression of ARID1A in OCC cell lines with ARID1A deletion also induced a G1 arrest (Guan et al., 2011).

In vivo, mice injected with OSE4 cells expressing shArid1a developed large tumours, when compared to mice injected with OSE4 cells expressing shGFP (Guan et al., 2011). Similarly, many groups have

shown that Snf5 null mice rapidly develop aggressive tumours, similar to human MRT, suggesting that mutations in SWI/SNF genes are drivers of cancers, rather than passenger mutations (Guidi et al., 2001; Roberts et al., 2000; Roberts et al., 2002). These results together with our data showing that SWI/SNF are important regulators of senescence, suggests that targeted mutations in SWI/SNF proteins may favour the bypass of senescence in pre-cancerous cells.

Epigenetic silencing of SWI/SNF genes also leads to loss of expression. The catalytic subunit BRM is frequently silenced by an unknown post-transcriptional mechanism, and silencing is restored by the use of HDAC inhibitors (Glaros et al., 2007; Yamamichi et al., 2005). In pancreatic cancer cell lines, ARID1B is frequently silenced by promoter hypermethylation; expression can also be restored by using HDAC inhibitors, providing a therapeutic window of opportunity in tumours where SWI/SNF components are epigenetically silenced (Khursheed et al., 2013).

5.4. The clinical utility of targeting the SWI/SNF complex in cancer detection and therapy

As mutations in SWI/SNF subunits have a significant role in the progression of particular tumours, loss of expression of these SWI/SNF components may be used as a biomarker for carcinogenesis (Jones et al., 2010; Varela et al., 2011; Versteege et al., 1998; Wang et al., 2011). A number of studies have proposed that the expression pattern of SWI/SNF subunits can be used as biomarkers of certain disease states (da Costa et al., 2013; Li et al., 2011a; Oike et al., 2013). For example, there is a significant reduction in SNF5 expression in metastatic melanoma compared with dysplastic nevi, suggesting that loss of SNF5 correlates with the loss of the senescent state (Lin et al., 2009; Mooi and Peeper, 2006). Furthermore negative SNF5 expression correlated with metastasis, poor patient survival and an increased resistance to chemotherapy, and therefore SNF5 expression may be used to predict the response to treatment and survival in patients with melanoma (Li et al., 2011a; Lin et al., 2009; Moore et al., 2012).

Loss of PBRM1 expression occurs in approximately 40-70% of clear cell renal cell carcinoma (ccRCC) and is associated with advanced tumour stage and poor patient prognosis (da Costa et al., 2013; Numata et al., 2013; Pawlowski et al., 2013; Varela et al., 2011). Thus PBRM1 expression is a promising biomarker for predicting survival outcome, however further work is needed before it can be used clinically to enable personalised therapy (Poste, 2011; Vasudev et al., 2012). Similarly in ovarian clear cell carcinoma (OCCC), ARID1A mutations occur in more than 50% of tumours, and loss of ARID1A expression is an early event in the development of OCCC from endometriosis (Jones et al., 2010; Yamamoto et al., 2012a, b). Further studies have assessed the value of using ARID1A as a biomarker in OCCC however as with PBRM1, this is yet to be followed up in a clinical setting (Kobel et al., 2013; Samartzis et al., 2012).

Interestingly, mutations in either ARID1A or ARID1B occur in approximately 11% of neuroblastomas, however structural rearrangements in ARID1B occur at a much higher frequency (Sausen et al., 2013). Sausen et al. reported that in 74 primary tumours and cell lines studied, at least one structural alteration was detected at the MYCN, ARID1B or ALK loci in all tumours (Sausen et al., 2013). These rearrangements can be detected from circulating tumour DNA in the blood and may be used as biomarkers of neuroblastoma as they are not present in normal cells (Sausen et al., 2013). Since neuroblastoma is a highly aggressive cancer with low patient survival outcomes, it has been proposed that detection of these chromosomal rearrangements can be used as a non-invasive method to identify residual disease, following surgery (Morgenstern et al., 2013; Sausen et al., 2013).

It has been proposed that epigenetic alterations may substitute for genomic instability in the progression of lethal cancers (McKenna and Roberts, 2009; Wilson et al., 2010). SNF5 deficient cancers are highly aggressive however tumour cells appear genomically stable, diploid and predominantly devoid of other mutations (McKenna et al., 2008). In contrast to genetic mutations, epigenetic modifications are reversible, and therefore are strong candidates for therapeutic

intervention in cancers driven by mutations in a single epigenetic regulator (Rodriguez-Paredes and Esteller, 2011). Indeed, specific inhibitors targeting chromatin remodelling proteins have been successful in preclinical trials and multiple drugs are currently into phase III clinical trials (Helin and Dhanak, 2013).

As SWI/SNF mutations are largely inactivating and involve the deregulation of multiple survival pathways; efforts are focused on targeting these cancers by synthetic lethality (C.W.M. Roberts unpublished data, (Oike et al., 2013)). Alternatively therapies may be designed to target downstream effectors that are hyperactivated by SWI/SNF loss. In particular a number of studies have shown that the SWI/SNF complex antagonises Polycomb activity, and inhibiting EZH2 in these cancers reduces tumour growth (Wilson et al., 2010; Young and Jacks, 2010). EZH2 is the catalytic component of the PRC2 complex, and is overexpressed in a number of cancers (Bachmann et al., 2006; Kleer et al., 2003; Varambally et al., 2002). Recently, specific chemical EZH2 inhibitors have been designed and tested for their anti-proliferative response in different cancers (McCabe et al., 2012), (Knutson et al., 2012; Qi et al., 2012). For some haematological and solid cancers EZH2 inhibitors have already entered clinical trials, including EPZ-6438 from Epizyme. Of interest, MRT with inactivated SNF5 are selectively killed upon treatment with EPZ-6438 (Knutson et al., 2013). Furthermore administration of EPZ-6438 to SNF5 null mice results in complete MRT regression (Knutson et al., 2013).

As the field progresses, future work must focus on elucidating the precise mechanism caused by SWI/SNF inactivation in cancer subtypes. This will allow highly specific drugs to be designed with the potential to increase efficacy and reduce side effects in patients. Furthermore, the use of biomarkers will permit personalised treatment opportunities and better prediction of responsiveness to certain drugs. These therapies will not only be useful in cancers with a high percentage of somatic SWI/SNF mutations, but also in cases where the targeting mechanism of the entire SWI/SNF complex is

disrupted, for example by fusion to oncogenic proteins (Kadoch and Crabtree, 2013) or by interaction with long non-coding RNAs (Prensner et al., 2013).

5.5. Concluding remark

Through the efforts of cancer genome sequencing, SWI/SNF proteins have now been recognised as *bona fide* tumour suppressors. Focus is currently being shifted into better understanding the mechanism of SWI/SNF tumour suppressive actions. Indeed in the last few years our knowledge of SWI/SNF subunits has vastly expanded, and many novel functions of the complex have been discovered. The precise mechanism of recruitment of these complexes to chromatin remains unclear, and may involve histone modifications or interactions with specific transcription factors or other proteins. SWI/SNF interacts with many cancer regulators including proteins involved in the DDR, nuclear hormone receptor signalling and tumour suppressor proteins p53 and RB1 (Figure 1.11).

What is most striking about the mutations of SWI/SNF proteins in cancer is that certain subunits are highly mutated exclusively in a particular cancer type, suggesting that the function of SWI/SNF is truly dependent on environmental cues and cell types studied. In our work I showed that ectopic expression of SWI/SNF subunits ARID1A, ARID1B, BRG1 and BRM induced premature senescence. Functional redundancy between these mutually exclusive SWI/SNF subunits is not frequently observed; however many SWI/SNF subunits have been linked to activation of the same tumour suppressive programs, namely the p53/$p21^{CIP1}$ and $p16^{INK4a}$/RB1 pathways (Bultman et al., 2000; Nagl et al., 2007; Wilson and Roberts, 2011).

Taken together, the work presented here and by others reveals the importance of SWI/SNF proteins in the induction and maintenance of senescence. Further work is needed to understand the exact contributions of particular SWI/SNF subunits in senescence, and therefore expand our understanding of the roles of this highly diverse complex in cancer and ageing. This will aid the development of

targeted therapies, which is currently hindered by the lack of mechanistic understanding by which epigenetic mutations promote tumourigenesis. Fully realising the function that epigenetic regulators, such as ARID1B, have on tumour progression could result in more specific and effective drugs for the treatment of cancers principally driven by reversible epigenetic instability.

References

Acosta, J.C., Banito, A., Wuestefeld, T., Georgilis, A., Janich, P., Morton, J.P., Athineos, D., Kang, T.W., Lasitschka, F., Andrulis, M.*, et al.* (2013). A complex secretory program orchestrated by the inflammasome controls paracrine senescence. Nat Cell Biol.

Acosta, J.C., O'Loghlen, A., Banito, A., Guijarro, M.V., Augert, A., Raguz, S., Fumagalli, M., Da Costa, M., Brown, C., Popov, N.*, et al.* (2008). Chemokine signaling via the CXCR2 receptor reinforces senescence. Cell *133*, 1006-1018.

Adkins, M.W., Howar, S.R., and Tyler, J.K. (2004). Chromatin disassembly mediated by the histone chaperone Asf1 is essential for transcriptional activation of the yeast PHO5 and PHO8 genes. Molecular cell *14*, 657-666.

Adkins, M.W., Williams, S.K., Linger, J., and Tyler, J.K. (2007). Chromatin disassembly from the PHO5 promoter is essential for the recruitment of the general transcription machinery and coactivators. Mol Cell Biol *27*, 6372-6382.

Adler, A.S., Sinha, S., Kawahara, T.L., Zhang, J.Y., Segal, E., and Chang, H.Y. (2007). Motif module map reveals enforcement of aging by continual NF-kappaB activity. Genes Dev *21*, 3244-3257.

Agger, K., Cloos, P.A., Rudkjaer, L., Williams, K., Andersen, G., Christensen, J., and Helin, K. (2009). The H3K27me3 demethylase JMJD3 contributes to the activation of the INK4A-ARF locus in response to oncogene- and stress-induced senescence. Genes Dev *23*, 1171-1176.

Alani, R.M., Young, A.Z., and Shifflett, C.B. (2001). Id1 regulation of cellular senescence through transcriptional repression of p16/Ink4a. Proc Natl Acad Sci U S A *98*, 7812-7816.

Alcorta, D.A., Xiong, Y., Phelps, D., Hannon, G., Beach, D., and Barrett, J.C. (1996). Involvement of the cyclin-dependent kinase inhibitor p16 (INK4a) in replicative senescence of normal human fibroblasts. Proc Natl Acad Sci U S A *93*, 13742-13747.

Alessio, N., Squillaro, T., Cipollaro, M., Bagella, L., Giordano, A., and Galderisi, U. (2010). The BRG1 ATPase of chromatin remodeling complexes is involved in modulation of mesenchymal stem cell senescence through RB-P53 pathways. Oncogene *29*, 5452-5463.

Aoyagi, S., Narlikar, G., Zheng, C., Sif, S., Kingston, R.E., and Hayes, J.J. (2002). Nucleosome remodeling by the human SWI/SNF complex requires transient global disruption of histone-DNA interactions. Mol Cell Biol *22*, 3653-3662.

Arkan, M.C., Hevener, A.L., Greten, F.R., Maeda, S., Li, Z.W., Long, J.M., Wynshaw-Boris, A., Poli, G., Olefsky, J., and Karin, M. (2005). IKK-beta links inflammation to obesity-induced insulin resistance. Nat Med *11*, 191-198.

Astle, M.V., Hannan, K.M., Ng, P.Y., Lee, R.S., George, A.J., Hsu, A.K., Haupt, Y., Hannan, R.D., and Pearson, R.B. (2012). AKT induces senescence in human cells via mTORC1 and p53 in the absence of DNA damage: implications for targeting mTOR during malignancy. Oncogene *31*, 1949-1962.

Bachmann, I.M., Halvorsen, O.J., Collett, K., Stefansson, I.M., Straume, O., Haukaas, S.A., Salvesen, H.B., Otte, A.P., and Akslen, L.A. (2006). EZH2 expression is associated with high proliferation rate and aggressive tumor subgroups in cutaneous melanoma and cancers of the endometrium, prostate, and breast. Journal of clinical oncology : official journal of the American Society of Clinical Oncology *24*, 268-273.

Baker, D.J., Wijshake, T., Tchkonia, T., LeBrasseur, N.K., Childs, B.G., van de Sluis, B., Kirkland, J.L., and van Deursen, J.M. (2011). Clearance of p16Ink4a-positive senescent cells delays ageing-associated disorders. Nature *479*, 232-236.

Bandyopadhyay, D., Curry, J.L., Lin, Q., Richards, H.W., Chen, D., Hornsby, P.J., Timchenko, N.A., and Medrano, E.E. (2007). Dynamic assembly of chromatin complexes during cellular senescence: implications for the growth arrest of human melanocytic nevi. Aging cell *6*, 577-591.

Banito, A., Rashid, S.T., Acosta, J.C., Li, S., Pereira, C.F., Geti, I., Pinho, S., Silva, J.C., Azuara, V., Walsh, M.*, et al.* (2009). Senescence impairs successful reprogramming to pluripotent stem cells. Genes Dev *23*, 2134-2139.

Barradas, M., Anderton, E., Acosta, J.C., Li, S., Banito, A., Rodriguez-Niedenfuhr, M., Maertens, G., Banck, M., Zhou, M.M., Walsh, M.J.*, et al.* (2009). Histone demethylase JMJD3 contributes to epigenetic control of INK4a/ARF by oncogenic RAS. Genes Dev *23*, 1177-1182.

Bartkova, J., Rezaei, N., Liontos, M., Karakaidos, P., Kletsas, D., Issaeva, N., Vassiliou, L.V., Kolettas, E., Niforou, K., Zoumpourlis, V.C.*, et al.* (2006). Oncogene-induced senescence is part of the tumorigenesis barrier imposed by DNA damage checkpoints. Nature *444*, 633-637.

Battaglioli, E., Andres, M.E., Rose, D.W., Chenoweth, J.G., Rosenfeld, M.G., Anderson, M.E., and Mandel, G. (2002). REST repression of neuronal genes requires components of the hSWI.SNF complex. J Biol Chem *277*, 41038-41045.

Becker, T.M., Haferkamp, S., Dijkstra, M.K., Scurr, L.L., Frausto, M., Diefenbach, E., Scolyer, R.A., Reisman, D.N., Mann, G.J., Kefford, R.F.*, et al.* (2009). The chromatin remodelling factor BRG1 is a novel binding partner of the tumor suppressor p16INK4a. Molecular cancer *8*, 4.

Belandia, B., Orford, R.L., Hurst, H.C., and Parker, M.G. (2002). Targeting of SWI/SNF chromatin remodelling complexes to estrogen-responsive genes. EMBO J *21*, 4094-4103.

Ben-Porath, I., and Weinberg, R.A. (2005). The signals and pathways activating cellular senescence. Int J Biochem Cell Biol *37*, 961-976.

Berman, J.R., and Kenyon, C. (2006). Germ-cell loss extends C. elegans life span through regulation of DAF-16 by kri-1 and lipophilic-hormone signaling. Cell *124*, 1055-1068.

Bernards, R., Brummelkamp, T.R., and Beijersbergen, R.L. (2006). shRNA libraries and their use in cancer genetics. Nat Methods *3*, 701-706.

Berns, K., Hijmans, E.M., Mullenders, J., Brummelkamp, T.R., Velds, A., Heimerikx, M., Kerkhoven, R.M., Madiredjo, M., Nijkamp, W., Weigelt, B.*, et al.* (2004). A large-scale RNAi screen in human cells identifies new components of the p53 pathway. Nature *428*, 431-437.

Beroukhim, R., Mermel, C.H., Porter, D., Wei, G., Raychaudhuri, S., Donovan, J., Barretina, J., Boehm, J.S., Dobson, J., Urashima, M.*, et al.* (2010). The landscape of somatic copy-number alteration across human cancers. Nature *463*, 899-905.

Biegel, J.A., Zhou, J.Y., Rorke, L.B., Stenstrom, C., Wainwright, L.M., and Fogelgren, B. (1999). Germ-line and acquired mutations of INI1 in atypical teratoid and rhabdoid tumors. Cancer Res *59*, 74-79.

Birmingham, A., Selfors, L.M., Forster, T., Wrobel, D., Kennedy, C.J., Shanks, E., Santoyo-Lopez, J., Dunican, D.J., Long, A., Kelleher, D.*, et al.* (2009). Statistical methods for analysis of high-throughput RNA interference screens. Nat Methods *6*, 569-575.

Blackburn, E.H. (2001). Switching and signaling at the telomere. Cell *106*, 661-673.

Bochar, D.A., Wang, L., Beniya, H., Kinev, A., Xue, Y., Lane, W.S., Wang, W., Kashanchi, F., and Shiekhattar, R. (2000). BRCA1 is associated with a human SWI/SNF-related complex: linking chromatin remodeling to breast cancer. Cell *102*, 257-265.

Bodnar, A.G., Ouellette, M., Frolkis, M., Holt, S.E., Chiu, C.P., Morin, G.B., Harley, C.B., Shay, J.W., Lichtsteiner, S., and Wright, W.E. (1998). Extension of life-span by introduction of telomerase into normal human cells. Science *279*, 349-352.

Boeger, H., Griesenbeck, J., Strattan, J.S., and Kornberg, R.D. (2003). Nucleosomes unfold completely at a transcriptionally active promoter. Molecular cell *11*, 1587-1598.

Boeger, H., Griesenbeck, J., Strattan, J.S., and Kornberg, R.D. (2004). Removal of promoter nucleosomes by disassembly rather than sliding in vivo. Molecular cell *14*, 667-673.

Bollag, G., Clapp, D.W., Shih, S., Adler, F., Zhang, Y.Y., Thompson, P., Lange, B.J., Freedman, M.H., McCormick, F., Jacks, T.*, et al.* (1996). Loss of NF1 results in activation of the Ras signaling pathway and leads to aberrant growth in haematopoietic cells. Nat Genet *12*, 144-148.

Bosse, T., Ter Haar, N.T., Seeber, L.M., Diest, P.J., Hes, F.J., Vasen, H.F., Nout, R.A., Creutzberg, C.L., Morreau, H., and Smit, V.T. (2013). Loss of ARID1A expression and its relationship with PI3K-Akt pathway alterations, TP53 and microsatellite instability in endometrial cancer. Modern pathology : an official journal of the United States and Canadian Academy of Pathology, Inc.

Bourgo, R.J., Siddiqui, H., Fox, S., Solomon, D., Sansam, C.G., Yaniv, M., Muchardt, C., Metzger, D., Chambon, P., Roberts, C.W.*, et al.* (2009). SWI/SNF deficiency results in aberrant chromatin organization, mitotic failure, and diminished proliferative capacity. Molecular biology of the cell *20*, 3192-3199.

Bracken, A.P., Kleine-Kohlbrecher, D., Dietrich, N., Pasini, D., Gargiulo, G., Beekman, C., Theilgaard-Monch, K., Minucci, S., Porse, B.T., Marine, J.C.*, et al.* (2007). The Polycomb group proteins bind throughout the INK4A-ARF locus and are disassociated in senescent cells. Genes Dev *21*, 525-530.

Braig, M., Lee, S., Loddenkemper, C., Rudolph, C., Peters, A.H., Schlegelberger, B., Stein, H., Dorken, B., Jenuwein, T., and Schmitt, C.A. (2005). Oncogene-induced senescence as an initial barrier in lymphoma development. Nature *436*, 660-665.

Bric, A., Miething, C., Bialucha, C.U., Scuoppo, C., Zender, L., Krasnitz, A., Xuan, Z., Zuber, J., Wigler, M., Hicks, J.*, et al.* (2009). Functional identification of tumor-suppressor genes through an in vivo RNA interference screen in a mouse lymphoma model. Cancer Cell *16*, 324-335.

Brummelkamp, T.R., Bernards, R., and Agami, R. (2002a). Stable suppression of tumorigenicity by virus-mediated RNA interference. Cancer Cell *2*, 243-247.

Brummelkamp, T.R., Bernards, R., and Agami, R. (2002b). A system for stable expression of short interfering RNAs in mammalian cells. Science *296*, 550-553.

Brummelkamp, T.R., Kortlever, R.M., Lingbeek, M., Trettel, F., MacDonald, M.E., van Lohuizen, M., and Bernards, R. (2002c). TBX-3, the gene mutated in Ulnar-Mammary Syndrome, is a negative regulator of p19ARF and inhibits senescence. J Biol Chem *277*, 6567-6572.

Bultman, S., Gebuhr, T., Yee, D., La Mantia, C., Nicholson, J., Gilliam, A., Randazzo, F., Metzger, D., Chambon, P., Crabtree, G.*, et al.* (2000). A Brg1 null mutation in the mouse reveals functional differences among mammalian SWI/SNF complexes. Molecular cell *6*, 1287-1295.

Burrows, A.E., Smogorzewska, A., and Elledge, S.J. (2010). Polybromo-associated BRG1-associated factor components BRD7 and BAF180 are critical regulators of p53 required for induction of replicative senescence. Proc Natl Acad Sci U S A *107*, 14280-14285.

Busuttil, R.A., Rubio, M., Dolle, M.E., Campisi, J., and Vijg, J. (2003). Oxygen accelerates the accumulation of mutations during the senescence and immortalization of murine cells in culture. Aging cell *2*, 287-294.

Cairns, B.R., Kim, Y.J., Sayre, M.H., Laurent, B.C., and Kornberg, R.D. (1994). A multisubunit complex containing the SWI1/ADR6, SWI2/SNF2, SWI3, SNF5, and SNF6 gene products isolated from yeast. Proc Natl Acad Sci U S A *91*, 1950-1954.

Cao, R., Wang, L., Wang, H., Xia, L., Erdjument-Bromage, H., Tempst, P., Jones, R.S., and Zhang, Y. (2002). Role of histone H3 lysine 27 methylation in Polycomb-group silencing. Science *298*, 1039-1043.

Carlson, M., Osmond, B.C., and Botstein, D. (1981). Mutants of yeast defective in sucrose utilization. Genetics *98*, 25-40.

Chai, J., Charboneau, A.L., Betz, B.L., and Weissman, B.E. (2005). Loss of the hSNF5 gene concomitantly inactivates p21CIP/WAF1 and p16INK4a activity associated with replicative senescence in A204 rhabdoid tumor cells. Cancer Res *65*, 10192-10198.

Chandra, T., Kirschner, K., Thuret, J.Y., Pope, B.D., Ryba, T., Newman, S., Ahmed, K., Samarajiwa, S.A., Salama, R., Carroll, T.*, et al.* (2012). Independence of repressive histone marks and chromatin compaction during senescent heterochromatic layer formation. Molecular cell *47*, 203-214.

Chen, J., and Archer, T.K. (2005). Regulating SWI/SNF subunit levels via protein-protein interactions and proteasomal degradation: BAF155 and BAF170 limit expression of BAF57. Mol Cell Biol *25*, 9016-9027.

Chen, Z., Trotman, L.C., Shaffer, D., Lin, H.K., Dotan, Z.A., Niki, M., Koutcher, J.A., Scher, H.I., Ludwig, T., Gerald, W.*, et al.* (2005). Crucial role of p53-dependent cellular senescence in suppression of Pten-deficient tumorigenesis. Nature *436*, 725-730.

Cheng, S.W., Davies, K.P., Yung, E., Beltran, R.J., Yu, J., and Kalpana, G.V. (1999). c-MYC interacts with INI1/hSNF5 and requires the SWI/SNF complex for transactivation function. Nat Genet *22*, 102-105.

Chiba, H., Muramatsu, M., Nomoto, A., and Kato, H. (1994). Two human homologues of Saccharomyces cerevisiae SWI2/SNF2 and Drosophila brahma are transcriptional coactivators cooperating with the estrogen receptor and the retinoic acid receptor. Nucleic acids research *22*, 1815-1820.

Choi, H.I., Choi, G.I., Kim, E.K., Choi, Y.J., Sohn, K.C., Lee, Y., Kim, C.D., Yoon, T.J., Sohn, H.J., Han, S.H.*, et al.* (2011). Hair greying is associated with active hair growth. The British journal of dermatology *165*, 1183-1189.

Cichowski, K., Santiago, S., Jardim, M., Johnson, B.W., and Jacks, T. (2003). Dynamic regulation of the Ras pathway via proteolysis of the NF1 tumor suppressor. Genes Dev *17*, 449-454.

Clapier, C.R., and Cairns, B.R. (2009). The biology of chromatin remodeling complexes. Annual review of biochemistry *78*, 273-304.

Collado, M., Blasco, M.A., and Serrano, M. (2007). Cellular senescence in cancer and aging. Cell *130*, 223-233.

Collado, M., Gil, J., Efeyan, A., Guerra, C., Schuhmacher, A.J., Barradas, M., Benguria, A., Zaballos, A., Flores, J.M., Barbacid, M.*, et al.* (2005). Tumour biology: senescence in premalignant tumours. Nature *436*, 642.

Collado, M., Medema, R.H., Garcia-Cao, I., Dubuisson, M.L., Barradas, M., Glassford, J., Rivas, C., Burgering, B.M., Serrano, M., and Lam, E.W. (2000). Inhibition of the phosphoinositide 3-kinase pathway induces a senescence-like arrest mediated by p27Kip1. J Biol Chem *275*, 21960-21968.

Coppe, J.P., Desprez, P.Y., Krtolica, A., and Campisi, J. (2010). The senescence-associated secretory phenotype: the dark side of tumor suppression. Annual review of pathology *5*, 99-118.

Coppe, J.P., Patil, C.K., Rodier, F., Sun, Y., Munoz, D.P., Goldstein, J., Nelson, P.S., Desprez, P.Y., and Campisi, J. (2008). Senescence-associated secretory phenotypes reveal cell-nonautonomous functions of oncogenic RAS and the p53 tumor suppressor. PLoS biology *6*, 2853-2868.

Cote, J., Quinn, J., Workman, J.L., and Peterson, C.L. (1994). Stimulation of GAL4 derivative binding to nucleosomal DNA by the yeast SWI/SNF complex. Science *265*, 53-60.

Counter, C.M., Avilion, A.A., LeFeuvre, C.E., Stewart, N.G., Greider, C.W., Harley, C.B., and Bacchetti, S. (1992). Telomere shortening associated with chromosome instability is arrested in immortal cells which express telomerase activity. EMBO J *11*, 1921-1929.

Courtois-Cox, S., Genther Williams, S.M., Reczek, E.E., Johnson, B.W., McGillicuddy, L.T., Johannessen, C.M., Hollstein, P.E., MacCollin, M., and Cichowski, K. (2006). A negative feedback signaling network underlies oncogene-induced senescence. Cancer Cell *10*, 459-472.

Courtois-Cox, S., Jones, S.L., and Cichowski, K. (2008). Many roads lead to oncogene-induced senescence. Oncogene *27*, 2801-2809.

Cowin, P.A., Anglesio, M., Etemadmoghadam, D., and Bowtell, D.D. (2010). Profiling the cancer genome. Annual review of genomics and human genetics *11*, 133-159.

Cremer, T., and Cremer, C. (2001). Chromosome territories, nuclear architecture and gene regulation in mammalian cells. Nat Rev Genet *2*, 292-301.

Cuaz-Perolin, C., Billiet, L., Bauge, E., Copin, C., Scott-Algara, D., Genze, F., Buchele, B., Syrovets, T., Simmet, T., and Rouis, M. (2008). Antiinflammatory and antiatherogenic effects of the NF-kappaB inhibitor acetyl-11-keto-beta-boswellic acid in LPS-challenged ApoE-/- mice. Arteriosclerosis, thrombosis, and vascular biology *28*, 272-277.

Cummings, S.D., Ryu, B., Samuels, M.A., Yu, X., Meeker, A.K., Healey, M.A., and Alani, R.M. (2008). Id1 delays senescence of primary human melanocytes. Molecular carcinogenesis *47*, 653-659.

Czermin, B., Melfi, R., McCabe, D., Seitz, V., Imhof, A., and Pirrotta, V. (2002). Drosophila enhancer of Zeste/ESC complexes have a histone H3 methyltransferase activity that marks chromosomal Polycomb sites. Cell *111*, 185-196.

d'Adda di Fagagna, F. (2008). Living on a break: cellular senescence as a DNA-damage response. Nat Rev Cancer *8*, 512-522.

d'Adda di Fagagna, F., Reaper, P.M., Clay-Farrace, L., Fiegler, H., Carr, P., Von Zglinicki, T., Saretzki, G., Carter, N.P., and Jackson, S.P. (2003). A DNA damage checkpoint response in telomere-initiated senescence. Nature *426*, 194-198.

da Costa, W.H., Rezende, M., Rocha, R.M., da Cunha, I.W., Carraro, D.M., Guimaraes, G.C., and de Cassio Zequi, S. (2013). PBRM1, a SWI/SNF complex subunit is a prognostic marker in clear cell renal cell carcinoma. BJU international.

Dallas, P.B., Cheney, I.W., Liao, D.W., Bowrin, V., Byam, W., Pacchione, S., Kobayashi, R., Yaciuk, P., and Moran, E. (1998). p300/CREB binding protein-related protein p270 is a component of mammalian SWI/SNF complexes. Mol Cell Biol *18*, 3596-3603.

Dankort, D., Filenova, E., Collado, M., Serrano, M., Jones, K., and McMahon, M. (2007). A new mouse model to explore the initiation, progression, and therapy of BRAFV600E-induced lung tumors. Genes Dev *21*, 379-384.

Dastidar, R.G., Hooda, J., Shah, A., Cao, T.M., Henke, R.M., and Zhang, L. (2012). The nuclear localization of SWI/SNF proteins is subjected to oxygen regulation. Cell & bioscience *2*, 30.

Debacq-Chainiaux, F., Erusalimsky, J.D., Campisi, J., and Toussaint, O. (2009). Protocols to detect senescence-associated beta-galactosidase (SA-betagal) activity, a biomarker of senescent cells in culture and in vivo. Nature protocols *4*, 1798-1806.

Debernardi, S., Bassini, A., Jones, L.K., Chaplin, T., Linder, B., de Bruijn, D.R., Meese, E., and Young, B.D. (2002). The MLL fusion partner AF10 binds GAS41, a protein that interacts with the human SWI/SNF complex. Blood *99*, 275-281.

Debril, M.B., Gelman, L., Fayard, E., Annicotte, J.S., Rocchi, S., and Auwerx, J. (2004). Transcription factors and nuclear receptors interact with the SWI/SNF complex through the BAF60c subunit. J Biol Chem *279*, 16677-16686.

Decristofaro, M.F., Betz, B.L., Rorie, C.J., Reisman, D.N., Wang, W., and Weissman, B.E. (2001). Characterization of SWI/SNF protein expression in human breast cancer cell lines and other malignancies. J Cell Physiol *186*, 136-145.

Demidenko, Z.N., Shtutman, M., and Blagosklonny, M.V. (2009a). Pharmacologic inhibition of MEK and PI-3K converges on the mTOR/S6 pathway to decelerate cellular senescence. Cell Cycle *8*, 1896-1900.

Demidenko, Z.N., Zubova, S.G., Bukreeva, E.I., Pospelov, V.A., Pospelova, T.V., and Blagosklonny, M.V. (2009b). Rapamycin decelerates cellular senescence. Cell Cycle *8*, 1888-1895.

Di Micco, R., Fumagalli, M., Cicalese, A., Piccinin, S., Gasparini, P., Luise, C., Schurra, C., Garre, M., Nuciforo, P.G., Bensimon, A.*, et al.* (2006). Oncogene-induced senescence is a DNA damage response triggered by DNA hyper-replication. Nature *444*, 638-642.

Dietrich, N., Bracken, A.P., Trinh, E., Schjerling, C.K., Koseki, H., Rappsilber, J., Helin, K., and Hansen, K.H. (2007). Bypass of senescence by the polycomb group protein CBX8 through direct binding to the INK4A-ARF locus. EMBO J *26*, 1637-1648.

Dillon, N., and Festenstein, R. (2002). Unravelling heterochromatin: competition between positive and negative factors regulates accessibility. Trends in genetics : TIG *18*, 252-258.

Dimauro, T., and David, G. (2009). Chromatin modifications: the driving force of senescence and aging? Aging *1*, 182-190.

Dimri, G.P. (2005). What has senescence got to do with cancer? Cancer Cell *7*, 505-512.

Dimri, G.P., Lee, X., Basile, G., Acosta, M., Scott, G., Roskelley, C., Medrano, E.E., Linskens, M., Rubelj, I., Pereira-Smith, O.*, et al.* (1995). A biomarker that identifies senescent human cells in culture and in aging skin in vivo. Proc Natl Acad Sci U S A *92*, 9363-9367.

Donet, E., Bayo, P., Calvo, E., Labrie, F., and Perez, P. (2008). Identification of novel glucocorticoid receptor-regulated genes involved in epidermal homeostasis and hair follicle differentiation. The Journal of steroid biochemistry and molecular biology *108*, 8-16.

Drost, J., Mantovani, F., Tocco, F., Elkon, R., Comel, A., Holstege, H., Kerkhoven, R., Jonkers, J., Voorhoeve, P.M., Agami, R.*, et al.* (2010). BRD7 is a candidate tumour suppressor gene required for p53 function. Nat Cell Biol *12*, 380-389.

Dunaief, J.L., Strober, B.E., Guha, S., Khavari, P.A., Alin, K., Luban, J., Begemann, M., Crabtree, G.R., and Goff, S.P. (1994). The retinoblastoma protein and BRG1 form a complex and cooperate to induce cell cycle arrest. Cell *79*, 119-130.

Echeverri, C.J., and Perrimon, N. (2006). High-throughput RNAi screening in cultured cells: a user's guide. Nat Rev Genet *7*, 373-384.

el-Deiry, W.S., Tokino, T., Velculescu, V.E., Levy, D.B., Parsons, R., Trent, J.M., Lin, D., Mercer, W.E., Kinzler, K.W., and Vogelstein, B. (1993). WAF1, a potential mediator of p53 tumor suppression. Cell *75*, 817-825.

Elbashir, S.M., Harborth, J., Lendeckel, W., Yalcin, A., Weber, K., and Tuschl, T. (2001). Duplexes of 21-nucleotide RNAs mediate RNA interference in cultured mammalian cells. Nature *411*, 494-498.

Esteller, M., Silva, J.M., Dominguez, G., Bonilla, F., Matias-Guiu, X., Lerma, E., Bussaglia, E., Prat, J., Harkes, I.C., Repasky, E.A.*, et al.* (2000). Promoter hypermethylation and BRCA1 inactivation in sporadic breast and ovarian tumors. Journal of the National Cancer Institute *92*, 564-569.

Euskirchen, G.M., Auerbach, R.K., Davidov, E., Gianoulis, T.A., Zhong, G., Rozowsky, J., Bhardwaj, N., Gerstein, M.B., and Snyder, M. (2011). Diverse roles and interactions of the SWI/SNF chromatin remodeling complex revealed using global approaches. PLoS Genet *7*, e1002008.

Fellmann, C., Zuber, J., McJunkin, K., Chang, K., Malone, C.D., Dickins, R.A., Xu, Q., Hengartner, M.O., Elledge, S.J., Hannon, G.J.*, et al.* (2011). Functional identification of optimized RNAi triggers using a massively parallel sensor assay. Molecular cell *41*, 733-746.

Feser, J., Truong, D., Das, C., Carson, J.J., Kieft, J., Harkness, T., and Tyler, J.K. (2010). Elevated histone expression promotes life span extension. Molecular cell *39*, 724-735.

Fisher (1925). Statistical Methods for Research Workers (Oliver and Boyd).

Flores-Alcantar, A., Gonzalez-Sandoval, A., Escalante-Alcalde, D., and Lomeli, H. (2011). Dynamics of expression of ARID1A and ARID1B subunits in mouse embryos and in cells during the cell cycle. Cell and tissue research *345*, 137-148.

Fonagy, A., Swiderski, C., Ostrovsky, A.M., Bolton, W.E., and Freeman, J.W. (1994). Effect of nucleolar P120 expression level on the proliferation capacity of breast cancer cells. Cancer Res *54*, 1859-1864.

Foster, K.S., McCrary, W.J., Ross, J.S., and Wright, C.F. (2006). Members of the hSWI/SNF chromatin remodeling complex associate with and are phosphorylated by protein kinase B/Akt. Oncogene *25*, 4605-4612.

Fryer, C.J., and Archer, T.K. (1998). Chromatin remodelling by the glucocorticoid receptor requires the BRG1 complex. Nature *393*, 88-91.

Fujimoto, A., Totoki, Y., Abe, T., Boroevich, K.A., Hosoda, F., Nguyen, H.H., Aoki, M., Hosono, N., Kubo, M., Miya, F.*, et al.* (2012). Whole-genome sequencing of liver cancers identifies etiological influences on mutation patterns and recurrent mutations in chromatin regulators. Nat Genet *44*, 760-764.

Funayama, R., Saito, M., Tanobe, H., and Ishikawa, F. (2006). Loss of linker histone H1 in cellular senescence. The Journal of cell biology *175*, 869-880.

Futreal, P.A., and Barrett, J.C. (1991). Failure of senescent cells to phosphorylate the RB protein. Oncogene *6*, 1109-1113.

Gangaraju, V.K., and Bartholomew, B. (2007). Dependency of ISW1a chromatin remodeling on extranucleosomal DNA. Mol Cell Biol *27*, 3217-3225.

Garcia-Cao, I., Garcia-Cao, M., Tomas-Loba, A., Martin-Caballero, J., Flores, J.M., Klatt, P., Blasco, M.A., and Serrano, M. (2006). Increased p53 activity does not accelerate telomere-driven ageing. EMBO Rep *7*, 546-552.

Gartel, A.L., Goufman, E., Tevosian, S.G., Shih, H., Yee, A.S., and Tyner, A.L. (1998). Activation and repression of p21(WAF1/CIP1) transcription by RB binding proteins. Oncogene *17*, 3463-3469.

Gerland, L.M., Peyrol, S., Lallemand, C., Branche, R., Magaud, J.P., and Ffrench, M. (2003). Association of increased autophagic inclusions labeled for beta-galactosidase with fibroblastic aging. Exp Gerontol *38*, 887-895.

Gil, J., Bernard, D., Martinez, D., and Beach, D. (2004). Polycomb CBX7 has a unifying role in cellular lifespan. Nat Cell Biol *6*, 67-72.

Gil, J., and Peters, G. (2006). Regulation of the INK4b-ARF-INK4a tumour suppressor locus: all for one or one for all. Nat Rev Mol Cell Biol *7*, 667-677.

Giraud, S., Hurlstone, A., Avril, S., and Coqueret, O. (2004). Implication of BRG1 and cdk9 in the STAT3-mediated activation of the p21waf1 gene. Oncogene *23*, 7391-7398.

Glaros, S., Cirrincione, G.M., Muchardt, C., Kleer, C.G., Michael, C.W., and Reisman, D. (2007). The reversible epigenetic silencing of BRM: implications for clinical targeted therapy. Oncogene *26*, 7058-7066.

Gonzalez-Zulueta, M., Bender, C.M., Yang, A.S., Nguyen, T., Beart, R.W., Van Tornout, J.M., and Jones, P.A. (1995). Methylation of the 5' CpG island of the p16/CDKN2 tumor suppressor gene in normal and transformed human tissues correlates with gene silencing. Cancer Res *55*, 4531-4535.

Gray-Schopfer, V.C., Cheong, S.C., Chong, H., Chow, J., Moss, T., Abdel-Malek, Z.A., Marais, R., Wynford-Thomas, D., and Bennett, D.C. (2006). Cellular senescence in naevi and immortalisation in melanoma: a role for p16? British journal of cancer *95*, 496-505.

Greider, C.W., and Blackburn, E.H. (1985). Identification of a specific telomere terminal transferase activity in Tetrahymena extracts. Cell *43*, 405-413.

Guan, B., Wang, T.L., and Shih Ie, M. (2011). ARID1A, a factor that promotes formation of SWI/SNF-mediated chromatin remodeling, is a tumor suppressor in gynecologic cancers. Cancer Res *71*, 6718-6727.

Guarente, L. (1987). Regulatory proteins in yeast. Annual review of genetics *21*, 425-452.

Guidi, C.J., Sands, A.T., Zambrowicz, B.P., Turner, T.K., Demers, D.A., Webster, W., Smith, T.W., Imbalzano, A.N., and Jones, S.N. (2001). Disruption of Ini1 leads to peri-implantation lethality and tumorigenesis in mice. Molecular and Cellular Biology *21*, 3598-3603.

Ha, L., Ichikawa, T., Anver, M., Dickins, R., Lowe, S., Sharpless, N.E., Krimpenfort, P., Depinho, R.A., Bennett, D.C., Sviderskaya, E.V.*, et al.* (2007). ARF functions as a melanoma tumor suppressor by inducing p53-independent senescence. Proc Natl Acad Sci U S A *104*, 10968-10973.

Hargreaves, D.C., and Crabtree, G.R. (2011). ATP-dependent chromatin remodeling: genetics, genomics and mechanisms. Cell research *21*, 396-420.

Harley, C.B., Futcher, A.B., and Greider, C.W. (1990). Telomeres shorten during ageing of human fibroblasts. Nature *345*, 458-460.

Harrison, D.E., Strong, R., Sharp, Z.D., Nelson, J.F., Astle, C.M., Flurkey, K., Nadon, N.L., Wilkinson, J.E., Frenkel, K., Carter, C.S.*, et al.* (2009). Rapamycin fed late in life extends lifespan in genetically heterogeneous mice. Nature *460*, 392-395.

Harvey, M., Sands, A.T., Weiss, R.S., Hegi, M.E., Wiseman, R.W., Pantazis, P., Giovanella, B.C., Tainsky, M.A., Bradley, A., and Donehower, L.A. (1993). In vitro growth characteristics of embryo fibroblasts isolated from p53-deficient mice. Oncogene *8*, 2457-2467.

Hayflick, L. (1965). The Limited in Vitro Lifetime of Human Diploid Cell Strains. Exp Cell Res *37*, 614-636.

Hayflick, L. (1997). Mortality and immortality at the cellular level. A review. Biochemistry Biokhimiia *62*, 1180-1190.

Hayflick, L., and Moorhead, P.S. (1961). The serial cultivation of human diploid cell strains. Exp Cell Res *25*, 585-621.

Helin, K., and Dhanak, D. (2013). Chromatin proteins and modifications as drug targets. Nature *502*, 480-488.

Herman, J.G., Latif, F., Weng, Y., Lerman, M.I., Zbar, B., Liu, S., Samid, D., Duan, D.S., Gnarra, J.R., Linehan, W.M.*, et al.* (1994). Silencing of the VHL tumor-suppressor gene by DNA methylation in renal carcinoma. Proc Natl Acad Sci U S A *91*, 9700-9704.

Herman, J.G., Merlo, A., Mao, L., Lapidus, R.G., Issa, J.P., Davidson, N.E., Sidransky, D., and Baylin, S.B. (1995). Inactivation of the CDKN2/p16/MTS1 gene is frequently associated with aberrant DNA methylation in all common human cancers. Cancer Res *55*, 4525-4530.

Hermeking, H., Lengauer, C., Polyak, K., He, T.C., Zhang, L., Thiagalingam, S., Kinzler, K.W., and Vogelstein, B. (1997). 14-3-3 sigma is a p53-regulated inhibitor of G2/M progression. Molecular cell *1*, 3-11.

Hirao, A., Kong, Y.Y., Matsuoka, S., Wakeham, A., Ruland, J., Yoshida, H., Liu, D., Elledge, S.J., and Mak, T.W. (2000). DNA damage-induced activation of p53 by the checkpoint kinase Chk2. Science *287*, 1824-1827.

Hirschhorn, J.N., Brown, S.A., Clark, C.D., and Winston, F. (1992). Evidence that SNF2/SWI2 and SNF5 activate transcription in yeast by altering chromatin structure. Genes Dev *6*, 2288-2298.

Hiyama, H., Iavarone, A., and Reeves, S.A. (1998). Regulation of the cdk inhibitor p21 gene during cell cycle progression is under the control of the transcription factor E2F. Oncogene *16*, 1513-1523.

Ho, L., Jothi, R., Ronan, J.L., Cui, K., Zhao, K., and Crabtree, G.R. (2009a). An embryonic stem cell chromatin remodeling complex, esBAF, is an essential component of the core pluripotency transcriptional network. Proc Natl Acad Sci U S A *106*, 5187-5191.

Ho, L., Ronan, J.L., Wu, J., Staahl, B.T., Chen, L., Kuo, A., Lessard, J., Nesvizhskii, A.I., Ranish, J., and Crabtree, G.R. (2009b). An embryonic stem cell chromatin remodeling complex, esBAF, is essential for embryonic stem cell self-renewal and pluripotency. Proc Natl Acad Sci U S A *106*, 5181-5186.

Hoare, M., Young, A.R., and Narita, M. (2011). Autophagy in cancer: having your cake and eating it. Seminars in cancer biology *21*, 397-404.

Hong, H., Takahashi, K., Ichisaka, T., Aoi, T., Kanagawa, O., Nakagawa, M., Okita, K., and Yamanaka, S. (2009). Suppression of induced pluripotent stem cell generation by the p53-p21 pathway. Nature *460*, 1132-1135.

Hu, G., and Luo, J. (2012). A primer on using pooled shRNA libraries for functional genomic screens. Acta biochimica et biophysica Sinica *44*, 103-112.

Huang, C.H., Mandelker, D., Gabelli, S.B., and Amzel, L.M. (2008a). Insights into the oncogenic effects of PIK3CA mutations from the structure of p110alpha/p85alpha. Cell Cycle *7*, 1151-1156.

Huang, S., Risques, R.A., Martin, G.M., Rabinovitch, P.S., and Oshima, J. (2008b). Accelerated telomere shortening and replicative senescence in human fibroblasts overexpressing mutant and wild-type lamin A. Exp Cell Res *314*, 82-91.

Hulsebos, T.J., Plomp, A.S., Wolterman, R.A., Robanus-Maandag, E.C., Baas, F., and Wesseling, P. (2007). Germline mutation of INI1/SMARCB1 in familial schwannomatosis. Am J Hum Genet *80*, 805-810.

Hutter, E., Renner, K., Pfister, G., Stockl, P., Jansen-Durr, P., and Gnaiger, E. (2004). Senescence-associated changes in respiration and oxidative phosphorylation in primary human fibroblasts. Biochem J *380*, 919-928.

Iakova, P., Awad, S.S., and Timchenko, N.A. (2003). Aging reduces proliferative capacities of liver by switching pathways of C/EBPalpha growth arrest. Cell *113*, 495-506.

Ichinose, H., Garnier, J.M., Chambon, P., and Losson, R. (1997). Ligand-dependent interaction between the estrogen receptor and the human homologues of SWI2/SNF2. Gene *188*, 95-100.

Inoue, H., Giannakopoulos, S., Parkhurst, C.N., Matsumura, T., Kono, E.A., Furukawa, T., and Tanese, N. (2011). Target genes of the largest human SWI/SNF complex subunit control cell growth. Biochem J *434*, 83-92.

Isakoff, M.S., Sansam, C.G., Tamayo, P., Subramanian, A., Evans, J.A., Fillmore, C.M., Wang, X., Biegel, J.A., Pomeroy, S.L., Mesirov, J.P.*, et al.* (2005). Inactivation of the Snf5 tumor suppressor stimulates cell cycle progression and cooperates with p53 loss in oncogenic transformation. Proc Natl Acad Sci U S A *102*, 17745-17750.

Ishimi, Y., Kojima, M., Takeuchi, F., Miyamoto, T., Yamada, M., and Hanaoka, F. (1987). Changes in chromatin structure during aging of human skin fibroblasts. Exp Cell Res *169*, 458-467.

Ishizaka, A., Mizutani, T., Kobayashi, K., Tando, T., Sakurai, K., Fujiwara, T., and Iba, H. (2012). Double plant homeodomain (PHD) finger proteins DPF3a and -3b are required as transcriptional co-activators in SWI/SNF complex-dependent activation of NF-kappaB RelA/p50 heterodimer. J Biol Chem *287*, 11924-11933.

Itahana, K., Campisi, J., and Dimri, G.P. (2004). Mechanisms of cellular senescence in human and mouse cells. Biogerontology *5*, 1-10.

Jackson, A.L., Burchard, J., Schelter, J., Chau, B.N., Cleary, M., Lim, L., and Linsley, P.S. (2006). Widespread siRNA "off-target" transcript silencing mediated by seed region sequence complementarity. RNA *12*, 1179-1187.

Jackson, A.L., and Linsley, P.S. (2010). Recognizing and avoiding siRNA off-target effects for target identification and therapeutic application. Nature reviews Drug discovery *9*, 57-67.

Jacobs, J.J., Keblusek, P., Robanus-Maandag, E., Kristel, P., Lingbeek, M., Nederlof, P.M., van Welsem, T., van de Vijver, M.J., Koh, E.Y., Daley, G.Q.*, et al.* (2000). Senescence bypass screen identifies TBX2, which represses Cdkn2a (p19(ARF)) and is amplified in a subset of human breast cancers. Nat Genet *26*, 291-299.

Jacobs, J.J., Kieboom, K., Marino, S., DePinho, R.A., and van Lohuizen, M. (1999). The oncogene and Polycomb-group gene bmi-1 regulates cell proliferation and senescence through the ink4a locus. Nature *397*, 164-168.

Johnson, B.R., Nitta, R.T., Frock, R.L., Mounkes, L., Barbie, D.A., Stewart, C.L., Harlow, E., and Kennedy, B.K. (2004). A-type lamins regulate retinoblastoma protein function by promoting subnuclear localization and preventing proteasomal degradation. Proc Natl Acad Sci U S A *101*, 9677-9682.

Jones, P.A., and Baylin, S.B. (2002). The fundamental role of epigenetic events in cancer. Nat Rev Genet *3*, 415-428.

Jones, S., Wang, T.L., Shih Ie, M., Mao, T.L., Nakayama, K., Roden, R., Glas, R., Slamon, D., Diaz, L.A., Jr., Vogelstein, B.*, et al.* (2010). Frequent mutations of chromatin remodeling gene ARID1A in ovarian clear cell carcinoma. Science *330*, 228-231.

Kadoch, C., and Crabtree, G.R. (2013). Reversible disruption of mSWI/SNF (BAF) complexes by the SS18-SSX oncogenic fusion in synovial sarcoma. Cell *153*, 71-85.

Kadoch, C., Hargreaves, D.C., Hodges, C., Elias, L., Ho, L., Ranish, J., and Crabtree, G.R. (2013). Proteomic and bioinformatic analysis of mammalian SWI/SNF complexes identifies extensive roles in human malignancy. Nat Genet.

Kamijo, T., Zindy, F., Roussel, M.F., Quelle, D.E., Downing, J.R., Ashmun, R.A., Grosveld, G., and Sherr, C.J. (1997). Tumor suppression at the mouse INK4a locus mediated by the alternative reading frame product p19ARF. Cell *91*, 649-659.

Kang, H., Cui, K., and Zhao, K. (2004). BRG1 controls the activity of the retinoblastoma protein via regulation of p21CIP1/WAF1/SDI. Mol Cell Biol *24*, 1188-1199.

Kang, T.W., Yevsa, T., Woller, N., Hoenicke, L., Wuestefeld, T., Dauch, D., Hohmeyer, A., Gereke, M., Rudalska, R., Potapova, A.*, et al.* (2011). Senescence surveillance of pre-malignant hepatocytes limits liver cancer development. Nature *479*, 547-551.

Kaplon, J., Zheng, L., Meissl, K., Chaneton, B., Selivanov, V.A., Mackay, G., van der Burg, S.H., Verdegaal, E.M., Cascante, M., Shlomi, T.*, et al.* (2013). A key role for mitochondrial gatekeeper pyruvate dehydrogenase in oncogene-induced senescence. Nature *498*, 109-112.

Kassabov, S.R., Zhang, B., Persinger, J., and Bartholomew, B. (2003). SWI/SNF unwraps, slides, and rewraps the nucleosome. Molecular cell *11*, 391-403.

Kennedy, A.L., Morton, J.P., Manoharan, I., Nelson, D.M., Jamieson, N.B., Pawlikowski, J.S., McBryan, T., Doyle, B., McKay, C., Oien, K.A.*, et al.* (2011). Activation of the PIK3CA/AKT pathway suppresses senescence induced by an activated RAS oncogene to promote tumorigenesis. Molecular cell *42*, 36-49.

Kenneth, N.S., Mudie, S., van Uden, P., and Rocha, S. (2009). SWI/SNF regulates the cellular response to hypoxia. J Biol Chem *284*, 4123-4131.

Kenyon, C.J. (2010). The genetics of ageing. Nature *464*, 504-512.

Keppler, B.R., and Archer, T.K. (2010). Ubiquitin-dependent and ubiquitin-independent control of subunit stoichiometry in the SWI/SNF complex. J Biol Chem *285*, 35665-35674.

Khavari, P.A., Peterson, C.L., Tamkun, J.W., Mendel, D.B., and Crabtree, G.R. (1993). BRG1 contains a conserved domain of the SWI2/SNF2 family necessary for normal mitotic growth and transcription. Nature *366*, 170-174.

Khursheed, M., Kolla, J.N., Kotapalli, V., Gupta, N., Gowrishankar, S., Uppin, S.G., Sastry, R.A., Koganti, S., Sundaram, C., Pollack, J.R.*, et al.* (2013). ARID1B, a member of the human SWI/SNF chromatin remodeling complex, exhibits tumour-suppressor activities in pancreatic cancer cell lines. British journal of cancer *108*, 2056-2062.

Kia, S.K., Gorski, M.M., Giannakopoulos, S., and Verrijzer, C.P. (2008). SWI/SNF mediates polycomb eviction and epigenetic reprogramming of the INK4b-ARF-INK4a locus. Mol Cell Biol *28*, 3457-3464.

Kidder, B.L., Palmer, S., and Knott, J.G. (2009). SWI/SNF-Brg1 regulates self-renewal and occupies core pluripotency-related genes in embryonic stem cells. Stem Cells *27*, 317-328.

Kim, J.S., Lee, C., Bonifant, C.L., Ressom, H., and Waldman, T. (2007). Activation of p53-dependent growth suppression in human cells by mutations in PTEN or PIK3CA. Mol Cell Biol *27*, 662-677.

Kleer, C.G., Cao, Q., Varambally, S., Shen, R., Ota, I., Tomlins, S.A., Ghosh, D., Sewalt, R.G., Otte, A.P., Hayes, D.F.*, et al.* (2003). EZH2 is a marker of aggressive breast cancer and promotes neoplastic transformation of breast epithelial cells. Proc Natl Acad Sci U S A *100*, 11606-11611.

Knutson, S.K., Warholic, N.M., Wigle, T.J., Klaus, C.R., Allain, C.J., Raimondi, A., Porter Scott, M., Chesworth, R., Moyer, M.P., Copeland, R.A.*, et al.* (2013). Durable tumor regression in genetically altered malignant rhabdoid tumors by inhibition of methyltransferase EZH2. Proc Natl Acad Sci U S A *110*, 7922-7927.

Knutson, S.K., Wigle, T.J., Warholic, N.M., Sneeringer, C.J., Allain, C.J., Klaus, C.R., Sacks, J.D., Raimondi, A., Majer, C.R., Song, J.*, et al.* (2012). A selective inhibitor of EZH2 blocks H3K27 methylation and kills mutant lymphoma cells. Nature chemical biology *8*, 890-896.

Kobel, M., Kalloger, S.E., Lee, S., Duggan, M.A., Kelemen, L.E., Prentice, L., Kalli, K.R., Fridley, B.L., Visscher, D.W., Keeney, G.L.*, et al.* (2013). Biomarker-based ovarian carcinoma typing: a histologic investigation in the ovarian tumor tissue analysis consortium. Cancer epidemiology, biomarkers & prevention : a publication of the American Association for Cancer Research, cosponsored by the American Society of Preventive Oncology *22*, 1677-1686.

Koch, C.M., Joussen, S., Schellenberg, A., Lin, Q., Zenke, M., and Wagner, W. (2012). Monitoring of cellular senescence by DNA-methylation at specific CpG sites. Aging cell *11*, 366-369.

Koch, C.M., Reck, K., Shao, K., Lin, Q., Joussen, S., Ziegler, P., Walenda, G., Drescher, W., Opalka, B., May, T.*, et al.* (2013). Pluripotent stem cells escape from senescence-associated DNA methylation changes. Genome research *23*, 248-259.

Kohashi, K., Izumi, T., Oda, Y., Yamamoto, H., Tamiya, S., Taguchi, T., Iwamoto, Y., Hasegawa, T., and Tsuneyoshi, M. (2009). Infrequent SMARCB1/INI1 gene alteration in epithelioid sarcoma: a useful tool in distinguishing epithelioid sarcoma from malignant rhabdoid tumor. Human pathology *40*, 349-355.

Kolesnichenko, M., Hong, L., Liao, R., Vogt, P.K., and Sun, P. (2012). Attenuation of TORC1 signaling delays replicative and oncogenic RAS-induced senescence. Cell Cycle *11*, 2391-2401.

Kong, Y., Cui, H., and Zhang, H. (2011). Smurf2-mediated ubiquitination and degradation of Id1 regulates p16 expression during senescence. Aging cell *10*, 1038-1046.

Korber, P., Barbaric, S., Luckenbach, T., Schmid, A., Schermer, U.J., Blaschke, D., and Horz, W. (2006). The histone chaperone Asf1 increases the rate of histone eviction at the yeast PHO5 and PHO8 promoters. J Biol Chem *281*, 5539-5545.

Kortlever, R.M., Higgins, P.J., and Bernards, R. (2006). Plasminogen activator inhibitor-1 is a critical downstream target of p53 in the induction of replicative senescence. Nat Cell Biol *8*, 877-884.

Kortschak, R.D., Tucker, P.W., and Saint, R. (2000). ARID proteins come in from the desert. Trends in biochemical sciences *25*, 294-299.

Kotake, Y., Zeng, Y., and Xiong, Y. (2009). DDB1-CUL4 and MLL1 mediate oncogene-induced p16INK4a activation. Cancer Res *69*, 1809-1814.

Kouzarides, T. (2007). Chromatin modifications and their function. Cell *128*, 693-705.

Kreiger, P.A., Judkins, A.R., Russo, P.A., Biegel, J.A., Lestini, B.J., Assanasen, C., and Pawel, B.R. (2009). Loss of INI1 expression defines a unique subset of pediatric undifferentiated soft tissue sarcomas. Modern pathology : an official journal of the United States and Canadian Academy of Pathology, Inc *22*, 142-150.

Krishnamurthy, J., Torrice, C., Ramsey, M.R., Kovalev, G.I., Al-Regaiey, K., Su, L., and Sharpless, N.E. (2004). Ink4a/Arf expression is a biomarker of aging. The Journal of clinical investigation *114*, 1299-1307.

Krtolica, A., Parrinello, S., Lockett, S., Desprez, P.Y., and Campisi, J. (2001). Senescent fibroblasts promote epithelial cell growth and tumorigenesis: a link between cancer and aging. Proc Natl Acad Sci U S A *98*, 12072-12077.

Kuilman, T., Michaloglou, C., Mooi, W.J., and Peeper, D.S. (2010). The essence of senescence. Genes Dev *24*, 2463-2479.

Kuilman, T., and Peeper, D.S. (2009). Senescence-messaging secretome: SMS-ing cellular stress. Nat Rev Cancer *9*, 81-94.

Kurz, D.J., Decary, S., Hong, Y., and Erusalimsky, J.D. (2000). Senescence-associated (beta)-galactosidase reflects an increase in lysosomal mass during replicative ageing of human endothelial cells. Journal of cell science *113 (Pt 20)*, 3613-3622.

Kuwahara, Y., Charboneau, A., Knudsen, E.S., and Weissman, B.E. (2010). Reexpression of hSNF5 in malignant rhabdoid tumor cell lines causes cell cycle arrest through a p21(CIP1/WAF1)-dependent mechanism. Cancer Res *70*, 1854-1865.

Kwon, H., Imbalzano, A.N., Khavari, P.A., Kingston, R.E., and Green, M.R. (1994). Nucleosome disruption and enhancement of activator binding by a human SW1/SNF complex. Nature *370*, 477-481.

Kyoung Kim, H., Kyoung Kim, Y., Song, I.H., Baek, S.H., Lee, S.R., Hye Kim, J., and Kim, J.R. (2005). Down-regulation of a forkhead transcription factor, FOXO3a, accelerates cellular senescence in human dermal fibroblasts. The journals of gerontology Series A, Biological sciences and medical sciences *60*, 4-9.

Lasorella, A., Iavarone, A., and Israel, M.A. (1996). Id2 specifically alters regulation of the cell cycle by tumor suppressor proteins. Mol Cell Biol *16*, 2570-2578.

Laurent, B.C., Treitel, M.A., and Carlson, M. (1990). The SNF5 protein of Saccharomyces cerevisiae is a glutamine- and proline-rich transcriptional activator that affects expression of a broad spectrum of genes. Mol Cell Biol *10*, 5616-5625.

Laurent, B.C., Treitel, M.A., and Carlson, M. (1991). Functional interdependence of the yeast SNF2, SNF5, and SNF6 proteins in transcriptional activation. Proc Natl Acad Sci U S A *88*, 2687-2691.

Lavigne, M., Eskeland, R., Azebi, S., Saint-Andre, V., Jang, S.M., Batsche, E., Fan, H.Y., Kingston, R.E., Imhof, A., and Muchardt, C. (2009). Interaction of HP1 and Brg1/Brm with the globular domain of histone H3 is required for HP1-mediated repression. PLoS Genet *5*, e1000769.

Leal, J.F., Fominaya, J., Cascon, A., Guijarro, M.V., Blanco-Aparicio, C., Lleonart, M., Castro, M.E., Ramon, Y.C.S., Robledo, M., Beach, D.H.*, et al.* (2008). Cellular senescence bypass screen identifies new putative tumor suppressor genes. Oncogene *27*, 1961-1970.

Lee, A.C., Fenster, B.E., Ito, H., Takeda, K., Bae, N.S., Hirai, T., Yu, Z.X., Ferrans, V.J., Howard, B.H., and Finkel, T. (1999). Ras proteins induce senescence by altering the intracellular levels of reactive oxygen species. J Biol Chem *274*, 7936-7940.

Lee, B.Y., Han, J.A., Im, J.S., Morrone, A., Johung, K., Goodwin, E.C., Kleijer, W.J., DiMaio, D., and Hwang, E.S. (2006). Senescence-associated beta-galactosidase is lysosomal beta-galactosidase. Aging cell *5*, 187-195.

Lee, C., Kim, J.S., and Waldman, T. (2007a). Activated PI3K signaling as an endogenous inducer of p53 in human cancer. Cell Cycle *6*, 394-396.

Lee, D., Kim, J.W., Seo, T., Hwang, S.G., Choi, E.J., and Choe, J. (2002a). SWI/SNF complex interacts with tumor suppressor p53 and is necessary for the activation of p53-mediated transcription. J Biol Chem *277*, 22330-22337.

Lee, H.C., Yin, P.H., Chi, C.W., and Wei, Y.H. (2002b). Increase in mitochondrial mass in human fibroblasts under oxidative stress and during replicative cell senescence. Journal of biomedical science *9*, 517-526.

Lee, J.W., Soung, Y.H., Kim, S.Y., Lee, H.W., Park, W.S., Nam, S.W., Kim, S.H., Lee, J.Y., Yoo, N.J., and Lee, S.H. (2005). PIK3CA gene is frequently mutated in breast carcinomas and hepatocellular carcinomas. Oncogene *24*, 1477-1480.

Lee, Y.S., Sohn, D.H., Han, D., Lee, H.W., Seong, R.H., and Kim, J.B. (2007b). Chromatin remodeling complex interacts with ADD1/SREBP1c to mediate insulin-dependent regulation of gene expression. Mol Cell Biol *27*, 438-452.

Legakis, J.E., Koepke, J.I., Jedeszko, C., Barlaskar, F., Terlecky, L.J., Edwards, H.J., Walton, P.A., and Terlecky, S.R. (2002). Peroxisome senescence in human fibroblasts. Molecular biology of the cell *13*, 4243-4255.

Lei, I., Gao, X., Sham, M.H., and Wang, Z. (2012). SWI/SNF protein component BAF250a regulates cardiac progenitor cell differentiation by modulating chromatin accessibility during second heart field development. J Biol Chem *287*, 24255-24262.

Lessard, J., Wu, J.I., Ranish, J.A., Wan, M., Winslow, M.M., Staahl, B.T., Wu, H., Aebersold, R., Graef, I.A., and Crabtree, G.R. (2007). An essential switch in subunit composition of a chromatin remodeling complex during neural development. Neuron *55*, 201-215.

Li, H., Collado, M., Villasante, A., Strati, K., Ortega, S., Canamero, M., Blasco, M.A., and Serrano, M. (2009). The Ink4/Arf locus is a barrier for iPS cell reprogramming. Nature *460*, 1136-1139.

Li, J., Yen, C., Liaw, D., Podsypanina, K., Bose, S., Wang, S.I., Puc, J., Miliaresis, C., Rodgers, L., McCombie, R.*, et al.* (1997). PTEN, a putative protein tyrosine phosphatase gene mutated in human brain, breast, and prostate cancer. Science *275*, 1943-1947.

Li, J., Zhang, Z., and Li, G. (2011a). Patient outcome prediction using multiple biomarkers in human melanoma: A clinicopathological study of 118 cases. Experimental and therapeutic medicine *2*, 131-135.

Li, Q., Zhang, Y., Fu, J., Han, L., Xue, L., Lv, C., Wang, P., Li, G., and Tong, T. (2013). FOXA1 mediates p16(INK4a) activation during cellular senescence. EMBO J *32*, 858-873.

Li, S., Liu, C., Li, N., Hao, T., Han, T., Hill, D.E., Vidal, M., and Lin, J.D. (2008). Genome-wide coactivation analysis of PGC-1alpha identifies BAF60a as a regulator of hepatic lipid metabolism. Cell metabolism *8*, 105-117.

Li, X.S., Trojer, P., Matsumura, T., Treisman, J.E., and Tanese, N. (2010). Mammalian SWI/SNF--a subunit BAF250/ARID1 is an E3 ubiquitin ligase that targets histone H2B. Mol Cell Biol *30*, 1673-1688.

Li, Z.Y., Yang, Y., Ming, M., and Liu, B. (2011b). Mitochondrial ROS generation for regulation of autophagic pathways in cancer. Biochem Biophys Res Commun *414*, 5-8.

Liaw, D., Marsh, D.J., Li, J., Dahia, P.L., Wang, S.I., Zheng, Z., Bose, S., Call, K.M., Tsou, H.C., Peacocke, M.*, et al.* (1997). Germline mutations of the PTEN gene in Cowden disease, an inherited breast and thyroid cancer syndrome. Nat Genet *16*, 64-67.

Lickert, H., Takeuchi, J.K., Von Both, I., Walls, J.R., McAuliffe, F., Adamson, S.L., Henkelman, R.M., Wrana, J.L., Rossant, J., and Bruneau, B.G. (2004). Baf60c is essential for function of BAF chromatin remodelling complexes in heart development. Nature *432*, 107-112.

Ligresti, G., Militello, L., Steelman, L.S., Cavallaro, A., Basile, F., Nicoletti, F., Stivala, F., McCubrey, J.A., and Libra, M. (2009). PIK3CA mutations in human solid tumors: role in sensitivity to various therapeutic approaches. Cell Cycle *8*, 1352-1358.

Lin, A.W., Barradas, M., Stone, J.C., van Aelst, L., Serrano, M., and Lowe, S.W. (1998). Premature senescence involving p53 and p16 is activated in response to constitutive MEK/MAPK mitogenic signaling. Genes Dev *12*, 3008-3019.

Lin, H., Wong, R.P., Martinka, M., and Li, G. (2009). Loss of SNF5 expression correlates with poor patient survival in melanoma. Clinical cancer research : an official journal of the American Association for Cancer Research *15*, 6404-6411.

Lin, H., Wong, R.P., Martinka, M., and Li, G. (2010). BRG1 expression is increased in human cutaneous melanoma. The British journal of dermatology *163*, 502-510.

Link, K.A., Burd, C.J., Williams, E., Marshall, T., Rosson, G., Henry, E., Weissman, B., and Knudsen, K.E. (2005). BAF57 governs androgen receptor action and androgen-dependent proliferation through SWI/SNF. Mol Cell Biol *25*, 2200-2215.

Liu, B., Chen, Y., and St Clair, D.K. (2008). ROS and p53: a versatile partnership. Free radical biology & medicine *44*, 1529-1535.

Liu, M., Lee, M.H., Cohen, M., Bommakanti, M., and Freedman, L.P. (1996). Transcriptional activation of the Cdk inhibitor p21 by vitamin D3 leads to the induced differentiation of the myelomonocytic cell line U937. Genes Dev *10*, 142-153.

Liu, Q., Guntuku, S., Cui, X.S., Matsuoka, S., Cortez, D., Tamai, K., Luo, G., Carattini-Rivera, S., DeMayo, F., Bradley, A.*, et al.* (2000). Chk1 is an essential kinase that is regulated by Atr and required for the G(2)/M DNA damage checkpoint. Genes Dev *14*, 1448-1459.

Lizardi, P.M., Forloni, M., and Wajapeyee, N. (2011). Genome-wide approaches for cancer gene discovery. Trends in biotechnology *29*, 558-568.

Lorch, Y., Zhang, M., and Kornberg, R.D. (1999). Histone octamer transfer by a chromatin-remodeling complex. Cell *96*, 389-392.

Luger, K., Mader, A.W., Richmond, R.K., Sargent, D.F., and Richmond, T.J. (1997). Crystal structure of the nucleosome core particle at 2.8 A resolution. Nature *389*, 251-260.

Luo, J., Emanuele, M.J., Li, D., Creighton, C.J., Schlabach, M.R., Westbrook, T.F., Wong, K.K., and Elledge, S.J. (2009). A genome-wide RNAi screen identifies multiple synthetic lethal interactions with the Ras oncogene. Cell *137*, 835-848.

MacKeigan, J.P., Murphy, L.O., and Blenis, J. (2005). Sensitized RNAi screen of human kinases and phosphatases identifies new regulators of apoptosis and chemoresistance. Nat Cell Biol *7*, 591-600.

Macleod, K.F., Sherry, N., Hannon, G., Beach, D., Tokino, T., Kinzler, K., Vogelstein, B., and Jacks, T. (1995). p53-dependent and independent expression of p21 during cell growth, differentiation, and DNA damage. Genes Dev *9*, 935-944.

Mason, D.X., Jackson, T.J., and Lin, A.W. (2004). Molecular signature of oncogenic ras-induced senescence. Oncogene *23*, 9238-9246.

Mathon, N.F., Malcolm, D.S., Harrisingh, M.C., Cheng, L., and Lloyd, A.C. (2001). Lack of replicative senescence in normal rodent glia. Science *291*, 872-875.

McCabe, M.T., Ott, H.M., Ganji, G., Korenchuk, S., Thompson, C., Van Aller, G.S., Liu, Y., Graves, A.P., Della Pietra, A., 3rd, Diaz, E.*, et al.* (2012). EZH2 inhibition as a therapeutic strategy for lymphoma with EZH2-activating mutations. Nature *492*, 108-112.

McKenna, E.S., and Roberts, C.W.M. (2009). Epigenetics and cancer without genomic instability. Cell Cycle *8*, 23-26.

McKenna, E.S., Sansam, C.G., Cho, Y.J., Greulich, H., Evans, J.A., Thom, C.S., Moreau, L.A., Biegel, J.A., Pomeroy, S.L., and Roberts, C.W. (2008). Loss of the epigenetic tumor suppressor SNF5 leads to cancer without genomic instability. Mol Cell Biol *28*, 6223-6233.

Meacham, C.E., Ho, E.E., Dubrovsky, E., Gertler, F.B., and Hemann, M.T. (2009). In vivo RNAi screening identifies regulators of actin dynamics as key determinants of lymphoma progression. Nat Genet *41*, 1133-1137.

Melov, S., Coskun, P.E., and Wallace, D.C. (1999). Mouse models of mitochondrial disease, oxidative stress, and senescence. Mutation research *434*, 233-242.

Meng, Z.X., Li, S., Wang, L., Ko, H.J., Lee, Y., Jung, D.Y., Okutsu, M., Yan, Z., Kim, J.K., and Lin, J.D. (2013). Baf60c drives glycolytic metabolism in the muscle and improves systemic glucose homeostasis through Deptor-mediated Akt activation. Nat Med *19*, 640-645.

Merlo, A., Herman, J.G., Mao, L., Lee, D.J., Gabrielson, E., Burger, P.C., Baylin, S.B., and Sidransky, D. (1995). 5' CpG island methylation is associated with transcriptional silencing of the tumour suppressor p16/CDKN2/MTS1 in human cancers. Nat Med *1*, 686-692.

Meyer, M., and Kircher, M. (2010). Illumina sequencing library preparation for highly multiplexed target capture and sequencing. Cold Spring Harbor protocols *2010*, pdb prot5448.

Michaloglou, C., Vredeveld, L.C., Soengas, M.S., Denoyelle, C., Kuilman, T., van der Horst, C.M., Majoor, D.M., Shay, J.W., Mooi, W.J., and Peeper, D.S. (2005). BRAFE600-associated senescence-like cell cycle arrest of human naevi. Nature *436*, 720-724.

Mills, A.A. (2010). Throwing the cancer switch: reciprocal roles of polycomb and trithorax proteins. Nat Rev Cancer *10*, 669-682.

Modena, P., Lualdi, E., Facchinetti, F., Galli, L., Teixeira, M.R., Pilotti, S., and Sozzi, G. (2005). SMARCB1/INI1 tumor suppressor gene is frequently inactivated in epithelioid sarcomas. Cancer Res *65*, 4012-4019.

Moiseeva, O., Bourdeau, V., Roux, A., Deschenes-Simard, X., and Ferbeyre, G. (2009). Mitochondrial dysfunction contributes to oncogene-induced senescence. Mol Cell Biol *29*, 4495-4507.

Mollinari, C., Reynaud, C., Martineau-Thuillier, S., Monier, S., Kieffer, S., Garin, J., Andreassen, P.R., Boulet, A., Goud, B., Kleman, J.P.*, et al.* (2003). The mammalian passenger protein TD-60 is an

RCC1 family member with an essential role in prometaphase to metaphase progression. Dev Cell *5*, 295-307.

Monahan, B.J., Villen, J., Marguerat, S., Bahler, J., Gygi, S.P., and Winston, F. (2008). Fission yeast SWI/SNF and RSC complexes show compositional and functional differences from budding yeast. Nat Struct Mol Biol *15*, 873-880.

Mooi, W.J., and Peeper, D.S. (2006). Oncogene-induced cell senescence--halting on the road to cancer. N Engl J Med *355*, 1037-1046.

Moore, D.A., Pringle, J.H., and Saldanha, G.S. (2012). Prognostic tissue markers in melanoma. Histopathology *60*, 679-689.

Morgenstern, D.A., Baruchel, S., and Irwin, M.S. (2013). Current and future strategies for relapsed neuroblastoma: challenges on the road to precision therapy. Journal of pediatric hematology/oncology *35*, 337-347.

Morin, G.B. (1989). The human telomere terminal transferase enzyme is a ribonucleoprotein that synthesizes TTAGGG repeats. Cell *59*, 521-529.

Moshkin, Y.M., Armstrong, J.A., Maeda, R.K., Tamkun, J.W., Verrijzer, P., Kennison, J.A., and Karch, F. (2002). Histone chaperone ASF1 cooperates with the Brahma chromatin-remodelling machinery. Genes Dev *16*, 2621-2626.

Muchardt, C., Reyes, J.C., Bourachot, B., Leguoy, E., and Yaniv, M. (1996). The hbrm and BRG-1 proteins, components of the human SNF/SWI complex, are phosphorylated and excluded from the condensed chromosomes during mitosis. EMBO J *15*, 3394-3402.

Muchardt, C., and Yaniv, M. (1993). A human homologue of Saccharomyces cerevisiae SNF2/SWI2 and Drosophila brm genes potentiates transcriptional activation by the glucocorticoid receptor. EMBO J *12*, 4279-4290.

Muchardt, C., and Yaniv, M. (1999). ATP-dependent chromatin remodelling: SWI/SNF and Co. are on the job. Journal of molecular biology *293*, 187-198.

Muller, J., Hart, C.M., Francis, N.J., Vargas, M.L., Sengupta, A., Wild, B., Miller, E.L., O'Connor, M.B., Kingston, R.E., and Simon, J.A. (2002). Histone methyltransferase activity of a Drosophila Polycomb group repressor complex. Cell *111*, 197-208.

Nagl, N.G., Jr., Patsialou, A., Haines, D.S., Dallas, P.B., Beck, G.R., Jr., and Moran, E. (2005). The p270 (ARID1A/SMARCF1) subunit of mammalian SWI/SNF-related complexes is essential for normal cell cycle arrest. Cancer Res *65*, 9236-9244.

Nagl, N.G., Jr., Wang, X., Patsialou, A., Van Scoy, M., and Moran, E. (2007). Distinct mammalian SWI/SNF chromatin remodeling complexes with opposing roles in cell-cycle control. EMBO J *26*, 752-763.

Naidu, S.R., Love, I.M., Imbalzano, A.N., Grossman, S.R., and Androphy, E.J. (2009). The SWI/SNF chromatin remodeling subunit BRG1 is a critical regulator of p53 necessary for proliferation of malignant cells. Oncogene *28*, 2492-2501.

Napolitano, M.A., Cipollaro, M., Cascino, A., Melone, M.A., Giordano, A., and Galderisi, U. (2007). Brg1 chromatin remodeling factor is involved in cell growth arrest, apoptosis and senescence of rat mesenchymal stem cells. Journal of cell science *120*, 2904-2911.

Narita, M., Krizhanovsky, V., Nunez, S., Chicas, A., Hearn, S.A., Myers, M.P., and Lowe, S.W. (2006). A novel role for high-mobility group a proteins in cellular senescence and heterochromatin formation. Cell *126*, 503-514.

Narita, M., Nunez, S., Heard, E., Lin, A.W., Hearn, S.A., Spector, D.L., Hannon, G.J., and Lowe, S.W. (2003a). Rb-mediated heterochromatin formation and silencing of E2F target genes during cellular senescence. Cell *113*, 703-716.

Narita, M., Nunez, S., Heard, E., Narita, M., Lin, A.W., Hearn, S.A., Spector, D.L., Hannon, G.J., and Lowe, S.W. (2003b). Rb-mediated heterochromatin formation and silencing of E2F target genes during cellular senescence. Cell *113*, 703-716.

Narita, M., Young, A.R., Arakawa, S., Samarajiwa, S.A., Nakashima, T., Yoshida, S., Hong, S., Berry, L.S., Reichelt, S., Ferreira, M.*, et al.* (2011). Spatial coupling of mTOR and autophagy augments secretory phenotypes. Science *332*, 966-970.

Nasmyth, K., Seddon, A., and Ammerer, G. (1987). Cell cycle regulation of SW15 is required for mother-cell-specific HO transcription in yeast. Cell *49*, 549-558.

Neigeborn, L., and Carlson, M. (1984). Genes affecting the regulation of SUC2 gene expression by glucose repression in Saccharomyces cerevisiae. Genetics *108*, 845-858.

Neumann, B., Held, M., Liebel, U., Erfle, H., Rogers, P., Pepperkok, R., and Ellenberg, J. (2006). High-throughput RNAi screening by time-lapse imaging of live human cells. Nat Methods *3*, 385-390.

Ni, Z., and Bremner, R. (2007). Brahma-related gene 1-dependent STAT3 recruitment at IL-6-inducible genes. J Immunol *178*, 345-351.

Nie, Z., Xue, Y., Yang, D., Zhou, S., Deroo, B.J., Archer, T.K., and Wang, W. (2000). A specificity and targeting subunit of a human SWI/SNF family-related chromatin-remodeling complex. Mol Cell Biol *20*, 8879-8888.

Nie, Z., Yan, Z., Chen, E.H., Sechi, S., Ling, C., Zhou, S., Xue, Y., Yang, D., Murray, D., Kanakubo, E.*, et al.* (2003). Novel SWI/SNF chromatin-remodeling complexes contain a mixed-lineage leukemia chromosomal translocation partner. Mol Cell Biol *23*, 2942-2952.

Nishio, K., Inoue, A., Qiao, S., Kondo, H., and Mimura, A. (2001). Senescence and cytoskeleton: overproduction of vimentin induces senescent-like morphology in human fibroblasts. Histochemistry and cell biology *116*, 321-327.

Numata, M., Morinaga, S., Watanabe, T., Tamagawa, H., Yamamoto, N., Shiozawa, M., Nakamura, Y., Kameda, Y., Okawa, S., Rino, Y.*, et al.* (2013). The clinical significance of SWI/SNF complex in pancreatic cancer. International journal of oncology *42*, 403-410.

O'Sullivan, R.J., and Karlseder, J. (2012). The great unravelling: chromatin as a modulator of the aging process. Trends in biochemical sciences *37*, 466-476.

O'Sullivan, R.J., Kubicek, S., Schreiber, S.L., and Karlseder, J. (2010). Reduced histone biosynthesis and chromatin changes arising from a damage signal at telomeres. Nat Struct Mol Biol *17*, 1218-1225.

Ohtani, N., Zebedee, Z., Huot, T.J., Stinson, J.A., Sugimoto, M., Ohashi, Y., Sharrocks, A.D., Peters, G., and Hara, E. (2001). Opposing effects of Ets and Id proteins on p16INK4a expression during cellular senescence. Nature *409*, 1067-1070.

Oike, T., Ogiwara, H., Tominaga, Y., Ito, K., Ando, O., Tsuta, K., Mizukami, T., Shimada, Y., Isomura, H., Komachi, M.*, et al.* (2013). A synthetic lethality-based strategy to treat cancers harboring a genetic deficiency in the chromatin remodeling factor BRG1. Cancer Res *73*, 5508-5518.

Olovnikov, A.M. (1973). A theory of marginotomy. The incomplete copying of template margin in enzymic synthesis of polynucleotides and biological significance of the phenomenon. J Theor Biol *41*, 181-190.

Ondrusova, L., Vachtenheim, J., Reda, J., Zakova, P., and Benkova, K. (2013). MITF-independent pro-survival role of BRG1-containing SWI/SNF complex in melanoma cells. PloS one *8*, e54110.

Ong, S.E., Blagoev, B., Kratchmarova, I., Kristensen, D.B., Steen, H., Pandey, A., and Mann, M. (2002). Stable isotope labeling by amino acids in cell culture, SILAC, as a simple and accurate approach to expression proteomics. Molecular & cellular proteomics : MCP *1*, 376-386.

Otsuki, T., Furukawa, Y., Ikeda, K., Endo, H., Yamashita, T., Shinohara, A., Iwamatsu, A., Ozawa, K., and Liu, J.M. (2001). Fanconi anemia protein, FANCA, associates with BRG1, a component of the human SWI/SNF complex. Human molecular genetics *10*, 2651-2660.

Owen-Hughes, T., Utley, R.T., Cote, J., Peterson, C.L., and Workman, J.L. (1996). Persistent site-specific remodeling of a nucleosome array by transient action of the SWI/SNF complex. Science *273*, 513-516.

Pang, J.H., and Chen, K.Y. (1994). Global change of gene expression at late G1/S boundary may occur in human IMR-90 diploid fibroblasts during senescence. J Cell Physiol *160*, 531-538.

Paradis, V., Youssef, N., Dargere, D., Ba, N., Bonvoust, F., Deschatrette, J., and Bedossa, P. (2001). Replicative senescence in normal liver, chronic hepatitis C, and hepatocellular carcinomas. Human pathology *32*, 327-332.

Parrinello, S., Samper, E., Krtolica, A., Goldstein, J., Melov, S., and Campisi, J. (2003). Oxygen sensitivity severely limits the replicative lifespan of murine fibroblasts. Nat Cell Biol *5*, 741-747.

Passos, J.F., Saretzki, G., Ahmed, S., Nelson, G., Richter, T., Peters, H., Wappler, I., Birket, M.J., Harold, G., Schaeuble, K.*, et al.* (2007). Mitochondrial dysfunction accounts for the stochastic heterogeneity in telomere-dependent senescence. PLoS biology *5*, e110.

Pawlowski, R., Muhl, S.M., Sulser, T., Krek, W., Moch, H., and Schraml, P. (2013). Loss of PBRM1 expression is associated with renal cell carcinoma progression. Int J Cancer *132*, E11-17.

Peng, C., Liu, H.Y., Zhou, M., Zhang, L.M., Li, X.L., Shen, S.R., and Li, G.Y. (2007). BRD7 suppresses the growth of Nasopharyngeal Carcinoma cells (HNE1) through negatively regulating beta-catenin and ERK pathways. Molecular and cellular biochemistry *303*, 141-149.

Pepperkok, R., and Ellenberg, J. (2006). High-throughput fluorescence microscopy for systems biology. Nat Rev Mol Cell Biol *7*, 690-696.

Perk, J., Iavarone, A., and Benezra, R. (2005). Id family of helix-loop-helix proteins in cancer. Nat Rev Cancer *5*, 603-614.

Peterson, C.L. (1996). Multiple SWItches to turn on chromatin? Curr Opin Genet Dev *6*, 171-175.

Peterson, C.L., Dingwall, A., and Scott, M.P. (1994). Five SWI/SNF gene products are components of a large multisubunit complex required for transcriptional enhancement. Proc Natl Acad Sci U S A *91*, 2905-2908.

Peterson, C.L., and Herskowitz, I. (1992). Characterization of the yeast SWI1, SWI2, and SWI3 genes, which encode a global activator of transcription. Cell *68*, 573-583.

Phelan, M.L., Sif, S., Narlikar, G.J., and Kingston, R.E. (1999). Reconstitution of a core chromatin remodeling complex from SWI/SNF subunits. Molecular cell *3*, 247-253.

Poste, G. (2011). Bring on the biomarkers. Nature *469*, 156-157.

Prensner, J.R., Iyer, M.K., Sahu, A., Asangani, I.A., Cao, Q., Patel, L., Vergara, I.A., Davicioni, E., Erho, N., Ghadessi, M.*, et al.* (2013). The long noncoding RNA SChLAP1 promotes aggressive prostate cancer and antagonizes the SWI/SNF complex. Nat Genet *45*, 1392-1398.

Puri, P.L., and Mercola, M. (2012). BAF60 A, B, and Cs of muscle determination and renewal. Genes Dev *26*, 2673-2683.

Qi, W., Chan, H., Teng, L., Li, L., Chuai, S., Zhang, R., Zeng, J., Li, M., Fan, H., Lin, Y.*, et al.* (2012). Selective inhibition of Ezh2 by a small molecule inhibitor blocks tumor cells proliferation. Proc Natl Acad Sci U S A *109*, 21360-21365.

Rada-Iglesias, A., Bajpai, R., Swigut, T., Brugmann, S.A., Flynn, R.A., and Wysocka, J. (2011). A unique chromatin signature uncovers early developmental enhancers in humans. Nature *470*, 279-283.

Rai, T.S., and Adams, P.D. (2012). Lessons from senescence: Chromatin maintenance in non-proliferating cells. Biochimica et biophysica acta *1819*, 322-331.

Rangarajan, A., and Weinberg, R.A. (2003). Opinion: Comparative biology of mouse versus human cells: modelling human cancer in mice. Nat Rev Cancer *3*, 952-959.

Reinke, H., and Horz, W. (2003). Histones are first hyperacetylated and then lose contact with the activated PHO5 promoter. Molecular cell *11*, 1599-1607.

Reisman, D., Glaros, S., and Thompson, E.A. (2009). The SWI/SNF complex and cancer. Oncogene *28*, 1653-1668.

Reisman, D.N., Sciarrotta, J., Wang, W., Funkhouser, W.K., and Weissman, B.E. (2003). Loss of BRG1/BRM in human lung cancer cell lines and primary lung cancers: correlation with poor prognosis. Cancer Res *63*, 560-566.

Reya, T., Morrison, S.J., Clarke, M.F., and Weissman, I.L. (2001). Stem cells, cancer, and cancer stem cells. Nature *414*, 105-111.

Reyes, J.C., Muchardt, C., and Yaniv, M. (1997). Components of the human SWI/SNF complex are enriched in active chromatin and are associated with the nuclear matrix. The Journal of cell biology *137*, 263-274.

Richmond, T.J., and Davey, C.A. (2003). The structure of DNA in the nucleosome core. Nature *423*, 145-150.

Riedel, C.G., Dowen, R.H., Lourenco, G.F., Kirienko, N.V., Heimbucher, T., West, J.A., Bowman, S.K., Kingston, R.E., Dillin, A., Asara, J.M.*, et al.* (2013). DAF-16 employs the chromatin remodeller SWI/SNF to promote stress resistance and longevity. Nat Cell Biol *15*, 491-501.

Ring, H.Z., Vameghi-Meyers, V., Wang, W., Crabtree, G.R., and Francke, U. (1998). Five SWI/SNF-related, matrix-associated, actin-dependent regulator of chromatin (SMARC) genes are dispersed in the human genome. Genomics *51*, 140-143.

Robbins, E., Levine, E.M., and Eagle, H. (1970). Morphologic changes accompanying senescence of cultured human diploid cells. J Exp Med *131*, 1211-1222.

Roberts, C.W.M., Galusha, S.A., McMenamin, M.E., Fletcher, C.D.M., and Orkin, S.H. (2000). Haploinsufficiency of Snf5 (integrase interactor 1) predisposes to malignant rhabdoid tumors in mice. P Natl Acad Sci USA *97*, 13796-13800.

Roberts, C.W.M., Leroux, M.M., Fleming, M.D., and Orkin, S.H. (2002). Highly penetrant, rapid tumorigenesis through conditional inversion of the tumor suppressor gene Snf5. Cancer Cell *2*, 415-425.

Rodriguez-Paredes, M., and Esteller, M. (2011). Cancer epigenetics reaches mainstream oncology. Nat Med *17*, 330-339.

Ross, S., Cheung, E., Petrakis, T.G., Howell, M., Kraus, W.L., and Hill, C.S. (2006). Smads orchestrate specific histone modifications and chromatin remodeling to activate transcription. EMBO J *25*, 4490-4502.

Rozenblatt-Rosen, O., Rozovskaia, T., Burakov, D., Sedkov, Y., Tillib, S., Blechman, J., Nakamura, T., Croce, C.M., Mazo, A., and Canaani, E. (1998). The C-terminal SET domains of ALL-1 and TRITHORAX interact with the INI1 and SNR1 proteins, components of the SWI/SNF complex. Proc Natl Acad Sci U S A *95*, 4152-4157.

Ryme, J., Asp, P., Bohm, S., Cavellan, E., and Farrants, A.K. (2009). Variations in the composition of mammalian SWI/SNF chromatin remodelling complexes. Journal of cellular biochemistry *108*, 565-576.

Sage, J., Mulligan, G.J., Attardi, L.D., Miller, A., Chen, S., Williams, B., Theodorou, E., and Jacks, T. (2000). Targeted disruption of the three Rb-related genes leads to loss of G(1) control and immortalization. Genes Dev *14*, 3037-3050.

Saha, A., Wittmeyer, J., and Cairns, B.R. (2002). Chromatin remodeling by RSC involves ATP-dependent DNA translocation. Genes Dev *16*, 2120-2134.

Sakai, T., Toguchida, J., Ohtani, N., Yandell, D.W., Rapaport, J.M., and Dryja, T.P. (1991). Allele-specific hypermethylation of the retinoblastoma tumor-suppressor gene. Am J Hum Genet *48*, 880-888.

Samartzis, E.P., Samartzis, N., Noske, A., Fedier, A., Caduff, R., Dedes, K.J., Fink, D., and Imesch, P. (2012). Loss of ARID1A/BAF250a-expression in endometriosis: a biomarker for risk of carcinogenic transformation? Modern pathology : an official journal of the United States and Canadian Academy of Pathology, Inc *25*, 885-892.

Samuels, Y., Wang, Z., Bardelli, A., Silliman, N., Ptak, J., Szabo, S., Yan, H., Gazdar, A., Powell, S.M., Riggins, G.J.*, et al.* (2004). High frequency of mutations of the PIK3CA gene in human cancers. Science *304*, 554.

Saramaki, A., Banwell, C.M., Campbell, M.J., and Carlberg, C. (2006). Regulation of the human p21(waf1/cip1) gene promoter via multiple binding sites for p53 and the vitamin D3 receptor. Nucleic acids research *34*, 543-554.

Sausen, M., Leary, R.J., Jones, S., Wu, J., Reynolds, C.P., Liu, X., Blackford, A., Parmigiani, G., Diaz, L.A., Jr., Papadopoulos, N.*, et al.* (2013). Integrated genomic analyses identify ARID1A and ARID1B alterations in the childhood cancer neuroblastoma. Nat Genet *45*, 12-17.

Schlabach, M.R., Luo, J., Solimini, N.L., Hu, G., Xu, Q., Li, M.Z., Zhao, Z., Smogorzewska, A., Sowa, M.E., Ang, X.L.*, et al.* (2008). Cancer proliferation gene discovery through functional genomics. Science *319*, 620-624.

Scott, C.L., Gil, J., Hernando, E., Teruya-Feldstein, J., Narita, M., Martinez, D., Visakorpi, T., Mu, D., Cordon-Cardo, C., Peters, G.*, et al.* (2007). Role of the chromobox protein CBX7 in lymphomagenesis. Proc Natl Acad Sci U S A *104*, 5389-5394.

Selman, C., Tullet, J.M., Wieser, D., Irvine, E., Lingard, S.J., Choudhury, A.I., Claret, M., Al-Qassab, H., Carmignac, D., Ramadani, F.*, et al.* (2009). Ribosomal protein S6 kinase 1 signaling regulates mammalian life span. Science *326*, 140-144.

Serrano, M., Hannon, G.J., and Beach, D. (1993). A new regulatory motif in cell-cycle control causing specific inhibition of cyclin D/CDK4. Nature *366*, 704-707.

Serrano, M., Lin, A.W., McCurrach, M.E., Beach, D., and Lowe, S.W. (1997). Oncogenic ras provokes premature cell senescence associated with accumulation of p53 and p16INK4a. Cell *88*, 593-602.

Seshadri, T., and Campisi, J. (1990). Repression of c-fos transcription and an altered genetic program in senescent human fibroblasts. Science *247*, 205-209.

Sevenet, N., Lellouch-Tubiana, A., Schofield, D., Hoang-Xuan, K., Gessler, M., Birnbaum, D., Jeanpierre, C., Jouvet, A., and Delattre, O. (1999). Spectrum of hSNF5/INI1 somatic mutations in human cancer and genotype-phenotype correlations. Human molecular genetics *8*, 2359-2368.

Severino, J., Allen, R.G., Balin, S., Balin, A., and Cristofalo, V.J. (2000). Is beta-galactosidase staining a marker of senescence in vitro and in vivo? Exp Cell Res *257*, 162-171.

Shain, A.H., Giacomini, C.P., Matsukuma, K., Karikari, C.A., Bashyam, M.D., Hidalgo, M., Maitra, A., and Pollack, J.R. (2012). Convergent structural alterations define SWItch/Sucrose NonFermentable

(SWI/SNF) chromatin remodeler as a central tumor suppressive complex in pancreatic cancer. Proc Natl Acad Sci U S A *109*, E252-259.

Shain, A.H., and Pollack, J.R. (2013). The spectrum of SWI/SNF mutations, ubiquitous in human cancers. PloS one *8*, e55119.

Shanahan, F., Seghezzi, W., Parry, D., Mahony, D., and Lees, E. (1999). Cyclin E associates with BAF155 and BRG1, components of the mammalian SWI-SNF complex, and alters the ability of BRG1 to induce growth arrest. Mol Cell Biol *19*, 1460-1469.

Shay, J.W., Pereira-Smith, O.M., and Wright, W.E. (1991). A role for both RB and p53 in the regulation of human cellular senescence. Exp Cell Res *196*, 33-39.

Shelton, D.N., Chang, E., Whittier, P.S., Choi, D., and Funk, W.D. (1999). Microarray analysis of replicative senescence. Current biology : CB *9*, 939-945.

Shendure, J., and Ji, H. (2008). Next-generation DNA sequencing. Nature biotechnology *26*, 1135-1145.

Sherr, C.J., and DePinho, R.A. (2000). Cellular senescence: mitotic clock or culture shock? Cell *102*, 407-410.

Sherr, C.J., and McCormick, F. (2002). The RB and p53 pathways in cancer. Cancer Cell *2*, 103-112.

Shi, S., Gronthos, S., Chen, S., Reddi, A., Counter, C.M., Robey, P.G., and Wang, C.Y. (2002). Bone formation by human postnatal bone marrow stromal stem cells is enhanced by telomerase expression. Nature biotechnology *20*, 587-591.

Shimi, T., Butin-Israeli, V., Adam, S.A., Hamanaka, R.B., Goldman, A.E., Lucas, C.A., Shumaker, D.K., Kosak, S.T., Chandel, N.S., and Goldman, R.D. (2011). The role of nuclear lamin B1 in cell proliferation and senescence. Genes Dev *25*, 2579-2593.

Shumaker, D.K., Dechat, T., Kohlmaier, A., Adam, S.A., Bozovsky, M.R., Erdos, M.R., Eriksson, M., Goldman, A.E., Khuon, S., Collins, F.S.*, et al.* (2006). Mutant nuclear lamin A leads to progressive alterations of epigenetic control in premature aging. Proc Natl Acad Sci U S A *103*, 8703-8708.

Shvarts, A., Brummelkamp, T.R., Scheeren, F., Koh, E., Daley, G.Q., Spits, H., and Bernards, R. (2002). A senescence rescue screen identifies BCL6 as an inhibitor of anti-proliferative p19(ARF)-p53 signaling. Genes Dev *16*, 681-686.

Siddiqui, H., Solomon, D.A., Gunawardena, R.W., Wang, Y., and Knudsen, E.S. (2003). Histone deacetylation of RB-responsive promoters: requisite for specific gene repression but dispensable for cell cycle inhibition. Mol Cell Biol *23*, 7719-7731.

Sif, S., Stukenberg, P.T., Kirschner, M.W., and Kingston, R.E. (1998). Mitotic inactivation of a human SWI/SNF chromatin remodeling complex. Genes Dev *12*, 2842-2851.

Silva, J.M., Li, M.Z., Chang, K., Ge, W., Golding, M.C., Rickles, R.J., Siolas, D., Hu, G., Paddison, P.J., Schlabach, M.R.*, et al.* (2005). Second-generation shRNA libraries covering the mouse and human genomes. Nat Genet *37*, 1281-1288.

Silva, J.M., Marran, K., Parker, J.S., Silva, J., Golding, M., Schlabach, M.R., Elledge, S.J., Hannon, G.J., and Chang, K. (2008). Profiling essential genes in human mammary cells by multiplex RNAi screening. Science *319*, 617-620.

Sims, D., Mendes-Pereira, A.M., Frankum, J., Burgess, D., Cerone, M.A., Lombardelli, C., Mitsopoulos, C., Hakas, J., Murugaesu, N., Isacke, C.M.*, et al.* (2011). High-throughput RNA interference screening using pooled shRNA libraries and next generation sequencing. Genome biology *12*, R104.

Singhal, N., Graumann, J., Wu, G., Arauzo-Bravo, M.J., Han, D.W., Greber, B., Gentile, L., Mann, M., and Scholer, H.R. (2010). Chromatin-Remodeling Components of the BAF Complex Facilitate Reprogramming. Cell *141*, 943-955.

Smith, C.L., Horowitz-Scherer, R., Flanagan, J.F., Woodcock, C.L., and Peterson, C.L. (2003). Structural analysis of the yeast SWI/SNF chromatin remodeling complex. Nature structural biology *10*, 141-145.

Smolen, G.A., Zhang, J., Zubrowski, M.J., Edelman, E.J., Luo, B., Yu, M., Ng, L.W., Scherber, C.M., Schott, B.J., Ramaswamy, S.*, et al.* (2010). A genome-wide RNAi screen identifies multiple RSK-dependent regulators of cell migration. Genes Dev *24*, 2654-2665.

Sohn, D.H., Lee, K.Y., Lee, C., Oh, J., Chung, H., Jeon, S.H., and Seong, R.H. (2007). SRG3 interacts directly with the major components of the SWI/SNF chromatin remodeling complex and protects them from proteasomal degradation. J Biol Chem *282*, 10614-10624.

Staal, A., Enserink, J.M., Stein, J.L., Stein, G.S., and van Wijnen, A.J. (2000). Molecular characterization of celtix-1, a bromodomain protein interacting with the transcription factor interferon regulatory factor 2. J Cell Physiol *185*, 269-279.

Stankunas, K., Hang, C.T., Tsun, Z.Y., Chen, H., Lee, N.V., Wu, J.I., Shang, C., Bayle, J.H., Shou, W., Iruela-Arispe, M.L.*, et al.* (2008). Endocardial Brg1 represses ADAMTS1 to maintain the microenvironment for myocardial morphogenesis. Dev Cell *14*, 298-311.

Steelman, L.S., Chappell, W.H., Abrams, S.L., Kempf, R.C., Long, J., Laidler, P., Mijatovic, S., Maksimovic-Ivanic, D., Stivala, F., Mazzarino, M.C.*, et al.* (2011). Roles of the Raf/MEK/ERK and PI3K/PTEN/Akt/mTOR pathways in controlling growth and sensitivity to therapy-implications for cancer and aging. Aging *3*, 192-222.

Stein, G.H., Beeson, M., and Gordon, L. (1990). Failure to phosphorylate the retinoblastoma gene product in senescent human fibroblasts. Science *249*, 666-669.

Stein, G.H., Drullinger, L.F., Robetorye, R.S., Pereira-Smith, O.M., and Smith, J.R. (1991). Senescent cells fail to express cdc2, cycA, and cycB in response to mitogen stimulation. Proc Natl Acad Sci U S A *88*, 11012-11016.

Stein, G.H., Drullinger, L.F., Soulard, A., and Dulic, V. (1999). Differential roles for cyclin-dependent kinase inhibitors p21 and p16 in the mechanisms of senescence and differentiation in human fibroblasts. Mol Cell Biol *19*, 2109-2117.

Stephens, P.J., Tarpey, P.S., Davies, H., Van Loo, P., Greenman, C., Wedge, D.C., Nik-Zainal, S., Martin, S., Varela, I., Bignell, G.R.*, et al.* (2012). The landscape of cancer genes and mutational processes in breast cancer. Nature *486*, 400-404.

Stern, M., Jensen, R., and Herskowitz, I. (1984). Five SWI genes are required for expression of the HO gene in yeast. Journal of molecular biology *178*, 853-868.

Strobeck, M.W., Knudsen, K.E., Fribourg, A.F., DeCristofaro, M.F., Weissman, B.E., Imbalzano, A.N., and Knudsen, E.S. (2000). BRG-1 is required for RB-mediated cell cycle arrest. Proc Natl Acad Sci U S A *97*, 7748-7753.

Strober, B.E., Dunaief, J.L., Guha, and Goff, S.P. (1996). Functional interactions between the hBRM/hBRG1 transcriptional activators and the pRB family of proteins. Mol Cell Biol *16*, 1576-1583.

Su, L., Hershberger, R.J., and Weissman, I.L. (1993). LYAR, a novel nucleolar protein with zinc finger DNA-binding motifs, is involved in cell growth regulation. Genes Dev *7*, 735-748.

Sudarsanam, P., Iyer, V.R., Brown, P.O., and Winston, F. (2000). Whole-genome expression analysis of snf/swi mutants of Saccharomyces cerevisiae. Proc Natl Acad Sci U S A *97*, 3364-3369.

Sun, A., Tawfik, O., Gayed, B., Thrasher, J.B., Hoestje, S., Li, C., and Li, B. (2007). Aberrant expression of SWI/SNF catalytic subunits BRG1/BRM is associated with tumor development and increased invasiveness in prostate cancers. The Prostate *67*, 203-213.

Swarbrick, A., Roy, E., Allen, T., and Bishop, J.M. (2008). Id1 cooperates with oncogenic Ras to induce metastatic mammary carcinoma by subversion of the cellular senescence response. Proc Natl Acad Sci U S A *105*, 5402-5407.

Szerlong, H., Hinata, K., Viswanathan, R., Erdjument-Bromage, H., Tempst, P., and Cairns, B.R. (2008). The HSA domain binds nuclear actin-related proteins to regulate chromatin-remodeling ATPases. Nat Struct Mol Biol *15*, 469-476.

Tacutu, R., Budovsky, A., Yanai, H., and Fraifeld, V.E. (2011). Molecular links between cellular senescence, longevity and age-related diseases - a systems biology perspective. Aging *3*, 1178-1191.

Takahashi, K., and Yamanaka, S. (2006). Induction of pluripotent stem cells from mouse embryonic and adult fibroblast cultures by defined factors. Cell *126*, 663-676.

Takai, H., Smogorzewska, A., and de Lange, T. (2003). DNA damage foci at dysfunctional telomeres. Current biology : CB *13*, 1549-1556.

Takayama, M.A., Taira, T., Tamai, K., Iguchi-Ariga, S.M., and Ariga, H. (2000). ORC1 interacts with c-Myc to inhibit E-box-dependent transcription by abrogating c-Myc-SNF5/INI1 interaction. Genes to cells : devoted to molecular & cellular mechanisms *5*, 481-490.

Takeuchi, J.K., and Bruneau, B.G. (2009). Directed transdifferentiation of mouse mesoderm to heart tissue by defined factors. Nature *459*, 708-711.

Takubo, K., Aida, J., Izumiyama-Shimomura, N., Ishikawa, N., Sawabe, M., Kurabayashi, R., Shiraishi, H., Arai, T., and Nakamura, K. (2010). Changes of telomere length with aging. Geriatrics & gerontology international *10 Suppl 1*, S197-206.

Tamkun, J.W., Deuring, R., Scott, M.P., Kissinger, M., Pattatucci, A.M., Kaufman, T.C., and Kennison, J.A. (1992). brahma: a regulator of Drosophila homeotic genes structurally related to the yeast transcriptional activator SNF2/SWI2. Cell *68*, 561-572.

Tanaka, T., Suh, K.S., Lo, A.M., and De Luca, L.M. (2007). p21WAF1/CIP1 is a common transcriptional target of retinoid receptors: pleiotropic regulatory mechanism through retinoic acid receptor (RAR)/retinoid X receptor (RXR) heterodimer and RXR/RXR homodimer. J Biol Chem *282*, 29987-29997.

Tilstra, J.S., Robinson, A.R., Wang, J., Gregg, S.Q., Clauson, C.L., Reay, D.P., Nasto, L.A., St Croix, C.M., Usas, A., Vo, N.*, et al.* (2012). NF-kappaB inhibition delays DNA damage-induced senescence and aging in mice. The Journal of clinical investigation *122*, 2601-2612.

Trobaugh-Lotrario, A.D., Tomlinson, G.E., Finegold, M.J., Gore, L., and Feusner, J.H. (2009). Small cell undifferentiated variant of hepatoblastoma: adverse clinical and molecular features similar to rhabdoid tumors. Pediatric blood & cancer *52*, 328-334.

Trotter, K.W., and Archer, T.K. (2004). Reconstitution of glucocorticoid receptor-dependent transcription in vivo. Mol Cell Biol *24*, 3347-3358.

Trouche, D., Le Chalony, C., Muchardt, C., Yaniv, M., and Kouzarides, T. (1997). RB and hbrm cooperate to repress the activation functions of E2F1. Proc Natl Acad Sci U S A *94*, 11268-11273.

Tsikitis, M., Zhang, Z., Edelman, W., Zagzag, D., and Kalpana, G.V. (2005). Genetic ablation of Cyclin D1 abrogates genesis of rhabdoid tumors resulting from Ini1 loss. Proc Natl Acad Sci U S A *102*, 12129-12134.

Tu, Z., Zhuang, X., Yao, Y.G., and Zhang, R. (2013). BRG1 Is Required for Formation of Senescence-Associated Heterochromatin Foci Induced by Oncogenic RAS or BRCA1 Loss. Mol Cell Biol *33*, 1819-1829.

Udugama, M., Sabri, A., and Bartholomew, B. (2011). The INO80 ATP-dependent chromatin remodeling complex is a nucleosome spacing factor. Mol Cell Biol *31*, 662-673.

Valencia-Sanchez, M.A., Liu, J., Hannon, G.J., and Parker, R. (2006). Control of translation and mRNA degradation by miRNAs and siRNAs. Genes Dev *20*, 515-524.

Varambally, S., Dhanasekaran, S.M., Zhou, M., Barrette, T.R., Kumar-Sinha, C., Sanda, M.G., Ghosh, D., Pienta, K.J., Sewalt, R.G., Otte, A.P.*, et al.* (2002). The polycomb group protein EZH2 is involved in progression of prostate cancer. Nature *419*, 624-629.

Varela, I., Tarpey, P., Raine, K., Huang, D., Ong, C.K., Stephens, P., Davies, H., Jones, D., Lin, M.L., Teague, J.*, et al.* (2011). Exome sequencing identifies frequent mutation of the SWI/SNF complex gene PBRM1 in renal carcinoma. Nature *469*, 539-542.

Vasudev, N.S., Selby, P.J., and Banks, R.E. (2012). Renal cancer biomarkers: the promise of personalized care. BMC medicine *10*, 112.

Vermeulen, M., Hubner, N.C., and Mann, M. (2008). High confidence determination of specific protein-protein interactions using quantitative mass spectrometry. Current opinion in biotechnology *19*, 331-337.

Versteege, I., Medjkane, S., Rouillard, D., and Delattre, O. (2002). A key role of the hSNF5/INI1 tumour suppressor in the control of the G1-S transition of the cell cycle. Oncogene *21*, 6403-6412.

Versteege, I., Sevenet, N., Lange, J., Rousseau-Merck, M.F., Ambros, P., Handgretinger, R., Aurias, A., and Delattre, O. (1998). Truncating mutations of hSNF5/INI1 in aggressive paediatric cancer. Nature *394*, 203-206.

Vignali, M., Hassan, A.H., Neely, K.E., and Workman, J.L. (2000). ATP-dependent chromatin-remodeling complexes. Mol Cell Biol *20*, 1899-1910.

Vlcek, S., and Foisner, R. (2007). A-type lamin networks in light of laminopathic diseases. Biochimica et biophysica acta *1773*, 661-674.

Vogelstein, B., Papadopoulos, N., Velculescu, V.E., Zhou, S., Diaz, L.A., Jr., and Kinzler, K.W. (2013). Cancer genome landscapes. Science *339*, 1546-1558.

Vousden, K.H., and Lu, X. (2002). Live or let die: the cell's response to p53. Nat Rev Cancer *2*, 594-604.

Vradii, D., Wagner, S., Doan, D.N., Nickerson, J.A., Montecino, M., Lian, J.B., Stein, J.L., van Wijnen, A.J., Imbalzano, A.N., and Stein, G.S. (2006). Brg1, the ATPase subunit of the SWI/SNF chromatin remodeling complex, is required for myeloid differentiation to granulocytes. J Cell Physiol *206*, 112-118.

Wajapeyee, N., Serra, R.W., Zhu, X., Mahalingam, M., and Green, M.R. (2008). Oncogenic BRAF induces senescence and apoptosis through pathways mediated by the secreted protein IGFBP7. Cell *132*, 363-374.

Wang, K., Kan, J., Yuen, S.T., Shi, S.T., Chu, K.M., Law, S., Chan, T.L., Kan, Z., Chan, A.S., Tsui, W.Y.*, et al.* (2011). Exome sequencing identifies frequent mutation of ARID1A in molecular subtypes of gastric cancer. Nat Genet *43*, 1219-1223.

Wang, W., Cote, J., Xue, Y., Zhou, S., Khavari, P.A., Biggar, S.R., Muchardt, C., Kalpana, G.V., Goff, S.P., Yaniv, M.*, et al.* (1996a). Purification and biochemical heterogeneity of the mammalian SWI-SNF complex. EMBO J *15*, 5370-5382.

Wang, W., Xue, Y., Zhou, S., Kuo, A., Cairns, B.R., and Crabtree, G.R. (1996b). Diversity and specialization of mammalian SWI/SNF complexes. Genes Dev *10*, 2117-2130.

Wang, X., Nagl, N.G., Wilsker, D., Van Scoy, M., Pacchione, S., Yaciuk, P., Dallas, P.B., and Moran, E. (2004). Two related ARID family proteins are alternative subunits of human SWI/SNF complexes. Biochem J *383*, 319-325.

Wang, Y., Wong, R.H., Tang, T., Hudak, C.S., Yang, D., Duncan, R.E., and Sul, H.S. (2013). Phosphorylation and recruitment of BAF60c in chromatin remodeling for lipogenesis in response to insulin. Molecular cell *49*, 283-297.

Watanabe, T., Semba, S., and Yokozaki, H. (2011). Regulation of PTEN expression by the SWI/SNF chromatin-remodelling protein BRG1 in human colorectal carcinoma cells. British journal of cancer *104*, 146-154.

Watkins, S.J., and Norbury, C.J. (2004). Cell cycle-related variation in subcellular localization of eIF3e/INT6 in human fibroblasts. Cell proliferation *37*, 149-160.

Watson, J.D. (1972). Origin of concatemeric T7 DNA. Nat New Biol *239*, 197-201.

Webb, A.E., and Brunet, A. (2013). FOXO flips the longevity SWItch. Nat Cell Biol *15*, 444-446.

Wei, W., Hemmer, R.M., and Sedivy, J.M. (2001). Role of p14(ARF) in replicative and induced senescence of human fibroblasts. Mol Cell Biol *21*, 6748-6757.

Westbrook, T.F., Martin, E.S., Schlabach, M.R., Leng, Y., Liang, A.C., Feng, B., Zhao, J.J., Roberts, T.M., Mandel, G., Hannon, G.J.*, et al.* (2005). A genetic screen for candidate tumor suppressors identifies REST. Cell *121*, 837-848.

Whitehouse, I., Flaus, A., Cairns, B.R., White, M.F., Workman, J.L., and Owen-Hughes, T. (1999). Nucleosome mobilization catalysed by the yeast SWI/SNF complex. Nature *400*, 784-787.

Wiegand, K.C., Shah, S.P., Al-Agha, O.M., Zhao, Y., Tse, K., Zeng, T., Senz, J., McConechy, M.K., Anglesio, M.S., Kalloger, S.E.*, et al.* (2010). ARID1A mutations in endometriosis-associated ovarian carcinomas. N Engl J Med *363*, 1532-1543.

Willis, M.S., Homeister, J.W., Rosson, G.B., Annayev, Y., Holley, D., Holly, S.P., Madden, V.J., Godfrey, V., Parise, L.V., and Bultman, S.J. (2012). Functional redundancy of SWI/SNF catalytic subunits in maintaining vascular endothelial cells in the adult heart. Circulation research *111*, e111-122.

Wilson, B.G., and Roberts, C.W. (2011). SWI/SNF nucleosome remodellers and cancer. Nat Rev Cancer *11*, 481-492.

Wilson, B.G., Wang, X., Shen, X., McKenna, E.S., Lemieux, M.E., Cho, Y.J., Koellhoffer, E.C., Pomeroy, S.L., Orkin, S.H., and Roberts, C.W. (2010). Epigenetic antagonism between polycomb and SWI/SNF complexes during oncogenic transformation. Cancer Cell *18*, 316-328.

Winston, F., and Carlson, M. (1992). Yeast SNF/SWI transcriptional activators and the SPT/SIN chromatin connection. Trends in genetics : TIG *8*, 387-391.

Wolffe, A.P. (1994). Transcriptional activation. Switched-on chromatin. Current biology : CB *4*, 525-528.

Wong, A.K., Shanahan, F., Chen, Y., Lian, L., Ha, P., Hendricks, K., Ghaffari, S., Iliev, D., Penn, B., Woodland, A.M.*, et al.* (2000). BRG1, a component of the SWI-SNF complex, is mutated in multiple human tumor cell lines. Cancer Res *60*, 6171-6177.

Wu, C.I., and Li, W.H. (1985). Evidence for higher rates of nucleotide substitution in rodents than in man. Proc Natl Acad Sci U S A *82*, 1741-1745.

Wu, J.I., Lessard, J., and Crabtree, G.R. (2009). Understanding the words of chromatin regulation. Cell *136*, 200-206.

Wu, J.I., Lessard, J., Olave, I.A., Qiu, Z., Ghosh, A., Graef, I.A., and Crabtree, G.R. (2007). Regulation of dendritic development by neuron-specific chromatin remodeling complexes. Neuron *56*, 94-108.

Wuestefeld, T., Pesic, M., Rudalska, R., Dauch, D., Longerich, T., Kang, T.W., Yevsa, T., Heinzmann, F., Hoenicke, L., Hohmeyer, A.*, et al.* (2013). A Direct In Vivo RNAi Screen Identifies MKK4 as a Key Regulator of Liver Regeneration. Cell *153*, 389-401.

Wurster, A.L., Precht, P., and Pazin, M.J. (2011). NF-kappaB and BRG1 bind a distal regulatory element in the IL-3/GM-CSF locus. Molecular immunology *48*, 2178-2188.

Xi, Q., He, W., Zhang, X.H., Le, H.V., and Massague, J. (2008). Genome-wide impact of the BRG1 SWI/SNF chromatin remodeler on the transforming growth factor beta transcriptional program. J Biol Chem *283*, 1146-1155.

Xu, Y., Yan, W., and Chen, X. (2010). SNF5, a core component of the SWI/SNF complex, is necessary for p53 expression and cell survival, in part through eIF4E. Oncogene *29*, 4090-4100.

Xu, Y., Zhang, J., and Chen, X. (2007). The activity of p53 is differentially regulated by Brm- and Brg1-containing SWI/SNF chromatin remodeling complexes. J Biol Chem *282*, 37429-37435.

Xue, W., Zender, L., Miething, C., Dickins, R.A., Hernando, E., Krizhanovsky, V., Cordon-Cardo, C., and Lowe, S.W. (2007). Senescence and tumour clearance is triggered by p53 restoration in murine liver carcinomas. Nature *445*, 656-660.

Xue, Y., Canman, J.C., Lee, C.S., Nie, Z., Yang, D., Moreno, G.T., Young, M.K., Salmon, E.D., and Wang, W. (2000). The human SWI/SNF-B chromatin-remodeling complex is related to yeast rsc and localizes at kinetochores of mitotic chromosomes. Proc Natl Acad Sci U S A *97*, 13015-13020.

Yamamichi, N., Yamamichi-Nishina, M., Mizutani, T., Watanabe, H., Minoguchi, S., Kobayashi, N., Kimura, S., Ito, T., Yahagi, N., Ichinose, M.*, et al.* (2005). The Brm gene suppressed at the post-

transcriptional level in various human cell lines is inducible by transient HDAC inhibitor treatment, which exhibits antioncogenic potential. Oncogene *24*, 5471-5481.

Yamamoto, S., Tsuda, H., Takano, M., Tamai, S., and Matsubara, O. (2012a). Loss of ARID1A protein expression occurs as an early event in ovarian clear-cell carcinoma development and frequently coexists with PIK3CA mutations. Modern pathology : an official journal of the United States and Canadian Academy of Pathology, Inc *25*, 615-624.

Yamamoto, S., Tsuda, H., Takano, M., Tamai, S., and Matsubara, O. (2012b). PIK3CA mutations and loss of ARID1A protein expression are early events in the development of cystic ovarian clear cell adenocarcinoma. Virchows Archiv : an international journal of pathology *460*, 77-87.

Yan, Z., Cui, K., Murray, D.M., Ling, C., Xue, Y., Gerstein, A., Parsons, R., Zhao, K., and Wang, W. (2005). PBAF chromatin-remodeling complex requires a novel specificity subunit, BAF200, to regulate expression of selective interferon-responsive genes. Genes Dev *19*, 1662-1667.

Yan, Z., Wang, Z., Sharova, L., Sharov, A.A., Ling, C., Piao, Y., Aiba, K., Matoba, R., Wang, W., and Ko, M.S. (2008). BAF250B-associated SWI/SNF chromatin-remodeling complex is required to maintain undifferentiated mouse embryonic stem cells. Stem Cells *26*, 1155-1165.

Yoo, A.S., Staahl, B.T., Chen, L., and Crabtree, G.R. (2009). MicroRNA-mediated switching of chromatin-remodelling complexes in neural development. Nature *460*, 642-646.

Young, A.R., Narita, M., Ferreira, M., Kirschner, K., Sadaie, M., Darot, J.F., Tavare, S., Arakawa, S., Shimizu, S., and Watt, F.M. (2009). Autophagy mediates the mitotic senescence transition. Genes Dev *23*, 798-803.

Young, N.P., and Jacks, T. (2010). Tissue-specific p19Arf regulation dictates the response to oncogenic K-ras. Proc Natl Acad Sci U S A *107*, 10184-10189.

Yu, J., Putcha, P., Califano, A., and Silva, J.M. (2013). Pooled shRNA screenings: computational analysis. Methods Mol Biol *980*, 371-384.

Yuge, M., Nagai, H., Uchida, T., Murate, T., Hayashi, Y., Hotta, T., Saito, H., and Kinoshita, T. (2000). HSNF5/INI1 gene mutations in lymphoid malignancy. Cancer genetics and cytogenetics *122*, 37-42.

Zebedee, Z., and Hara, E. (2001). Id proteins in cell cycle control and cellular senescence. Oncogene *20*, 8317-8325.

Zender, L., Xue, W., Zuber, J., Semighini, C.P., Krasnitz, A., Ma, B., Zender, P., Kubicka, S., Luk, J.M., Schirmacher, P.*, et al.* (2008). An oncogenomics-based in vivo RNAi screen identifies tumor suppressors in liver cancer. Cell *135*, 852-864.

Zhan, X., Shi, X., Zhang, Z., Chen, Y., and Wu, J.I. (2011). Dual role of Brg chromatin remodeling factor in Sonic hedgehog signaling during neural development. Proc Natl Acad Sci U S A *108*, 12758-12763.

Zhang, H.S., Gavin, M., Dahiya, A., Postigo, A.A., Ma, D., Luo, R.X., Harbour, J.W., and Dean, D.C. (2000). Exit from G1 and S phase of the cell cycle is regulated by repressor complexes containing HDAC-Rb-hSWI/SNF and Rb-hSWI/SNF. Cell *101*, 79-89.

Zhang, R., Chen, W., and Adams, P.D. (2007). Molecular dissection of formation of senescence-associated heterochromatin foci. Mol Cell Biol *27*, 2343-2358.

Zhang, R., Poustovoitov, M.V., Ye, X., Santos, H.A., Chen, W., Daganzo, S.M., Erzberger, J.P., Serebriiskii, I.G., Canutescu, A.A., Dunbrack, R.L.*, et al.* (2005). Formation of MacroH2A-containing senescence-associated heterochromatin foci and senescence driven by ASF1a and HIRA. Dev Cell *8*, 19-30.

Zhang, Z.K., Davies, K.P., Allen, J., Zhu, L., Pestell, R.G., Zagzag, D., and Kalpana, G.V. (2002). Cell cycle arrest and repression of cyclin D1 transcription by INI1/hSNF5. Mol Cell Biol *22*, 5975-5988.

Zhao, K., Wang, W., Rando, O.J., Xue, Y., Swiderek, K., Kuo, A., and Crabtree, G.R. (1998). Rapid and phosphoinositol-dependent binding of the SWI/SNF-like BAF complex to chromatin after T lymphocyte receptor signaling. Cell *95*, 625-636.

Zhou, J., Ma, J., Zhang, B.C., Li, X.L., Shen, S.R., Zhu, S.G., Xiong, W., Liu, H.Y., Huang, H., Zhou, M.*, et al.* (2004). BRD7, a novel bromodomain gene, inhibits G1-S progression by transcriptionally regulating some important molecules involved in ras/MEK/ERK and Rb/E2F pathways. J Cell Physiol *200*, 89-98.

Zhu, J., Woods, D., McMahon, M., and Bishop, J.M. (1998). Senescence of human fibroblasts induced by oncogenic Raf. Genes Dev *12*, 2997-3007.

Zindy, F., Eischen, C.M., Randle, D.H., Kamijo, T., Cleveland, J.L., Sherr, C.J., and Roussel, M.F. (1998). Myc signaling via the ARF tumor suppressor regulates p53-dependent apoptosis and immortalization. Genes Dev *12*, 2424-2433.

Zraly, C.B., Middleton, F.A., and Dingwall, A.K. (2006). Hormone-response genes are direct in vivo regulatory targets of Brahma (SWI/SNF) complex function. J Biol Chem *281*, 35305-35315.

Appendix

Table A1. Inferences from test NGS run at CSC. (A) Comparison of hairpins detected from the same Solexa library, run on two different lanes of a flowcell. Hairpins with the most frequently occurring reads from beginning (day 0) and end (day 26) time points are shown to identify variations during cluster formation. Underlined hairpins do not correlate as highly enriched in both lanes.

A

Day 0 - Lane 1				Day 0 - Lane 2			
Hairpin ID	Number of reads	Proportion of total reads	Hairpin rank	Hairpin ID	Number of reads	Proportion of total reads	Hairpin rank
255411	16224	0.022	1	255411	16818	0.013	1
227797	14395	0.019	2	227797	15991	0.012	2
313708	9158	0.012	3	313708	9931	0.008	5
315123	6232	0.008	4	315123	6586	0.005	14
224512	6093	0.008	5	224512	12839	0.010	3
345046	6068	0.008	6	409046	10576	0.008	4
265589	5422	0.007	7	265589	6376	0.005	16
227227	5088	0.007	8	227227	9168	0.007	6
242174	4843	0.007	9	294529	8192	0.006	8
292091	4837	0.007	10	292091	7913	0.006	10
289507	4804	0.006	11	291552	6831	0.005	12
484108	4801	0.006	12	254108	6163	0.005	19
412353	4686	0.006	13	371450	6551	0.005	15
299510	4659	0.006	14	299510	8303	0.006	7
298236	4540	0.006	15	298236	6799	0.005	13
299585	4533	0.006	16	299585	7641	0.006	11
225410	4502	0.006	17	251616	6340	0.005	17
295248	4442	0.006	18	304239	6296	0.005	18
246874	4279	0.006	19	246874	7997	0.006	9
487004	4240	0.006	20	270196	6141	0.005	20

B

Day 26 - Lane 1				Day 26 - Lane 2			
Hairpin ID	Number of reads	Proportion of total reads	Hairpin rank	Hairpin ID	Number of reads	Proportion of total reads	Hairpin rank
227797	557443	0.610	1	227797	602086	0.467	1
421869	62830	0.069	2	421869	114086	0.089	2
240150	53696	0.059	3	240150	99634	0.077	3
322345	21905	0.024	4	322345	48689	0.038	5
267420	21493	0.024	5	267420	48970	0.038	4
326037	20867	0.023	6	326037	43905	0.034	6
345038	12546	0.014	7	345038	27094	0.021	7
307744	11916	0.013	8	307744	22457	0.017	8
345037	6758	0.007	9	345037	14318	0.011	10
244423	6750	0.007	10	244423	17200	0.013	9
224512	6389	0.007	11	224512	11977	0.009	12
282103	5785	0.006	12	282103	10790	0.008	13
380153	5455	0.006	13	380153	12188	0.009	11
302435	5192	0.006	14	424211	7352	0.006	18
299585	4763	0.005	15	299585	7984	0.006	15
476556	4632	0.005	16	476556	9218	0.007	14
322064	3843	0.004	17	322064	7626	0.006	16
285671	3726	0.004	18	285671	7490	0.006	17
236688	3501	0.004	19	236688	7304	0.006	19
450546	3447	0.004	20	315231	6022	0.005	20

Table A2. Differential gene expression of ARID1B knockdown cells during OIS. * validated by RT-qPCR.

Gene name	Gene	Fold change shARID1B-3/vector
late cornified envelope 2C	LCE2C*	0.29
late cornified envelope 2A	LCE2A*	0.35
late cornified envelope 2B	LCE2B	0.35
late cornified envelope 1F	LCE1F	0.42
secreted phosphoprotein 1	SPP1*	0.42
matrix metallopeptidase 3 (stromelysin 1, progelatinase)	MMP3	0.46
serpin peptidase inhibitor, clade B (ovalbumin), member 7	SERPINB7	0.52
vitamin D (1,25- dihydroxyvitamin D3) receptor	VDR	0.52
growth arrest-specific 6	GAS6	0.52
keratin associated protein 2-4	KRTAP2-4	0.53
keratin associated protein 2-1	KRTAP2-1	0.53
colony stimulating factor 2 (granulocyte-macrophage)	CSF2	0.54
ankyrin repeat domain 1	ANKRD1	0.55
latent transforming growth factor beta binding protein 2	LTBP2	0.58
tumor necrosis factor, alpha-induced protein 6	TNFAIP6	0.60
AT rich interactive domain 1B (SWI1-like)	ARID1B*	0.60
semaphorin 7A, GPI membrane anchor	SEMA7A	0.60
transgelin 3	TAGLN3	0.60
SMAD specific E3 ubiquitin protein ligase 2	SMURF2	0.61
matrix metallopeptidase 10 (stromelysin 2)	MMP10	0.62
NUAK family, SNF1-like kinase, 1	NUAK1	0.62
NLR family, pyrin domain containing 10	NLRP10	0.63
v-ets erythroblastosis virus E26 oncogene homolog 1	ETS1	0.65
tumor necrosis factor (ligand) superfamily, member 15	TNFSF15	0.68
growth differentiation factor 15	GDF15*	0.68
E2F transcription factor 7	E2F7*	0.68
chemokine (C-X-C motif) ligand 5	CXCL5	0.68
transmembrane protein 156	TMEM156	0.69
cyclin-dependent kinase inhibitor 1A (p21, Cip1)	CDKN1A*	0.72
inhibitor of DNA binding 4, dominant negative helix-loop-helix protein	ID4	1.61
inhibitor of DNA binding 2, dominant negative helix-loop-helix protein	ID2	2.00
inhibitor of DNA binding 3, dominant negative helix-loop-helix protein	ID3	2.45
inhibitor of DNA binding 1, dominant negative helix-loop-helix protein	ID1	3.34

Table A3. pGIPZ pool coverage determined by HTS. Amplified pGIPZ library pools were prepared from plasmid stocks and transformation efficiencies were calculated by counting the number of colonies arising from parallel pUC DNA transformations at different dilutions. IMR-90 were infected with the indicated pGIPZ pool and collected 2 days post infection. Custom Solexa libraries were prepared and sequenced as before. Proportions of reads in a sample were calculated to assess the shRNAs represented per pool. shRNAs detected are predominantly pool specific as indicated by corresponding plate numbers.

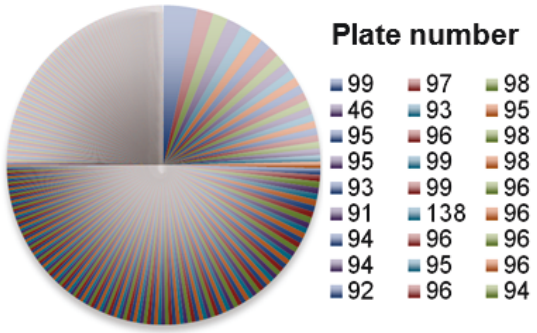
Pool	Plates	Transformation efficiency	Number of shRNAs detected	Proportions of reads/hairpin (plate number indicates origin of highly enriched hairpins)
9 (1000 shRNAs)	91-100	4.21×10^5	1065	

Table A4. Copy number deletions in ARID1B are significant across cancers. ARID1B is significantly focally deleted (Q-value<0.25) across the entire dataset of 3131 tumours. However ARID1B is not located within a "focal peak region of deletion" which are regions most likely to contain the gene or genes being targeted by significant deletions. ARID1B is significantly focally deleted and is located within a focal peak region of deletion in breast and ovarian cancers (Adapted from www.broadinstitute.org/tumorscape and Beroukhim et al. 2010)

Cancer Subset	In Peak?	Nearest Peak	#Genes in Peak	Q-value
all_cancers	No	chr6:161626932-163103553	1	5.86E-7
Breast	Yes	chr6:155684256-170747902	66	1.62E-4
Ovarian	Yes	chr6:144467714-170747902	120	0.0265

Table A5. cDNA constructs.

Vector	cDNA	Antibiotic resistance	Addgene reference
pBABE	Empty Vector	Puromycin	-
pGIPZ	Empty Vector	Puromycin	-
LXSN	Empty Vector	Puromycin	-
pRS	Empty Vector	Puromycin	-
pBABE	GFP	Puromycin	-
pBABE	RAS^{G12V}	Puromycin	-
pBABE	ARID1A	Puromycin	-
pBABE	ARID1B	Puromycin	-
pLNC	RAS:ER	Neomycin	-
pLPC	Cherry	Puromycin	-
LXSN	E6	Puromycin	-
LXSN	E7	Puromycin	-
LXSN	E6/E7	Puromycin	-
pLNCX	$PIK3CA^{H1047R}$	Neomycin	25635
pBABE	BRG1	Puromycin	1959
pBABE	BRM	Puromycin	1961

Table A6. shRNA target sequences.

Construct	Target sequence
MLP m-shp53	CACTACAAGTACATGTGTA
MLP m-shp16/Arf	CCGCTGGGTGCTCTTTGTGT
pRS m-shArid1b	AAGGCGAAAGATTACCTCAAA
pRS shARID1B-1	CACAACCAGTCTTGAAACAAA
pRS shARID1B-2	AAGCAAATTGACTTTAAAGAA
pRS shARID1B-3	ACCATGAAGACTTGAACTTAA
pRS shp16	GAGGAGGTGCGGGCGCTGC
pRS shp53	GTAGATTACCACTGGAGTC
pRS shp21	TCCCACAATGCTGAATATACA
pGIPZ shp53-1	TAACTGCAAGAACATTTCT
pGIPZ shp53-2	TACACATGTAGTTGTAGTG
pGIPZ shp53-3	TCTCTTCCTCTGTGCGCCG
pGIPZ shp16-1	TGCCCATCATCATCACCTG
pGIPZ shp16-2	ACACAAAGAGCACCCAGCG
pGIPZ shp16-3	TGAGCTGAAGCTATGCCCG

Table A7. Solexa PCR primers.

Primer	Sequence (5’ to 3’)
p5 miR3'	aatgatacggcgaccaccgactaaagtagccccttg
p7 Loop primer	caagcagaagacggcatacgatagtgaagccacaga
Solexa barcode 1	caagcagaagacggcatacgaaaatagtgaagccacaga
Solexa barcode 2	caagcagaagacggcatacgaaactagtgaagccacaga
Solexa barcode 3	caagcagaagacggcatacgaaagtagtgaagccacaga
Solexa barcode 4	caagcagaagacggcatacgaaattagtgaagccacaga
Solexa barcode 5	caagcagaagacggcatacgaacatagtgaagccacaga
Solexa barcode 6	caagcagaagacggcatacgaacctagtgaagccacaga
Solexa barcode 7	caagcagaagacggcatacgaacgtagtgaagccacaga
Solexa barcode 8	caagcagaagacggcatacgaacttagtgaagccacaga
Solexa barcode 9	caagcagaagacggcatacgaagatagtgaagccacaga
Solexa barcode 10	caagcagaagacggcatacgaagctagtgaagccacaga
Solexa barcode 11	caagcagaagacggcatacgaaggtagtgaagccacaga
Solexa barcode 12	caagcagaagacggcatacgaagttagtgaagccacaga
Solexa barcode 13	caagcagaagacggcatacgaatatagtgaagccacaga
Solexa barcode 14	caagcagaagacggcatacgaatctagtgaagccacaga
Solexa barcode 15	caagcagaagacggcatacgaatgtagtgaagccacaga

Table A8. Sequencing primers

Primer	Sequence (5’ to 3’)
pBABE F	CTTTATCCAGCCCTCAC
pBABE R	ACCCTAACTGACACACATTC
pRS F	GCTGACGTCATCAACCCGCT
pRS R	TGTGAGGGACAGGGGAG
Solexa primer	TAGCCCCTTGAATTCCGAGGCAGTAGGCA
pGIPZ F	TGGAAACACTTGCTGGGATT
pGIPZ R	GCTCCTAAAGTAGCCCCTTG

Table A9. RT-qPCR primers.

Target gene	Sequence (5’ to3’)
ARID1A	CCCCTCAATGACCTCCAGTA
	CTGGAAATCCCTGATGTGCT
Arid1b	CCTGGAAAATCCAACCATGA
	GTCTACAAGCAGCCAGGGAG
ARID1B	CTGTCGCCTCAGAGAC
	GTTCGATAAAAGCGCCAT
ARID2	CTGGCGCTGTCCTGCCATGT

	CAGCGGTGTCTGTTGGGCAGT
β-GUS	CTCATTTGGAATTTTGCCGATT
	CCGAGTGAAGATCCCCTTTTTA
BAF155	GGGCCTTTGGCCTACCAGCC
	CAGATGCCACGCGAGGGTCC
BAF170	GGAATGGGTACGACCAGTCA
	CATCTTCCACAGATGCCTCA
BRD7	GCTCCTGGCTACTCCATGAT
	TCATTCCTGAGTGCAACAGC
BRG1	CATCACCCCCATCCAGAA
	CTCAATGGTCGCTTTGGTTC
CDKN1a	CCTGTCACTGTCTTGTACCCT
	GCGTTTGGAGTGGTAGAAATCT
E2F7	GGAAAGGCAACAGCAAACTCT
	TGGGAGAGCACCAAGAGTAGAAGA
GDF15	AGGGCGGCCCGAGAGATACG
	AGTGCTGCTGAAGGAGATGCCTGA
INHBA	GCTGTTCCTGACTCGGCAAACGT
	GGATACTCACGCCAGAAGTGCGG
INK4a	CGGTCGGAGGCCGATCCAG
	GCGCCGTGGAGCAGCAGCAGCT
INK4B	GAATGCGCGAGGAGAACAAG
	CCATCATCATGACCTGGATCG
LCE2A	CACCCAAGTGTCCTCCAAAG
	CCCCAGAAGGTTCACACTCA
LCE2B	CCGACTGCTGTGAGAGTGAA
	TTGAGGTGCTCCATCAAGTG
P53	CCGCAGTCAGATCCTAGCG
	AATCATCCATTGCTTGGGACG
PBRM1	GTGTGATGAACCAAGGAGTGGC
	GATATGGAGGTGGTGCCTGCTG
PGC1a	GGCAGGCCTCAGATCTAAAAGTCA
	GCATCATGGGAGCCTTCTTGTC
Rps14	GACCAAGACCCCTGGACCT
	CCCCTTTTCTTCGAGTGCTA
SMARCB1	GGATGGCAACGATGAGAAGT
	CTGTTCCTCTTGGCCTTCTG
SPP1	TTGCAGCCTTCTCAGCCAA
	CAAAAGCAAATCACTGCAATTCTC

Table A10. Primers for cloning.

Primer	Sequence (5' to 3')
ARID1B SalI forward	cagagagaaagctctggGTCGACcgatacc
ARID1B SalI reverse	ggGTCGACtcataactgcccaatctgaaacagtacatca
Lumican BamH1 forward	acctgGGATTCatttgccaaaaatgagtctaagtgc
Lumican EcoR1 reverse	acctgGAATTCttaattaagagtgactt

Table A11. Antibodies.

Target	Clone/Lot	Company	Catalogue no.	Source	Application
ARID1B	A301-047A-1	Bethyl	A301-047A	Rabbit	IF, IP
ARID1B	M01	Abgent	AT1189a	Mouse	IF
ARID1B	R06587	Sigma	HPA016511	Rabbit	IF
ARID1A	M01	Abgent	AT1188a	Mouse	IF
SNF5	R07906	Sigma	HPA018248	Rabbit	IF
BRG1	1147182	abcam	ab4081	Rabbit	IF, IP
BRM	GR5208-2	abcam	ab15597	Rabbit	IF
BrdU	PRB-1	Invitrogen	A21303	Mouse	IF
p16INK4a	JC-8	Santa Cruz	sc-56330	Mouse	IF
p21Waf1/Cip1	12D1	Cell Signaling	2947	Rabbit	IF
p53	DO-1	Santa Cruz	sc-126	Mouse	IF
P-AKT Ser473	193H12	Cell Signaling	4085	Rabbit	IF
IgG control	GR63825-D	abcam	ab46540	Rabbit	IP
H3K27me3	JBC1873477	Millipore	07-449	Rabbit	IF
H3K9me3	1971290	Millipore	07-442	Rabbit	IF
P-AKT Ser473	193H12	Cell Signaling	4085	Rabbit	IF
Anti-Mouse IgG	Alexa Fluor® 488	Invitrogen	A11029	Goat	IF
Anti-Mouse IgG	Alexa Fluor® 594	Invitrogen	A11032	Goat	IF
Anti-Rabbit IgG	Alexa Fluor® 488	Invitrogen	A11034	Goat	IF
Anti-Rabbit IgG	Alexa Fluor® 594	Invitrogen	A11037	Goat	IF

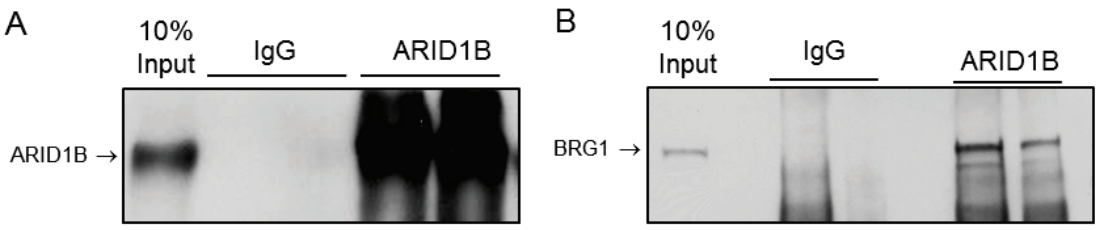


Figure A1. Validation of ARID1B antibody for immunoprecipitation. (A) nuclear extracts (2mg for IP, 200μg for input) were prepared and ARID1B was immunoprecipitated using 10 μg Bethyl A301-047A-1 antibody. For blotting immunoprecipitated ARID1B, Abgent MO1 which recognizes an upstream epitope, was used at 1 μg/ml. (B) Co-immunoprecipitation of SWI/SNF components was assessed by detecting immunoprecipitated BRG1 in ARID1B pull-downs.